More Than Meets the Eye: Molecular Diversity of the Intrinsically Photosensitive Ganglion Cells Regulating Circadian Photoentrainment

By

Daniel Joseph Berg

BA, Lawrence University, 2008

Thesis

Submitted in partial fulfillment of the requirements for the

Degree of Doctorate in the Department of Molecular Biology, Cellular Biology, and Biochemistry at Brown University

Providence, Rhode Island

May 2018

Signature Page

This thesis by Daniel Joseph Berg is accepted in its present form by the Department of Molecular Biology, Cellular Biology, and Biochemistry as satisfying the thesis requirements for the degree of Doctor of Philosophy.

Date _____ **_____**

David Berson, Ph.D., Thesis Advisor

Date _____ **_____**

Gary Wessel, Ph.D., Committee Chair

Date _____ **_____**

Gilad Barnea, Ph.D., Committee Member

Date _____ **_____**

Eric Morrow, Ph.D., Committee Member

Date _____ **_____**

Joshua Sanes, Ph.D., Outside Reader

Date _____ **_____**

Andrew G. Campbell, Ph.D., Dean of Graduate School

Abstract of "More Than Meets the Eye: Molecular Diversity of the Intrinsically Photosensitive Ganglion Cells Regulating Circadian Photoentrainment," by Daniel Joseph Berg, Ph.D., Brown University, June 2017

The retina as a model system has helped to understand the genetic programs responsible for generating the cellular diversity in the nervous system. Intrinsically photosensitive retinal ganglion cells (ipRGCs) are rare mammalian photoreceptors essential for non-image-forming vision functions, such as circadian entrainment and the pupillary light reflex. The ipRGCs comprise multiple subtypes distinguishable by morphology, physiology, projections, and levels of expressed Opn4, the ipRGC photopigment.

Although substantial progress has been achieved over the years, comprehensive classification of ipRGCs on a molecular basis has yet to be realized. Examination of ipRGC gene expression profiles could provide insights into the function adult ipRGCs. In Chapter 2, I discuss how I developed a comprehensive, sensitive, and accurate means to test for genes differentially expressed in ipRGCs compared to generic RGCs. The purity of the isolated ipRGCs was demonstrated by the very low abundance of mRNAs unique to retinal cell types other than ipRGCs (e.g., rhodopsin in rods) and highly significant enrichment for transcripts unique to ipRGCs (e.g. melanopsin, PACAP, Trpc7 and Eomes/Tbr2). Our data revealed dozens of genes not previously known to be highly enriched in ipRGCs including phototransduction machinery, transcription factors, and beneficial tools for ipRGC survival.

The next frontier in understanding the diversity and classification of subtypes is through the integration of molecular, anatomical, and physiological criteria. As I discuss in Chapter 3, my initial goal after the completion of my transcriptomics studies was to test whether the differentially

expressed genes truly were restricted to ipRGCs, and if so, integrate this new molecular information with the wealth of knowledge that is already known about the ipRGC family members. One of the genes that caught our eye was Rasgrp1, a Ras GEF (guanine nucleotide exchange factor). Rasgrp1-expressing ganglion cells were demonstrated to be overwhelmingly ipRGCs, but broke the mold of what we have been traditionally calling distinct ipRGC subtypes. Rasgrp1 was determined to be expressed in most M1 ipRGCs, but a portion of M2 and M5/6 cells also appear to express the protein. The phototransduction cascade in ipRGCs is known to elevate diacylglycerol and intracellular calcium, both known to activate Rasgrp1. Preliminary evidence suggests that Rasgrp1 is well-positioned to provide a unique form of Ras signaling to a subset of ipRGCs. The transcription factor Tbx20 also stood out to us from our gene expression analysis for its potential to be a driving force in maintaining the adult identity of ipRGCs. Surprisingly, Tbx20 was also determined to be expressed in a subpopulation of ipRGCs that was not restricted to a single, established type. The integration of the two new ipRGC markers, Rasgrp1 and Tbx20, paints an even more complex picture. Finally, I tested how this expression pattern correlates with known brain circuitry to the region in the brain responsible for circadian time-keeping. These findings continue to support the notion that ipRGCs are incredibly specialized and diverse, a characteristic that is expected to exist across the nervous system.

For my fourth chapter, I discuss a fortuitous transgenic reporter mouse line that we pursued because it allowed us to study not only an amacrine cell type that is electrically coupled to ipRGCs, but it has also allowed us to characterize a new subtype of RGC, the R-type. The Rbp4-cre transgenic reporter line revealed a sparse labeling of RGCs, as well as labeling of amacrine cells across the retina. Closer inspection of Rbp4-labeled RGCs revealed bistratified dendrites with ON dendritic arbors in close proximity to processes of starburst amacrine cells and OFF arbors that

costratified with M1-ipRGCs. This “R-type” was determined to have intriguing physiology. The bistratified R-type was solely ON-responsive despite having OFF-arbors, a feature that is similar to known ipRGC types with OFF-arbors receiving ectopic ON cone bipolar input. We have leveraged this Cre-based reporter to also test a distinct type of amacrine cell that is gap junction coupled to ipRGCs.

DANIEL BERG

320-266-3375

Daniel_Berg@Brown.edu

EDUCATION

Brown University Providence, RI

PhD – Molecular, Cellular Biology and Biochemistry (MCB) program 2017

David Berson laboratory (Neuroscience department)

Doctoral Dissertation: More Than Meets the Eye: Molecular Diversity of the Intrinsically Photosensitive Ganglion Cells Regulating Circadian Photoentrainment

Lawrence University Appleton, WI

Bachelor of Arts – Biology-Chemistry and Neuroscience Interdisciplinary 2008

Magna cum laude honors in Independent Study, "Potassium Channel Interactions Modify Male Mating Behavior of *Caenorhabditis elegans*"

RESEARCH EXPERIENCE

Brown University (Providence, RI) 9/2010-6/2017

PhD (MCB) – laboratory of Dr. David Berson (Neuroscience)

- To understand the molecular identity and diversity of a specialized type of neuron in the mouse eye, I designed and implemented new methods to assess the transcriptional profile of purified intrinsically photosensitive retinal ganglion cells (ipRGCs). I successfully: 1) dissected and enzymatically dissociated retinas, 2) isolated a pure population of the rare fluorescently labeled ipRGCs (0.01% of retinal cells), 2) prepared the tiny amount of isolated genetic material for robust RNA-sequencing, and 3) used bioinformatics pipelines (Cuffdiff and EdgeR) to determine differential gene expression of ipRGCs relative to generic RGCs.
- I seamlessly transitioned from dozens of differentially expressed genes revealed by an avalanche of RNA-seq data to more targeted studies such as the quantification of protein coexpression in retrograde labeled brain circuits using confocal microscopy.
- I have identified multiple distinct molecular subtypes of ipRGCs and clarified how these subtypes can potentially be linked to specialized visual functions by parallel brain circuits.
- I collaborated to identify a Cre-based mouse reporter that labels a novel type of retinal ganglion cell definable by a unique set of physiological, circuitry, molecular and morphological criteria.
- I was part of a team effort to develop a method that will permit correlated light and serial EM observations on genetically identified neurons.
- Expertise in extensive molecular and cell biology techniques including: tissue microdissection, enzymatic tissue dissociation, fluorescence activated cell sorting (FACS), Magnetic-activated cell sorting (MACS), mRNA extraction, cDNA and sequencing library preparation, Covaris cDNA shearing, Qubit and nanodrop DNA quantification, Illumina RNA-seq, differential expression analysis, multi-channel tissue immunofluorescence and co-expression analysis, confocal imaging, cell culture, *in situ* hybridization, molecular cloning, neuroanatomy, live animal handling and genotyping, and anesthetized animal surgery.

Columbia University (New York, NY) 10/2009-8/2010
Technician B – laboratory of Dr. Iva Greenwald (Biochemistry and Molecular Biophysics)

- I genetically characterized the suppressor candidate genes in gain of function *glp-1* and hypermorphic *lin-12* backgrounds.
- I constructed expression vectors to drive SID-1 expression at critical points in *C. elegans* vulval cell fate decision to allow for efficient RNAi silencing as a tool for future identification of additional factors.

University of Minnesota (Minneapolis, MN) 2/2008-9/2009
Junior Scientist – laboratory of Dr. Ann Rougvie (Genetics, Cell Biology, Development)

- I examined relationship between *eak-4* and *lin-42* in *C. elegans* stress response using quantitative Western Blot analysis, dauer formation and alae formation assays, and daf-16::GFP localization assays.
- I utilized genetic crosses to create strains for analysis of genes interacting with *lin-42* in *C. elegans* developmental timing and the dauer formation pathway.
- I recombineered *lin-42* locus to generate differentially labeled isoforms in a single construct to visualize localization in *C. elegans*.

Lawrence University (Appleton, WI) 6/2006-12/2007
Research Assistant - laboratory of Dr. Elizabeth De Stasio (Biology)

- I developed *C. elegans* male mating assays to quantify the effect of *sup-9* mutations on males' ability to respond to hermaphrodite contact and complete tight ventral turns necessary for the mating process.
- I constructed and verified plasmids containing *sup-9* bait and *sup-18* prey vectors for the Split-Ubiquitin Yeast Two-Hybrid system.

PUBLICATIONS

Berg D, Kartheiser K, Leyrer M, Saali A, Woods J, and Berson D (to be submitted to eLife 2017) Molecular Diversity of the Intrinsically Photosensitive Ganglion Cells Regulating Circadian Photoentrainment. (pre-print manuscript available upon request)

Sabbah S, **Berg D**, Papendorp C, Briggman K, Berson D (2017) A Cre Mouse Line for Probing Irradiance- and Direction-Encoding Retinal Networks. eNeuro

CONFERENCE PRESENTATIONS

Berg D, Sabbah S, and Berson D (2015) Genetic identification of a novel bistratified retinal ganglion cell type. Society for Neuroscience (SFN) meeting. San Diego, CA (Poster)

Berg D, Kartheiser K, and Berson D (2014) Molecular Diversity of ipRGCs: Implications for Specialized Ras Signaling. FASEB conference Saxtons River, Vermont (Poster)

Berg D and Berson D (2013) RNA-seq Sheds light on Molecular Diversity in Intrinsically Photosensitive Retinal Ganglion Cells (ipRGCs). SFN meeting. San Diego, CA (Poster)

Berg D and Berson D (2012) Methods for Probing Molecular Diversity in Intrinsically Photosensitive Ganglion Cells. FASEB conference Steamboat Springs, CO (Poster)

Acknowledgements

The Berson laboratory was a source of comradery, deep knowledgebase, teamwork, and expertise that helped me grow in important ways that I couldn't even imagine beforehand.

- My PhD advisor, **David Berson**, believed in my research potential and gave me a chance at a time when I needed it most. None of the research I have accomplished during my PhD would have been possible without his support, promotion of independence, and an endless supply of optimism. David helped me build a strong research foundation for my future development as a postdoc and beyond.
- **Dianne and Kimmy Boghossian** do not receive enough credit for making research possible in the Berson lab. When I first came to the lab, I had many big requests on their time and energy to manage ordering lists of reagents and heavily expand the mouse colony for my studies. At a minimum, my research would not have been able to be completed nearly as efficiently without their help throughout the process. They made the lab environment warm and provided a source of stability and reliability.
- **Jordan Renna** provided an exceptional source for thoughtful discussion about experiments, life and everything in between. He provided multiple examples of fruitful collaboration that benefited all stages of my research program.
- **Shai Sabbah** provided much appreciated friendship in and out of lab. His expert experimental prowess and collaboration was vital to turning a side project into a full publication.
- **Katherine Kartheiser** was a talented undergraduate researcher that I had the pleasure of mentoring for two years. I was continuously impressed by her self-drive as well as capacity for growth, discipline, and enthusiastic about science.

- **Megan Leyrer** had a similar background in molecular biology that facilitated the development of new lines of research in the lab. She collaborated with me on multiple projects and was essential to acquiring important pieces of my research program.
- **Ryan Maloney** taught me much about mentorship during our partnership to complete the Sheridan Center Mentorship program with our mentees. His inquisitive nature always made it a joy to share conversations.
- **Michelle Fogerson** was an exceptional team player that always made time to help others. She demonstrated an impressive ability to decipher complex neural circuits, build new experimental setups, and think deeply about science.
- **Lauren Quattrochi** was the one who first pointed me in the direction of the "research playground" that was David Berson's laboratory and helped me significantly during my challenging transition into the Berson lab.
- **Maureen Estevez** enthusiasm and passion for teaching was truly infectious and inspired many students and colleagues including myself.

My committee pushed me to reach my full potential during my PhD by accepting nothing less than the best from me.

- **Gary Wessel** was an exceptional chair of my committee and provided insightful, critical, and constructive analysis throughout my time at Brown. His promotion of unbiased research inquiry ("to test a hypothesis" versus "to prove") will be a lesson I will always carry with me.

- **Gilad Barnea** promoted me to keep the big picture in mind and provided an expert perspective into mouse genetics. He openly allowed me to use his laboratory's equipment to test out experiments and generally helped me push forward my research.
- **Eric Morrow** provided a valuable perspective of retinal transcriptome analysis and mammalian neurobiology that helped me develop my research mentality.
- My outside reader, **Josh Sanes**, has been generous with his time to have indepth discussions with me at conferences about research and the academic career path. He shared his special, deep wisdom of many aspects the specialization and classification of retinal ganglion cells types.

I dedicate this PhD thesis to my parents, **Joe and Theresa Berg**. They always seem to see the best in me and have provided an endless source of love and support. They provided the support structure and believed in me every step of the way. They prioritized my education and provided me the confidence and space to explore and develop my identity.

The greatest discovery I made during my time at Brown University was **Irina Calciu** during a fortuitous MCB-sponsored Halloween party. From the beginning, she fostered in me a strength and confidence that I had been searching for. She has provided love and support while I clawed through some of the lowest lows and was the reason why I could find the highest highs in my life. I admire her curiosity, impeccable instincts and tenacity in research. Through it all, she has provided life balance with tennis games and trips to foreign lands of Romania, Sweden, Denmark, and Germany. Through it all, she has pushed me to have an honest perspective on life filled with hope, confidence, and optimism for where life will take me in the future alongside my better half.

TABLE OF CONTENTS

Title Page **i**

Copyright Page **ii**

Signature Page **iii**

Abstract **iv**

Curriculum Vitae **vii**

Acknowledgements **ix**

Table of Contents **xii**

List of Figures and Tables **xvii**

CHAPTER 1: Theory and practice of classification 1

Part 1: Classification of organisms **2**

1.1 Aristotle's observation-based science and classification 2

1.2 Francis Bacon and objectivity in classification 3

1.3 The taxonomy system of Linnaeus 4

1.4 Whewell philosophy of natural classification 5

1.5 Darwin's theory of evolution 12

1.6 The Modern Synthesis 15

Part 2: Classification of retinal ganglion cells **18**

2.1 The fundamental organization of the retina 18

2.2 The initial studies of retinal ganglion cell (RGC) diversity 19

2.3 Application of taxonomy systems to ganglion cell classification 21

2.4 Unsupervised cluster analysis based on Whewell Maxim 25

2.5 The immense parallel processing capabilities of diverse retinal cell types 27

2.6 Classification with comprehensive physiological and anatomical criteria 27

2.7 Mosaicism as an organizing principle of ganglion cell types 29

2.8 Molecular criteria for ganglion cell classification 30

Part 3: Devo-Evo and retinal cell type diversification **33**

3.1 Reintroduction of structuralism thinking into evolutionary biology 33

3.2 Biological types are individuals, not classes 34

3.3 The sister cell model and the origin of cell types 37

3.4 Origin and diversification of retinal cell types 40

Part 4: Summary **43**

Figures **46**

CHAPTER 2: Assembling a molecular parts list for ipRGCs **48**

Our third type of photoreceptor proves to be a needle in a haystack 50

Discovery of intrinsically photosensitive retinal ganglion cell (ipRGCs) 51

Phototransduction capabilities of ipRGCs 53

Multiple ipRGC types beyond original M1 type 54

The establishment of diversity within the retina 56

ipRGCs are the first-born photoreceptors 61

Filling the void: Identification of a molecular parts list for ipRGCs 62

Methods **67**

Results **74**

Cell composition and purity of isolated ipRGCs and generic RGCs 75

Identification of differentially expressed genes in ipRGCs 78

ipRGC phototransduction machinery 79
Molecular programs of ipRGCs 81
Additional genes of interest 83
Comparison of the genes differentially expressed in Opn4-based reporters 84
ipRGC retinal circuitry development 86
Discussion 87
Clarification of the ipRGC phototransduction cascade 89
Specialized heparin sulfate modifications 91
Developmental control of ipRGC circuit formation 92
Enhancement of ipRGC survival 95
Comparison with other studies 96
Further considerations 98
Conclusion 100
Figures 101
CHAPTER 3: Molecular diversity of ipRGCs regulating circadian rhythms **123**
Introduction **124**
Rasgrp1 provides specialized Ras signaling at the Golgi 124
Tbx20 has a dual role as both a transcriptional activator and repressor 126
Results **130**
Rasgrp1 is selectively expressed in ipRGCs 130
Rasgrp1 is expressed in a diverse subpopulation of multiple ipRGC types 132
Tbx20 is expressed in a diverse subset of ipRGCs 133
Tbx20 is expressed in M5/6 ipRGCs 135

Molecular diversity of Rasgrp1 and Tbx20 expression in ipRGCs 136
Molecular diversity of SCN-projecting ipRGCs 137
Functional testing of Rasgrp1 139
Discussion **140**
What type(s) of adult ipRGCs express Rasgrp1? 141
What is the function of Rasgrp1 in adult ipRGCs? 142
Central brain targets of Rasgrp1-expressing ipRGCs 144
What type of amacrine cells express Rasgrp1? 145
Future directions of Rasgrp1 studies 146
Tbx20 is expressed in a diverse set of ipRGC subtypes 148
What is the function of Tbx20 in adult ipRGCs? 149
Classification of ipRGC subtypes 151
Identification of genes differentially expressed in adult ipRGCs 153
Methods **154**
Figures **160**
References **169**
CHAPTER 4: A Cre mouse line for the study of irradiance-encoding in the retina **203**
Summary and Significance Statement **204**
Introduction **205**
Methods **207**
Results **215**
Small subsets of amacrine and ganglion cells are marked in Rbp4-Cre mice 215
Rbp4-Cre labels a subpopulation of displaced polyaxonal amacrine cells 216

Rbp4-Cre labels a sparse population of bistratified amacrine cells 217

RACs have sustained irradiance-encoding light responses 217

RACs are tracer coupled to selected ipRGCs and ACs 219

Rbp4-Cre marks two types of bistratified RGCs 220

Morphology of the R-cell 220

R-cells have sustained ON irradiance-encoding light-evoked responses 221

Serial electron microscopy reconstruction of an R-cell and its synaptic inputs 222

A novel bipolar cell type – cone BC Type 0 224

Morphology and physiology of RDS cells 225

Axonal projections of Rbp4-Cre RGCs 226

Discussion **228**

RACs form a wide-field lateral inhibitory network coupled to ipRGCs 228

R-cell – an ON bistratified ganglion cell type 231

RDS – A direction selective cell in the Rbp4-Cre mouse 234

Tables and Figures **237**

References **260**

CHAPTER 5: Closing thoughts **267**

References **272**

LIST OF FIGURES AND TABLES

Chapter 1: Introduction

Figure 1. Visual processing in the retina. **46**

Figure 2. Retinal ganglion cell morphological diversity. **47**

Chapter 2: Assembling a molecular parts list for intrinsically photosensitive retinal ganglion cells (ipRGCs)

Figure 1. The intrinsically photosensitive retinal ganglion cells (ipRGCs) are distinguished, in part, by their special ability to independently respond to light stimulation **101**

Figure 2. Transgenic mouse reporters have revealed multiple, anatomically distinct ipRGC subtypes **102**

Figure 3. The generation and differentiation of the many types of neurons in the eye have a stereotyped timing and molecular program. **103**

Figure 4. Coexpression of BAC transgenic Opn4-GFP reporter with Opn4 immunoreactivity. **104**

Figure 5. Experimental design of the isolation and differential expression analysis of ipRGCs compared to generic RGCs. **105**

Figure 6. Steps involved with processing mRNA extracted from purified cell populations and preparing for RNA-sequencing **106**

Figure 7. Sequencing reads and differential analysis pipeline. **107**

Figure 8. EdgeR multi-dimensional scaling (MDS) plot visualizes the overall similarity between expression profiles of different samples. **108**

Figure 9. Visualization strategy of differential gene expression analysis in ipRGCs compared to generic RGCs. **109**

Figure 10. Heat map of known cell type marker gene expression in the retina to assess purity and cell composition of ipRGC and generic RGC samples. **110**

Figure 11. Heat map of genes differentially expressed in ipRGCs. **111**

Figure 12. Heat map of genes that are potentially relevant to the Opn4-mediated phototransduction signaling cascade. **114**

Figure 13. Heat map of genes with previously described functions in the phototransduction cascade. **115**

Figure 14. Heat map of genes encoding transcription factors that have a particular temporal pattern of differential expression in ipRGCs. **117**

Figure 15. Heat map of genes encoding channels and receptors. **118**

Figure 16. Heat map of genes differentially expressed in adult ipRGCs labeled by the Opn4-Cre/ZEG (M1-M6 ipRGCs) reporter compared to Opn4-GFP (M1-M3 ipRGCs) **120**

Figure 17. Heat map of genes relevant for development of ipRGCs. **121**

Figure 18. Comparison of other gene expression studies of ipRGCs to our dataset. **122**

Chapter 3: Molecular Diversity of the Intrinsically Photosensitive Ganglion Cells Regulating Circadian Photoentrainment

Figure 1. Rasgrp1 is selectively expressed in ipRGCs. **160**

Figure 2. Rasgrp1 is selectively expressed in a subset of morphologically diverse set of ipRGC subtypes. **161**

Figure 3. Colocalization study of Tbx20-expression in ipRGC subtypes. **162**

Figure 4. Complex pattern of Rasgrp1-Tbx20-Brn3b co-expression suggests further diversity in ipRGC family. **163**

Figure 5. SCN-projecting ipRGCs are molecularly diverse patterns of Rasgrp1 and Tbx20 expression. **164**

Figure 6. Rasgrp1-Cre expressing RGCs have axon terminals in a wide range of subconscious visual targets. **165**

Figure 7. Rasgrp1 is localized to the Golgi in ipRGCs via an Opn4-independent process. **166**

Figure 8. Phenotype analysis of anatomical defects suggest Rasgrp1 does not have an important circuit-based neuron function. **167**

Figure 9. Current model of ipRGC family members integrating molecular, physiology, brain circuitry, and morphology. **168**

Chapter 4: Cre mouse line for probing irradiance- and direction-encoding retinal networks

Table 1. Summary (average ± s.d.) of morphological properties of RGCs and ACs in the GCL of Rbp4-Cre mouse **236**

Figure 1. Density of Rbp4 ACs and RGCs varies across the retina **237**

Figure 2. Morphology of Rbp4-Cre-positive cells of the inner retina. **238**

Figure 3. Morphology of ACs labeled in the Rbp4-Cre mouse line. **240**

Figure 4. RACs have sustained irradiance-encoding light responses even under blockade of chemical synapses. **243**

Figure 5. RACs are tracer-coupled to M2 ipRGCs and other neurons of the GCL. **246**

Figure 6. Morphology of the R-cell — a bistratified RGC labeled in the Rbp4-Cre line. **248**

Figure 7. Rbp4 R-cells show sustained irradiance-encoding light-evoked responses. **250**

Figure 8. Serial EM reconstruction of an Rbp4 RGC and its synaptic inputs. **252**

Figure 9. A novel OFF bipolar cell, Type 0. **254**

Figure 10. Morphology of DS RGCs in the Rbp4-Cre mouse. **255**

Figure 11. Brain projections of Rbp4 RGCs, and R-cells alone **258**

CHAPTER 1: Theory and practice of classification: from organism to retinal ganglion cell

The potential of an animal to achieve its versatile behavioral repertoires critically depends on the specialization of cells making up the central nervous system and the establishment of distinct neuronal connections. Millions of years of evolution have generated a vast array of innovative sensory systems that connect organisms with their surroundings, instructs their behavior, and has the potential to provide a survival edge to a species for generations. The retina is an ideal model system for neuroscientists to study neuron diversification and function specialization. A necessary first step has required the conceptual and experimental challenges involved with classifying cell types in a way that fosters scientific communication and understanding of natural visual processing. Neuroscientists have looked to taxonomists for guidance considering their accumulated wisdom gained while attempting to classify the immense diversity of living things. The classification of organisms has a long history dating back to the Ancient Greeks and continues to improve to this day. In this introductory chapter, I first provided an overview of this history to provide context to the foundation that has been laid down for the classification of retinal neurons. Looking back on this history has provided important lessons for neuroscientists, but has also promoted some assumptions that evolutionary biologists are only recently beginning to provide innovative, albeit preliminary, solutions. I identify the source of these assumptions, when possible, during my introduction of taxonomy's history in the hopes that this will lead to a more comprehensive understanding of the best practices for modern-day retinal neuron classification. I close this portion of the introduction with an overview of devo-evo, a modern-day revolution that is occurring in evolutionary biology that is already impacting cell type classification (inspired primarily by works of (Wagner, 2014)and (Arendt et al., 2016).

PART 1: CLASSIFICATION OF ORGANISMS

1.1 Aristotle's observation-based science and classification

Aristotle, the Father of Science, was the first to attempt a classification of all kinds of living organisms according to their natural relationships, a process now called taxonomy (Moore, 1999). Aristotle recognized that animals had striking biological similarities among them, denoting the ones seemingly of the same kind as species. He grouped the types of creatures according to their similarities: those that live on land and those that live in the water; those with red blood and those without. His main contribution to classification is the realization that there are natural groups of living things based on mode of reproduction, properties and function of structure, physiology, and behavior. Aristotle considered species to be fixed and eternal. Further, he considered organisms to be objects that have two kinds of "Being": Potential (their matter) and Actual (their form) (Wagner, 2014). For example, an acorn has the potential to grow into a living oak tree, with its universal "oakness" not being affected if it loses a tree branch.

Observation-based science, as exemplified by Aristotle's studies of living things, was considered by him to be the best way to discover the fundamental principles in the natural world. Aristotle was the first to recognize the importance of empiricism, careful observation and measurements, being the starting point to successful scientific inquiry. This view dissented altogether from Plato, his tutor, who did not see the benefits of measuring anything since all knowledge could be obtained through reflection and reason. Aristotle, in contrast, promoted the revolutionary idea that knowledge could only be gathered by acquired experience, which is grounded by what was already known to be true by observed facts. Aristotle also put forth a system of reasoning called induction, which inferred beyond what is known strictly by observation. This

cognitive process of progressing from particular cases to their generalities was explained by Aristotle:

> The way of reasoning, is the same in philosophy, and in any art or science: we must collect the facts, and the things to which the facts happen, and must have as large a supply of these as possible, and then we must examine them according to the terms of our syllogisms…Induction, and Syllogism from Induction, is when we attribute one extreme term to the middle by means of the other. (cited in(Whewell, 1847)

This line of reasoning is illustrated by one of Aristotle's examples, "We find that several animals which are deficient in bile are long-lived, as man, the horse, the mule; hence we infer that *all* animals which are deficient in bile are long-lived" (cited in(Whewell, 1847). However, Aristotle's method of induction became tarnished by his refusal to limit assumptions and subjectivity from his interpretations. As William Whewell described, "his opinions rested, not upon sound inductions, gathered in each case from the phenomena by means of appropriate Ideas; but upon the loose and vague generalizations which are implied in the common use of speech" (Whewell, 1847).

1.2 Francis Bacon and objectivity in classification

A growing number of scientists and philosophers began questioning the subjectivity of perception during the seventeenth century. In the many centuries since Aristotle, a vibrant scientific exchange was fostered across Europe due to the accumulation of scientific collections and the invention of printing press promoted efficient scientific publications (Vogt, 2008). In 1620, Francis Bacon believed that Aristotle's approach needed to be modified to better reflect the realities and growing needs in scientific investigation (Alban, 1620). Bacon agreed that all

knowledge must begin with observation. His major methodological improvement came from his requirement that the description of observation should be represented as empirical facts, disconnected from preconceived ideas, conclusions, or explanations (MOORE, 1986). Further, he redesigned the induction-based philosophy of the scientific method to promote continuous advancement by incremental steps through successive gradations of generality, in contrast to leaping from special facts to loose and vague universals that was common with Aristotle (Whewell, 1847). Inspired by Bacon's work, taxonomists began excluding subjectivity related to individual observations and focused more heavily on traits that are able to provide reliable biological classification (Vogt, 2008).

1.3 The taxonomy system of Linnaeus

Classification methods became formalized by Linnaeus during the eighteenth century. For Linnaeus, like most biologists of that time, there was no philosophical problem with the incredible diversity of organisms or occurrences of common characteristics. He believed, "There are as many species as the Infinite Being produced diverse forms in the beginning" (Linné, 2010); quoted in (Wilkins, 2009). Linnaeus thought that it was his duty to discover God's handiwork in nature. Classifying the stream of new types of plants, animals, and minerals entering Europe from around the world was becoming an escalating problem for taxonomists, fueled by miscommunication and confusion. Linnaeus made the pragmatic decision to limit the required observations to a few identifiable criteria, making classification a less subjective process for taxonomists (Linné, 1751; Hacking, 2007). Further, he provided standardization for the construction of hierarchical classifications (lower classes nested within higher classes), including a clear and simple nomenclature system. This greatly facilitated information storage and retrieval, as well as opened

up communication among taxonomists. The system was flexible enough to allow rearrangements in classification organization. However, many inconsistent and contradicting classifications amassed over time and began making the classification criteria seem arbitrary (Vogt, 2008). Interest was surging for a greater understanding of dynamics underlying nature's great diversity.

1.4 Whewell philosophy of natural classification

The question of what made a classification natural or artificial was on the minds of botanists, zoologists and mineralogists in the first half of the nineteenth century. The philosopher and historian of science William Whewell recognized that the issue wasn't as straightforward as artificial systems simply being entirely arbitrary(Whewell, 1847; Winsor, 2003). Instead, natural systems needed to be able to identify and eliminate arbitrary characters from all groupings. He was generally impressed by the progress that naturalists were making in the "classificatory sciences" and their attempts to identify groups that were not artificial. He summarizes these attempts into three types: blind trial, general comparison, and subordination of characters:

> The attempts at Natural Classification are of three sorts; according as they are made by the process of *blind trial*, of *general comparison*, or of *subordination of characters*. The process of Blind Trial professes to make its classes by attention to *all* the characters, but without proceeding methodically. The process of General Comparison professes to enumerate all the characters, and forms its classes by the *majority*. Neither of these methods can really be carried into effect. The method of Subordination of Characters considers some characters as *more important* than others; and this method gives more consistent results than the others. This method, however, does not depend upon the Idea of Likeness only, but introduces the Idea of Organization or Function. (Whewell, 1847)

The Blind Trial method stems from the taxonomist pursuing a vague feeling of likeness between things as a whole and a general affinity among classes. For Linnaeus, his "natural taxonomy" system does not use traits to distinguish one plant or animal from another, but is meant to portray their "nature" defined in terms of the "symmetry of all parts." (cited in Whewell, 1847). What emerges is a unique whole represented as a general picture of interrelated parts and properties, whose differences and similarities are then compared to other such wholes. The logic of restricting his definitions to the sexual organs for plants was that, to him, these were not simply parts of the plant, but rather a representation of the final form of the plant in its entirety (Whewell, 1847). However, although Linnaeus successfully develops a very good and useful artificial taxonomy, he never reached the point of obtaining a natural classification system (Whewell, 1847). On the one hand, taking his process seriously to the fullest extent leads to an extreme splitting of species divisions considering that all characteristics of the organism are considered and that each of these become necessary and sufficient to be grouped as a species. However, the system quickly becomes arbitrary if only a subset of characteristics are used to define a species. Whewell concludes that Linnaeus does not provide justification for his classification being natural—failing in the end to provide a method that would determine the system of characters that delineates groups (Whewell, 1847). Whewell goes on to infer that these limitations come from his fixation on morphological similarities on the surface of organisms and refusal to consider the underlying causal relationships that they depend on:

> This persuasion was the result of his having refused to admit into his mind any idea more profound than that notion of resemblance of which he had made so much and such successful use; he would not attempt to unravel the ideas of symmetry and of function on

> which the clear establishment of natural relations must depend. He even despised the study of the inner organization of plants. (Whewell, 1847)

The General Comparison method is portrayed by Whewell (1847) as being a means to provide a more systematic, structured system of classification to overcome the obscure practices arising from general feelings of resemblance. Along these lines, Michel Adanson decided that basing classification studies on a few characters like sex organs is arbitrary and leads to artificial classifications (cited in Whewell, 1847). In contrast, Adanson thought that using as many characters as possible to distinguish resemblance would directly result in more natural groupings. Therefore, he examined all distinguishable parts of the plant (65 different characters), constructed a comprehensive description of each trait, and then differentiated his natural families by comparing all differences and similarities with all of the other plants. Adanson approach is innovative and he is valiant for going down such a labor-intensive route, but it suffers greatly from its epic proportions and aimless process. The work alone is prohibitive. Whewell notes that just one of the sixty-five artificial systems comprised ten classes that are further split into ninety-three sections (Whewell, 1847). By the end, there are two enduring flaws that prove fatal for this system: 1) the taxonomist can never know that all possible relevant properties of the plant are considered in the classification and 2) an incorrect assumption is made that all possible artificial systems are equally important for natural classification (Whewell, 1847). Similar to Linnaeus and the blind trial method, general comparison suffered in this case because of its reliance on "mere external and detached resemblance" and failure to take into account the relative importance of organs and their characters (Whewell, 1847). Whewell attributes whatever success Adanson's classification has to

the “dim feeling of affinity, by which he was unconsciously guided, than to the help he derived from his numerical processes” (Whewell, 1847).

Whewell (1847) recognized that general comparisons become more attainable if some resemblances are able to be considered more important than others, a logical leap he calls subordination of characters. However, this presents challenges when trying to dissociate each organ and living component in a way that their relative values can be assessed without having preconceived notions that could lead to artificial classifications:

> It is easy to see that some organs are more essential than others to the existence of an organized being; the organs of nutrition, for example, more essential than those of locomotion. But at the same time it is clear that any *arbitrary* assumption of a certain scale of relative values of different kinds of characters will lead only to an Artificial System...It is clear that this relation of importance of organs and functions must be collected by the study of the organized beings; and cannot be determined a priori, without depriving us of all right to expect a general accordance between our system and the arrangment of nature. We see, therefore, that our notion of Natural Affinity involves in it this consequence;--that it is not to be made out by an *arbitrary* subordination of characters (Whewell, 1847).

Alexander Pope expressed this dilemma another way, “Like following life through creatures you dissect, you lose it in the moment you detect.” (cited in (WAGNER, 2000). In the case of Whewell’s method subordination of characters, this problem is conceptual. The initial step of identifying the “natural” suture lines to dissect and subsequently assess the different components has the potential to create arbitrary divisions that would obfuscate the phenomena that is trying to be understood (Wagner, 2014).

The classifications discussed so far have been based on resemblances, but to get a natural classification you have to go beyond similarity of morphological traits to what Whewell calls Natural Affinity:

> The assumption that there is a Natural System, an assumption made by all philosophical botanists, implies a belief in the existence of Natural Affinity, and is carried into effect by means of principles which are involved in that Idea. (Whewell, 1847)

To find Natural Affinity, Whewell urges taxonomists to recognize the integration of living things. An organism is a multi-part system with the organs and different components having a function that works in unison with the rest. The concept of function is able to relate individual morphological traits to the whole organism, allowing further correspondence to other traits as well.

Even before Darwin, this interdependence and function-structure relationship was often attributed to fine-tuned adaptation (Wilkins, 2010), but Whewell strongly argues that it also suggests a natural affinity:

> It has sometimes been asserted that if we were to classify any of the departments of organized nature by means of one function, and then by means of another, the two classifications, if each strictly consistent with itself, would be consistent with each other. Such an assertion is perhaps more than we are entitled to make with confidence; but it shows very well what is meant by Affinity. The disposition to believe such a general identity of all partial natural classifications, shows how readily we fix upon the notion of Affinity, as a general result of the causes which determine the forms of living things. When these causes or principles, of whatever nature they are conceived to be, vary so as to modify one part of the organization of being, they also modify another: and thus the groups which

> exhibit this variation of the fundamental principles of form, are the same, whether the manifestation of the change be sought in one part or in another of the organized structure. The groups thus formed are related by Affinity; and in proportion as we find the evidence of more functions and more organs to the propriety of our groups, we are more and more satisfied that they are Natural Classes. It appears, then, that our Idea of Affinity involves the conviction of the *coincidence of natural arrangements formed on different functions*; and this, rather than the principle of the subordination of some characters to others, is the true ground of the natural method of Classification (Whewell, 1847).

Whewell's suggestion to determine natural classes by demonstrating a similarity of gradation between multiple different characters effectively disposes of assumptions that one resemblance is more important in the classification than another. Whewell creates a Maxim for testing whether the classification system is natural: "that the arrangement obtained from one set of characters coincides with the arrangement obtained from another set" (Whewell, 1847). Whewell provides the following example of Natural Affinity as applied to minerology. Minerals were classified according to external properties (such as hardness, lustre, and color) in parallel to other researchers classifying those minerals based on chemical constitution. Whewell finds that "each of these arrangements is true and natural, then, and then only, when it coincides with the other." (Whewell, 1847). In contrast, every classification of minerals that disagrees is considered to be "merely arbitrary."

For Whewell, this Maxim fulfills a valuable confirmation criteria that he calls "jumping together" or "consilience" of inductions. Whewell explains:

> "the evidence in favour of our induction is of a much higher and more forcible character when it enables us to explain and determine cases of a *kind different* from those which were contemplated in the formation of our hypothesis. The instances in which this have occurred, indeed, impress us with a conviction that the truth of our hypothesis is certain" (Whewell, 1858).

For Whewell, natural classes are formed inductively considering their Natural Affinity. Further, he thought that these natural classes are not bound by definitions, but are instead organized around an exemplary type or specimen:

> "[A natural class] is determined, not by a boundary line without, but by a central point within; not by what it strictly excludes, but by what it eminently includes; by an example, not by a precept; in short, instead of a Definition, we have a Type for our director" (Whewell, 1847).

This can also be termed the "method of exemplars" rather than adopting Whewell's label of "type method" to avoid the current improper condemnation of "typological thinking" as essentialism (Mayr, 1968; Winsor, 2003; Levit and Meister, 2006; Winsor, 2006; Wilkins, 2013). Although species were considered simple objects comparable to minerals, Whewell allowed for variation among his natural classes (Whewell, 1847). Additionally, he accommodated loose clustering of properties and allowed for the presence of individuals intermediate between groups. Whewell illustrates that "[intermediates] would not destroy the reality of the generic groups, any more than the scattered trees of the intervening plain prevent our speaking intelligibly of the distinct forests of two separate hills (Whewell, 1847)." These concepts prevent natural classes

from being associated with necessary and sufficient conditions and vindicates Whewell from his posthumous ties with essentialism.

1.5 Darwin's theory of evolution

Two conflicting ways of thinking have been battling for superiority since the dawn of evolutionary biology (Amundson, 2005; Wagner, 2014). On the one side are "functionalists," who explains traits of organisms by their functional and adaptive values. This view has come to be called adaptationism due to the belief that the functions of a trait is precisely adapted to their environment by natural selection. On the other side, "structuralists" are interested in the manifestations of "unity of type" exemplified by organisms with disparate ways of life having similarities in their morphology. Modern day structuralists attack adaptionists' belief that each character of an organism is directly selected for its adaptive value (Gould and Lewontin, 1979).

In the late eighteenth century, Charles Darwin was joining the ranks of naturalists that were aiming to "develop an all-encompassing theory of life's diversity in all its forms" (Thomson, 2009; Wagner, 2014). In parallel to Darwin's pursuits, Richard Owen was impressed by the incredible progress that chemists and mineralists were making devising the periodic table of elements and classifying minerals based on symmetry properties of their crystals, respectively (Rupke, 1994; Wagner, 2014). Wishing to describe the organization of body parts in a more formulaic way, he considered an animal's homologs to be likened to the anatomical "atoms" of the body (Wagner, 2014). His comparison of mammalian limbs revealed what he called "unity of type," in which the form and structure of the bat's wing and mole's shovel were found to have similarities despite being responsible for very different functions (flying versus digging) (Owen, 1849). These results were in conflict with the perception that function is inextricably linked to structure. Further, Owen

defined homologous characters as, “the same organ in different animals under every variety of form or function”(Owen, 1843). However, Owen’s definition was poorly equipped to explain the common occurrence of homologous characters being distributed as nested sets (hierarchies). Darwin was able to seamlessly incorporate Owen’s “structuralist” claims into his own theory of evolution by descent with modification and lineage splitting (Darwin, 1859). A bifurcating tree of descent was able to explain the hierarchical organization of homologous characters. After Darwin published the Origin of Species (1859), comparative anatomy became a popular topic and homologies (especially morphological) became prized for their potential to provide evidence for triangulating phylogenetic relationships. Homology and the unity of type were repurposed as means to trace the evolutionary history of organisms. Homologies were no longer considered for their potential to explain the causal mechanisms underlying morphological resemblances and the structuralist arguments became dormant for almost a century (Wagner, 2014).

The revelation of common descent helped naturalists understand what makes biological classification different from classification taking place in other sciences(Ghiselin et al., 2007). In the physical and chemical sciences, the natural classes are grounded on similarity of properties that do not change. Elements of the periodic table, such as gold, relates to atomic structure that is grounded by the laws of nature. All and only gold atoms will eternally contain an established number of protons that discriminate them from all of the other elements on the periodic table. Until Darwin’s theory of evolution, taxonomists and philosophers considered species to be similarly fixed and timeless, as John Ray stated, "the Works created by God at the first, and conserved to this Day in the Same State and Condition in which they were first made." (Ray, 1691; Moore et al., 2010) This was in stark contrast to Darwin’s theory of evolution, which argued that life on earth has had a much more complex history (Darwin, 1859). In an evolving world of living things,

"There is no holding nature still and looking at it" (Whitehead, 1920; Rieppel, 2009). The causal basis of biological classification is understood as "history and process" (Ghiselin et al., 2007). Although taxonomists continued to use morphological similarities between organisms as tools for their classifications schemes, the grounds of classification ultimately became common descent. Further, concepts such as Natural Affinity could still provide an indication of "naturalness," but the underlying reason for this association was common descent.

Darwin's theory of Natural Selection was less well received due to a lack of explanatory mechanism. Genetics was a newborn field of study while Darwin was writing Origin of the Species. More than 40 years passed before Mendel's work on the mode of inheritance was rediscovered. In the first half of the 20th century, genetics began providing workable models of chromosomes and genes as fundamental hereditary units and provided the theory of natural selection with much needed explanatory mechanisms. This new knowledge fostered the general sense that Darwin's original theories needed some modifications and updates. Beginning in the 1930s, multiple high-impact books and articles were published by Fisher, Dobzhansky, Mayr, Simpson, and many others, that aimed to integrate evidence for evolution from multiple fields, including genetics, paleontology, systematics, and cytology. The result was a theory of evolution that came to be known as the "Modern Synthesis". The Modern Synthesis proposed that evolution is a gradual process explained by the accumulation of small genetic changes in populations, which is regulated by natural selection on phenotypic variation over long periods of time (Mayr 1982; Futuyama 1986).

1.6 The Modern Synthesis

The packaging of the Modern Synthesis was unfortunately done using incomplete knowledge, in part because important aspects of life such as the molecular biology and biochemistry of the gene were not yet known (Rose and Oakley, 2007). This allowed population geneticists to freely extrapolate from simple models of genomes, adopting the notion that hereditary information was malleable and easily shaped by natural selection (Rose and Oakley, 2007). Further, strong natural selection was assumed to erase the evolutionary history of traits below the level of the organism. In other words, "species were the durable units of evolution while organs, genes, and cells evolved to match the functional demands placed on those species"(Rose and Oakley, 2007). The conceptualization of organisms became that of "vehicles" transporting and replicating genes (Dawkins, 1978; Wagner, 2014). The definition of homologies also became modified by Mayr, "Attributes of two organisms are homologous when they are derived from an equivalent characteristic of the common ancestor" (Mayr, 1982; Wagner, 2014). In contrast to Owen's definition ("the same organ in different animals under every variety of form and function"), the newly adopted homology definition no longer considers organs or other biological parts and "[homologous similarities] are merely the ancestral characters that happened by coincidence to survive" (Williams, 1992; Amundson, 2005; Wagner, 2014). The view that genes are exquisitely tuned to the organism's current functional requirements also manifested as the incorrect assumption that species mostly contain different sets of genes (Rose and Oakley, 2007; Wagner, 2014).

The Modern Synthesis of evolution also became limited in scope due to entire branches of biology being condemned as "typological," which Mayr wrongly treated as synonymous with essentialism (Mayr, 1968). The Modern Synthesis considered concepts like body plans to be

considered as "types," leading to their associated developmental and variational commonalities dismissed as "relevant causal factors" (Wagner, 2014). In effect, only differences revealing at the organism level were considered, excluding any tendencies for underlying different forms of genes and phenotypes. Consequently, this had the effect of excluding fields such as embryology and developmental biology from being incorporated into the Modern Synthesis. Mayr and others also propagated an 'essentialism story' that attacked opposing taxonomic methods and philosophies (Winsor, 2003; Levit and Meister, 2006; Winsor, 2006; Wilkins, 2013). As explained by Marc Ereshefsky, "Prior to the acceptance of evolutionary theory, essentialism was the standard mode of classification in biological taxonomy" (Ereshefsky, 2000; Winsor, 2003). According to the essentialism story, Linnaeus was an earnest follower of neo-Platonic and Aristolian ideals, which is a gross oversimplification of his classification system:

> Essential characters are merely diagnostic aids, and no more are thought by pre-Darwinians or post-Darwinians to be the *causes* of particular species than a cross-vein on a wing used to identify a Tetriphid fruit fly is the cause of it being the sort of animal it is. (Wilkins, 2010).

By association, taxonomists and philosophers after Linnaeus were also portrayed as propagating the ideas of Platonic types. In regards to Whewell, Mayr and Bock state,

> "The use of this pre-evolutionary concept of affinity/homology is difficult for present-day biologists to understand as it was part of the then widespread acceptance of essentialism…But prior to the acceptance of evolution no one could explain this natural affinity or knew how to determine it" (Mayr and Bock, 2002)

As discussed earlier, Whewell does not promote essentialism, but instead arrives at types through a "consilience" of inductions and in turn treats types as the anchor points for taxonomic descriptions, explicitly not being defined by a list of essential characters:

> "…the object of our study is *kinds* of things, not one of which kinds can be rigorously defined, yet all of them are sufficiently definite. In these cases we may indeed give a specific description of one of the kinds, and may call it a definition; but it is clear that such a definition does not contain the essence of the thing. …But no one would say that [the description of the Rose Tribe] was our essential conception of a rose, to be substituted for it in all cases of doubt or obscurity, by way of making our reasonings perfectly clear" (Whewell, 1840).

As Mary Winsor (2003) put it, "Whewell congratulated pre-Darwinian taxonomists for not adhering to the rigid ideal of definition used in the mathematical sciences." Owen is given a similar treatment by the designers of the Modern Synthesis and his notion of homology is summarily dismissed until more recent reappraisal has been made possible (Wagner, 2014). The causal basis for organismal similarity underlying both cases of Whewell's affinity and Owen's homology, as well as the fields of development and embryology, were all open questions prior to Darwin's publication of Origin of the Species (1859). Afterwards, the answer was provided indisputably and forcefully by common descent and the tenets of the Modern Synthesis, but that proved to only be part of the story as will be discussed later.

PART 2: CLASSIFICATION OF RETINAL GANGLION CELLS

2.1 The fundamental organization of the retina

Vision is the conduit through which we perceive the outside world. The mammalian retina extracts features from the visual world, encodes them in spike trains of specific retinal ganglion cell types (RGCs), and conveys them along the axons to visual brain centers (Figure 1). The thin size, accessibility, transparency, stereotyped organization, and origins from the brain made the vertebrate retina an ideal model system for neuroanatomical studies by the great Santiago Ramon y Cajal and generations of researchers since. The retina contains five basic neuronal classes (photoreceptors, horizontal, bipolar, amacrine, and ganglion cells) and two types of glial cell (Muller glia and astrocytes) (Figure 1B). The retina neuron cell bodies are organized in three layers. The photoreceptors exist in the outermost nuclear layer (ONL); horizontal cells, bipolar cells, and amacrine cells are distributed throughout the inner nuclear layer (INL); while the ganglion cell layer (GCL) contains nuclei of retinal ganglion cells. Light entering the eye counter-intuitively passes through the extent of the retinal tissue to reach the light-sensitive photoreceptors at the back of the retina, where it creates a photochemical reaction and hyperpolarization of the photoreceptors (Figure 1). The activation of these cells is communicated to bipolar cells in the outer plexiform layer (OPL). Bipolar cells and photoreceptors transmit light information over a wide dynamic range of intensity using graded potentials, rather than the action potentials used by most neurons (Figure 1B). These graded synaptic output signals are transferred via the release of the neurotransmitter glutamate at a special type of chemical synapse, called the ribbon synapse. Depolarization of bipolar cells leads to transfer of the light signal to retinal ganglion cell dendrites in the inner plexiform layer (IPL). Activated retinal ganglion cells will then conduct action

potentials along their axons to the brain (Figure 1B). Synaptic input with bipolar cells from the horizontal cells and amacrine cells provide further processing and filtering of the light signal through lateral inhibition in the OPL and INL, respectively. A tremendous amount of visual processing occurs between the absorption of light by photoreceptors to the ganglion cell axons that transmit the multiple channels of visual information from the retina to the brain.

2.2 The initial studies of retinal ganglion cell diversity

Cajal (1893) recognized the morphological diversity of retinal ganglion cells in the process of carefully characterizing his Golgi stained vertebrate retinas (Cajal, 1892)(Figure 2A). He was able to classify many varieties of RGCs by their overall size as well as the morphology and level of branching of their dendrites. He understood that the composition of retinal ganglion cells were similar across vertebrate retinas. These initial classification studies were extended by Polyak (1941) who provided an more extensive classification of primate RGCs (Polyak, 1941). Hartline (1938) realized that RGCs do not have a homogeneous physiological response to light and was the first to classify them based on their receptive field properties (Hartline, 1938). He presented ganglion cells with flashing spots within the center of their receptive fields and was able to categorize them as responding only to the onset of light (ON cells), offset of light (OFF cells), or to both (ON-OFF cells). In 1953, Kuffler and Barlow described the concentric receptive field organization of ON- and OFF-center RGCs such that illuminating the surround zone antagonized the response of the center zone (BARLOW, 1953; KUFFLER, 1953). All RGCs were anticipated to share a similar center-surround antagonism and operate as the lowest level of a hierarchical signal processing pathway (Hubel and Wiesel, 1962).

Fundamental differences were soon observed among retinal ganglion cells' response properties and evidence quickly accumulated for additional retinal ganglion cell diversity. Barlow determined that a type of ON-OFF retinal ganglion cell in frogs are especially sensitive to moving stimuli across its receptive field, but not at all to stationary objects. Considering that these ON-OFF cells seemed to represent a type of cell having a specific functional role, Barlow started calling these cells "fly-detectors" (BARLOW, 1953). Thus began the practice of naming a cell type by its "trigger feature," the type of stimulus that was determined to most effectively activate the cell (BARLOW, 1953; MATURANA et al., 1960; BARLOW et al., 1964). The discovery of ON-OFF ganglion cells that respond to light spots moving in certain directions across their receptive fields led Barlow to name them "directionally selective" retinal ganglion cells (BARLOW et al., 1964). Additional studies of receptive fields of rabbit ganglion cells by Barlow and Levick in the 1960s lead to the classification of many more cell types, including ON-direction selective, ON-center, OFF-center, orientation-selective, and local edge detectors (BARLOW et al., 1964; LEVICK, 1967). In parallel, Enroth-Cugell and Robson classified ON-center and OFF-center cells from cat retinas into two types based on their contrast sensitivity and response properties to sine wave gratings (Enroth-Cugell and Robson, 1966). They decided to designate them with the open-ended names X and Y (Enroth-Cugell and Robson, 1966). The other ganglion cells were found to have receptive field properties similar to those found in rabbit ganglion cells such as on-off direction selective and local edge detectors (Stone and Fabian, 1966; Stone and Hoffman, 1972; Cleland and LEVICK, 1974). These cells in the cat retina were controversially grouped together as W-cells (Stone and Fukuda, 1974). Further confusion arose when the X, Y, and W types classified primarily by their physiological responses became correlated with the morphological types that went by the name of alpha, beta, and gamma (Enroth-Cugell and Robson,

1966; Boycott and Wässle, 1974; Cleland and LEVICK, 1974; LEVICK and Thibos, 1983). Understanding this newfound retinal diversity had the potential to dramatically rework the hierarchical scheme of visual processing (Rowe, 2012). The lack of an agreed on classification methodology for studying ganglion cell diversity and the disagreement on naming strategy lead to an energetic discourse among multiple research groups (Rowe and Stone, 1977; Hughes, 1979; Rowe and Stone, 1979; Rodieck and Brening, 1983).

2.3 Application of taxonomy systems to ganglion cell classification

Tyner (1975) introduced neuroscientists to the idea that classifying neuronal populations should consider implementing the methods and concepts that have been developed by taxonomists in their classification of plants and animals (Tyner, 1975). In particular, Tyner highlighted the following best-practices: 1) classification of neuron types should be arranged hierarchically; 2) any type should be recognized based on a large number of features (not a single feature); 3) each type is not rigidly defined (may have fuzzy boundaries) with members having many, but not necessarily all features describing the type; 4) the arrangement of neuron types within the hierarchy should only be defined in operational terms, separate from descriptive features; 5) diversity and adaptive value of characters are generally beneficial to classification; and 6) classification schemes should be open to revision as new information become available. More pragmatic benefits include more efficient storage, retrieval, and communication among neuroscientists.

Rowe and Stone (1977) adapted Tyner's guiding principles to the study of retinal ganglion cells. Accordingly, they considered cell type classifications to be modifiable hypothesis of relationships between cell types that accomplish particular functions, instead of being explicit definitions. Further, the functional roles of neuron types suggested by the classification should be

defined in terms independent of the description of the neuron type. In general, Rowe and Stone first attempted to identify the signal processing operations underlying visual perception and then tried to identify cell types whose properties are well-suited for these operations. Their discussion also helped set guidelines for distinguishing between two different kinds of phenotypic variation (Rowe and Stone, 1977; 1980). The sort of variation that separates a rod cell from a ganglion cell or blue-sensitive cone from a red-sensitive cone was described as 'between-type' variation. In contrast, 'within-type' variation includes different morphology of the same cell type that correspond to a change of retina location or situations that individual neuron cell bodies reside in different layer than the others from the same type. They provided "local-edge detectors" and "sustained" as examples of classifiers improperly concentrating too much attention to a single physiology-based trait, which may introduce bias and compromise hypothesis-testing in future studies. Using the W/X/Y classification system as an example, they effectively argued that the neutral nomenclature and multi-parametric description was key to a beneficial classification that promoted open elaboration and modification in the future.

Along with the good practices promoted by taxonomists of the Modern Synthesis era, Rowe and Stone also adopted the incorrect assumption that organisms are exquisitely adapted to the needs of their environment:

> Each species plays a particular role in the ecosystem, and can be said to occupy an ecological niche within it. Analogously, groups of neurons within a neuronal system also interact with each other in order to perform certain operations. Each group of neurons contributes a particular component to the overall function of the system and can be tentatively said to occupy a functional niche within it. We would suggest that the functional

> roles played by various neurons do provide a basis for their classification into groups; and that the classification should be regarded as an hypothesis that particular groups of neurons fill particular functional niches. (Rowe and Stone, 1977)

In other words, evolution generates specialized cell types when needed, followed by selection of features that improve fitness and efficient cleansing of those that do not. The result is a notion of cell types that has morphological, physiological, and molecular properties aligned and integrated together to allow for a tight form to function correlation. The assumption that ganglion cells are fit for visual functions in a way that is perceivable by neuroscientists plays an important role in Rowe and Stone's classification system:

> Our view was that the starting point for any study of ganglion cell diversity should be the study of visual perception itself…Armed with that information, one could then identify cell groups whose descriptive features made them suitable candidates for performing particular operations. Furthermore, our view was that the labeling of such groups should be neutral (X, Y, W instead of brisk-sustained, brisk-transient, sluggish) in order to assure that the hypothesized relationships between cell groups and visual operations could accommodate new results and new ideas. (Rowe and Stone, 1977)

These presuppositions seem to be based on incomplete information adopted during the generation of the Modern Synthesis. As I will be exploring further later in this chapter, the resurgence of interest in "deep homology" in the 1980s revitalized support for Owen's earlier notion of "unity of type," in which similarity of form and structure in spite of differences in function (Wagner, 2014). The experimental evidence that has accumulated over the last thirty years suggests a much more complex, nonlinear system of ganglion cell types, with RGC types increasing from three to thirty 'functional' types over the last thirty years (see Sanes and Masland, 2015 for review). On a

more pragmatic note, despite the neutral nomenclature, the reliance on a conceptual subdivision of functional visual pathways may be dramatically different between neuroscientists and lead to irreconcilable differences of opinion towards ganglion cell classification.

Rowe and Stone (1977) also adopted Mayr's maligned interpretation of pre-Darwinian history and attacked opposing viewpoints as being "essentialistic."

> The method of classifying animals according to their 'essences', which stems from the Aristotelian and Platonic traditions, and which dominated all classificatory schemes until the 19th century, has been largely abandoned by modem taxonomists. Thus, the choice between the X/Y and sustained/transient terminologies is not simply a matter of which label to apply. Issues such as the use or avoidance of the Aristotelian concept of the 'essential nature' of a cell group are involved, as well as the ability of a scheme of classification to assimilate and adapt to new data.

They relentlessly point to Cleland and Levick (1972, 1974) as being "essentialistic" due to their contrasting views on nomenclature and classification strategy of the W/X/Y cells. I found it challenging to disentangle the incorrect presuppositions surrounding the "essentialistic" label from valid concerns about preconceived bias entering into the process of classifying ganglion cells. John Wilkins (2010) sees the essentialism label as a straw-man argument that should be disregarded:

> I consider, therefore, that essentialism is a straw-man target in biology… The requirement that classification be "theory-free" represents a now-defunct philosophy of science. It suffices that one does not use theory to support a classification that in turn is used to support the theory in a vicious circle.

Simpson (1961) suggests a more pragmatic approach, "The stablest classification is the most useful" (Simpson, 1961); cited by Mayr and Bock, 2002). Contrary to expectations, types classically named by Levick to be "local edge detectors" (LEDs) and "orientation-sensitive" continues to be used to this day (LEVICK, 1967; Cleland and LEVICK, 1974; He et al., 1998; Sanes and Masland, 2015). However, making homology statements between species remains a challenge. The W-, X-, Y-cells in the rabbit named primarily based on physiological criteria have been correlated, for the most part, with K, P, and M-cells in primate, respectively, which were named based on brain targets (Shapley and Hugh Perry, 1986; Casagrande, 1994). Controversy has occurred whether monkey midget ganglion cells are in fact homologous with cat beta ganglion cells (Kolb et al., 2001; Masland, 2004). A standardized way of naming neurons has not been agreed on, and is outside the scope of this document.

2.4 Unsupervised cluster analysis based on Whewell Maxim

Rodieck and Brening (1983) classification system for ganglion cells also prioritized being objective and strived to distinguish the 'natural cell types'. Their aim was to develop a classification system that is completely empirical. Mapping cell properties within parametric space were pursued by them to determine covariance of properties between cells that can provide empirical evidence for ganglion cell types. A 'natural cell type' was represented as a discrete cluster of individual cell measurements, with an objective reality and being distinct without intermediates in at least one dimension from every other cluster. Like Rowe and Stone (1977), they argued that neuron types are "discovered and demonstrated; they cannot be locked up by means of a definition." Any set of variables, with few exceptions, were eligible to build the multi-dimensional parametric space (Rodieck and Brening, 1983). They also did not set a limit to the

number of parameters used for clustering or have some parameters weighted more heavilty than others. They stated, “No error would occur if all of these parameters were included. This would increase the dimensionality of the parametric space, but would not create any more clusters than had only one been included” (Rodieck and Brening, 1983). They then proceeded to establish a method to distinguish whether a neuron type is ‘natural.’ Their method distinguished whether clusters form “Whewell affinities,’ which was based on Whewell’s Maxim, 'The arrangement obtained from one set of characters coincides with the arrangement obtained from another set' (Whewell, 1847). They tested this approach with ‘On-Center X’ and Off-Center X’ cells and found a ‘natural’ X type. However, classification of other groupings such as ‘W/X/Y’ was out of reach of their method.

The use of Whewell’s Maxim by Rodieck and Brening (1983) differed significantly from the process suggested in Whewell’s original descriptions. Their association of types with collections of empirically derived properties seems to align with Whewell’s suggested approach. However, they described a classification system that does not support individual intermediates and uses potentially limitless properties with no consideration of relative value or kinds of properties. These discrepancies make their method similar to the ‘general comparison’ attempt at natural classification as described by Whewell (1847) above. Therefore, Rodieck and Brening’s approach in practice likely suffers from similar issues as Adanson’s classification study, which was incredibly laborious, assumed incorrectly that all properties are equally valuable to natural classification, and can never be certain if all relevant cell properties are considered (Whewell, 1847). This approach has only been successfully applied once (Kock et al., 1989) and has not been adopted widely due to issues mentioned above: labor-intensive, open-ended implementation, and

immense amount of multidisciplinary data that is required from the same set of cells (Carcieri et al., 2003).

2.5 The immense parallel processing capabilities of diverse retinal cell types

The mature vertebrate retina encompasses morphologically and functionally distinct circuits that provide parallel processing of specific features from the complex visual scene (Figure 2B). The simplified visual pathway from photoreceptor to bipolar to ganglion cell to brain was an oversimplification. As Richard Masland (2001) stated, "The retina of 1980, containing only X and Y cells, now seems a stick figure" (Masland, 2001). Currently, there is considered to be at least 80 physiological and anatomically distinct neural cell types in the retina and more than 30 separate visual circuits sent along parallel pathways to the brain for further processing (Sanes and Masland, 2015; Baden et al., 2016). The characterization of the ganglion cells that make up these distinct circuits has been intensely studied for decades and the criteria for classifying their cell-type identity has become increasingly advanced. According to Sanes and Masland (2015), there are four main criteria that are used to classify RGCs: uniform morphology, uniform physiology, regular spacing, and similar gene expression. These criteria will be explored further below.

2.6 Comprehensive studies of physiological and anatomical criteria for ganglion cell classification

Over the last two decades, there has been multiple attempts at a complete catalogue of RGC types considering morphological and physiological criteria (Kong et al., 2005; Coombs et al., 2006; Völgyi et al., 2009; Baden et al., 2016; see Masland, 2012 for review). Kong et al., (2005) were able to describe morphological clusters that represent eleven cell types of mouse ganglion

cells. They found that deciding what constitutes an effective parameter space for cluster analysis is not a trivial decision. Some kind of parameter selection is required in order to make the cluster analysis viable because each additional parameter has the potential to generate additional variability, introduces potential error to the cluster analysis. They focused their 42 calculated parameters down to a selected three that they determined "were most likely to be effective ways to discriminate among the cells"(Kong et al., 2005). They note that:

> "Most meet Rodieck and Brening's (1983) criterion of coherent clusters. It is worth noting that this coherence would not have been true in a two-parameter sort. It is only with the addition of a third dimension that spaces between all the clusters become evident."

However, they also make explicit their finding that "excess parameters add little power but much variability and potential error to the analysis." Therefore, the limitless number of parameters for cluster analysis proposed by Rodieck and Brening (1983) does have its real-world drawbacks. More recently, at least fifteen morphological types were distinguished using unsupervised clustering together with genetic markers (Sümbül et al., 2014). In a large survey of mouse ganglion cell physiological properties, Farrow and Masland (2011) clustered ganglion cells by their light responses into twelve types. They limited their set of parameters to five for effective clustering analysis, reiterating the importance to reduce the number of parameters because the amount of required data was found to increase exponentially with each parameter added and "the concept of distance becomes less precise as the number of dimensions grows" (Beyer et al., 1999; Verleysen and François, 2005; Farrow and Masland, 2011). Unsupervised clustering considering both morphological and physiological properties has recently expanded the number of 'functional' RGC types to more than thirty in the mouse (Baden et al., 2016). How these types based on physiological

and morphological criteria correlate to the more than forty known visual brain targets of mouse RGCs remains unclear (Morin and Studholme, 2014; Dhande et al., 2015; Baden et al., 2016).

2.7 Mosaicism as an organizing principle of ganglion cell types

The organization of the retina is such that every part of an image is locally processed by parallel circuits to discriminate different properties such as color, movement, contrast, and brightness (Masland, 2001; Cook, 2003; Wässle, 2004; Baden et al., 2016). The receptive fields of particular RGC types independently 'tile' the entire retina to allow for uniform sampling of the visual scene (Wässle et al., 1981; Devries and Baylor, 1997; Rockhill et al., 2000; Ford and Feller, 2012). The tiling property of RGC types are also related to the formation of their cell bodies into 'neuronal mosaics,' repelling each other cell type so as to uniformly disperse across the retina. Mosaicism generally correlates well with other criteria such as morphology and physiology that have traditionally been used for the classification of RGCs:

> "A 'type' has come to be defined by the regular association of particular morphological, cytological, connectional, chemical, and physiological features, ...Each type, so defined, turns out to have a characteristic stoichiometry and distribution in the retinal mosaic, thus further supporting the idea that the type is fundamental." (Sterling, 1983)

These principles have helped to clarify some concepts of neuronal type classification. Similar to suggestions by Rodieck and Brening (1983), absolute soma size and the layer that the soma is residing (i.e., 'displaced' ganglion cell bodies in inner nuclear layer) is not well correlated with mosaics of ganglion cell types (Cook and Noden, 1998; Cook, 2003). Multiple RGC types have been validated by metrics associated with mosaicism, but a full inventory remains incomplete (Huberman et al., 2008b; Kim et al., 2008b; Huberman et al., 2009; Rivlin-Etzion et al., 2011).

2.8 Molecular criteria for ganglion cell classification

Distinguishing ganglion cell types by their molecular signatures has made great strides over the last two decades, but is still largely incomplete and exploratory (Dhande et al., 2015; Sanes and Masland, 2015). Only a few RGC types have been able to be distinguished based on a single gene, including the photopigment Opn4 expression in intrinsically photosensitive retinal ganglion cells (ipRGCs), the cell adhesion molecules JamB in J-RGCs, and CART (cocaine- and amphetamine-regulated transcript) distinguishes ON-OFF direction-selective RGCs (Hattar et al., 2002; Kim et al., 2008b; 2010; Kay et al., 2011). However, these are not simply single types, but have been determined to have heterogeneity. Multiple ipRGC subtypes have been revealed, with differing levels of Opn4 and no molecular signature that aligns with morphological or physiological differences (Berson et al., 2010; Ecker et al., 2010; Estevez et al., 2012; Hu et al., 2013). In the case of J-RGCs, their morphology and physiology is different depending on what region of the retina is under study (Kim et al., 2008b; Sanes and Masland, 2015). Additionally, JamB is also expressed in the outer retina and discrimination of J-RGCs would require including an additional RGC-specific marker, such as Rbpms (Daniele et al., 2007; Rodriguez et al., 2014; Sanes and Masland, 2015). Evidence is accumulating that multiple genes will generally be important for distinguishing RGC types. For example, a recent screen of transcription factor expression in the mouse retina revealed that Foxp2-expressing RGCs (F-RGCs) are further subdivided into a set of four types by the combinatorial expression of Foxp1 and members of the Pou4f1 family (Rousso et al., 2016). Morphological and physiological analysis determined that F-RGCs are two discrete pairs of ON and OFF ganglion cells—F-mini types are small-field direction-selective RGCs while F-midi types have a larger dendritic field and are not direction-

selective(Rousso et al., 2016). By current estimates, RGCs consist of more than 30 types with the majority still lacking any kind of molecular signature attributed to them (Sanes and Masland, 2015; Baden et al., 2016). Recent attempts at single-cell profiling, although successful at identifying an extensive molecular marker set for bipolar cells, has failed to account for the heterogeneity of RGC types (Macosko et al., 2015; Shekhar et al., 2016).

Transgenic mice have become valuable and widely used tools for studying neuronal cell types. In particular, "reporter mice" have been designed to express exogenous genes that encode fluorescent proteins, such as green fluorescent protein (GFP). This was first established with the "Green mouse," which expressed GFP ubiquitously in all cells by placing it under control of a constitutively active promoter (Okabe et al., 1997). Another reporter method uses the Cre/Lox system, which uses the ability of Cre recombinase to specifically recognize and delete specific DNA regions between sequences called Loxp sites (Sternberg, 1981; LAKSO et al., 1992; Kühn and Torres, 2002). The combination of Cre-expressing mice with Cre-dependent fluorescent reporters have allowed spatial and temporal control of genetic labeling subsets of neuron populations (Smith, 2011; Abe and Fujimori, 2013). Labeling by the reporter mouse is restricted to specific cell populations by inserting the cDNA of GFP, or Cre in the case of Cre/lox system, downstream of genetic regulatory elements (promoters and enhancers) that are only expressed in specific cell types. Reporter mice are generated by introducing exogeneous transgenes into the mouse genome generally by one of two methods: 1) random transgenesis into an unpredictable genomic integration site or 2) targeted transgenesis to a specific genomic locus by homologous recombination (Vacaru et al., 2014). Both methods have benefits and caveats. The latter, 'knock-in' approach, is generally faithful to anticipated gene expression pattern, but is technically more challenging and expensive. In contrast, the main limitation of random integration is that reporter

labeling may be incomplete, less restrictive, or entirely different from endogenous pattern of activity of the promoters. However, sometimes the random integration can produce a labeling pattern that does not recapitulate expected expression, but has a labeling pattern restricted in a way that still proves beneficial to the study cell subpopulations.

Reporter mice have proven invaluable for systematically linking physiological, anatomical, and molecular criteria for specific RGC types (Yonehara et al., 2008; Huberman et al., 2008b; Kim et al., 2008b; Huberman et al., 2009; Ecker et al., 2010; Kay et al., 2011; Osterhout et al., 2011; Trenholm et al., 2011; Dhande et al., 2013; Trenholm et al., 2013; Dhande et al., 2015; Sanes and Masland, 2015). In the case of ON-OFF dsRGCs, they are morphologically indistinguishable, but they can be subdivided further into four mosaics that are physiologically distinguishable as responding to stimuli motion in one of four directions: nasal, ventral, dorsal, and temporal (Oyster and BARLOW, 1967; Devries and Baylor, 1997; Borst and Euler, 2011; Vaney et al., 2012). Transgenic mouse reporters have helped resolve these four different subtypes, with reporters that have selective labeling correlating with ON-OFF dsRGCs that prefer nasal, ventral, or dorsal motion (Huberman et al., 2009; Kay et al., 2011; Rivlin-Etzion et al., 2011; Trenholm et al., 2011). Further, these reporters allowed researchers to decipher differences in the brain targets, including subtler lamination segregation, of On-Off dsRGCs (Huberman et al., 2009; Kay et al., 2011; Trenholme et al., 2011; Dhande, Estevez et al., 2013). Although reporter mice are experimentally useful as markers, some of these reporters were generated by random integration and determined to not reliably recapitulate endogenous gene expression (Haverkamp et al., 2009; Kay et al., 2011; Visser et al., 2015). Other reporters, such as PV-Cre and Pcp2-Cre, label multiple types, but still facilitates physiological and anatomical studies to narrow focus to particular RGC types (Münch et al., 2009; Farrow et al., 2013; Ivanova et al., 2013). The expression of GFP in specific RGC

types also facilitates targeted and efficient purification of labeled cells by fluorescence activated cell sorting (FACS) for system-wide gene expression profiling (Kay et al., 2011; Siegert et al., 2012).

PART 3: DEVO-EVO AND RETINAL CELL TYPE DIVERSIFICATION

3.1 Reintroduction of structuralism thinking into evolutionary biology

The Modern Synthesis portrayed different species of animals as being genetically constructed in entirely different ways over vast amounts of evolutionary time. Further, this view usually assumed that species formation prompted genes to diverge in a way that would match cells and organs to the specific functional demands of the species. Therefore, strong selective pressure was thought to essentially erase the evolutionary history of homologous genes in all but the most recent relatives. The possibility of widely shared characteristics being explained by the presence of homologous genes was rejected vigorously by Ernst Mayr in the 1960s:

> Much that has been learned about gene physiology makes it evident that the search for homologous genes is quite futile except in very close relatives. If there is only one efficient solution for a certain functional demand, very different gene complexes will come up with the same solution, no matter how different the pathway by which it is achieved. The saying, "Many roads lead to Rome" is as true in evolution as in daily affairs. (Mayr, 1963)

This fostered the view that "organisms are balls of wax in the hand of natural selection" with "no causally important structures remaining over longer periods of time" (Gould, 2002; Wagner, 2014).

The devo-evo revolution (also called Evo-Devo) in evolutionary biology was initiated by the discovery of conserved developmental genes controlling the formation and pattern of body

parts with similar function, but very different forms, in distantly related species (Wagner, 2014). It wasn't until the 1980s that some of the mysteries surrounding how dramatically disparate body forms develop among the diversity of species were solved (Gehring, 1998). Genes were presumed to play a fundamental role in evolution and development, but the actual process was left to a wide range of speculations. A key breakthrough was the discovery of homeobox (Hox) genes in the model organism, *Drosophila melanogaster*, that was determined to be important for controlling body organization during fly embryonic development (McGinnis et al., 1984; Scott and Weiner, 1984). Unexpectedly, most of these genes were discovered to have equivalent gene sequences in widely different vertebrate species as well, including frogs, birds, and mammals(Carrasco et al., 1984). These studies reawakened the possibility of homologous genes being conserved among different species for tens or hundreds of millions of years (Wagner, 2014). The concept of deep homology, dissimilar organs unexpectedly determined to be controlled by similar genes, also applied to specific complex organs such as the eye. Eyes were considered by biologists, including Ernst Mayr, to have evolved at least 40 times, correlating with the incredible diversity of light sensing organs across the animal species (Salvini-Plawen and Mayr, 1977). Surprisingly, the Pax-6 gene was determined to be important for not only development and formation of the fruit fly's compound eye, but also the "camera" eye of vertebrates, and the eyes of many other animals such as squid (Gehring, 2012).

3.2 Biological types are individuals, not classes

An important distinction between classes and individuals in evolutionary biology was made by Michael Ghiselin (Ghiselin, 1966; 1974; 1997; 2005; Ghiselin et al., 2007; Wagner, 2014). The inherent variation in biological species is now understood to be a fact of nature and the basis for

their being evolvable. No longer are species considered to operate in the realm of chemistry, in which elements such as oxygen have defining chemical properties. Ghiselin (1997) distinguishes biological species as "individuals," not classes that are considered to have defining properties. Further, individuals have parts that are spatiotemporally restricted, unlike classes that can occur anywhere and anytime. Since individuals are spatiotemporally restricted, they have definite historic beginnings and endings, continuity and change over time. Species, organisms, and cells can all be considered to have a birth, continuity over time, have a specific location in space, and a death (extinction, in the case of species; apoptosis in the case of cells). An individual is also considered to be concrete and able to engage in a process and have causal roles. In contrast, classes are abstract, their designation applying to anything with the defining properties, regardless of when and where the entity occurs in time and space. A mouse is one example of an individual, not a class: 1) it does not have a defining property; 2) it was born from another member of its species and will change dramatically over its lifetime; 3) losing its tail will not disqualify it from being the same mouse; and 4) eventually its existence will end through death. Similar concepts can be applied to organs (i.e. eyes) and cells (i.e. neurons) as individuals. Ghiselin (2005) extended this idea a step further, pointing out that homologs should also be considered as individuals instead of classes (Wagner, 2014). Ghistelin (2005) stated, "Homology is a relationship of correspondence between parts (individual homologues) of individual organisms, which are in turn parts of individual genealogical wholes." Further, homology applies to concrete parts (i.e., organs), have a beginning as a novelty, have continuity through inheritance along lineages, do not have defining properties, and come to an end when the lineages having the homologous part goes extinct.

How do biological individuals such as species or homologous organs become individualized? In the case of species, sexually reproducing organisms become individualized

species once they become reproductively isolated from other populations and therefore, form distinct lineage of descent:

> Members of a species have to have properties that are essential for these organisms and their descendants to be members of this species. Now that is not the same as forming a class, i.e. having defining properties. (Wagner, 2014)

Like species, homologous body parts exist in a lineage of descent that is distinct from other parts of the body. Further, the body part must become developmentally individualized in regards to other parts of the body for it to become a homolog (Wagner, 2014). Wagner (2014) makes an important distinction between "character identity" and "character state" to better understand the notion of homology as the "same organ in different species in every variety of shape and function."

> *Character identity* refers to that part of the organism that forms a lineage of descent with modifications (i.e., the thing that corresponds among different species like the forewing of a bee and that of a dragonfly). *Character states* are the different shapes and forms that a character can assume.

In other words, character identity and character states has a similar relationship as that found in genetics with gene identity and alleles, respectively (Wagner, 2014). Homology is regarded in terms of character identities, instead of character states. Character identity is a hypothesis, not a definition, that a body part has become individualized and was accordingly derived from the equivalent individualized body part in the most recent common ancestor. This does not, however, mean that the character identity is bound by phenotypic or genetic similarity. A body part is a beak, whether it is pouched beak of a pelican or the elongated beak of a hummingbird. Accordingly, a homolog is a body part that adopts form and/or functions that are shaped by natural selection (Wagner, 2014).

> "Homology is a reflection of the highly non-trivial manner in which developmental and genetic information is organized. Physical, descriptive distinctness is not sufficient to infer the kind of biological individuality that is necessary to recognize a part of the body as a homolog. Empirically, it is often difficult to recognize and decide upon whether two parts of the same body are individualized and, thus, should be treated as two different characters and merit distinct names."

Wagner (2014) makes sure to clarify that not every component of an animal is individualized and open to a homology statement. For example, red blood cells do not have biological individuality that would allow for comparisons even among close relatives, despite each individual cell being spatially segregated by a cell membrane. The reason is that individual red blood cells do not have a consistent difference from all other instances of red blood cells of the same type, having been generated using the same genetic program. In contrast, the individuality of hands depends on specific genetic programs throughout development and the life of the organism that leads to hands being distinct from feet and all other parts of the body.

3.3 The sister cell model and the origin of cell types

The sister cell type model proposes that the origin of cell types occurs by the splitting of multifunctional cell types into two more specialized descendent cells by the process of individuation (Arendt, 2008; Arendt et al., 2016). Initially, cells such as the epithelial muscle cells of some invertebrates play multiple functional roles of epidermal cell in combination with contracting like a muscle cell. Specialized sister cell types may arise through the gradual segregation of functions already present in the ancestral cell. In the case of epithelial muscle cells, the multifunction cell type split with some cells adopting the contractile function, while other cells

adopt epithelial functions (Mackie, 1970; Seipel et al., 2004; Arendt, 2008). Over time, the two sister cell types will form independent lineages of descent and modifications (Arendt, 2008). In contrast, divergence of function occurs when both sister cell types basically maintain their original functions initially, but the structure and functions of these cell types diverge over time. The diversification of sister cell types from an initially homogeneous ancestral cell type requires genetic individuation (Arendt et al., 2016). Genetic individuation signifies a cell type gaining evolutionary independence by having differential access to genomic information that expresses and maintains its distinct gene expression programs. This ability for an emergent cell type to express its set of genes independent from its evolutionary sister cell type requires a 'core regulatory complex' (CoRC) comprised of a unique combination of transcription factors (Arendt et al., 2016). The evolution of a new CoRC (i.e., transcription factor duplication and modifying protein-protein interactions of CoRC members) is important for ensuring regulatory independence and a stable cell type identity.

The above model of cell type identity proposed by Arendt and colleagues (2016) significantly impacts our comprehension of cell type homology. The structure of the core gene regulatory networks for individuating cell type identity may be disconnected from a particular cell phenotype:

> "There is little, if any, integration among the large number of target genes that are regulated by the core gene regulatory network. Target genes can be removed or added simply by adding or losing a cis-regulatory element that is responsive to the core transcription factor complex. This explains the fact that most morphological changes are due to mutations in cis-regulatory elements…" (Arendt et al., 2016)

Accordingly, variation in the phenotype should be allowed for a given cell type, given that cell identity is linked to its CoRC. Further, functional phenotypes can be deceptive for distinguishing cell identity:

> One has to look at more characters than just the functional phenotype to reliably recognize the identity of a cell. These other characters should preferably be gene products that are not directly related to cell function, but indicative of cell types regardless of cell function, such as the intermediate filaments and transcription factors. (Arendt et al., 2016)

Therefore, their model provides a mechanistic explanation of cell identity that emboldens Owen's (1848) original notion of homology: "[character identity] under every variety of form and function." Wagner (2014) concludes, "thinking about cell types as potential homologs forces us to look beyond or underneath the phenotypic characteristics that usually are associated with the notion of cell types."

There are multiple challenges obscuring a full understanding of how core gene regulatory networks impact cell identity (Wagner, 2014). Establishing cell identity may not be as simple as being controlled by a single core gene regulatory network. Instead, there is accumulating evidence that "the gene regulatory network state of a cell is governed not by one core network, but by a mosaic of densely interconnected network modules each of which, in isolation, might look like a core network" (Wagner, 2014). For example, gene expression studies of the hematopoetic lineage have revealed a more complex gene regulatory network than expected (Novershtern et al.2011; reference from Wagner, 2014). Hematopoiesis is a stepwise process that generates all lineages of the blood cell types (Orkin and Zon, 2008). Earlier studies suggested that hematopoiesis is controlled by a core of a small number of transcription factors that are lineage-specific and determine terminal differentiation (Iwasaki and Akashi, 2007). However, a large number of

transcription factors were recently determined to be differentially expressed across multiple lineages and controlling a dense, interconnected network of gene expression (Novershtern et al., 2011). Additionally, the evolutionary history of cell type individuation may not be strictly correlated with developmental lineage (Arendt et al., 2016; Wagner, 2014). The sister cell type model implies that emergent sister cell types arise from regulatory network changes promoting the functional specialization of terminally differentiated cells during evolution. Therefore, the sister cell type model is only meant to be applied to the study of terminally differentiated cell types (Wagner, 2014).

3.4 Origin and diversification of retinal cell types

The sister cell type model is well illustrated by the evolutionary diversification pattern of photoreceptor cell types in the retina. For more than a century, photoreceptors have been classified into two types primarily based on the morphology of membrane that incorporates photosensitive pigment molecules (Schultze, 1866). The ciliary photoreceptors are most commonly shown as the vertebrate rods and cones, with outer segments that contain discs of folded membranes. In contrast, rhabdomeric types are commonly found in invertebrates, like *Drosophila melanogaster*, and have membranous microvilli. Based on morphology, photoreceptors were assumed to evolve independently more than 40 times (Salvini-Plawen and Mayr, 1977). Recently, photoreceptors have been determined to be broadly homologous and are not independently derived photoreceptors (Arendt, 2003; 2008; Arendt et al., 2016). All photoreceptors similarly use opsins which are all demonstrated to be homologous by phylogenetic analysis. Further, they have also converged on using homologous molecular machinery upon activation of the opsin to initiate signal transduction as well as for the quenching of activated opsin. Additionally, molecular program involved in

photoreceptors differentiation share a core set of transcription factors including Pax6 (ortholog of *Drosophila eyeless*) (Arendt, 2003; 2008; Arendt et al., 2016).

Evolutionary biologists have only recently been able to determine whether ciliary and rhabdomeric photoreceptors are individualized types arising from duplications of an ancestral photoreceptor type (sister cell types), or whether they are true homologs (also called orthomorphs) that are two different character states of a strictly homologous cell type (Wagner, 2014). In-depth molecular comparisons of ciliary and rhabdomeric photoreceptors suggest that they are sister cell types (Arendt, 2003; 2008; Arendt et al., 2016). The visual pigments expressed in ciliary (c-opsins) and rhabdomeric (r-opsins) are paralogs, forming by duplication of ancient opsin and then evolving new functions (Arendt, 2003). Further, they have two different downstream phototransduction cascades—ciliary photoreceptors use a G_q-phospholipase C signalling that induces a depolarizing response to light while rhabdomeric photoreceptors use a G_t-cyclic GMP signaling that induces a hyperpolarizing response to light (Lamb, 2013). Additionally, rhabdomeric photoreceptors continue expressing Pax6, while ciliary photoreceptor differentiation requires the rx (retinal homeobox) transcription factor (Arendt, 2003). Finding animals with both cell types coexisting is an important means to distinguish whether rhabdomeric and ciliary photoreceptors are sister cell types (Wagner, 2014; Arendt et al., 2016). Indeed, the chordate amphioxus and the marine worm Platynereis are examples that have both photoreceptor types (WHITTLE and GOLDING, 1974; Arendt et al., 2004; Lacalli, 2004; Hobert, 2011). Therefore, rhabdomeric and ciliary photoreceptors are considered sister cell types by a divergence of functions—they retain the majority of cellular functions and structure, but diverge over time.

Rods and cones have been proposed to have a sister cell type relationship with bipolar cells, having derived from an ancient ciliary photoreceptor type that had photosensitive cilium combined

with axonal terminals on ganglion cells (Arendt, 2008). Through a function segregation process akin to 'division of labor,' bipolar cells retained the interneuron connection to ganglion cells (losing light-sensing capabilities), while rods and cones kept the ability to respond to light but lost synaptic connection to ganglion cells (Arendt et al., 2009). In the vertebrate retina, bipolar cells have inherited many properties similar to rods and cones including their synaptic ribbon structures, G-protein signaling cascade, and the fact that some bipolar cells have a structure (Landolt's club) like the photoreceptor inner segment (Lamb et al., 2007; Arendt, 2008). They also share similar terminal selectors (Otx2, Crx, and Rx) as well as molecular machinery of ribbon synapses. The diversification of bipolar lineage from rods and cones has been proposed to involve the selective retention of two homeobox genes, Chx10 and Vsx, in bipolar cells, that were lost in photoreceptors. The functional segregation of bipolar cells may also explain the evolution of fundamental neuronal circuits in the retina. In this scenario, the emergent bipolar cell type becomes an interneuron due to it retaining synaptic connections with retinal ganglion cells and their sister cell types rods and cones (Arendt, 2008).

The vertebrate retinal ganglion cells, amacrine cells, and horizontal cells are all derived sister cells of rhabdomeric photoreceptor precursors, despite their disparate appearances (Arendt et al., 2016). Surprisingly, a subset of retinal ganglion cells have been determined to be intrinsically photosensitive (ipRGCs) (Berson et al., 2002). Further, ipRGCs respond to light using the photopigment melanopsin, a homolog of r-opsin, and a photoransduction cascade involving G_q-PLC that is also reminiscent of rhabdomeric photoreceptors (Arendt, 2003; Isoldi et al., 2005; Koyanagi et al., 2005; Plachetzki et al., 2010). Further, they express the transcription factor Pax6, which is also distinctive of rhabdomeric cells (Arendt et al., 2003). Therefore, vertebrate ipRGCs are likely descendants and true homologs of rhabdomeric photoreceptors, which have since

evolved a specialized role in non-visual functions, such as circadian photoentrainment and pupillary light reflex (Arendt et al., 2008; Arendt et al., 2016). Amacrine and ganglion cells inherited expression of atonal homologs, Math1 and Math3, and are considered more closely related to eachother than to horizontal cells (Arendt et al., 2003). In summary, vertebrate rods, cone, and bipolar cells originated from an ancient ciliary photoreceptor cell, while the ganglion cells, amacrine cells, and horizontal cells are ancestors of rhabdomeric photorepector cells. Molecular fingerprinting combined with anatomical and functional properties have been used to disentangle sister cell type relationships in the evolution of the vertebrate retina cell diversification.

PART 4: SUMMARY

1. Incorporating taxonomy best practices helped to provide a framework for careful, unbiased, multiparametric, and useful classification system of ganglion cell types. Contaminating negative aspects such as unproductive accusations of "essentialism" and considerations for neurons being ideally fit for visual functions has become dispensed with over time with dramatic increase in multi-disciplinary knowledge of RGC types.
2. There are four main criteria that are used to classify RGCs: uniform morphology, uniform physiology, regular spacing, and similar gene expression (Sanes and Masland, 2015).
3. Morphological and physiological criteria continue to provide the most complete characterization of retinal ganglion cell types. Mosaicism revealed by morphological studies is a powerful test to validate natural subdivision of RGC types.
4. Brain targets have become loosely associated with RGC types, but remain a challenge to conclusively correlate with a given type or set of types.

5. Molecular information remains to be the most incomplete criteria for distinguishing RGC types and is poorly understood in relation to the other criteria. Further, gene and protein expression are primarily used as means to "mark" or provide a "reporter system" for enabling further study of other criteria such as morphology or physiology.
6. The comparison of multiple, different types of criteria is proving to be the most informative for retinal neuron classification (allows for Whewell's 'consilience of inductions').
7. The devo-evo revolution reinstated Owen's homology definition of "[character identity] under every variety of form and function." Evolutionary biology notions such as common descent and natural selection still remain critically important, but it is in a more balanced perspective of underlying structure and causal mechanisms that may not allow for a precise fit of form to function. This has important clarifications for cell type studies.
8. Biological species and cell types should be considered as "individuals," not classes that are considered to have defining properties.
9. *Character identity* refers to that part of the organism that forms a lineage of descent with modifications (i.e., the thing that corresponds among different species like the forewing of a bee and that of a dragonfly). *Character states* are the different shapes and forms that a character can assume.
10. Cell types are the lowest level of biological organization that character identity can be considered. A 'core regulatory complex' (CoRC) is considered important for ensuring regulatory independence (individuation) and a stable cell type identity. Target genes of CoRC are more easily changed (by altering regulatory sequence) and accounts for relative disconnect between cell identity and other phenotypic characteristics like morphology.

11. The origin and diversification of retinal cell types occurs at least in part by the sister cell type model.
12. Many challenges remain for distinguishing cell identity of ganglion cell types. Of particular interest is strong possibility that mammalian neuron identity is controlled by not a single CoRC, but multiple that are overlapping. For example, certain properties of retinal neurons such as mosaicism may be controlled by one CoRC, while another property such as visual brain targets may be controlled by another. More challenging will be the anticipated cases that not all properties are strictly individualized of a given cell type, therefore allowing broad variation in one or a number of properties. This will be especially confounding if there is incredible variation in properties normally used for designating cell type classification such as morphology.
13. The next frontier in understanding the diversity and classification of RGC types continues to be the integration of terminal differentiation program (requiring CoRCs) with the cell type phenotype distinguishable by anatomical, circuitry, and physiological criteria.

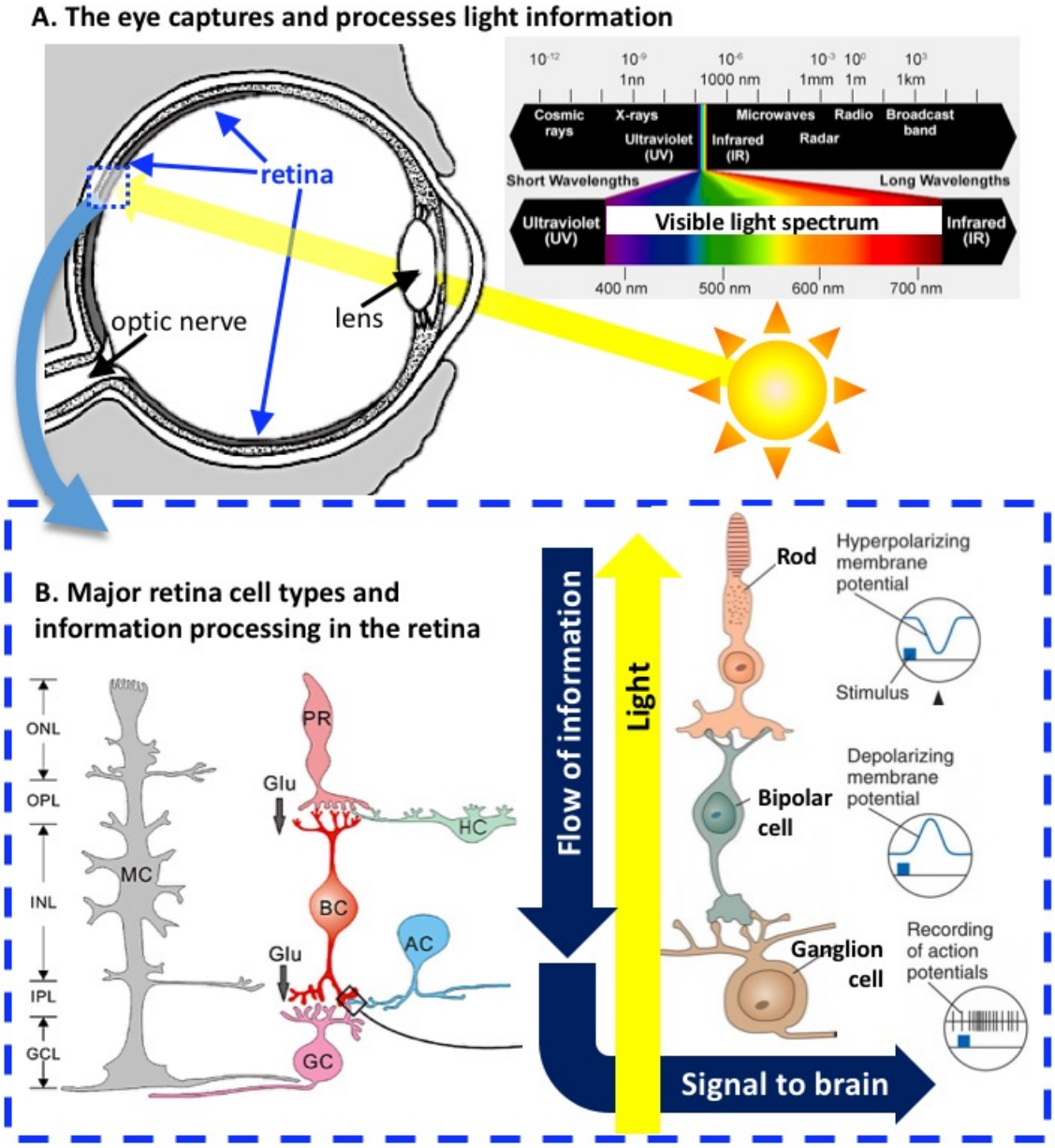

Figure 1. A) The visible spectrum corresponds to the entire electromagnetic spectrum. Light enters the eye and is focused by the lens onto a thin layer of neural tissue called the retina. **B)** The retina has a complex, stereotyped organization of neurons and glia that processes light information and transmits that information to the brain. Light is captured primarily by photoreceptors (PR), which communicate with bipolar cells (BC) and horizontal cells (HC). Then, bipolar cells form synapses with amacrine cells (AC) and retinal ganglion cells (GC), the sole output neuron the retina. ONL = Outer nuclear lear, OPL = outer plexiform layer, INL = inner nuclear layer, IPL = inner plexiform layer, GCL = ganglion cell layer, Glu = Glutamate

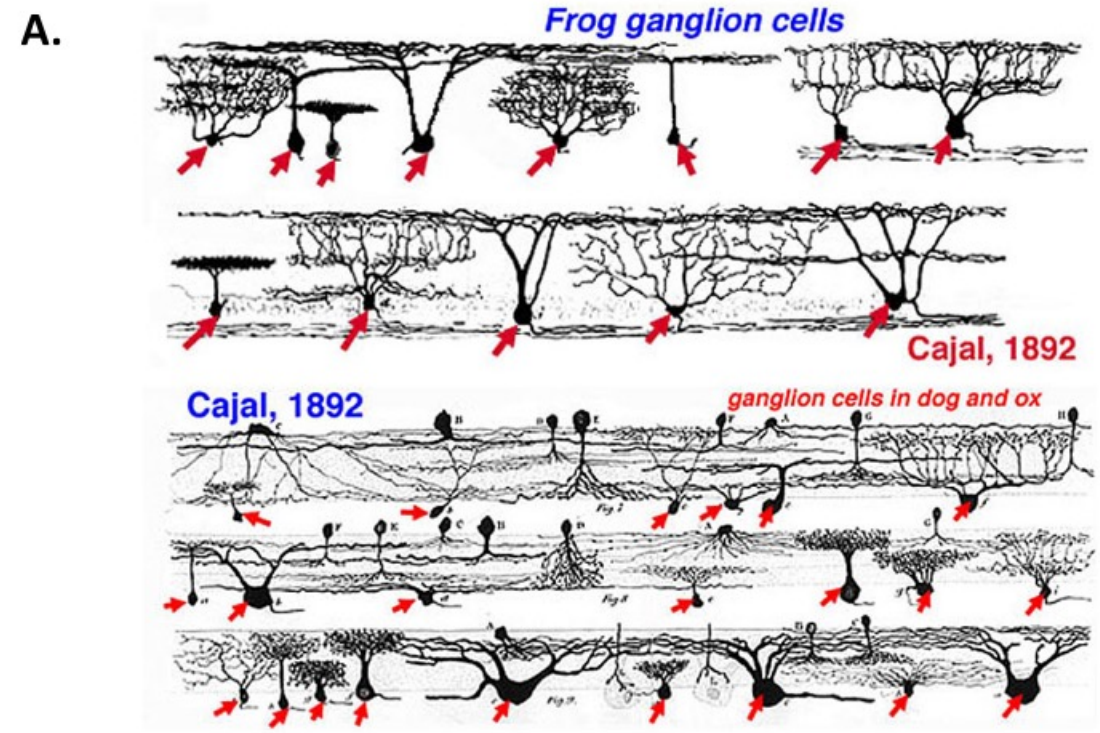

Figure 2. A) Cajal's drawings of morphologically diverse ganglion cells from Golgi stained vertebrate retinas. **B)** Extraordinary neuronal specialization in the form of diversity is present in the retina and throughout the parallel processing of information in the central brain.

Chapter 2:

Assembling a molecular parts list for intrinsically photosensitive retinal ganglion cells (ipRGCs)

Research was designed by DJ Berg and DM Berson.

Experiments were conducted, analyzed, and reported by DJ Berg.

Vision is the primary sense that most mammals, including humans and mice, use to evaluate the external environment and prompt behavior that is important for their survival. Mammalian eyes provides two functionally distinct visual pathways: image forming and non-image forming vision. Image-forming vision mediates conscious vision, involving the formation of detailed images (includes color and spatial light-dependent information) and the tracking of moving objects. In contrast, non-image forming (NIF) vision detects the ambient light intensity (irradiance) for the regulation of behavioral and physiological functions, including the entrainment of an animal's internal body clock to the environmental light-dark cycle (circadian photoentrainment) and the pupillary light reflex. Circadian rhythms are biological rhythms in physiology and behavior that are synchronized to the 24-hour light-dark cycle linked to the rotation of Earth around its axis. Most animals have adapted their circadian rhythms to best account for predictable environmental factors (i.e., gather food and avoid predators) and confine their activities to certain times during the day and night. Diurnal animals, such as humans, are most active during the day, while nocturnal animals such as mice, are most active at night. In mammals, circadian rhythms are coordinated by an internal 'clock' located in the hypothalamus called the suprachiasmatic nucleus (SCN). Light 'photoentrains' the circadian clock in the SCN, keeping an animal's biological rhythms synchronized to environmental time. A direct connection between the retina and SCN via the retinohypothalamic tract enables circadian photoentrainment. Photic input from the eye is essential for circadian photoentrainment, as demonstrated by the failure of mice to synchronize their sleep-wake cycle to a 24-hour pattern of light-dark after eye removal. The pupillary light reflex (PLR), another component of the NIF visual system, is a reflex that regulates the pupil's diameter in relation to the intensity of light reaching the retina, thereby adjusting the intensity of light that enters the eye.

Our third type of photoreceptor proves to be a needle in a haystack

The classical photoreceptors, rods and cones, transform light energy into an electrical signal and convey information for both image- and non-image-forming visual functions through RGCs. Rods and cones were thought for decades to be the only photoreceptors in the retina. In the 1920s, Clyde Keeler fortuitously stumbled on a genetic mutation in mice that manifested as a dramatic loss of rod and cone photoreceptors in the outer retina(Keeler, 1927). Without these light sensing cells, the mice were essentially blind. Being a careful scientist, Keeler followed up these initial studies with further behavioral testing and surprisingly found that the blind mice's pupil's shrank in response to light! This was completely paradoxical considering that the only known photoreceptors in the eye were ultimately destroyed by this genetic mutation. There remained many questions about how the brain was receiving this mysterious light signal or whether it was due to incomplete loss of photoreceptors, but no clear answers were revealed for decades. Keeler's original "blind" mice were not maintained and were lost to history. However, more than 50 years later, Ebihara and Tsuji (1980) rediscovered the phenomenon of persistent behavioral light responses in retinal degeneration mouse model (*rd*, now called *rd1*)with an extensive loss of classical photoreceptors (Ebihara and Tsuji, 1980). In particular, they determined that *rd1* mice were still able to entrain their circadian locomotor activity to the day-night cycle. In the 1990s, Russell Foster and colleagues expanded upon the work with retinal degeneration mouse models by, in part, genetically ablating photoreceptors using transgenic mice lacking cone cells crossed with *rd1* mice that had degenerative rods (Foster et al., 1991; Freedman et al., 1999; Lucas et al., 1999). These 'rodless/coneless' mice still maintained normal circadian photoentrainment (Freedman et al., 1999; Lucas et al., 1999). Importantly, eye removal completely eliminated

photoentrainment, demonstrating that a photoreceptive cell remained intact within the eyes of animals having complete degeneration of the classic photoreceptors in the outer retina (Nelson and Zucker, 1981; Laemle and Ottenweller, 1998; Sexton et al., 2012). Foster and colleagues also replicated Keeler's earlier work; demonstrating that retinal degeneration models of classic photoreceptors still retained normal pupillary light reflex (Lucas et al., 2001). The mounting pile of evidence for a third photoreceptor lead to an intense hunt to try to identify this alternate means of light sensing.

Discovery of the specialized intrinsically photosensitive retinal ganglion cell (ipRGCs)

A combination of studies finally established the presence of an inner retina photoreceptor (Figure 1a). Ignacio Provencio (2000) revealed the sparse expression of a novel light-sensitive protein melanopsin (also known as Opn4) in the ganglion cell layer of mammalian retina (Provencio et al., 2000). In 2002, my PhD advisor David Berson and his group here at Brown University joined the hunt by using a retrograde axonal tracing technique to fluorescently label the RGCs that make specific, direct connections to the brain's circadian pacemaker, the suprachiasmatic nucleus (SCN) of the hypothalamus(Berson et al., 2002). Follow-up electrophysiological recording made the important discovery that these SCN-projecting RGCs generated strong, prolonged electrical responses to light, even when pharmacologically blocking all synaptic input from classic rod and cone photoreceptors and physically isolated from the retina circuit. The unique capacity of these RGCs to respond to light independent of rods and cones lead Berson to name them intrinsically photosensitive retinal ganglion cells (ipRGCs). In parallel, Samer Hattar and colleagues engineered transgenic mice to label the axons of ipRGCs for studying central brain targets (Hattar et al., 2002). They determined that ipRGCs project their axons to

multiple non-visual centers of the brain beyond the SCN; including the olivary pretectal nucleus essential for regulating the reflexive pupillary light response and the intergeniculate leaflet (IGL) of the geniculate nucleus that has modulatory roles in circadian rhythm behavior. Furthermore, they clarified that the Opn4-expressing ipRGCs are exceedingly rare (2.5% of rat RGCs; 1% of mouse RGCs). The Opn4-expressing ipRGCs have since been identified to play important roles in non-image forming behavior in many mammalian species including mice, rats, 'blind' naked mole rats, cats, and primates (Hannibal et al., 2002b).

Intensive studies of the originally described "M1 type" of ipRGCs over the last 15 years has revealed many special attributes that distinguishes them from traditional RGCs. M1 ipRGCs express high levels of the blue-light sensitive photopigment melanopsin (Opn4) and, as their name suggests, can directly respond to light without the need for rod or cone input. Although ipRGCs have Opn4-mediated light responses, they also receive synaptic input from rod- and cone-driven circuits like other RGCs (Dacey et al., 2005; Perez-Leon et al., 2006; Wong et al., 2007a; Wong, 2012; Weng et al., 2013; Zhao et al., 2014). A defining feature of the M1-type is their stereotypical, sparse dendrites stratifying in the outermost margin of the canonical "OFF-sublamina" of the inner plexiform layer (IPL) (Baver et al., 2008; Berson et al., 2010). Defying expectations, M1 ipRGCs paradoxically receive sustained ON physiological input via *en passant* synapses with the ON bipolar pathway(Dumitrescu et al., 2009). The repertoire of specialized M1 ipRGCs retinal circuitry also includes reciprocal intraretinal interactions with dopaminergic amacrine cells (Zhang et al., 2008; Xue et al., 2011). Both the intrinsic and the extrinsic photoresponses of M1 ipRGCs are remarkably tonic, consistent with their role in long-term irradiance coding (Wong, 2012). This behaviorally-relevant light information is sent along the axons of M1 ipRGCs to the hypothalamic circadian clock for the photoentrainment of circadian rhythms, to a midbrain nucleus that drives

pupillary constriction, and to many other NIF brain regions. Additionally, M1 ipRGCs also have demonstrated a remarkable survival ability in experimental models such as intraocular hypertension, optic nerve injury, glutamate-induced excitotoxicity, and glaucoma(Cui et al., 2015).

Phototransduction capabilities of ipRGCs

The expression of Opn4 photopigment in ipRGCs endows them with their defining properties as a light-sensing projection neuron (Figure 1b). The Opn4 phototransduction cascade is mediated by members of the Gq/11 family of G proteins and the signalling enzyme phospholipase C-β4 (PLCβ4) (Graham et al., 2008; Xue et al., 2011). Furthermore, light leads to depolarization and action potentials in ipRGCs through a Gq-mediated signaling cascade via opening of the heteromeric transient receptor potential (TRP) channels TRPC6 and TRPC7 (Melyan et al., 2005; Panda et al., 2005; Qiu et al., 2005; Peirson and Foster, 2006; Graham et al., 2008; Perez Leighton et al., 2011). The relatively low levels of melanopsin expression in ipRGCs (1/10,000 of rhodopsin density in rods) leads to light responses that have slower onset, are less sensitive, and more sustained than that found in rods and cones (Tu et al., 2005; Do et al., 2009).

The Opn4 photopigment and phototransduction machinery of ipRGCs more closely resembles that found in invertebrate rhabdomeric photoreceptors than ciliary photoreceptors such as mammalian rods and cones (Panda et al., 2003; Baver et al., 2008; Hankins et al., 2008). The mechanism of chromophore regeneration is another major difference between ciliary and rhapdomeric opsins. Rods and cones require regeneration of chromophore in a second cell type, the retinal pigment epithelium (RPE), which supplies retinal and vitamin A required for their photoreceptors' response to light photons. The RPE also contains the enzymatic machinery required to recycle used all-trans retinal to the operational 11-cis-retinal(Palczewski, 2006). In

contrast, ipRGCs are physically remote from the RPE and use a different mechanism similar to *Drosophila* opsins for photopigment formation and regeneration(Tu et al., 2005; Sexton et al., 2012). The melanopsin photopigment has been demonstrated to be bistable in ipRGCs and chromophore regeneration is an intrinsic capability(Melyan et al., 2005; Panda et al., 2005). However, there has been additional evidence that contacting Muller glial cells may provide parallel chromophore regeneration cycles, but we have yet to identify the molecular enzymatic machinery which is involved (Walker et al., 2008; Sexton et al., 2012).

Multiple ipRGC types beyond original M1 type

Until recently, the majority of research on ipRGCs has focused on the initially identified subtype (M1) and thought to comprise a relatively uniform population of RGCs that detect light levels and simply act as irradiance detectors (Berson et al., 2002; Hattar et al., 2002; Panda et al., 2002; Hannibal et al., 2002a; Hatori et al., 2008). Sophisticated morphological studies using a highly sensitive melanopsin antibody and mouse transgenics have recently uncovered a diverse assortment of five ipRGCs subtypes that differ in morphology, physiology and projections (Figure 2)(Berson et al., 2010; Ecker et al., 2010). The majority of retinal ganglion cells send their dendrites to stratify in either the outer sublamina of the inner plexiform layer (IPL) or the inner sublamina. The initially discovered ipRGC subtype M1 stratifies within the outer OFF sublamina, but predominately receives ON-input due to extraordinary “en passant” synaptic input from ON bipolar cell axons(Dumitrescu et al., 2009; Pickard et al., 2009; Schmidt and Kofuji, 2010; GRÜNERT et al., 2011). Additional morphological diversity in the ipRGC population was revealed using enhanced melanopsin immunohistochemistry and a Cre-based melanopsin reporter mouse system, which revealed at least five subtypes of ipRGCs (M1-M5) (Berson et al., 2010;

Ecker et al., 2010) (Figure 2).

The ipRGCs are now considered to consist of at least six anatomically distinct retinal subtypes, termed M1-M6 ipRGCs (Figure 2). The ipRGC family members are classified primarily by the differing levels of melanopsin expression and the morphology of their dendrites. The M2-type ipRGCs have complex dendritic fields that stratify exclusively in the ON sublamina of the IPL, while M3-types have a bistratified morphology with dendrites present in both the ON and OFF layers (Viney et al., 2007; Schmidt and Kofuji, 2009; Berson et al., 2010). Both M2 and M3 express significantly lower levels of melanopsin compared with M1-type ipRGCs (Berson et al., 2010; Schmidt and Kofuji, 2010). The M4 and M5 cells are monostratified with the ON layer of the IPL and are distinguished from M2 by their unique morphology (Ecker et al., 2010; Estevez et al., 2012). M4 cells have much larger somas and dendritic fields while M5 cells have small, highly branched dendritic arbors and small somas (Ecker et al., 2010; Estevez et al., 2012). The M6-type of ipRGCs have recently been differentiated from other ipRGC subtypes on the basis of its unusually highly branched bistratified arbor (Quattrochi et al., in preparation).

The physiological properties of the distinct ipRGC morphological subtypes were first tested when researchers recombineered a bacterial artificial chromosome (BAC) to label ipRGCs with enhanced GFP (eGFP) (Schmidt and Kofuji, 2010). The endogenous nature of the BAC derived melanopsin promoter representatively labels the M1, M2, and M3 ipRGC subtypes, with the remaining subtypes being undetectable (Hattar et al., 2006; Viney et al., 2007; Baver et al., 2008; Schmidt et al., 2008; Schmidt and Kofuji, 2009). The more recently discovered M2–M6 cells are capable of weaker intrinsic photoresponses than M1 cells, correlating with lower level of melanopsin (Schmidt and Kofuji, 2009). Synaptic input is more important for shaping the activity of M2-M6 ipRGCs than it is for M1 cells. The entire ipRGC family receive predominantly

sustained ON-input. The ON pathway influences to the bistratified M3 and M6 cells are presumably due to the OFF-stratifying dendrites receiving *en passant* synapses from ON bipolar cells, similar to that observed with M1 cells. Therefore, the entire ipRGC family is able to integrate their extrinsic and intrinsic light responses to provide long-term irradiance coding, despite their morphological and physiological diversity.

The M1-M6 ipRGC subtypes innervate multiple central brain targets, and participate in diverse visual functions (Figure 2c). The SCN receives projections primarily from M1 ipRGCs, but also a minor input from the M2 subtype(Viney et al., 2007; Baver et al., 2008). The ipRGCs project to distinct regions of the OPN; with M1 innervating the OPN shell, the critical relay station controlling the pupilary light response, and M2 axons arriving to the core of the OPN (Prichard et al., 2002; Baver et al., 2008; Güler et al., 2008); personal communication L. Quattrochi). The OPN also receives significant input from the recently described M6 ipRGCs (Figure 2) (Osterhout et al., 2011; 2014); Quattrochi et al., manuscript in preparation). Unexpectedly, M2-M4 ipRGCs have recently been shown to send projections to image-forming brain regions and to mediate coarse pattern vision (Ecker et al., 2010). Although it may be tempting to infer that different ipRGC subtypes mediate specialized visual functions on the basis of their anatomical projections, the roles performed by specific types of ipRGC remain largely undetermined.

The establishment of diversity within the retina

The immense diversity of neural cell types and connections arises from a layer of stem cells residing in the neural plate of the early embryo (Chow and Lang, 2003; Andreazzoli, 2009) (Figure 3). These stem cells create complex patterns of transcription to give rise to the panoply of newborn neurons and glial cells which progress through precise stepwise differentiation programs

to eventually generate the tremendous cellular diversity of the mature mammalian central nervous system. The vertebrate retina and spinal cord have proven to be invaluable model systems for defining the fate determination genes and transcription factors that mediate neurogenesis and neural circuit development (Cepko, 1999; Jessell, 2000; Dasen, 2009). A variety of transcription factors contribute to the specification and maturation of the early eye-field (Figure 3a) (Matsushima et al., 2011; Bassett and Wallace, 2012). Progenitor cells differentiate to express complex and distinct patterns of transcription factors(Reese, 2011). These cells continue to progress through precise stepwise differentiation programs to generate the tremendous cellular diversity of the mature central nervous system(Livesey and Cepko, 2001; Reese, 2011).

The main cell types that make up highly specialized retinal tissue are generated in an invariant order during embryonic neurogenesis; beginning with retinal ganglion cells, followed by cone photoreceptors, horizontal cells, and amacrine cells, and finishing with bipolar neurons, rod photoreceptors, and Muller glia (Young, 1985; Cepko et al., 1996). Transcription factors that drive the gene expression underlying cell differentiation also feed back negatively on genes that support pluripotency, thereby stabilizing the newly acquired state of differentiation (Mao et al., 2011). As the sole output neurons and the first neuronal lineage to differentiate from pluripotent progenitors in the developing retina and migrate to their target layer, it is no surprise that RGCs possess unique developmental features. Post-mitotic mouse RGCs can first be seen migrating to the appropriate position in the future ganglion cell layer (GCL) by embryonic day 11.5 (E11.5)(Young, 1985). A hierarchical cascade of a variety of transcription factors, including those of the basic helix-loop-helix and T-box families, is essential for proper RGC fate specification and terminal differentiation (Figure 1b) (Mu and Klein, 2004; Cayouette et al., 2006; Trimarchi et al., 2008). The sequential expression of the transcription factors Math5 (also called Atoh7), Brn3b (Pou4f2), and Tbr2

(Eomes) are essential for the majority of RGC differentiation, cell survival, neurite outgrowth, and axon pathfinding (Figure 3a) (Gan et al., 1996; Wang et al., 2001). Brn3b is one of the earliest markers of RGC differentiation and is expressed by E13.5 in newborn RGCs populating the GCL (Gan et al., 1996). Subsequent to Brn3b expression, Math5 becomes downregulated in those cells fated to become ganglion cells. At E14.5, Brn3b in turn drives expression of Tbr2 in differentiating RGCs and Tbr2 protein expression increases thereafter as they migrate to the GCL and undergo terminal differentiation, with a subset of cells coexpressing Brn3b. Tbr2 is necessary for orchestrating the general molecular program controlling axon outgrowth and myelination, which is important for proper optic nerve development (Mao et al., 2008). By the time the mouse is born, the projections from the majority of ganglion cells have already reached their central brain targets (McNeill et al., 2011). Further development of the retinal circuits and refinement of the retinofugal synapses occur to the extent that the visual system is essentially complete by the time the animal opens its eyes two weeks after birth (Huberman et al., 2008a; Ford and Feller, 2012).

Little is known for how the general embryonic developmental program leading to the terminal differentiation and stable maintenance of the more than 30 types of retinal ganglion cells in adulthood. Complex and yet poorly characterized combinations of transcription factors are certainly critical for co-regulating the different cell-specific gene expression underlying the specialized function of ipRGC types. Most melanopsin-containing ipRGCs are born between E11 and E15, similar to other RGCs (Drager, 1985; Rachel et al., 2002; Farah and Easter, 2005). However, some ipRGCs have recently been shown to follow a relatively delayed developmental time course, with ipRGC neurogenesis continuing beyond that of other RGCs (McNeill et al., 2011). These cells are born after Math5 is downregulated at E16, which suggests that some ipRGCs are specified independently of Math5 (Brown et al., 1998). Further, the innervation of the SCN

and OPN by M1 ipRGCs begins postnatally, unlike most RGCs, which innervate their image-forming targets during embryogenesis (Fox and Guido, 2011; McNeill et al., 2011) (Figure 3b). Additionally, although the Tbr2 transcription factor is required in early cell fate specification of embryonic RGCs, Tbr2 expression later becomes restricted and selectively expressed in adult ipRGCs (Mao et al., 2014; Sweeney et al., 2014).

Until recently, the majority of research on ipRGCs has focused on the initially identified subtype (M1), which is thought to comprise a relatively uniform population of RGCs that act as irradiance detectors (Berson et al., 2002; Hattar et al., 2002; Panda et al., 2002; Hannibal et al., 2002b; Hatori et al., 2008). Molecularly distinct developmental programs have discriminated between two distinct subpopulations of M1 ipRGCs, which are otherwise morphologically and physiologically homogeneous (Chen et al., 2011). The Brn3b transcription factor is not expressed in M1 ipRGCs that innervate the SCN, but it is expressed in M1 ipRGCs projecting to other non-image forming brain targets such as the OPN (Chen et al., 2011). Consistent with this innervation pattern, mice in which Brn3b-positive ipRGCs have been ablated demonstrate a severely impaired PLR, but have intact circadian photoentrainment (Chen et al., 2011). The case of Brn3b suggests further diversity of ipRGC types at the molecular level, but there are certainly additional molecular features important for the unique circuitry, physiology, and visual functions of ipRGCs. To date, there still remains an intellectual chasm between the well-described hierarchies of events that initially generate ganglion cells and how they become diversified into the more than 30 functionally distinct types distinguishable in adulthood (Figure 1).

The molecular adhesion code important for M1 ipRGC circuit development has started to become deciphered. The repertoire of specialized M1 ipRGCs retinal circuitry includes reciprocal intraretinal interactions with dopaminergic amacrine cells (DACs) in the uppermost sublaminas of

the IPL (Van Hook et al., 2012; Vuong et al., 2015; Prigge et al., 2016). DACs express the Sema6a receptor PlxnA4 (Matsuoka et al., 2011). Expression of Sema6a in the On layers of the IPL repulses Plxna4-expressing DAC dendrites and restricts their dendrites to the S1 sublamina of the IPL (Matsuoka et al., 2011). M1 ipRGCs were unexpectedly determined to not express either Sema6a or PlexinA4, but their dendritic architecture still becomes mislocalized when either gene is knocked out (Matsuoka et al., 2011). Therefore, these two cues are important for M1 ipRGCs synapse specificity, but are suggested to play important non-autonomous roles in ipRGC dendritic development (Figure 3c).

We lack essential knowledge of what gene regulatory programs are required throughout the lifespan of ipRGCs to maintain the specialized molecular identity, circuitry, and physiology required for a lifetime of normal neural function. Despite realizing melanopsin's vital role as a regulator of physiology and behavior in animals, effectively nothing is known about the molecular program regulating the dynamic melanopsin expression through embryonic birth to adult life of an ipRGC, but may require *Pax6* (Panda et al., 2002; Ruby et al., 2002; Sakamoto et al., 2004; Mathes et al., 2007; Chen et al., 2010). Attempts to decipher transcription factor binding motifs along the melanopsin promoter have failed to identify important regulatory elements (Sheely, 2011). Besides melanopsin, ipRGCs exclusively express pituitary adenylate cyclase–activating polypeptide (PACAP), which acts as a neurotransmitter to SCN target neurons (Hannibal et al., 2002a; Bergström et al., 2003; Fahrenkrug et al., 2004). There are undoubtedly many more synaptic proteins expressed by ipRGC subtypes that underlie their specialized communication between their set of pre- and post-synaptic circuit partners. A full understanding of the transcriptional program and specific genes connected to ipRGC subtype-specific neuronal function, morphology, and connectivity has remained out of reach.

ipRGCs are the first-born photoreceptors

The ipRGCs are photosensitive at birth in mice, making them the first functional retinal photoreceptors(Johnson et al., 2010). In newborn mice, even before eye opening, they drive light avoidance and play a role in patterning retinal blood vessels (Sekaran et al., 2005; Johnson et al., 2010; McNeill et al., 2011). The functioning of adult neural networks requires the creation of precise patterns of network formation during development. Spontaneous waves of depolarization sweep across the early postnatal mouse retina triggering correlated firing of neighboring RGCs. By the first postnatal week, RGC axons are already establishing and refining projections to the visual centers of the brain and depolarizing waves play a critical role in this process. This activity-dependent developmental program does not require light, since it takes place well before eye opening at P12 and before rod and cone photoreceptors are mature enough to drive light responses(Ford, 2011). Retinal waves are driven by a network of cholinergic starburst amacrine cells (SACs), which generate and propagate retinal waves through the release of acetylcholine onto both ganglion cells and other SACs (Ford, 2011). Light input through ipRGCs phototransduction has recently been shown to modulate retinal waves and enhances the segregation of retinogeniculate afferents (Renna et al., 2011). This is potentially due to unusual ipRGC intraretinal connections, known to exist in adulthood, which feed back onto dopaminergic amacrine cells (Zhang et al., 2008). Interestingly, the cholinergic starburst connections mediating retinal waves are eliminated by P9(Ford, 2011). This transition may partly reflect the maturation of GABAergic synapses, which switch polarity from excitatory to inhibitory. However, starburst cells also become insensitive to acetylcholine, thus reducing the mutual excitation among SACs that support the waves(Zhou, 1998). Changes in SAC-to-RGC signaling may contribute to the

fading of the waves. Retinal waves activate most, if not all ganglion cells, including ipRGCs(Renna et al., 2011). Currently, the evidence that the excitation of ganglion cells is mediated by ACh released from the starburst network and acting directly on nicotinic receptors on RGCs is relatively weak. This question thus needs to be examined more carefully, especially in ipRGCs because, at least in adulthood, ipRGCs appears to lack functional nAChRs and their dendrites no longer costratify with SACs (Wong et al., 2007b). These results demonstrate that ipRGCs play multiple developmental roles, including patterning of retinal blood vessels, neonatal bright light avoidance, and modulating early retinal activity that promotes RGC axonal refinements within the brain.

Filling the void: Identification of a molecular parts list for ipRGCs

Investigating which genes are selectively expressed in ipRGCs could dramatically enhance our understanding of their diversity. The basic molecular framework of the Opn4 phototransduction cascade, a major defining feature of ipRGCs, has begun to be identified (Hughes et al., 2012), for review). However, the precise cellular mechanisms of phototransduction in ipRGCs remains poorly characterized, especially compared to the depth of knowledge of neuroanatomical features of ipRGCs. Further, much of the molecular details remain unknown. It remains unclear at the molecular level how the important cellular differences between M1 ipRGCs, non-M1 ipRGCs, and the retinal ganglion cell population as a whole are developmentally differentiated and maintained through adulthood.

The tremendously diverse morphology, physiology and anatomy seen throughout the nervous system is due at least in part to profound variations in the type and amounts of RNA which drive the underlying molecular program. Initial studies used Northern blot analysis or quantitative

reverse transcriptase-PCR to study the messenger RNA (mRNA) expression transcribed from a limited number of genes. Currently, gene expression microarrays and RNA-seq are two popular ways of generating transcriptome data. The transcriptome ideally represents the relative abundances of the entire set of coding and non-coding transcripts from the corresponding genes of a cell. Gene expression profiling studies using microarrays have generated a considerable amount of information regarding the genes potentially involved in the development and differentiation of the vertebrate retina (Livesey et al., 2004; Mu et al., 2004). Microarrays are relatively cost-effective and quick means to obtain a general view of gene expression changes across development and cell type (Marioni et al., 2008; Malone and Oliver, 2011). However, microarrays suffer from false positives due to background hybridization, inability to detect splice variants or unknown genes, and limited accuracy of expression for transcripts in low abundance. Although microarrays are useful tools for transcriptomics, RNA-seq complements and extends microarray transcriptomics capabilities. In particular, high throughput sequencing provides direct measurement of transcript abundances, allows identification of alternative splicing events which may be of biological importance, and has much greater dynamic range. The caveats include a relatively high cost and a much more intensive data analysis requirement, both of which are increasingly becoming more accessible over time.

Transcriptome profiling is commonly used to identify statistically differentially expressed genes (DEGs). DEGs are determined by analyzing the relative amounts of mRNA expressed in two or more groups, usually a test case and a control group. Oftentimes, acquiring transcriptomics data is done prior to having a hypothesis about which genes will be differentially expressed given the particular experimental conditions. Instead, the thousands of genes that are analyzed simultaneously during RNA-seq or microarray experiments help to identify potential hypothesis

for future experiments and discoveries. This is in contrast to RT-PCR, which is a more targeted approach that depends on picking a few genes to be analyzed at a time. However, the large number of genes tested for differential gene expression profile using RNA-seq requires correcting for multiple comparisons (Noble, 2009). Traditional means to calculate statistical significance using p-values were only intended for single tests. The massive number of statistical tests required for differential expression analysis of thousands of genes in transcriptomics studies quickly escalates the likelihood of creating many erroneous "discoveries." The False Discovery Rate (FDR) is commonly used to compensate for multiple comparisons in large-scale gene expression profile data (Benjamini and Hochberg, 1995; Anders and Huber, 2010).

The extreme heterogeneity and disproportionate distribution of cell types in the mammalian nervous system imposes many challenges to the identification of DEGs. Until recently, most gene expression studies were done using populations of cells homogenized from tissue or homogeneous cell culture systems (Dougherty and Geschwind, 2005), for review). The cell types making up the brain are especially diverse and intermingled, limiting the detection of gene expression changes. Many cell types have been found that are exceptionally rare, but nonetheless have functionally important roles. Measurements of pooled cells only detect the averaged gene expression pattern, which is dominated by the most prevalent cell types. The small amount of genetic material provided by relatively rare cells means that most DEGs and gene expression changes will be below the levels of detection. Further, differences in gene expression of one cell type may be masked by an opposing change in expression of the same gene by different cell types. Another issue with using pooled cells for identifying DEGs is due to RNA-seq being a method that randomly samples transcripts in proportion to their abundances. Recurrent sampling of highly abundant transcripts uses a considerable portion of the available sequencing resources and decreases the capability to

detect relatively rare transcripts (Bloom et al., 2009; Robinson and Oshlack, 2010; Roberts and Pachter, 2011).

Numerous methods have been developed to simplify the cellular composition of neural samples and characterize the transcriptome of defined cell populations in live nervous system tissue (Kamme et al., 2003; Lobo et al., 2006; Nelson et al., 2006; Doyle et al., 2008; Heiman et al., 2008). A large number of GFP and Cre-transgenic reporter mice have been generated to label specific neuronal and glial cell populations in the nervous system (i.e., (Gavériaux-Ruff and Kieffer, 2007; Gong et al., 2007; Siegert et al., 2009; Ecker et al., 2010). The first task for directly measuring the transcriptomes of labeled cell types is the enzymatic dissociation of dissected tissue into its constituent individual cells for further selection. Second, labeled cells are selected from surrounding cells by methods including the low-throughput manual cell sorting or by high-throughput fluorescence activated cell sorting (FACS) (Lobo et al., 2006; Sugino et al., 2006). Third, the cell is lysed, RNA is extracted, and consequently processed for microarray or sequencing. In contrast to fluorescence based methods, immunopanning relies on antibodies against cell-type specific surface proteins to purify target cell subpopulations (Barres et al., 1988; 1992; Cahoy et al., 2008). A major challenge of dissociation-based isolation methods has been the inherent necessity to remove cells from their cellular-context that has the potential to decrease viability and initiate stress-induced gene expression changes due to mechanical shear forces throughout the process of preparation. This is especially the case for mature neurons, but procedural optimizations over the last decade has continued improve survivability (Arlotta et al., 2005; Lobo et al., 2006; Heiman et al., 2008).

The retina as a model system has helped to define the genetic programs generating the cellular diversity in the nervous system (Sanes and Masland, 2015), for review). A molecular

description of the distinct neural cell types has been hindered by the highly heterogeneous and intermixed circuitry. Previous studies have found some success in analyzing the whole retina as the source of identifying important molecular components and disease elements (Blackshaw et al., 2001; 2004; Livesey et al., 2004; Mu et al., 2004; Gamsiz et al., 2012). However, it remains difficult to assess the unique molecular characteristics of defined cell populations from these tissue homogenates due to the indistinguishable gene expression changes of relatively rare cell types and the averaging of gene expression levels throughout the system.

Previous attempts of resolving a "molecular parts list" using gene expression profiling of adult ipRGC types have been severely limited by the extreme heterogeneity of retinal tissue, rarity of ipRGCs, minuscule amount of accessible genetic material, and fragility of mature retinal neurons. However, the isolation of ipRGCs from the entire dissociated retina using either the Opn4 antibody-mediated isolation or direct isolation of reporter labeled ipRGCs with FACS has been plagued by low yield, inability to distinguish above background autofluorescence, and inclusion of contaminating cell populations such as rods (Hartwick et al., 2007; Siegert et al., 2012). For the transcriptome analysis of defined ipRGC subtypes, I have used the BAC transgenic *Opn4::GFP* reporter (fluorescently labels M1-M3 ipRGCs) and *Opn4::Cre* reporter system labeling M1-M5 ipRGC subtypes(Schmidt et al., 2008; Ecker et al., 2010). My process is a novel, unbiased gene expression profiling approach and has successfully identified more than 75 new genes that are candidates for selective expression in adult ipRGCs. The utility of this data is exemplified by the presence of all known molecular markers of the ipRGC family and absence of potential contaminating cell populations.

METHODS

For our transcriptomics studies, we used two ipRGC reporters available in the lab to identify selective gene expression in ipRGCs compared to RGCs as a whole: 1) BAC transgenic *Opn4-EGFP* Gensat mice from MMRRC (#033064-UCD) and 2) knock-in *Opn4-Cre* mice (obtained from S. Hattar; Ecker et al., 2010) with Cre-dependent GFP reporter (Z/EG obtained from Jackson labs; (Novak et al., 2000). The *Opn4-GFP* mice were maintained as heterozygotes on *C57/BL6* background while $Opn4^{Cre/+}$*;Z/EG* mice were generated by breeding homozygous *Opn4-Cre* mice with heterozygous *Z/EG* mice and maintained on mixed background. Although *Opn4-GFP* reporter labeling in ipRGCs has not been reported previously, a similar BAC transgenic strategy has been demonstrated to label M1-M3 ipRGCs (Schmidt et al., 2008). We tested the correlation of the *Opn4-GFP* reporter expression and endogenous melanopsin in RGCs. We used anti-melanopsin immunoreactivity label M1-M3 ipRGCs (Berson et al., 2010) and anti-EGFP antibodies in a whole-mount retina from an adult Opn4-EGFP mouse. Importantly, all *Opn4-GFP*+ RGCs were Opn4-immunopositive (n=60 GFP^+ cells across seven regions of one retina, Figure 4a). Unexpectedly, more than half of the Opn4-immunopositive M1-M3 ipRGCs were not labeled by the reporter (55%, n=133). Therefore, the coexpression of EGFP expression by the Opn4-GFP reporter is strongly correlated with M1-M3 ipRGCs, but only accounts for about half of the population. The other reporter system used in this study, $Opn4^{Cre/+}$ *; Z/EG* mice, has been previously demonstrated to label with EGFP all six known morphological types of ipRGCs), named M1–M6 (Ecker et al., 2010; Quattrochi et al., in preparation).

Two ages were chosen for retina tissue collection for purification of ipRGC neurons: Postnatal day 5 (+/- 1day) and young adult (P30 +/- 3 days). Three or more biological replicates were used for each dataset (three for postnatal day 4-6 (P4-6) Gensat *Opn4::GFP*, six replicates

for Gensat *Opn4::GFP*, four replicates for *Opn4::Cre/GFP* reporter). Each adult replicate required the pooled retinas from 15-20 transgenic mice to acquire suitable numbers of cells for the transcriptomics. These steps are outlined in much more depth and detail in the following sections.

The choice of transcriptomics preparation strategies and final readout of processed samples are interrelated and subject to a number of technical concerns vital to the success of transcriptomics analysis. Seven steps in the development and completion of the cell type-specific transcriptomics procedure of cells isolated from early postnatal and adult mouse retinas (Figure 4b). **First**, dissociation of retinal tissue to a cell suspension; **Second**, purification of RGCs; **Third**, FACS analysis and sorting; **Fourth**, extraction of RNA; **Fifth,** cDNA amplification because the resulting RNA is typically low in abundance; **Sixth**, shear cDNA into sequenceable fragments that are then sequenced with Illumina deep-sequencing; and **Finally**, the raw reads must be analyzed to identify differential expression of genes in ipRGCs.

Dissociation

The intertwined nature and tight cell–cell adhesions of neural cells make it difficult to separate cells without causing cellular damage and activating stress or cell death pathways. Therefore, vigorous dissociation of tissues can lead to activation of stress or cell death pathways and distort the resulting expression profile. However, poor dissociation can lead to a severe decrease in isolated cells and make downstream expression studies an impossibility. As a first step, we dissected retinal tissue, which we then digested in a protease solution to loosen and disrupt the intertwined neural cells into single cell suspensions for subsequent cell-type isolation. The essential components for proper dissociation included: the proteolytic enzyme papain L-cysteine to promote enzymatic activity, DNase for destroying the extremely sticky free DNA strands

released by damaged cells, and an absence of calcium from solutions to promote disruption of cell-cell adhesions (Barres et al., 1988). We further optimized cell viability and recovery by replacing dPBS with HibernateA and including B27 throughout the cell-isolation procedure (Brewer et al., 1993; Brewer, 1997; Brewer and Torricelli, 2007). The use of survival-promoting media such as Hibernate-A and supplements such as B27 was particularly relevant for adult neural dissociation since adult neurons have been demonstrated to be especially prone to cell death (Eide et al., 2005; Brewer and Torricelli, 2007). We incubated the dissected retinas in pre-activated protease solution and completed the cell dissociation by triturating the cells with a 1mL pipette tip.

RGC Pre-Enrichment

Pre-enrichment of ganglion cells prior to isolation of ipRGCs is necessary due to their extraordinary rarity in the retina. Ganglion cells only make up 1% of mouse retinal cells and only 1-5% of ganglion cells are ipRGCs (0.01-0.05% of retina cells) (Hattar et al., 2002; Ecker et al., 2010; Berson et al., 2010). In contrast, the classic photoreceptors rods and cones account for 75-80% of all mouse retinal cells (Jeon et al., 1998). Therefore, we pre-enriched for ganglion cells prior to positively selecting fluorescently labeled ipRGCs using fluorescence activated cell sorting. We incorporated an immunopanning system that has proven effective at isolating a homogeneous population of RGCs (Barres et al., 1988; Cahoy et al., 2008). Immunopanning takes advantage of the cell surface protein Thy1 which is shared among retinal ganglion cells (Barres et al., 1988). The classic immunopanning process uses antibodies raised against Thy1 to select the RGCs from the heterogeneous retinal cell suspension. We improved upon viability and reproducibility of the immunopanning procedure by adapting it to use a magnetic-activated cell sorting procedure (MACS, Miltenyi Biotec), eliminating the need for using harsh lysis treatment (data not shown).

We incubated the dissociated retinal cell solution with Thy1.2-conjugated magnetic nanoparticles which are retained in a magnetized column and the isolated RGCs can then be acquired (Haeryfar and Hoskin, 2004). In preparation for FACS, the DNA intercalating dye, 7-AAD, was added to the solution to discriminate dying cells that consequently had compromised cell membranes.

Fluoresence-Activated Cell Sorting (FACS)

We used a FACS Aria (BD Biosciences) electrostatic sorter to isolate a homogeneous GFP-labeled cell population from the dissociated RGC-enriched cell suspension of the transgenic melanopsin reporter mice (Figure 4). FACS has been successfully used previously to profile gene expression in cell subtypes of the nervous system (Lobo et al., 2006; Cahoy et al., 2008; Siegert et al., 2012). Live cell gating was achieved by excluding 7-AAD labeled cells (high fluorescence signal in far red emission). Fluorescently labeled ipRGCs were positively selected from the solution of enriched ganglion cells by their relatively high level of GFP fluorescence (FITC gating). In parallel, cells with relatively low GFP-fluorescence (low FITC) were also isolated and designated as a "generic RGC" control population for direct comparison with correlated ipRGC samples. The parallel isolation of generic RGCs was designed as an internal negative control for comparison with isolated ipRGCs. Accordingly, the generic RGC populations were treated with the same reagents, cytometer settings, centrifugation forces, and temperatures throughout the procedure. This is especially important for isolating adult RGC populations, since they are particularly susceptible to the stresses of FACS sorting(Lobo et al., 2006; Cahoy et al., 2008; Heiman et al., 2008). The large amount of small cellular debris generated during the dissociation process made it a challenge to keep the number of collected generic RGCs consistent with the rare ipRGCs. Cellular debris registers as being essentially non-fluorescent, is smaller and less complex

than the generic RGC population that is of the same relative size and complexity as the isolated GFP-positive cells. Therefore, we limited cell debris by acquiring the ipRGC (GFP+) and generic RGC (GFP-negative) populations with the same relative cell complexity (indicator of cell health) and cell size selection to exclude the relatively small cellular debris or doublets.

RNA Extraction

The small volumes allowed by the electrostatic FACSAria sorter allowed us to lyse sorted cells directly into Qiagen RLT buffer and directly proceed to RNA extraction using Minelute columns (Qiagen). The enriched RNA was treated on-column with DNase to remove any residual genomic DNA from the sample. RNA-processing was done in an enclosed RNase-free environment to limit degradation of RNA throughout the extraction process. Additionally, RNA integrity was analyzed using the Agilent 2100 Bioanalyzer and the PicoChip, which is able to qualitatively test the low RNA recovery samples (Figure 6a). Initially, we proceeded immediately with cDNA processing after RNA extraction. However, freezing at -80 degrees did not seem to effect RNA integrity since the frozen RNA samples still received RIN score of 9.0 or greater. Therefore, most of the cDNA libraries were prepared after storage of extracted RNA at -80 degrees Celsius.

cDNA Preparation

RNA-seq transcriptome analysis requires large amounts of RNA material using TruSeq, ranging on the order of 100-1000ng of total RNA. However, our improved method for isolating ipRGCs was able to isolate 12,000 GFP+ ipRGCs from nine postnatal day 5 (P5) transgenic reporter mice. This was only expected to provide about 12ng of extracted total RNA by qualitative

estimates considering that a single cell holds 5-10pg of total RNA. Further, twice as many adult mice of the same genotype were required to provide only 1,000 cells due the the relative fragility of adult retinal ganglion cells described above. Therefore, we decided that some form of amplification was necessary to study the molecular programs used by adult ipRGCs. The Nugen Ovation RNA amplification system was successfully used in microarray studies with as little as 500pg of total RNA input (Caretti et al., 2008; Clément-Ziza et al., 2009; Morse et al., 2010) (Figure 6b). In most cells, rRNA and tRNA is known to make up the majority of RNA species and mRNA is only a small fraction of the total RNA. Therefore, we figured that our sequencing data would largely be dominated by the uninformative results without somehow enriching for mRNA. Sequencing analysis using the Ovation system was reported to generate cDNA containing negligible rRNA reads (<4%), while providing a representative transcriptome with sufficient biological replicates(Tariq et al., 2011).

RNA-SEQ Library Preparation

We determined that the Truseq system was the necessary platform for my cDNA samples to produce the 10nM sequencing library concentration required at the on-site Genomics Core facility in preparation for 50bp single-end Illumina sequencing. Before preparing the library, we first sheared cDNA to the appropriate size, (200-300bp median) using the Covaris system (Figure 6c). Each sample was subsequently processed using a unique barcode adapter to allow for multiplexing multiple samples on the HiSeq (commonly 200million 50bp reads divided among sequencing samples). Excess adapter sequences was removed using Ampure bead isolation, which removes all DNA fragments less than 200bp. Finally, the Genomics Core completed the final quality control of the DNA library prior to sequencing: testing the library fragment size distribution

(High Sensitivity Bioanalyzer) and qPCR analysis using primers that match the library adapters (Quail et al., 2008) (Figure 6d).

Initially, we processed a large number of samples at once with multiplexed sequencing using HiSeq (8 samples per lane) to minimize high costs of sequencing at the expense of sequencing depth. We later reran many of the sequencing libraries with less multiplexing, enabling increased sequencing depth. The corresponding technical replicates were merged together for differential expression analysis (Figure 6E). The final read counts of each sample is shown in Figure 7a.

Differential gene and transcript expression analysis.

The completion of sequencing generated tens of millions of reads that are used to compare gene expression levels between isolated ipRGCs (GFP+) and generic RGCs (GFP-) (Figure 7a). Well-established, powerful RNA-seq differential expression analysis pipelines have been developed such as Cuffdiff, EdgeR, and DESeq (Anders and Huber, 2010; Trapnell et al., 2012; Anders et al., 2013). The Cuffdiff pipeline prioritizes isoform quantification and diversity (Trapnell et al., 2012). However, the short 50bp single-end reads that are generated in our study are not well-suited for prioritizing isoform discovery and analysis. Further, Cuffdiff does not fully take advantage of our purposeful pairwise-comparison between groups. In contrast, the EdgeR package is better suited for our purpose; it is designed to count the number of reads that align to an annotated gene (mouse reference genome, in our case) and subsequently performs statistical analysis on a generated table of counts to identify quantitative changes in expression levels between the two experimental samples (Figure 7b). EdgeR compares and retains the relationship between all pairs of experimental samples when calculating differential expression likelihood

(Anders et al., 2013). Of note, our analysis filtered out genes with very low counts, less than 1 count per million (cpm), in more than half of the samples used in the differential expression analysis. This is a common cutoff and considers 1) that a gene must be expressed at a minimum threshold in order to become biologically important and 2) that the inclusion of genes with very low counts may negatively affect the statistical approximations used by the EdgeR pipeline.

RESULTS

To better understand the molecular diversity within adult ipRGC populations, we developed methods to assess the transcriptional profile of these exceptionally rare, specialized retinal cells (see Methods, Figure 4). Intrinsically photosensitive retinal ganglion cells (ipRGCs), once considered an homogeneous population, are now known to be comprised of six subtypes distinguished by their distinct morphology, physiology, projections and level of Opn4 expression. We optimized a protocol to obtain different complements of ipRGC subtypes using two reporter systems (see Methods). We isolated populations of P5 and adult M1-M3 ipRGCs using the BAC transgenic *Opn4::GFP* reporter (see Methods). Additionally, we isolated the M1-M6 ipRGC population based on labeling by the *Opn4::Cre/GFP* reporter system (Ecker et al., 2010). We used fluorescently activated cell sorting (FACS) to positively-select the fluorescently labeled ipRGCs. We also isolated and processed generic RGCs in parallel with ipRGCs as an internal control and a means to distinguish relative transcript abundance. RNA-seq was used to generate gene expression profiles for ipRGCs and generic RGCs and enabled differential gene expression analysis. We used

EdgeR differential expression analysis to determine genes that had enriched expression in ipRGCs (see Methods).

Cell composition and purity of isolated ipRGCs and generic RGCs

To visualize general trends or biases in our gene expression profile datasets, we produced multidimensional scaling (MDS) 2D plots that show the relationship between all pairs of samples based on a count-specific pairwise distance measure (Anders et al., 2013) (Figure 8). MDS plots represent similar samples as being in closer proximity, while dissimilar samples are separated. The first dimension (x-axis) accounts for the greatest amount of the variance in the data and it generally, but not necessarily, distinguishes test from control samples. The second dimension (y-axis) is uncorrelated with the first and accounts for the next best variance possible. We observed that the ipRGCs and generic RGC samples were clearly separated along the first dimension, except for the 40 and 41 pair of samples that were distinct outliers along the second dimension. The second dimension loosely correlated with samples that were processed in parallel (i.e., 24 with 25; 40 with 41), confirming the paired nature of our experimental design. The generic RGC group of samples were less clustered together, suggesting they are more heterogeneous than the ipRGC group.

The data coming from our differential expression analysis suggested that our isolated ipRGCs were of high-purity and that the genetic material generated high-quality sequencing (Figures 9 and 10). As expected, the Opn4/Melanopsin gene was found to be differentially expressed and was one of the most highly enriched genes in ipRGCs across all studies. For example, Opn4 was enriched 40-fold in the ipRGC (GFP^+) population of the adult *Opn4-GFP* reporter (FDR $1x10^{-55}$). There was also a relatively very low, yet present, level of expression of Opn4 in the generic RGC samples (GFP-negative) as well, suggesting that some ipRGCs were

unable to be purified during our selection procedure. Possible explanations include the incomplete labeling of M1-M3 ipRGCs by the reporter system (see Methods), presence of low-expressing ipRGC types M4-M6 that are unlabeled by the Opn4-GFP reporter (Ecker et al., 2010). In addition to Opn4, other known ipRGC-expressing genes were also determined to be differentially expressed (FDR < 0.05, significantly expressed ipRGC samples, and absent or low expression in generic RGC samples) including Adcyap1, Tbr2, Trpc7, and to a lesser extent, Trpc6 (Hannibal et al., 2004; Xue et al., 2011; Mao et al., 2014; Sweeney et al., 2014; Sand et al., 2012). There appears a discrepancy between the residual low expression of the ipRGC molecular marker Opn4 and the seemingly absent expression of other known ipRGC markers in generic RGC samples. This may be due, in part, to Opn4 being especially abundant in ipRGCs to the extent that even a small minority within the pooled generic RGC population is sufficient to provide levels of overall Opn4 expression detectable by RNA-sequencing pipeline. In contrast, genes with relatively lower expression than Opn4 or restricted expression to a subset of ipRGCs may become thoroughly diluted by the vast amount of transcripts from the other cells in the generic RGC population. Indeed, Opn4 expression in the Opn4-GFP reporter is 88-, 37-, and 12-fold higher than Trpc7, Adcyap1, and Tbr2, respectively. These trends were observed across both reporter systems (*Opn4-GFP* and *Opn4-Cre/GFP*) as well as both ages (P5 and adult).

We found little or no evidence of contamination in ipRGCs (GFP+) samples. A major potential source of contamination are the abundant rod photoreceptors (Figure 9). They are the most abundant cell in the retina (>70% of all cells) and their photopigment, Rhodopsin, is expressed at extremely high levels. Therefore, the presence or absence of transcripts towards Rhodopsin is an important indicator of sample purity. Importantly, Rhodopsin expression was largely or completely absent in the positively isolated ipRGC (GFP+) populations. Specifically,

the Rhodopsin expression in adult ipRGC samples from *Opn4-GFP* and *Opn4-Cre/GFP* reporter mice were more than 150-fold less than that in generic RGCs (FDR<$6x10^{-9}$). Muller glia seems to be a major contaminant in the generic RGC population, with high expression of all known Muller markers including Glul, Apoe, Aqp4, and Vim. In contrast, the additional positive selection by fluorescence during the ipRGC isolation process seemed to significantly reduced the impact of Muller contamination (more than 50-fold decrease in most Muller cell marker expression compared to generic RGCs). The expression of several molecular markers for amacrine cells are present in ipRGC population, including Calb1, Gad1, Gfd2, and Slc6a9. However, none of these genes are known to be exclusively expressed in amacrine cells. Therefore, the impact of amacrine cell-derived transcripts existing in the ipRGC gene expression profile remains a challenge to determine (Cherry et al., 2009). The absence of horizontal cells in our ipRGC samples was confirmed by undetected expression of the horizontal cell marker Lhx1, but was confounded by the presence of another horizontal cell marker, Prox1 (Liu et al., 2000; Dyer et al., 2003). In general, the presence of non-RGCs in generic RGC populations is suggested by the more than five-fold reduction of ganglion cell markers (i.e., Rbpms and Sncg) in adult generic RGC samples compared to isolated ipRGCs (Soto et al., 2008; Rodriguez et al., 2014). In other words, whereas a pure population of ipRGCs will homogeneously express RGC markers, their relative abundance becomes less prevalent in generic RGC population due to the presence of rod and Muller glia contamination. In contrast, contaminating populations were significantly decreased or abolished in the samples from P5 *Opn4-GFP* mice. This may be due, at least in part, to the fact that the major contaminants rod photoreceptors and Muller glia are mostly generated postnatally, and therefore may not be as prevalent during the P5 time point (Young, 1985; Morrow et al., 1998; Matsushima et al., 2011). The discrepancy of samples 40 and 41 as observed in our MDS plots (Figure 8) were

unable to be correlated with any obvious differences in cell composition that would distinguish them from other samples. Overall, differential expression analysis comparing ipRGCs (GFP+) against generic RGCs (GFP-negative) suggests that the transcripts obtained were derived largely from ipRGCs.

Identification of differentially expressed genes in ipRGCs

To identify the set of differentially expressed genes in the ipRGC populations, we used the following strict criteria. First, we identified genes with low false discovery rate (FDR < 0.05) and high fold-change (greater than 2-fold) suggesting differential expression between GFP+ ipRGCs and GFP-negative generic RGCs. Second, we considered whether the differentially gene expression was corroborated across both reporters (*Opn4::GFP* labeling M1-M3 cells and the *Opn4::Cre/GFP* system that labels M1-M6 ipRGCs) and both ages (P5 and adult). Lack of expression in one case may suggest further refinement as age-dependent gene expression or ipRGC subtype expression. Third, we identified whether the differentially expressed genes have nearly absent gene expression in generic RGC samples to distinguish potential for selective gene expression in ipRGCs. This was distinguished both at the level of count-values and manual inspection of aligned raw reads using the Integrated Genome Viewer (IGV) (Thorvaldsdóttir and Robinson, 2013). Using IGV, we verified that the reads align with reference gene model for full-length coverage across multiple ipRGC replicates and that there were absent or partial reads aligned across the generic RGC replicates. Our gene expression data of the two Opn4 reporter systems has suggested more than 75 genes to be differentially expressed genes in ipRGCs, many of which have not been previously recognized (Figure 11).

ipRGC phototransduction machinery

Distinct from rod and cone photoreceptors, the light-activated Opn4 phototransduction cascade triggers a membrane bound signalling cascade including $G_{q/11}$ type G-proteins, the generation of 1,2-diacylglycerol (DAG) by PLCβ4, the opening of downstream TRPC6 and TRPC7 channels, and ultimately leads to the influx of calcium through L-type voltage-gated calcium channels (Hughes et al., 2012). As mentioned above, Opn4 and its key downstream light gated ion channel Trpc7 were determined to be differentially expressed in ipRGCs, with relatively low or absent levels of expression in GFP-negative RGCs (Figures 11a and 12). However, other phototransduction machinery components such as Trpc6 and PLCβ4 were found to be more ubiquitously expressed across RGCs, fitting with previously described expression patterns (Graham et al., 2008; Xue et al., 2011). Multiple genes were determined to be differentially expressed in ipRGCs that have known roles in connection with DAG and calcium signaling, including Rasgrp1 and Dgkg (Bivona et al., 2003b; Shulga et al., 2011) (Figure 11a and 12).

Only recently has the precise identity of the Gα subunits combination in ipRGCs been identified as redundantly expressing and signaling through the Gnaq, Gna11, or Gna14 subunits (Hughes et al., 2015). Our studies suggest a similar expression pattern, including a lack of Gna15 expression (Figure 12). Further, Gna14 was revealed to be differentially expressed in our P5 ipRGC samples, but it did not reach a statistical significant difference in adult *Opn4-GFP* ipRGCs.

Desensitization and adaptation mechanisms of Opn4 phototransduction process has also begun to be revealed. Beta-arrestin is the main player known for the phosphorylation-dependent deactivation of Opn4(Cameron and Robinson, 2014). Our gene expression profiles suggested that the beta-arrestins Arrb1 and Arrb2 are ubiquitously expressed across ipRGCs and generic RGCs (Figure 12). The Regulator of G-protein signaling (RGS) proteins negatively regulate GPCR

signaling by binding to activated G-alpha subunits and terminating the signaling cascade. Rgs17 and Rgs4 were both determined to be differentially expressed in ipRGCs (Figure 11a).

Many of the known classic phototransduction machinery were found to have absent expression (scarce or no read alignment) or were expressed solely in generic RGC control populations (for example, Rho, Gnat1 and Sag) (Figure 10 and 13). The majority of transducin genes known to be expressed in rods and cones did not have detectable levels of expression. However, Gnb1 was a notable exception and was found to be the highest expressing Gβ subunit in ipRGCs, with similar expression levels relative to generic RGCs. Additionally, Kcnh1, also known as ether-a-go-go (Eag1), was differentially expressed in ipRGCs (Figure 11B). Kcnh1 is a voltage-gated K+ channel that has been shown to be important for the dark current in the inner segment of rods(Frings et al., 1998). Our studies also suggested that the cyclic nucleotide gated channel subunit Cngb1 is differentially expressed in ipRGCs. However, we used IGV to visualize the raw reads aligning to Cngb1 and identified sparse, incomplete alignment of reads across the gene model and a pile-up of reads to a very limited region of the gene. Therefore, Cngb1 may be a false-positive due to an overamplification artifact. Additionally, Cngb1 function requires functional alpha subunits, which were not detected (Weitz et al., 2002; Zheng et al., 2002; Zhong et al., 2002).

Despite their distance from the outer retina, ipRGCs have been suggested to receive at least some support to their visual cycle from the outer retina (Díaz et al., 2016). One suggestion was that ipRGCs use the closely coupled Muller glia for chromophore regeneration support similarly to cones in the outer retina. In our studies, the Muller glia isomerase Degs1 was found to be expressed in ipRGCs, although at similar levels across ipRGC and generic ipRGC populations (Figure 13b). In addition to Muller glia, Des1 has been shown to be expressed in RGCs(Kaylor et

al., 2013). However, the prevalence of Muller glia contamination in generic RGC samples made the assessment of Degs1 differential expression in ipRGCs impossible (Figure 9). Other enzymes responsible for further processing of a functional chromophore were not significantly expressed in ipRGCs (Figure 13b).

Molecular programs of ipRGCSs

Complex genetic programs control the binary fate decisions giving rise to the specialized adult retina require the simultaneous activation and repression of genes by transcription factors. Little is known for how the general embryonic developmental program leads to the terminal differentiation of the more than 30 types of retinal ganglion cells in adulthood. The identification of transcription factors has the potential to identify parts of the molecular program important for maintenance of adult ipRGC neuronal identity, as well as potential identification of cell-type specific expression and function programs (100s of genes potentially regulated). Tbr2 was recently shown to continue expression in the majority of adult ipRGCs(Sweeney et al., 2014). Our studies suggest that Tbr2 as well as another T-box transcription factor, Tbx20, are selectively expressed in our gene expression profiling of adult ipRGCs (Figure 11a). Additionally, Irx6, Dmrtb1, Nr4a3, and Pou6f2 differential expression pattern suggested that they may play a role in adult ipRGCs. Most of these genes have well-described roles as broad lineage determinants in early retinal development(Zhou et al., 1996; Star et al., 2012). The neuron-derived orphan receptor 1 (Nor1, also called Nr4a3) is a nuclear receptor that was also found to be differentially expressed in ipRGCs. The RNA-binding protein Elavl2 was differentially expressed and has been shown to play important roles in neuron differentiation and survival by effecting mRNA metabolism through binding to RNA stability elements (Fornaro et al., 2007; Hinman and Lou, 2008). Pathway analysis

(DAVID) of differentially expressed genes in ipRGCs suggested specialization in heparan sulfate biosynthesis, including Hs3st4, Hs3st2, Hs6st2, Ndst4, and Gpc5 (Figure 11B). Heparan sulfate is functionally diverse, mainly due to the precise arrangement of sulfate group motifs that selectively bind to other effector proteins (Poulain and Yost, 2015).

Determining differentially *repressed* genes in adult ipRGCs was confounded by the high amount of contaminants in generic RGC populations. We could not decipher whether a gene with relatively low expression in ipRGCs was the result of non-RGC populations contaminating the generic RGC control population. In contrast, the P5 generic RGC samples from the *Opn4-GFP* reporter seemed to have greatly reduced levels of contamination and similar levels of RGC marker expression (Figure 10). This made it possible to identify genes more weakly expressed in ipRGCs than in generic RGCs in early postnatal development (Figure 14). Our studies suggest that the transcription factor JUN (Jun Proto-Oncogene) may be differentially repressed in ipRGCs. Differentially low gene expression of Satb1, Satb2, and Foxp2 in ipRGCs may reflect known restricted expression in the abundant F-RGCs that are likely present in generic RGC populations (Rousso et al., 2016). The Pou4f1 (Brn3a) and Pou4f3 (Brn3c) transcription factors were both differentially low in P5 ipRGCs, correlating with the known lack of expression in ipRGCs (Jain et al., 2012) (Figure 14). The transcriptional repressors Bcl11b (CTIP2), Irx4, and Tbr1 were all found to have significantly lower expression compared to generic RGCs. Further, Bcl11b has previously been shown to transcriptionally repress the expression of Cdkn1c (p57KIP2), a cyclin-dependent kinase inhibitor that was shown to be significantly higher expressing in P5 ipRGCs (Figure 11c) (Topark-Ngarm et al., 2006). The differentially repressed Irx4 transcription factor has been associated with controlling axon guidance through the negative regulation of Slit1 (Jin et al., 2003).

Additional differentially expressed genes in ipRGCs

We also identified a set of genes differentially expressed in ipRGCs having known roles in synaptic transmission, ion transport and cell communication, cell adhesion, survival, as well as numerous novel unclassified genes (Figure 11).

We explored the set of receptors that are expressed in ipRGCs. The ionotropic nicotinic acetylcholine receptors in ipRGCs were determined to consist of the α3, α4, and α6 subunits in combination with the β2 and β3 subunits (Figure 15a). The α3 and α4 were statistically borderline for being differentially expressed in ipRGCs. In agreement with previous studies, ipRGCs expressed the Drd1 (D1a) dopamine receptor, but had low or absent level of Drd2 expression (Van Hook et al., 2012) (Figure 15a). The serotonin receptors Htr1b, Htr1d, and Htr5a were modestly expressed in ipRGCs. The main glycine receptor subunits were determined to be the α1β heteromer (Figure 15b). The ipRGCs were also found to express a complex set of glutamate receptors (Figure 15b). In particular, the glutamate ionotropic receptor NMDA 3A (GRIN3A) was differentially expressed in ipRGCs. We did not detect expression of melatonin receptors in ipRGCs, in contrast to previous studies in rodent retina suggesting expression of Mtnr1a and Mtnr1b in M1- and M4-type ipRGCs (Sengupta et al., 2011; Pack et al., 2015; Sheng et al., 2015).

Differentially expressed genes with known roles regulating information processing at presynaptic active zones include Sh3gl3, Entpd1, Rab3b, Baiap3, Chl1, Sh3gl3, and Adra2a (Figure 11b). Multiple growth factors and neuropeptides were determined to be differentially expressed in adult ipRGCs (Bmp7, Fgf1, Gal, Gdf6, Grem1, Nmb and Nppb) (Figure 11b).

There is increasing evidence that ipRGCs are resistant to stress and able to survive under circumstances that are fatal for other retinal neurons (de Sevilla Müller et al., 2014; Cui et al.,

2015; Duan et al., 2015). We controlled for general stress-induced gene expression that is anticipated in the adult neurons in response to the harsh dissociation and FACS processing by processing the isolated ipRGCs in parallel with generic RGCs. This allowed us to identify survival induced molecular programs that are specific to ipRGCs compared to normal RGCs (Figure 11c). The genes Adcyap1/PACAP, Igf1, and Spp1/osteopontin were determined to be differentially expressed, all of which have previously described roles in promoting survivability in ipRGCs (Atlasz et al., 2010; Duan et al., 2015). We also identified an intriguing glial-neuronal relationship suggested by differential expression of Gldn, Cntn2, Lama4, and Astn2, and Thbs1 (Figure 11c). Many of these genes have been studied in the context of axon regeneration and could prove useful for identifying axon repair therapies in the future(Catherine Faivre-Sarrailh, 2013).

Comparison of the genes differentially expressed in *Opn4-GFP* versus *Opn4-Cre/ZEG*

In general, the two Opn4-based reporters were both supportive and cross-correlated for differentially expressed genes in ipRGCs. Our studies also allowed us to take advantage of the possibility to compare between the two reporters to ipRGC to further decipher subtype-specific expression (Figure 16). This comparison lead to the identification of 24 genes that were differentially expressed in the adult *Opn4-Cre/ZEG* reporter and had low or no apparent expression in the *Opn4-GFP* reporter, suggestive of selective expression in one or more of the M4-M6 ipRGC types. The neurexophilins Nxph1 and Nxph3 were found to be differentially expressed in the *Opn4-GFP* and *Opn4-Cre/ZEG* reporter, respectively (Figure 16). These proteins are known to bind α-neurexins in mice and have restricted expression patterns (Missler et al., 1998; Beglopoulos et al., 2005; Craig and Kang, 2007). Nxph3 has been suggested to play a functional role in specific neuronal circuits such as the startle response in mice. Several genes found to be expressed in *Opn4-*

Cre/ZEG specific genes have been shown to become up-regulated in diseased mammalian brains and murine models of vision loss, including Anxa2 and Gem (Eberhard et al., 1994; Wang et al., 2013; Wen et al., 2013; Yang et al., 2013; Xu et al., 2014). Anxa2 is a multifunctional protein that is a member of the annexin family and is important for mediating many calcium-dependent intracellular functions (Gerke and Moss, 2002; Moss and Morgan, 2004; Beglopoulos et al., 2005; Gerke et al., 2005; Singh, 2007; Bharadwaj et al., 2013; Madureira and Waisman, 2013). Gem is a small GTP-binding protein that is an atypical member of the Ras superfamily (Maguire et al., 1994; Fischer et al., 1996). The two main neuronal functions of Gem involves the regulation of voltage-gated Ca^{2+} channel activity and reorganization of the cytoskeleton (Béguin et al., 2001; Ward et al., 2002; Scamps et al., 2015). The differentially expressed genes Rbp4 (Serum Retinol binding protein 4) and retinoic acid receptor Rxrg have well-described roles in signaling by retinoids (Lane and Bailey, 2005; Maden, 2007; Li et al., 2014). Rbp4 binds retinol in the blood and assists in its transport to the retinal epithelial cells via the Stra6 receptor for the retinol/Rbp4 complex (Ruiz et al., 2012). Stra6 is known to be highly expressed in the outer retina, but there is no immunocytochemical evidence for Stra6 expression in the inner retinal neurons of the mouse (Ruiz et al., 2012; Dean Bok, personal communication). Rbp4 is known to be expressed in several brain regions, including the hippocampus (Komatsu et al., 2005; Goodman et al., 2012). In response to retinoid binding, heterodimers of retinoid A receptors (RAR) and retinoid X receptors (RXR) bind to specific retinoic acid-response elements (RARE) (Bastien and Rochette-Egly, 2004). In the mouse retina, Rxrg is known to suppress S opsin expression in immature cone photoreceptors and dorsal cones in the mature retina (Roberts et al., 2005). Rxrg has also been suggested to be an integral part of a retinoid pathway that controls the dopaminergic signaling that modulates affective behaviors in mice (Krzyzosiak et al., 2010). The Kcnk4/TRAAK gene encodes

a two-pore potassium channel subunit that was determined to be differentially expressed in the *Opn4-Cre/ZEG* reporter (Fink et al., 1998). Kcnk4 has been previously shown to be activated by polyunsaturated fatty acids-activated, mechanogated, and have expression in the retina, as well as other brain regions and the spinal cord (Fink et al., 1998; Maingret et al., 1999; Reyes et al., 2000). Additionally, our studies suggested that the Kcns3 potassium channel subunit has its expression restricted to the ipRGCs labeled by *Opn4-Cre/ZEG*, but this difference did not reach statistical significance (FDR 0.13). However, close inspection of reads aligning to Kcns3 using the integrated genome viewer (IGV) confirmed weak expression in ipRGCs and absent expression in generic RGCs for *Opn4-Cre/ZEG* samples (data not shown). Kcns3 is a member of the electrically silent voltage-gated potassium channels, which does not form functional channels by itself but instead modulates the biophysical properties of Kv2, a crucially important and ubiquitously expressed voltage-gated potassium channel (Shepard and Rae, 1999; Bocksteins and Snyders, 2012; Bocksteins, 2016). Lastly, the Sema3d gene encodes a member of the semaphoring family and was found to be differentially expressed in *Opn4-Cre/ZEG*. Sema3d is involved in axon guidance during neuronal development and has been found to be important for guiding retinal ganglion cell axons in developing zebrafish (Sakai and Halloran, 2006; Dell et al., 2013; Erskine and Herrera, 2014).

ipRGC retinal circuitry development

As suggested previously, the repulsive ligand Sema6a was determined to be significantly low expressing in ipRGCs compared to RGCs in postnatal development (Matsuoka et al., 2011) (Figure 17). However, we found that its receptor PlxnA4 was also differentially expressed in P5 ipRGCs (Figure 17). This is contrary to earlier findings suggesting that neither Sema6a or Plxna4

are expressed in ipRGCs, despite Plxna4 expression in DACs from (Matsushima et al., 2011). Another semaphorin, Sema5a, is also significantly enriched in developing ipRGCs. The cell adhesion molecule DscamL1 seems to be relatively low in ipRGCs during development, but the closely related immunoglobulin superfamily (IgSF) adhesion molecules Sidekick-1 and Sidekick-2 are enriched in developing ipRGCs. Unc5a and Unc5d were significantly expressed across development, and continue to be enriched into adulthood in ipRGCs as well. Both Unc5d and Unc5a are known to have distinct laminar expression patterns that coincide with stereotyped S1 OFF-region dendrites of M1 and S5 ON-region dendrites of M2 ipRGCs (Visser et al., 2015). As expected, Unc5b was very low expressing, while Unc5C expression was insignificant in ipRGCs when compared against generic RGCs. Differentially expressed Salm5/Lrfn5, Clstn2, Thbs1, Lrrtm2, Pcdh19, Ptprm, and Lrrc4c/Ngl1 cell-adhesion molecules are additional candidates for being important for ipRGC excitatory synapse formation. The cell surface glycoprotein Mdga1 is also differentially expressed in developing ipRGCs and is known to influence the formation and maintenance of inhibitory synapses (Pettem et al., 2013).

DISCUSSION

The extraordinary complexity and heterogeneity of the mature retina has created an obstruction for clarifying the genes important for the specialized function of ipRGCs. Our investigation into the gene expression profile of ipRGCs had two primary aims. First, we developed and validated an expression profiling method that characterized the differential expression of a purified population of ipRGCs compared to enriched generic RGCs. Second, we evaluated the differentially expressed genes that may be functionally relevant to the specialized

Opn4-mediated phototransduction cascade, the molecular programs key to differentiation and maintenance of ipRGCs into adulthood, neuronal excitability, enhanced survivability, and circuit development.

In our study, we demonstrated a robust method that combined enrichment of RGCs by magnetic-activated cell sorting and FACS for positively selecting the rare fluorescently labeled ipRGCs in parallel with generic RGCs for comparison of relative gene expression. First, we demonstrated that our ipRGC populations differentially express all markers known to be expressed in ipRGCs. Further, the lack of marker expression from potential contaminating populations, including abundant rod photoreceptors, validated that we were able to obtain a highly pure population of ipRGCs. We successfully adapted our isolation processing procedures from developmental age P5 to young adults, despite increasing challenge to obtain viable mature neurons (Lobo et al., 2006). Representative of the increasingly fragility involved with isolating adult neurons, our biological replicates from young adult mice required ten-fold more retinal tissue compared to young P5 mice to obtain a similar number of ipRGCs. This striking decrease in acquiring efficiency in adulthood is largely due to the inability of adult retinal ganglion cells to compensate for dissociation of dendrites and axons and removal from retinal environment. Optimizations such as magnetic-activated cell sorting proved vital to promoting survivability since our original attempts using the two-step immunopanning process (Barres et al., 1988) to enrich RGCs proved ineffective at isolating sufficient numbers of healthy adult ipRGCs (data not shown). Our isolation method and differential expression analysis allowed us to identify more than 75 differentially expressed genes in ipRGCs compared to generic RGCs. These genes belong to diverse functional classes, including transcription factors, RNA binding proteins, signaling molecules, secreted proteins, neurotransmitter receptors, vesicle trafficking, protein modification,

survival, and more that remain unknown.

Clarification of the ipRGC phototransduction cascade

Despite there being incredible progress deciphering the molecular components of the ipRGC phototransduction cascade over the last decade, many questions remain unanswered or uncertain. Contrasting with other studies, the gene expression profiling studies of Siegert and colleagues (2012) did not detect Gnaq expression in ipRGCs while it appears to be among the highest expressing $G_{q/11}$ subunits in our study. To date, the $G_{\beta\gamma}$ complex remains unknown, despite it providing an essential element in GPCR signaling cascades and additional possibilities for signal specificity. The beta subunit Gnb1 is by far the highest expressing, having 15-fold higher expression than the other subunits Gnb2, Gnb4, or Gnb5; while Gnb3 shows no expression (Figure 10). The gamma subunit Gng4 is differentially expressed in ipRGCs, potentially providing additional complexity to the Opn4 phototransduction cascade (Figure 9). If Gng4 acts similar to other members of its class, it could potentially enhance the Gq/11 subunit binding with GPCRs such as Opn4. In *Drosophila* photoreceptors (physiologically similar to ipRGCs), disrupting DAG kinase activity by mutating rdga leads to the accumulation of DAG and subsequently alters downstream PKC and TRPC activity(Raghu et al., 2000; Delgado et al., 2014). Rasgrp1 has both a calcium and a diacylglycerol binding domain and has well-described role in lymphocytes as a Ras GEF, a nucleotide exchange factor activating Ras through the exchange of bound GDP for GTP activating Erk/MAP kinase cascades(Bivona et al., 2003b). Additionally, Dgkg is a diacylglycerol kinase that enzymatically phosphorylates diacylglycerol to produce phosphatidic acid (PA)(Shulga et al., 2011). Notably, both Rasgrp1 and Dgkg have been shown to be expressed and play as yet unknown roles in subpopulations of neurons throughout multiple brain regions

including the hippocampus and striatum but their function in the retina remain largely unknown(Pierret et al., 2000a; Adachi et al., 2005; Bungers, 2010). Diacylglycerol and calcium are also known to activate the protein kinase C family members Prkcd and Prkcq, which are serine- and threonine-specific protein kinases. PKC activity has been suggested to be important for deactivating TRPC activity in the invertebrate photoreceptors and potentially also for the Opn4 phototransduction cascade. Interestingly, another Prkcz disruption has been correlated with being important for ipRGC-mediated photoentrainment of circadian rhythms(Peirson et al., 2007). However, Prkcz is only moderately expressed and similar to control samples in our study. Additionally, Prkcz is functionally perplexing due to lack DAG and calcium binding domains traditional on PKC members and Prkcz has not been physiologically for a direct, specific role in ipRGC phototransduction(MELLOR and PARKER, 1998). The differentially expressed gene Pirt has been shown to Pirt regulates PIP_2-dependent activation of TRP channels (TrpV1 and Trpm8), but has not been directly tested with TrpC6/7 channels relevant for ipRGC phototransduction(Kim et al., 2008a). As negative regulators of GPCR signaling, the differentially expressed genes Rgs4 and Rgs17 could fine-tune Opn4 signaling(Mao et al., 2004; Ji et al., 2011). Both Rgs17 and Rgs4 have also been shown to regulate opioid signaling in the brain via the GPCR, Oprm1(Georgoussi et al., 2006; Rodríguez-Muñoz et al., 2008). Oprm1, another differentially expressed gene in ipRGCs, is responsible for a variety of cellular responses, of particular interest is the inactivation of L-type calcium channels (main calcium influx mechanism in ipRGCs) and activation of inward rectifying potassium channels that could lead to current inhibition and modulated physiology of ipRGCs (Moises et al., 1994; Diaz et al., 1995; Doğrul et al., 2001; Alvarez et al., 2002; Dang and Williams, 2005). The lack of rod contamination in our ipRGC samples allowed us to closely investigate the phototransduction cascade components that may be shared with the classic rod and

cone photoreceptors (Beech and Barnes, 1989; Frings et al., 1998). The visual cycle of ipRGCs has also been remained a challenge to clarify. The location of ipRGCs within the inner retina, far removed from the RPE-process of the chromophore regeneration in the outer retina, makes it challenging to think that ipRGCs are using a similar mechanism as rods and cones. Further, the ipRGCs are similar to their drosophila counterparts in that Opn4 is bistable, plausibly even tristable(Emanuel and Do, 2015). This ability allows Opn4 to photoisomerase the all-trans-retinal independent of additional enzymes by capturing a photon with a second wavelength. Even with this exceptional capability, ipRGCs are considered to require some kind of additional mode of chromophore regeneration(Díaz et al., 2016). The expression of the isomerase Degs1 by ipRGCs in our studies suggests that they may share some of the same chromophore regeneration machinery used by Muller glia. However, we were unable to find expression of additional enzymes that would be required to complete the visual cycle in ipRGCs.

Specialized heparin sulfate modifications

The biosynthesis of heparin sulfate is a complex, multi-step process that requires the coordination of multiple pieces of enzymatic machinery. The first modification that occurs is catalyzed by N-deacetylase/N-sulfotransferase (NDST) and replaces N-acetyl groups on GlcNAc residues with N-sulfate groups, a prerequisite for later modifications in heparin sulfate biosynthesis (Zhang et al., 2016). The differentially expressed gene Ndst4 has restricted expression in adult brain tissue and may have a more specific role in adulthood than the other NDST members (Aikawa et al., 2001). The heparin sulfate D-glucosaminyl 3-Osulfotransferase 2 and 4 (Hs3st2 and Hs3st4) enzymes generate 3-O sulfated glucosaminyl residues on heparin sulfate. The main known role for this modification is that it is used as a receptor by herpes simplex virus type 1 and

therefore promotes pathogenesis in expressing cells(O'Donnell et al., 2006). Although not fully explored in the retina, Hs3st2 and Hs3st4 are the major neural benefactor of 3-O-sulfated residues in neuron subpopulations and may therefore provide specific HS-dependent functions(Lawrence et al., 2007).

Developmental control of ipRGC circuit formation

The molecular adhesion code important for M1 ipRGC circuit development has started to become deciphered. The repertoire of specialized M1 ipRGCs retinal circuitry includes reciprocal intraretinal interactions with dopaminergic amacrine cells (DACs) in the uppermost sublaminas of the IPL. DACs express the Sema6a receptor PlxnA4. Expression of Sema6a in the On layers of the IPL repulses Plxna4-expressing DAC dendrites and restricts their dendrites to the S1 sublamina of the IPL (Matsuoka et al., 2011). However, M1 ipRGCs were determined to not express either Sema6a or PlexinA4 in their studies, despite the fact that the dendritic architecture became mislocalized if either gene was knocked out. Therefore, these two cues were found to be important for M1 ipRGCs synapse specificity, but Mastuoka et al., (2011) suggested that they play non-autonomous roles in ipRGC dendritic development. In contrast, our studies suggested that Plxna4 is differentially expressed in P5 ipRGCs, which aligns with the Plxna4-knockout mislocalization phenotype and suggests that ipRGCs share a similar adhesion protein code as DACs. Visualization limitations of Plxna4 immunofluorescence labeling may mean that its endogeneous expression level is too low to be detected in ipRGCs. In our case, it is hard to know what the endogenous level of Plxna4 mRNA is in developing M1 ipRGCs and whether it is translated to a level of protein expression that could make a biological impact. Our results agree with their finding that Sema6a is repressed in ipRGCs, relative to other ganglion cells (Matsuoka et al., 2011).

Our studies also suggest the differentially high expression of Mdga1 in developing ipRGCs. The role of Mdga1 in regulatng inhibitory synapse formation may establish key connections between ipRGCs and specific GABAergic amacrine populations (Lee et al., 2013; Pettem et al., 2013). Our studies suggest that adhesion molecules such as Unc5a and Unc5d continue to be enriched in ipRGCs into adulthood. Both Unc5d and Unc5a have been shown to have distinct laminar expression patterns that coincide with stereotyped S1 OFF-region dendrites of M1 and S5 ON-region dendrites of M2 ipRGCs. As expected, Unc5b is very low expressing, while Unc5C expression is insignificant in ipRGCs when compared against generic RGCs (Visser et al., 2015).

The highly specialized, yet morphologically and physiologically homogeneous, M1 ipRGCs seem to have parallel pathways for controlling non-image forming functions. How the shared molecular adhesion code in retinal development of M1 ipRGCs coordinates with the differential axon targeting in the brain remains unknown. Our gene expression profiling studies of P5 ipRGCs may reveal molecular mechanisms important for M1 axon development including 1) stalling of the growth cone prior to innervation, 2) leaving the optic nerve towards the SCN, and 3) innervation and refinement in functionally compartmentalized suprachiasmatic nucleus (reviewed by Fox and Guido, 2011). The same general process may also be similar, yet specialized, to M1 targeting to the OPN shell. Multiple genes identified by our studies to be differentially expressed in P5 ipRGCs may be relevant for ipRGC-specific axon targeting (Figure 16). Wnt4 is differentially expressed in postnatal ipRGC samples, but its expression is strikingly absent in adult ipRGCs and other RGCs. Wnt4 is known to be a secreted signaling protein that plays a chemoattractant role for regulating axon guidance during neuron development (Lyuksyutova et al., 2003; Mulligan and Cheyette, 2012). Tenm1 is significantly enriched during ipRGC postnatal

development and adulthood (Figure 16). Teneurins family members (Tenm2 and Tenm3) have well-characterized roles for promoting precise patterns of connectivity in the visual pathway(Leamey et al., 2007; 2008; Tran et al., 2015). They have homophilic adhesion properties, but there are also examples of heterophilic binding partners(Leamey and Sawatari, 2014). The metalloprotease Adam10 is differentially expressed in postnatal ipRGCs and has well-described roles in regulating axon growth cone pathfinding and retinal development (Mu et al., 2005; Brennaman et al., 2014; Toonen et al., 2016). The neural adhesion molecule CHL1 is differentially expressed in postnatal and adult ipRGCs and may mediate axon guidance and maintenance of neural circuits(Wright et al., 2007; Schlatter et al., 2008). This semaphorin Sema5a has been demonstrated to be important for the development of connections between neurons and inhibiting the growth of RGC axons, but was suggested glia-specific expression (Goldberg et al., 2004). The relatively low expression of the Irx4 transcriptional repressor found in our studies may also be relevant to molecular program controlling ipRGC axon pathfinding of in the developing retina (Jin et al., 2003).

The ipRGCs are known to have the capacity to shape the development of visual neural circuits (Renna et al., 2011). In mice, within a week of birth, RGC axons are already establishing and refining projections to visual brain centers, and retinal waves play a crucial role in this process. The starburst amacrine cells generate and propagate retinal waves through the release of acetylcholine (ACh), leading to the coordinated excitation of most, if not all RGCs, including ipRGCs (Renna et al., 2011). It is widely assumed that such excitation is also mediated by ACh released from the starburst network acting directly on nAChRs on the RGCs (Ford and Feller, 2012). However, it has remained unclear which subunits of nAChRs are expressed on ipRGCs during developmental retinal waves and whether they persist into adulthood despite their lack of

dendritic stratification in the appropriate layer to receive synaptic input from SACs and apparently lack functional nAChRs (Wong et al., 2007a; Ecker et al., 2010). Our studies suggest that multiple alpha subunits (α3, α4, and α6) are expressed in combination with the β2 and β3. In contrast, the gene expression profiling studies of Siegert et al., (2012) only deciphered α6 and β3 subunits, which were broadly expressed across all transgenic reporters that labeled RGC types. We did not distinguish any clear up- or down-regulation of cholinergic subunit expression between P5 and adult ipRGCs.

Enhancement of ipRGC survival

Our results have important implications for studying the increased survivability of ipRGCs in rodent models of retinal degeneration (Cui et al., 2015). The neuropeptide Adcyap1/PACAP was differentially expressed in our studies and has been previously shown to be specifically expressed in ipRGCs and play a neuroprotective role in animal models of RGC death in response to monosodium glutamate toxicity, mitochondrial dysfunction, and axotomy(Li et al., 2008; de Sevilla Müller et al., 2014; Cui et al., 2015). A major component of glaucoma is pro-death signaling pathways that are activated soon after axonal injury. In mouse glaucoma models, JUN-dependent pathways have been determined to be important for promoting axonal injury-induced death(Levkovitch-Verbin et al., 2005). In another study, decreasing JUN activation provides at least some protection to axotomied RGCs. Our studies suggest that the transcription factor JUN (Jun Proto-Oncogene) may be differentially repressed in ipRGCs. Therefore, reduced JUN signaling may provide beneficial to the survivability in ipRGCs. Increased glutamate release in the retina can lead to a deleterious rise in intracellular calcium that leads to degeneration in RGCs (Sucher et al., 1997). This process seems to be mediated by ionotropic NMDA receptors (Sucher

et al., 1997; Shen et al., 2006). NMDA-induced excitotoxicity is often used to study the mechanisms leading to RGC death and neuroprotection potential (Goldblum and Mittag, 2002; Niwa et al., 2016). M1 ipRGCs are especially resistant to glutamate-induced toxicity (DeParis et al., 2012). Our studies show that the modulatory subunit Grin3a is differentially expressed in ipRGCs and Grin3a has been shown to dramatically decrease calcium flow through NMDA channels and provide resistance against NMDA-mediated excitotoxicity(Henson et al., 2010; Cui et al., 2015). Expression localization studies have suggested that Grin3a is not selectively expressed in ipRGCs. However, it is possible that the combination of Grin3a with intrinsic photosensitivity capabilities allow ipRGCs to survive, while other Grin3a expressing RGC types may not survive our experimental processing prior to sequencing and gene expression analysis. In other words, the control samples enriching for generic RGCs may be biased against RGCs that are sensitive to stressful environments such as glutamate toxicity. This experimental caveat is especially relevant when looking for survival relevant genes in our differential expression analysis of ipRGCs. Finally, the differentially expressed transcription factor Nr4a3 is known to be induced as early immediate genes by stressors and play important role in maintaining cellular homeostasis (Safe et al., 2016).

Comparison with other ipRGC gene expression profiles

We also sought to compare our gene expression results with previous studies that have identified differential gene expression in ipRGCs (Figure 18). Siegert and colleagues (2012) used many different mouse reporters (including the *Opn4-Cre* system) to isolate different subsets of retinal cells for microarray gene expression profiling. Their study is similar in that it relied on harsh dissociation processing from FACS isolation of adult fluorescently labeled cells. Many of

the genes highlighted in their study were also determined to be differentially expressed in our study. However, the dozens of additional genes that we determined to have a high likelihood of differential expression in ipRGCs were were either undetected or indistinguishable across their gene expression profiles. This discrepancy of differentially expressed genes may be due, at least in part, to the following reasons. First, their study did not include a pre-enrichment step for retinal ganglion cells and, from our studies, makes it that much more challenging to isolate the rare labeled cells of interest (estimated 0.05% in the case of *Opn4-Cre* labeled ipRGCs) compared to the photoreceptors that account for 70-80% of retinal cells (Jeon et al., 1998). Indeed, their results were compromised from rod contamination across samples and they needed to compensate by the *post hoc* application of a strict differential expression threshold. Second, they did not include a control population to be processed in parallel to their isolated sample. We have found that providing an internal control by purifying generic RGCs in parallel to ipRGC samples was vital for controlling for stress-induced expression changes and the day-to-day variation across the many processing steps of the experiment and laboratory environment. Our ability to compare to generic RGCs allowed for broad correlations such as presence or lack of expression, despite the caveat that contaminating cell populations are present in the generic RGC population. Third, Siegert et al. used the microarray platform, which has limited coverage of probes along a target gene and has a smaller dynamic range compared to RNA-seq.

The other study that we compared against used the recently developed Drop-seq technology to process single cell suspensions from mouse retina for single-cell transcriptomic analysis at a massive scale(Macosko et al., 2015). Single cell technology is ideal, in principle, for the precise identification of an individual neurons molecular identity despite the extreme heterogeneity of the nervous system. The main challenge for this type of analysis stems from the

physical limits of capturing and sequencing a complete representation of the minuscule level of genetic material in a single neuron. Therefore, this technology operates best when multiple instances of a cell type transcriptional landscape can be compared and averaged. This is especially problematic for the retina tissue, which is not only extremely heterogeneous, but the odds of capturing the highly diverse subpopulations of neurons are especially low. Whereas there are roughly 30 distinguishable types of RGCs that total about 1% of retinal cells, there are less than a handful of photoreceptors that are far more common (75%). Indeed, their studies could definitively distinguish the main broad class of RGCs, but they required *post hoc* supervised analysis to distinguish a limited number of genes attributed to Opn4-positive cell clusters. They identified nine genes with a two-fold increase in expression compared to Opn4-negative cells. Three genes (Tbr2, Igf1, and Tbx20) were also found to be enriched in our ipRGC samples (Figure 18). In contrast, Tbx20 did not reach above threshold for Siegert et al., (2012), but it is among the highest expressing ipRGC-enriched genes in our study. Single-cell gene expression profiling methods such as Drop-Seq holds great promise and will certainly continue to be pursued more in future studies of neuron subtype gene expression. Recently, single-cell studies of pre-enriched bipolar cells were able to distinguish molecular markers for all previously recognized bipolar cell types (Shekhar et al., 2016). Future experiments with a pre-enrichment step for RGCs should help provide sufficient numbers to decipher subtype-specific programs of ipRGCs.

Further considerations

Our identification of differentially expressed genes in ipRGCs can not be assumed to be specific to ipRGCs or reflect the expression of functional proteins. Instead, DEGs should be treated as hypothesis for genes that are functionally relevant for ipRGC function. Although our selection

criteria dramatically decreased the potential heterogeneity obscuring differential gene expression in ipRGC, the transgenic reporters used in our studies are known to label multiple morphologically and physiologically distinct ipRGC types. For example, genes determined to be differentially expressed using the *Opn4-GFP* reporter can, at best, be inferred to have restricted expression within the M1-M3 ipRGC types. However, it would be impossible to know whether this gene is expressed in all M1-M3 types or a subset. Further, we can not assume that differentially expressed genes in our studies are uniquely expressed in ipRGCs and absent in non-ipRGCs. Our studies are based on relative abundance of ipRGCs compared to our generic RGC populations. We can not rule out scenarios that differentially expressed genes are enriched in ipRGCs, but are also expressed in additional subsets of other RGCs. Therefore, follow-up localization studies using *in situ* hybridization or immunofluorescence will be required to test the validity and cell type-specific expression of our proposed differentially expressed genes. Additionally, the study of transcriptomes and differential gene expression has certainly proven important for revealing otherwise unknown molecular underpinnings to specialized cell function. However, the transcription of genomic DNA to mRNA is only one of many intermediate steps to the synthesis of functional proteins(de Sousa Abreu et al., 2009; Maier et al., 2009; Koussounadis et al., 2015). Translational control, post-translational modifications, and subcellular localizations are examples of ways that the level and function of proteins can be decoupled from the relative abundance of mRNA expression. Additional immunofluorescence studies using protein peptide-specific antibodies is one way to test whether candidate differentially expressed genes are correlated at the protein level.

Conclusion

In conclusion, our results demonstrate a method to purify ipRGCs and identify an extensive list of more than 75 genes that are differentially expressed compared to generic RGCs. Of course, our identified DEGs in ipRGCs should not be considered a complete account of all genes relevant to ipRGC function. Instead, we hope that it will provide a beneficial resource that will generate hypothesis that lead to key insights into ipRGC function in non-image forming vision.

Figure 1. The intrinsically photosensitive retinal ganglion cells (ipRGCs) are distinguished, in part, by their special ability to independently respond to light stimulation. a) Distinguishing anatomical, molecular, physiological, and circuitry characteristics of the initially described ipRGC subtype "M1." b) The known mechanisms of Opn4 phototransduction cascade, distinct from the phototransduction machinery used by the relatively much more common rods and cone photoreceptors. Please see text for further details.

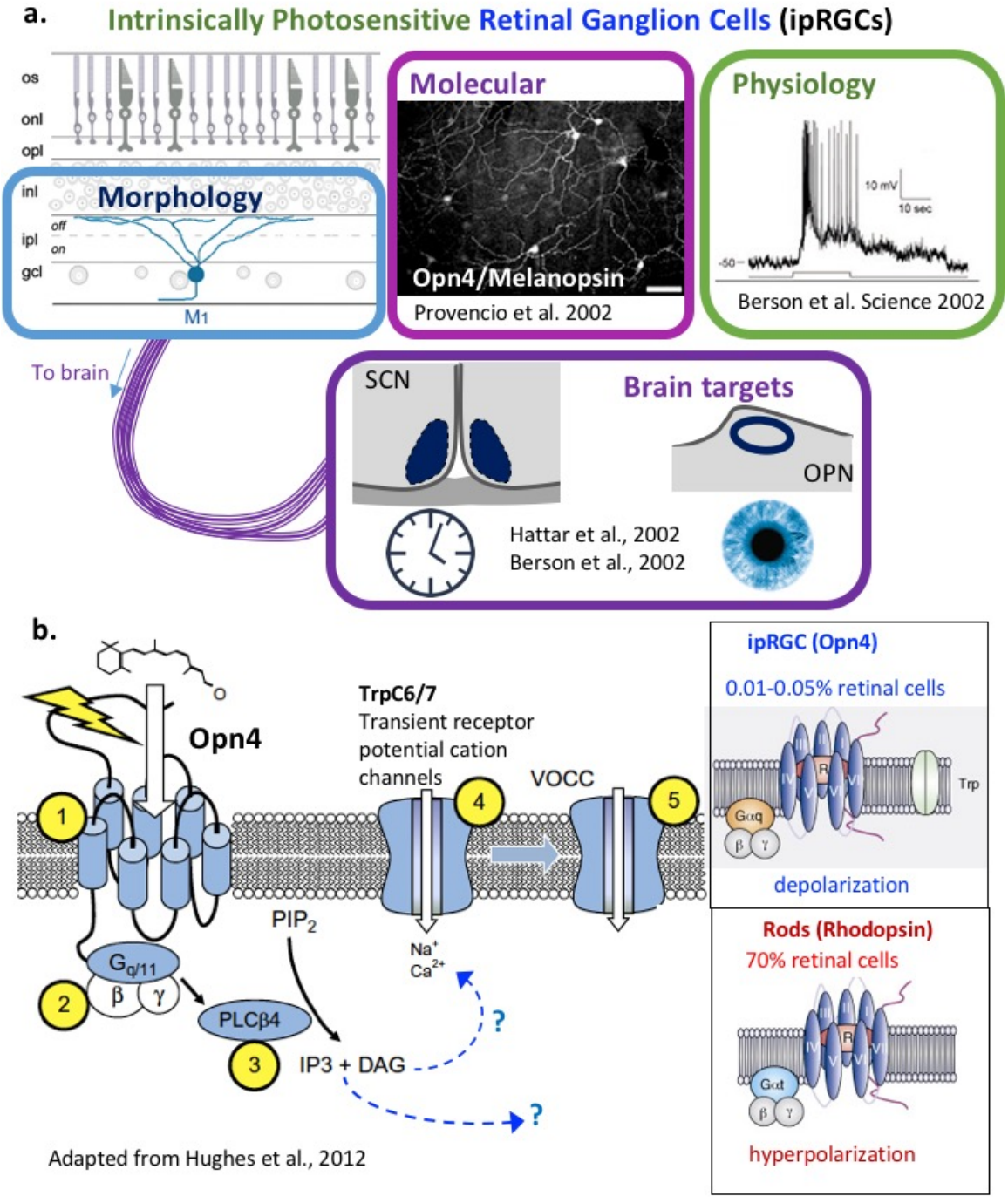

Figure 2. Transgenic mouse reporters have revealed multiple, anatomically distinct ipRGC subtypes. a) Schematic diagram of stratification and general dendritic architecture of M1-M6 ipRGCs (including recently described M5 and M6 types). Opn4-GFP reporter has enabled the study of M1-M3 ipRGC subtypes while the Opn4-Cre reporter system lead to the discovery of additional members (M4 and M5). b) The Cdh3-GFP reporter preferentially labels the newly classified M6 type and are considered to project to non-image forming targets olivary pretectal nucleus (OPN) and ventral lateral geniculate nucleus (vLGN). **c)** Summary schematic of predominant targets of ipRGC subtypes in the brain.

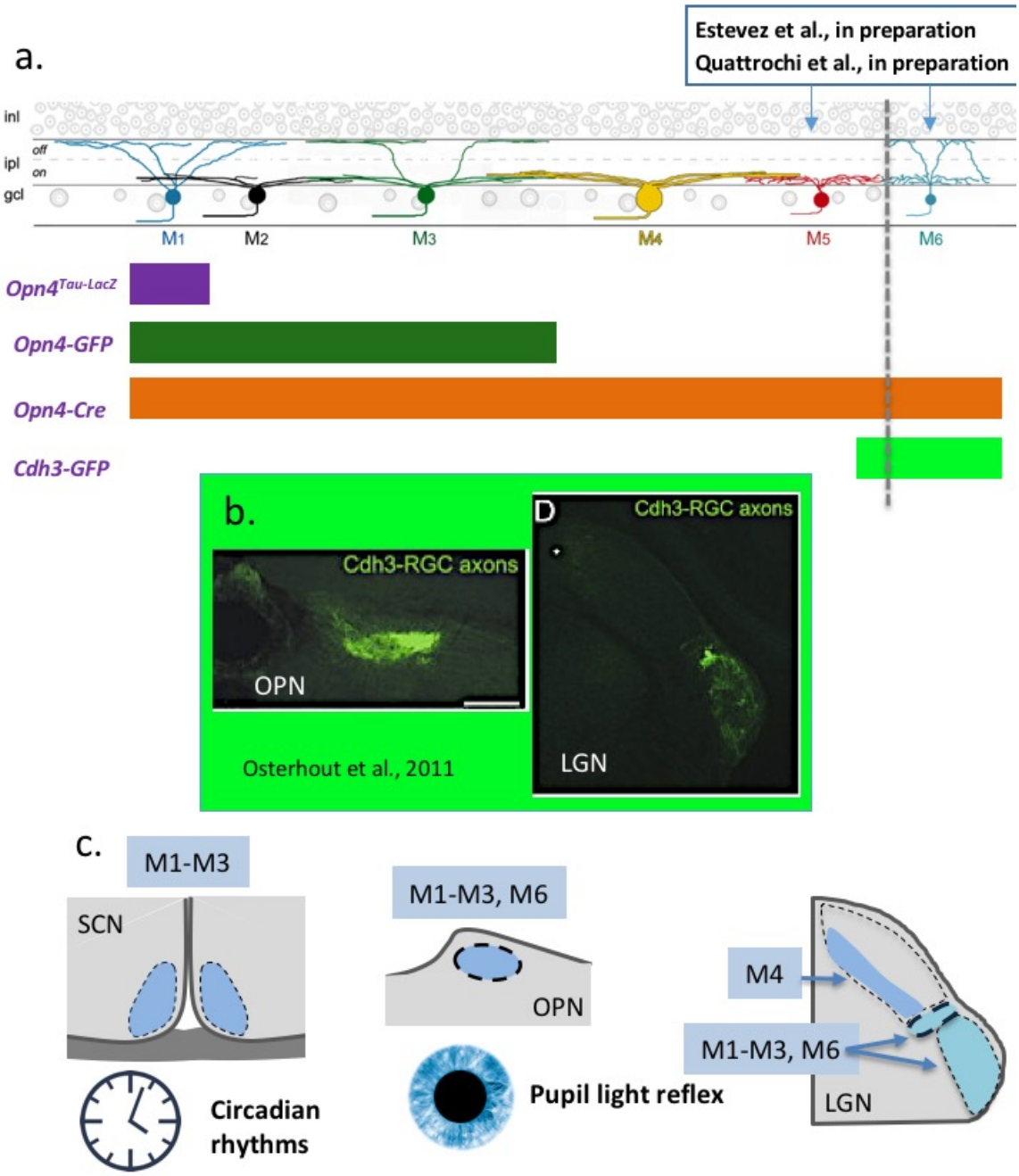

Figure 3. The generation and differentiation of the many types of neurons in the eye have a stereotyped timing and molecular program. a) RGCs progress through a stereotyped molecular program involving a hierarchy of transcription factors that sequentially differentiates the initial progenitor cell to a RGC fate. Although the developmental program is well-characterized, the program that leads to the terminal differentiation of the more than 30 subtypes of RGCs in the adult retina is poorly understood. b) Dendrite development of M1 ipRGCs. c) Development of M1 ipRGC axons targeting olivary pretectal nucleus (OPN) and suprachiasmatic nucleus (SCN).

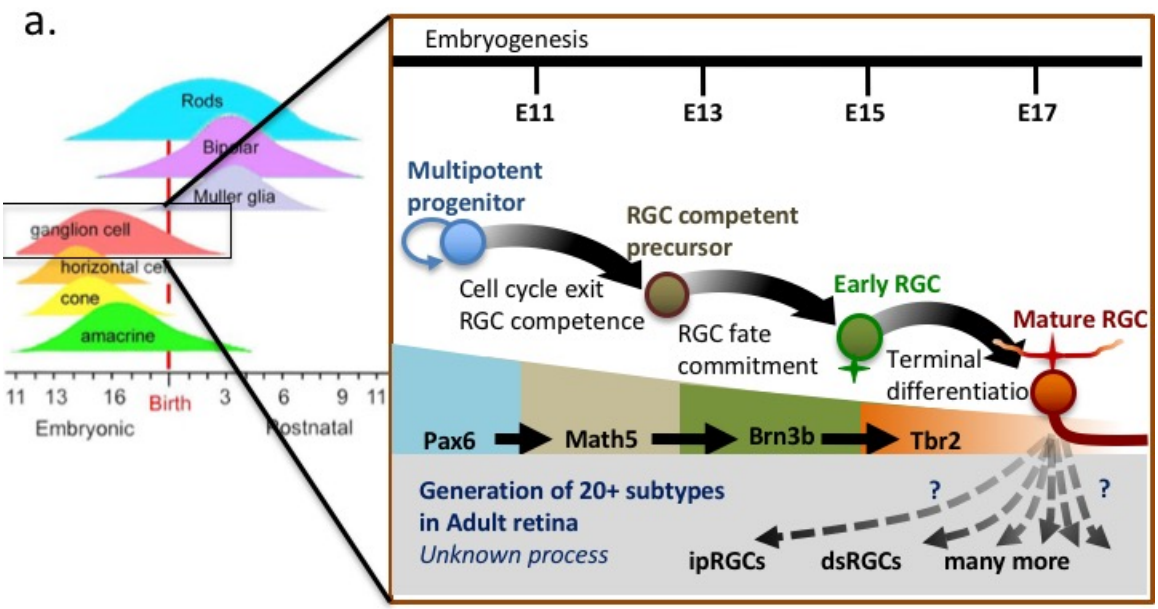

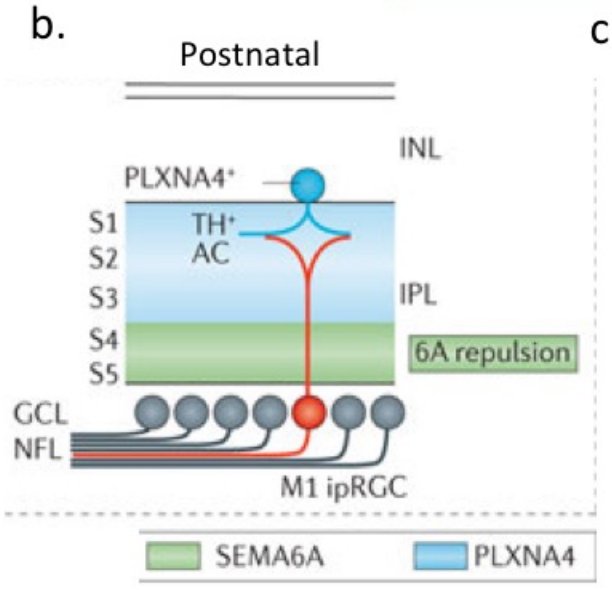

Pasterkamp et al., 2012

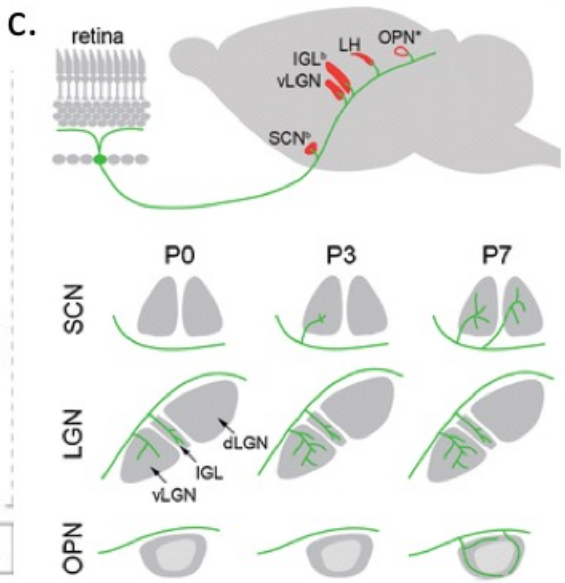

Fox and Guido, 2011

Figure 4A. Coexpression of BAC transgenic Opn4-GFP reporter with Opn4 immunoreactivity.

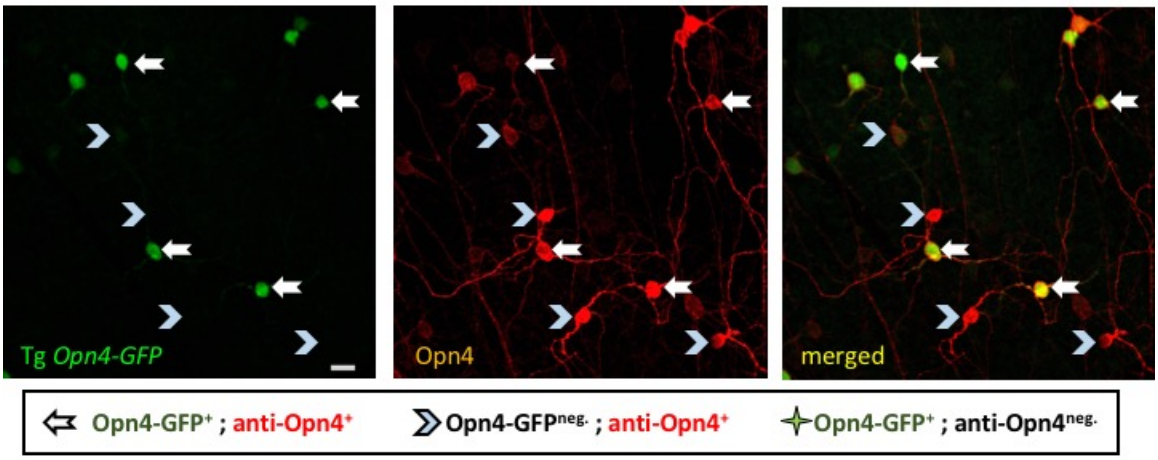

Immunofluorescence of anti-Opn4 staining of whole mount retina from transgenic Opn4-GFP mice with fluorescent protein expression in ipRGCs. Red, Opn4-immunolabeling; green, fluorescently labeled cells; yellow, merged co-localized labeling pattern. Scale bar, 20 µm.

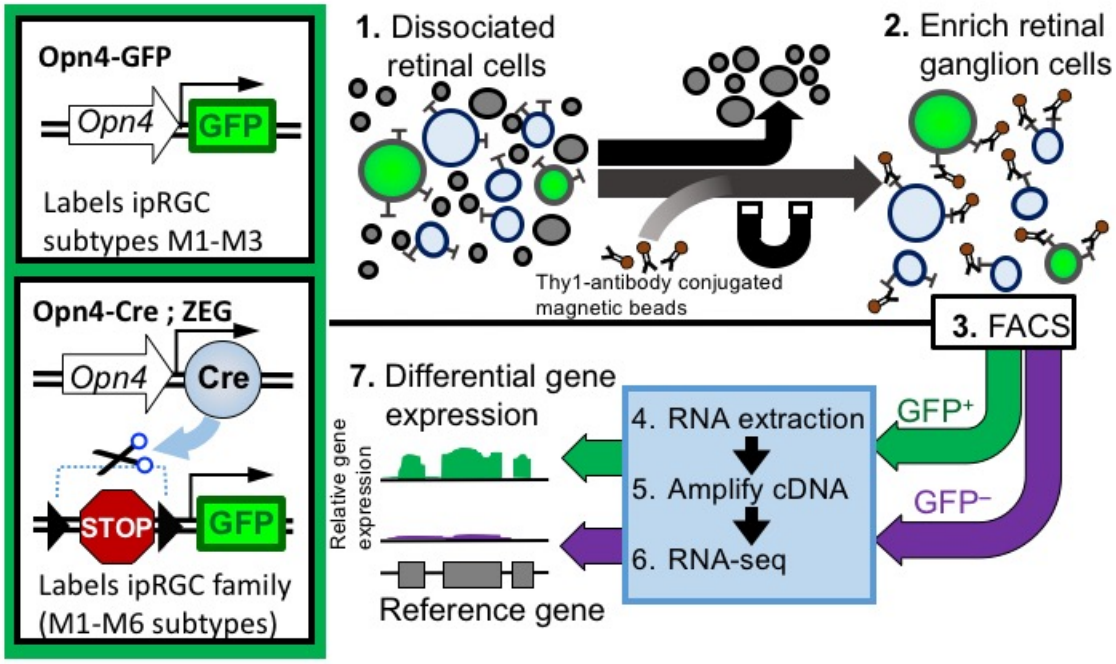

Figure 4B. Experimental design of gene expression profiling from purified ipRGCs and comparison with enriched RGCs. Left panel: Two transgenic reporters were used for gene expression profiling of ipRGCs. The BAC transgenic Opn4-GFP labels M1-M3 ipRGC subtypes while the Opn4-Cre combined with a cre-dependent GFP reporter labels M1-M6 ipRGCs. 1) enzymatically dissociated retinas for downstream isolation of cell populations. 2) The Thy-1 surface protein is enriched on retinal ganglion cells. Therefore, I used Thy1-conjugated magnetic beads to enrich for RGCs. 3) FACS isolation of GFPpositive cells (ipRGCs) and GFP-negative cells(RGCs). These two populations were simultaneously isolated in parallel to provide direct internal testing of ipRGCs versus RGCs under same treatment, conditions, and genetic background. 4-5) mRNA extraction, cDNA processing and amplification. 6) RNA-seq library preparation using Tru-Seq adapters. 7) illumina HiSeq, single-end, 50bp, multiplexed (concatenated additional technical replicates). Differential expression analysis using count-based EdgeR pipeline. See methods section for additional information.

Figure 5. A. Fluorescence activated cell sorting (FACS) gating strategy for isolating ipRGCs (GFP+) in parallel with GFP-negative cells that are enriched for RGCs. **B.** Healthy cells were selected against death marker 7-AAD (not G1). GFP+ and GFP- cells were selected based on intensity and similar relative cell size ultimately using gates G2A and G3A, respectively. C. Example sort from young adult, noticeably higher debri and cell death. **D.** Microscopy testing of accurate sorting of GFP+ cells.

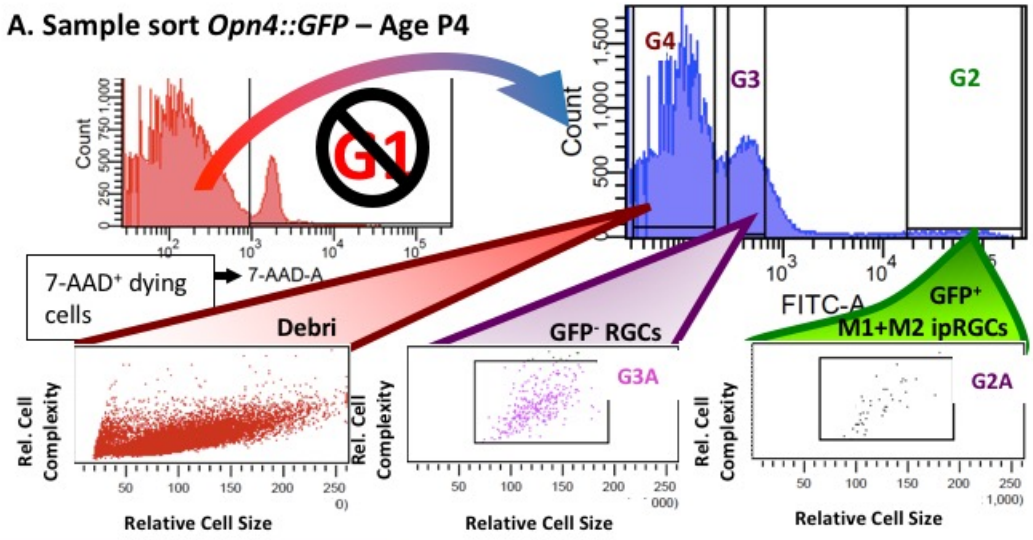

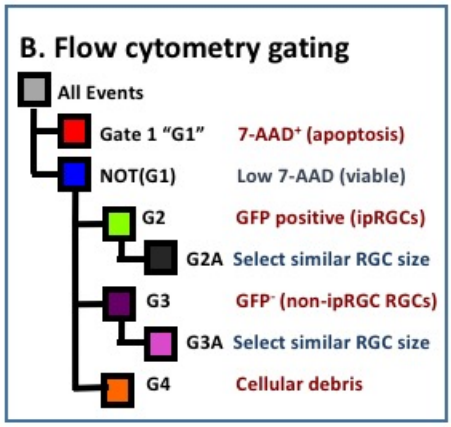

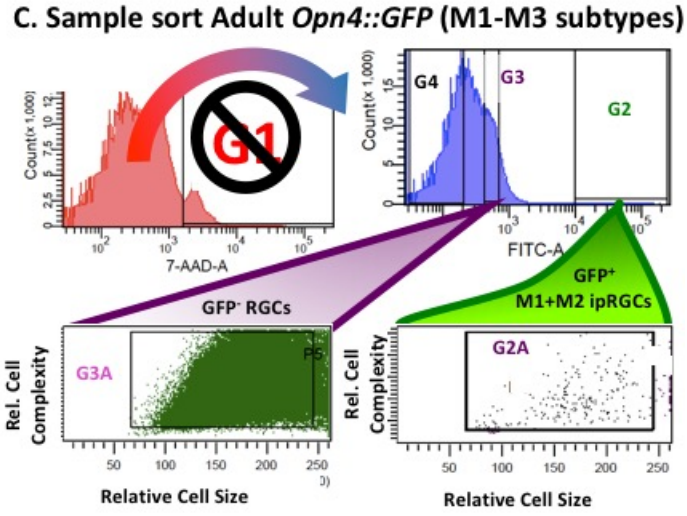

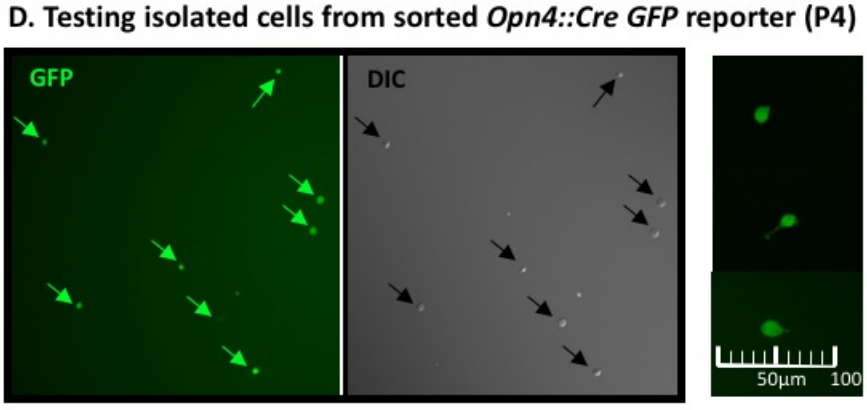

Figure 6. Steps involved with processing mRNA extracted from purified cell populations and preparing for RNA-sequencing

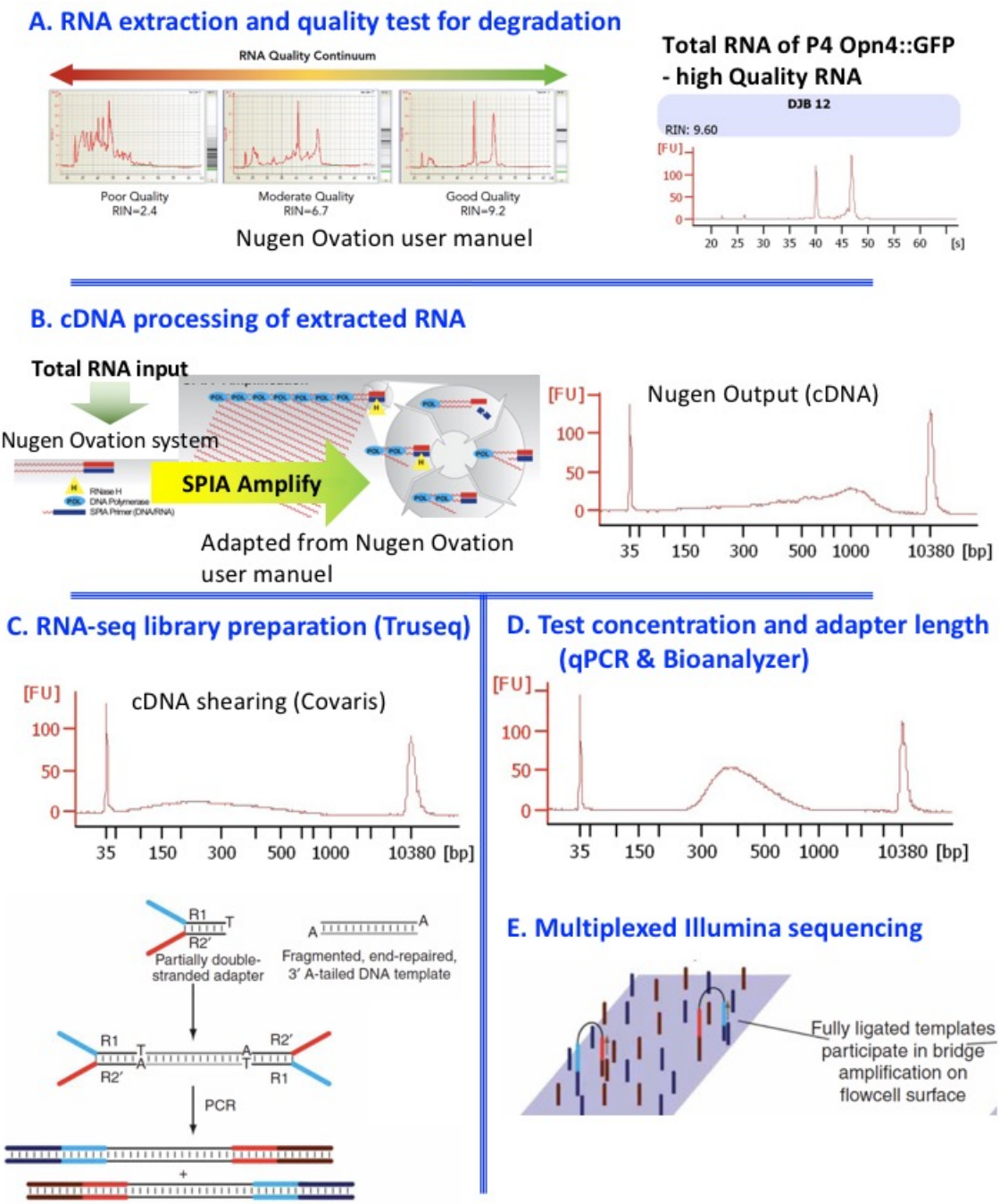

Figure 7. Sequencing reads and differential analysis pipeline. a) Summary of sequencing samples and resulting number of raw reads from sequencer. b) Pipeline

a.

Opn4-GFP
(M1-M3 ipRGCs)

raw reads	GFP+ sample		GFP- sample	raw reads
95016286	**DJB0007***		**DJB0008***	90897302
44201103	**DJB0030***		**DJB0031***	43690608
45578821	**DJB0028***		**DJB0029***	49110355
49661171	**DJB0016***		**DJB0021***	47265858
10724088	**DJB0036**		**DJB0037**	11294631
11377625	**DJB0038**		**DJB0039**	22789777

Opn4-Cre/ZEG
(M1-M6 ipRGCs)

raw reads	GFP+ sample		GFP- sample	raw reads
109774976	**DJB0005***		**DJB0006***	96032720
98636762	**DJB0022***		**DJB0023***	110267207
64188702	**DJB0032***		**DJB0035***	68930442
21602002	**DJB0040**		**DJB0041**	22028459

*** concatenated technical replicates**

b.

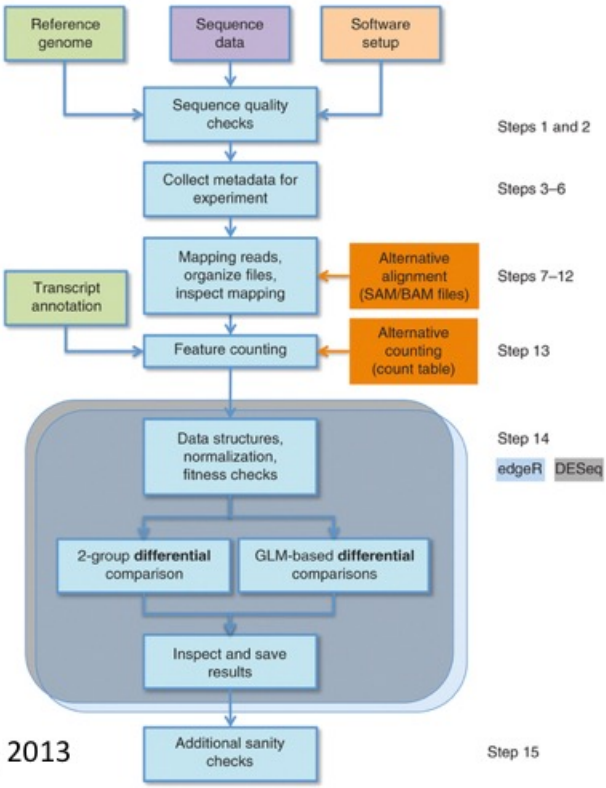

Anders et al., 2013

Figure 8. EdgeR multi-dimensional scaling (MDS) plot visualizes the overall similarity between expression profiles of different samples. Numbering system represents paired ipRGCs (GFP+) replicates with respective generic RGCs (GFP-) replicates (i.e., 03 processed in parallel with 04, 24 with 25, 42 with 43). Distances are approximately the log2 fold changes between samples. Green ovals represent ipRGC (GFP+) samples, while gray ovals represent generic RGC control samples. Adapted from EdgeR simple graphical output of individual samples in 2D space.

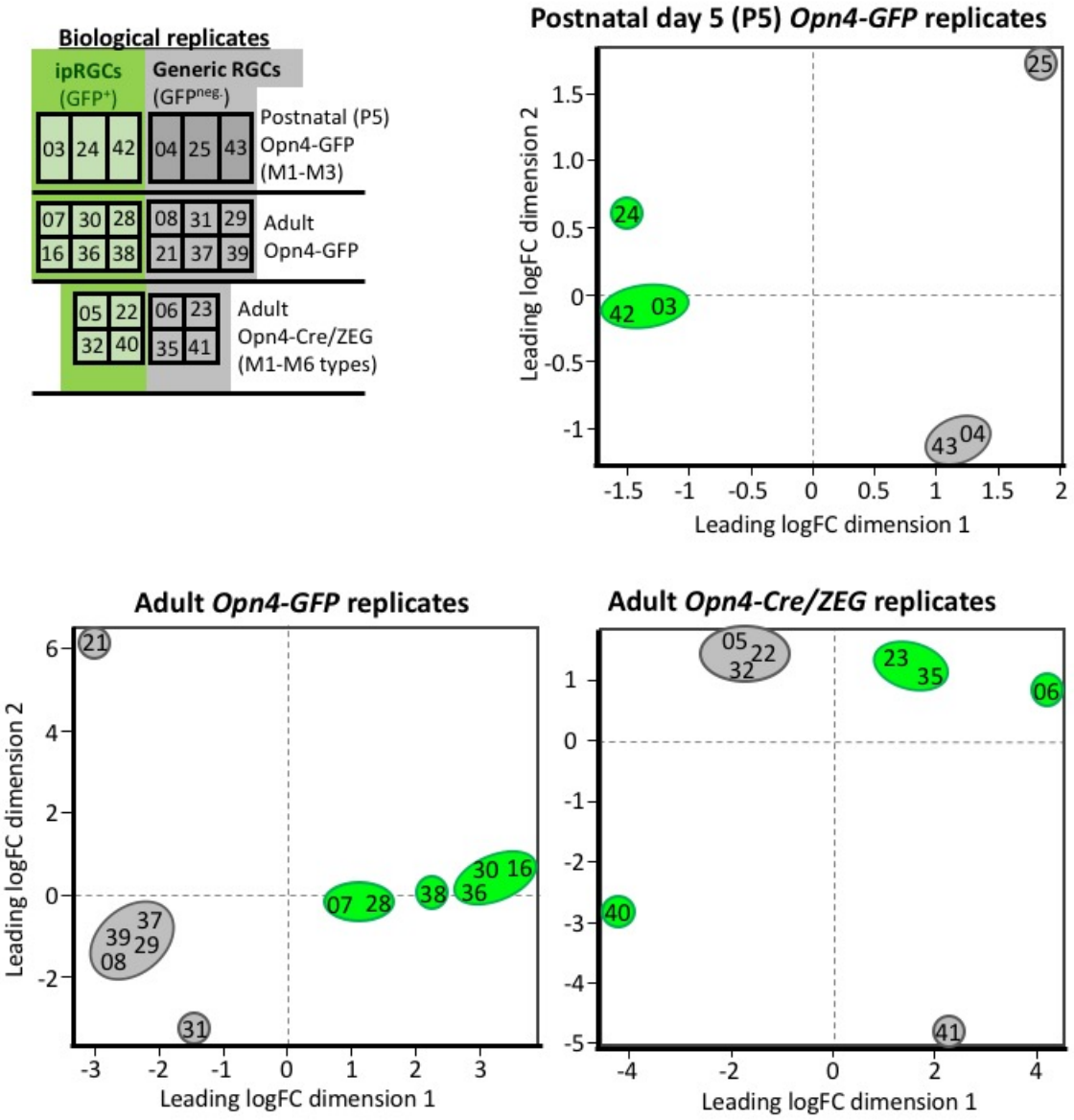

Figure 9. a) Raw reads were aligned to the genome and counts computed for each gene. b) Example heat map of expression for three hypothetical genes, including differentially expressed Opn4. Expression values are color-coded as represented in figure: blue indicates absent or low expression, red relatively moderate expression, and white indicates relatively highest expression (log2 scale). The median gene expression value across samples for (log2 scale) of ipRGCs (GFP+) and generic RGCs (GFP-negative) are flanking a bar-scale representation for fold-change (yellow indicates ipRGC-enriched expression, blue indicates enrichment in generic RGC samples. False discovery rate (FDR) symbolically represented as being statistically significant (green circle, <0.05), borderline (yellow triangle, <0.1), or not statistically significant (red diamond, >0.1). Genes much more highly expressed in ipRGCs relative to generic RGCs were identified primarily by high fold change (compare counts of ipRGCs vs. controls) and significant false discovery rate (FDR<0.05).

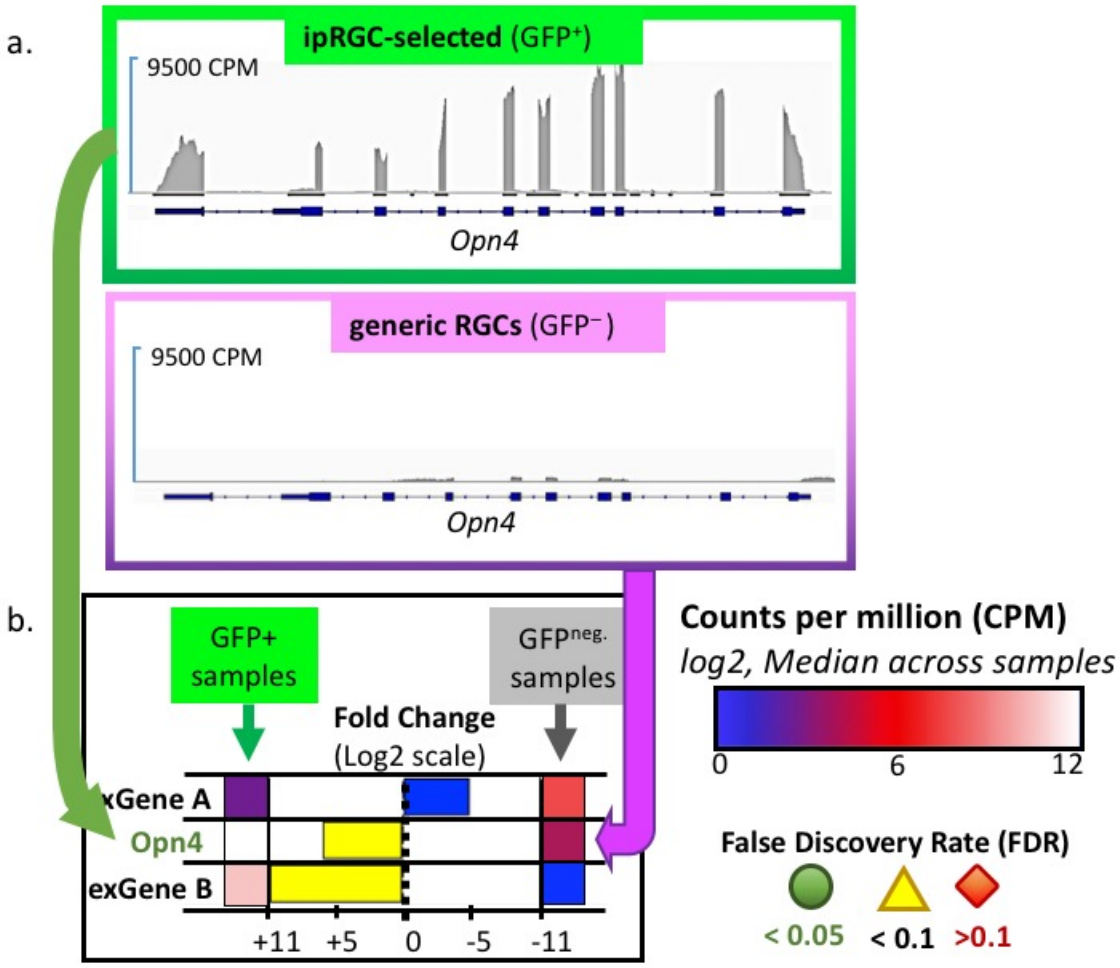

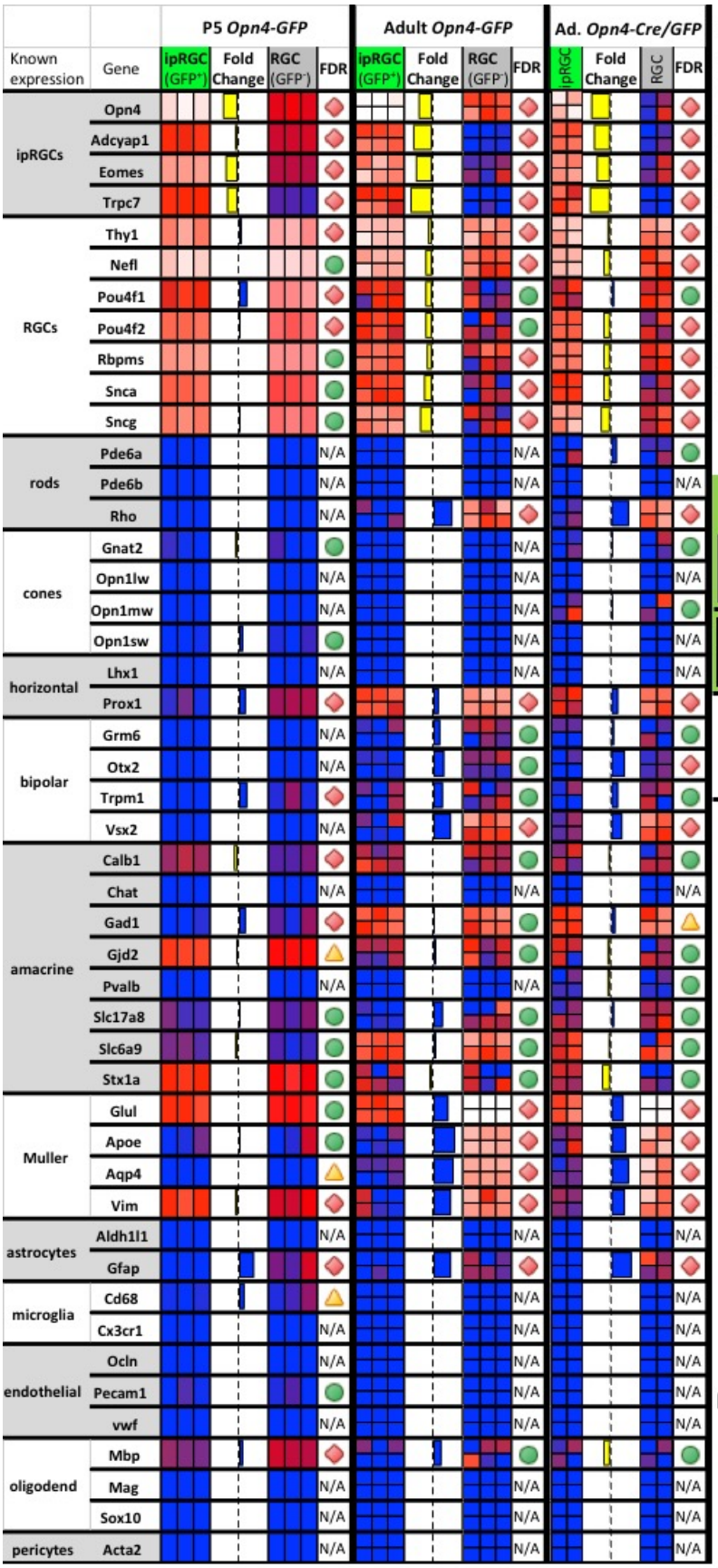

Figure 10. Heat map of known cell type marker gene expression in the retina to assess purity and cell composition of ipRGC and generic RGC samples. Shown are biological replicates tested for *Opn4-GFP* (P5 and adult) and *Opn4-Cre/GFP* reporters. Relative expression levels, fold change, and FDR are color-coded as indicated in the figure. White boxes indicate high gene expression, while blue represents little or no detected expression.

N/A = FDR not available due to gene expression count values being below detection (zeros) for all samples of given mouse reporter

Figure 11A. Heat map of genes differentially expressed in ipRGCs that have functional links to GPCR signaling and regulation of molecular programs. Relative expression levels, fold change, and FDR are color-coded as indicated in the figure.

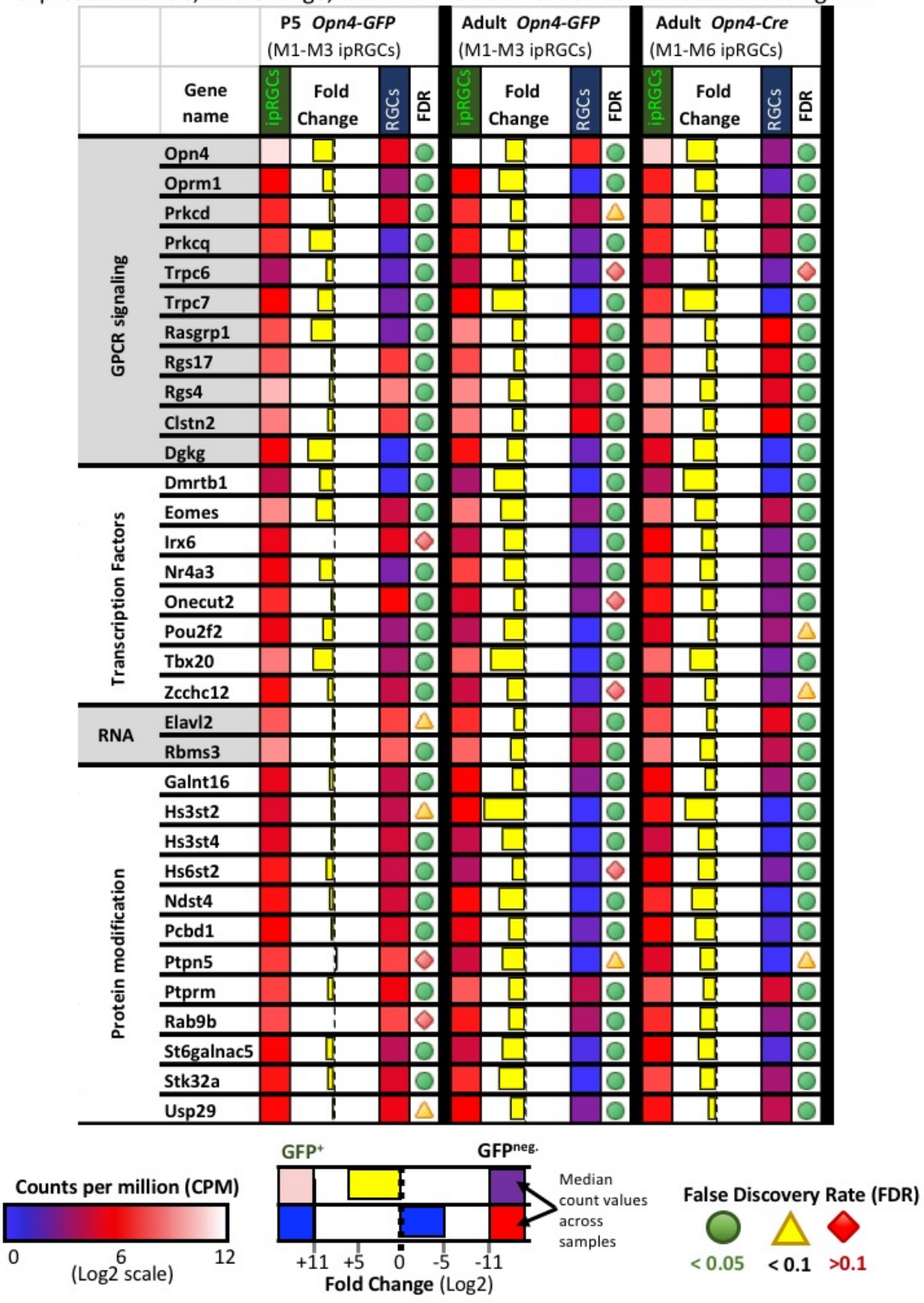

Figure 11B. Heat map of genes differentially expressed in ipRGCs that have functional links to neuron communication and organization. Relative expression levels, fold change, and FDR are color-coded as indicated in the figure.

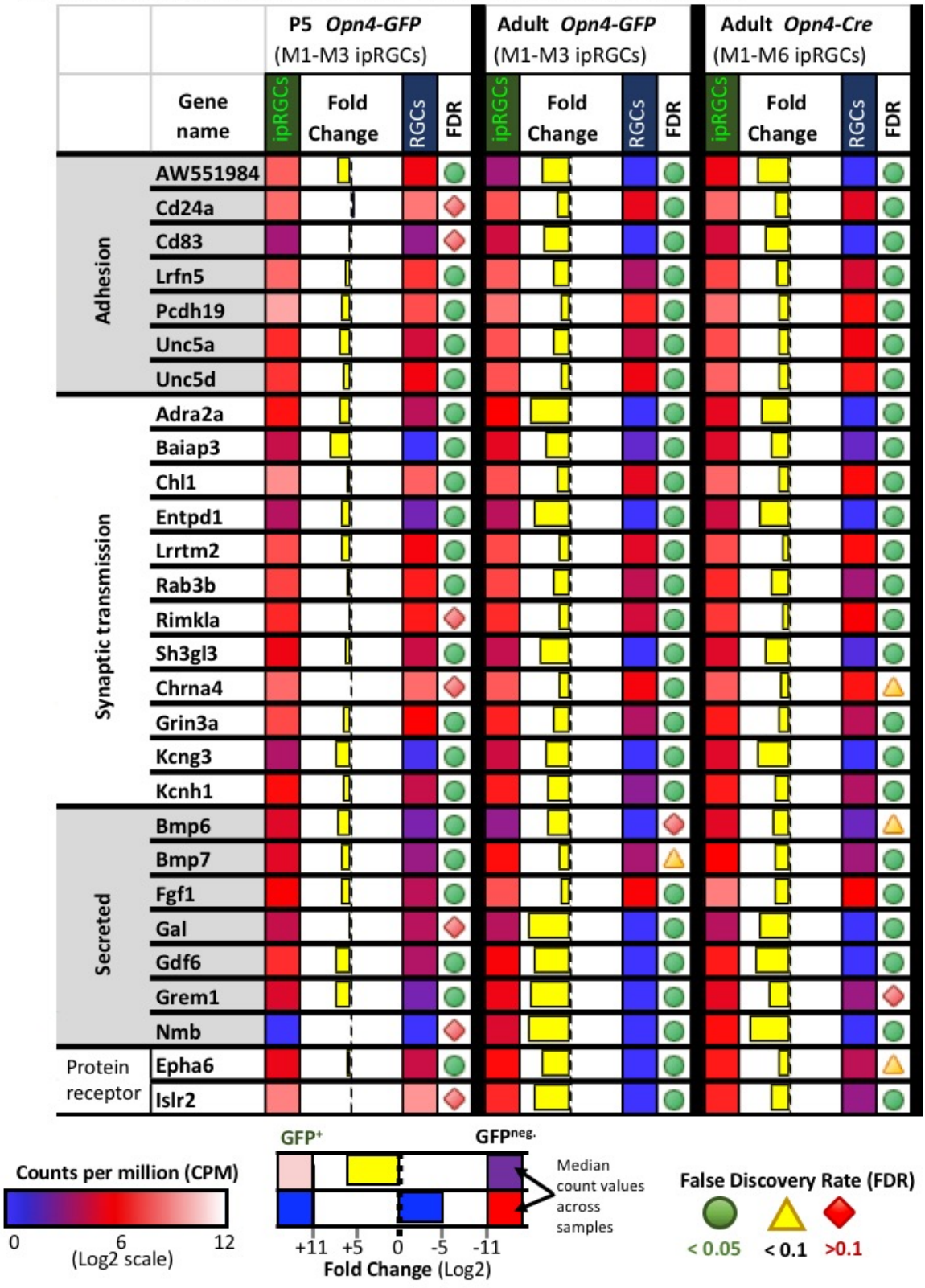

Figure 11C. Heat map of genes differentially expressed in ipRGCs that have functional links to neuron survival and neuron-glia interactions. Relative expression levels, fold change, and FDR are color-coded as indicated in the figure.

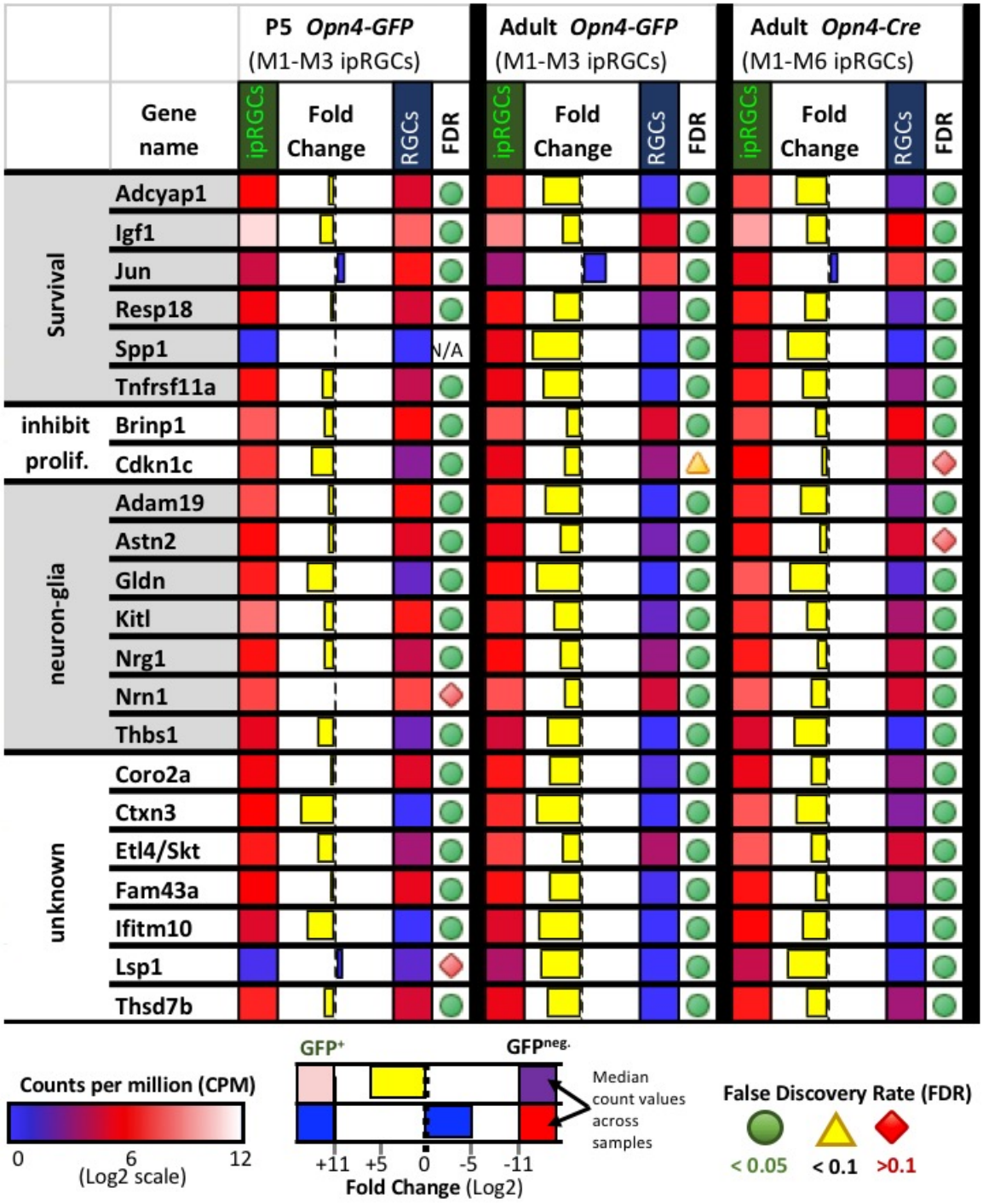

Figure 12. Heat map of genes that are potentially relevant to the Opn4-mediated phototransduction signaling cascade. Relative expression levels, fold change, and FDR are color-coded as indicated in the figure.

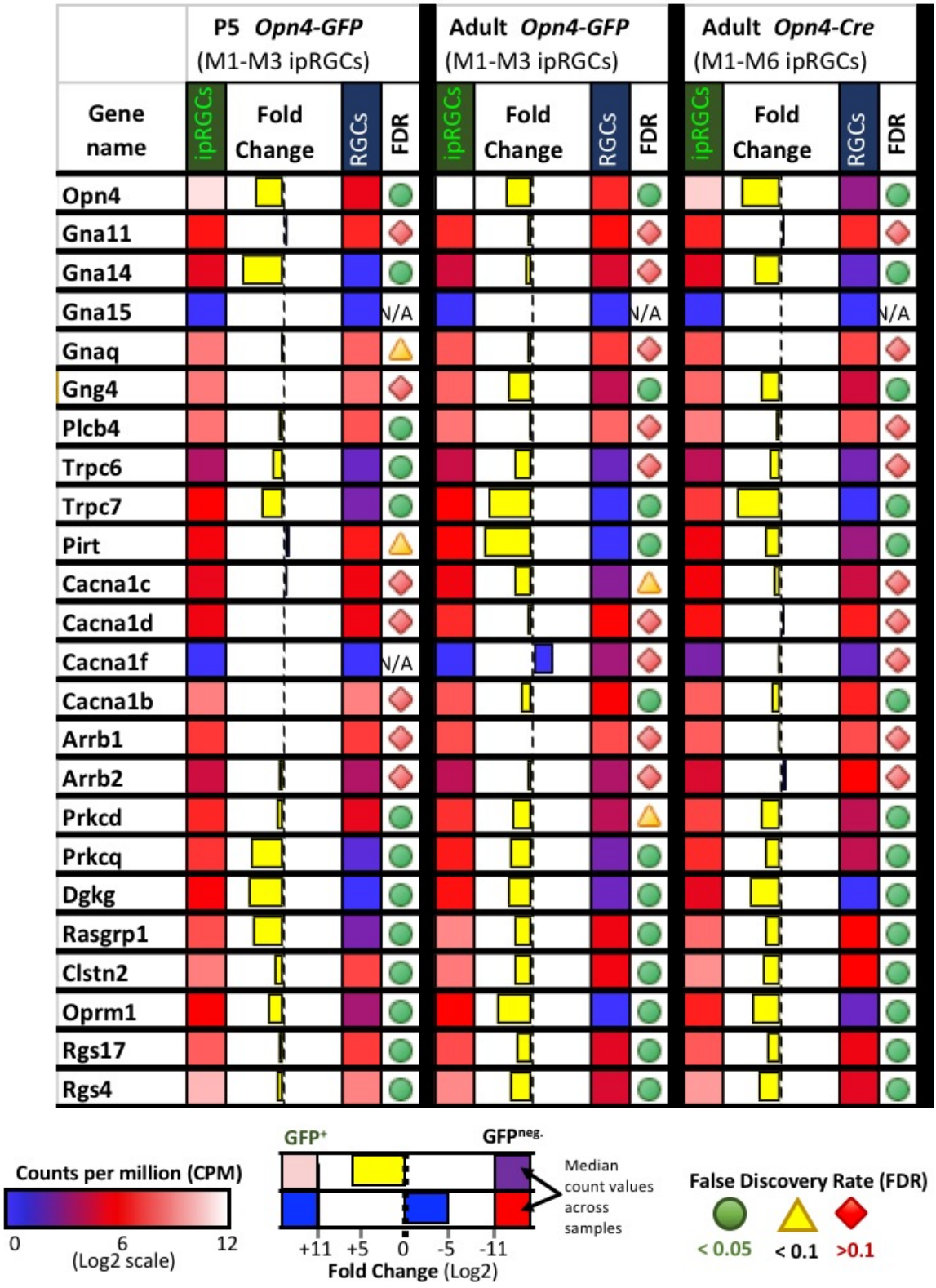

Figure 13A. Heat map of genes previously described to play a role in the light response of rod and cone photoreceptors. Relative expression levels, fold change, and FDR are color-coded as indicated in the figure.

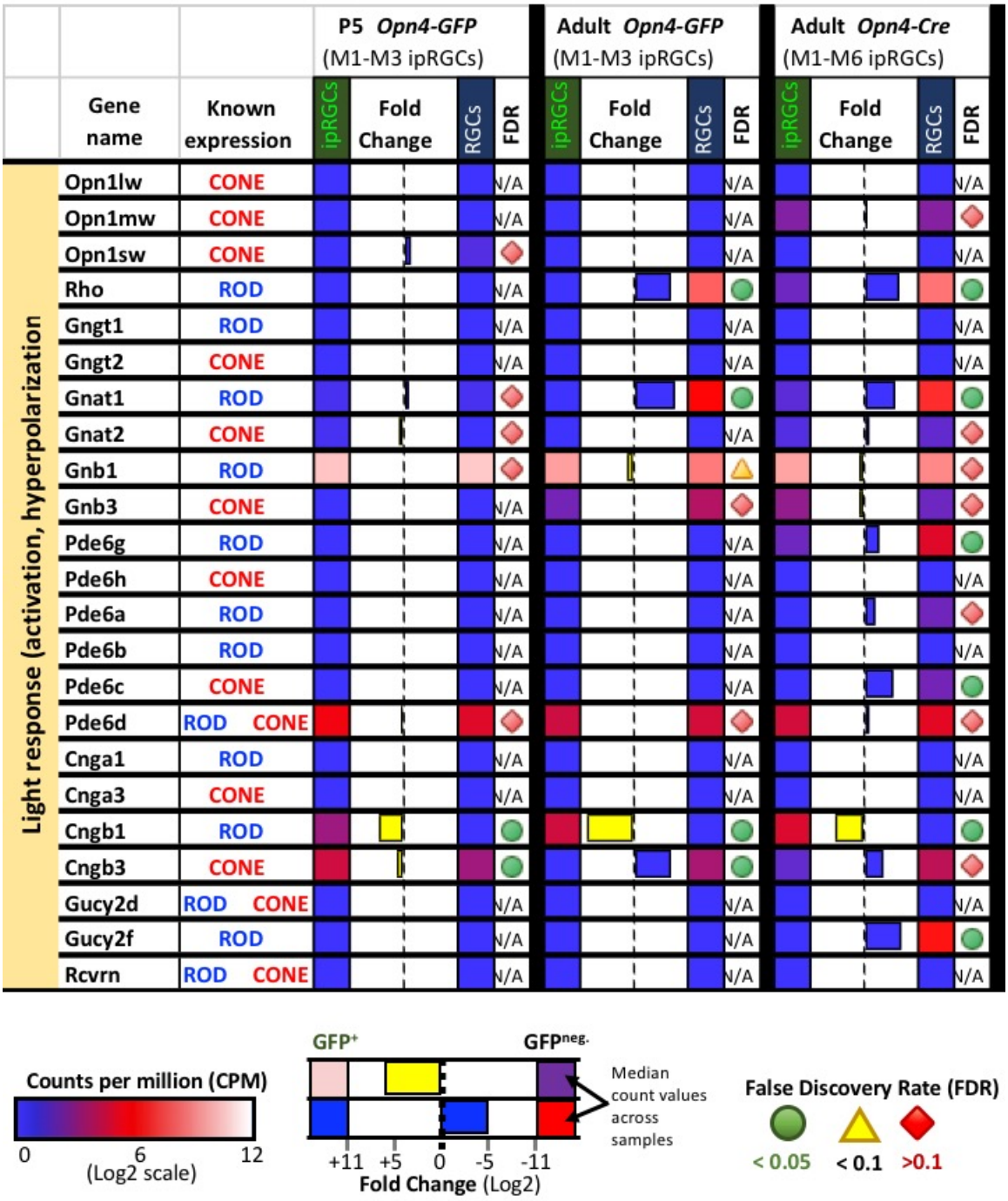

Figure 13B. Heat map of genes previously described to play a role during dark adaptation and chromophore regeneration of rod and cone photoreceptors. Relative expression levels, fold change, and FDR are color-coded as indicated in the figure.

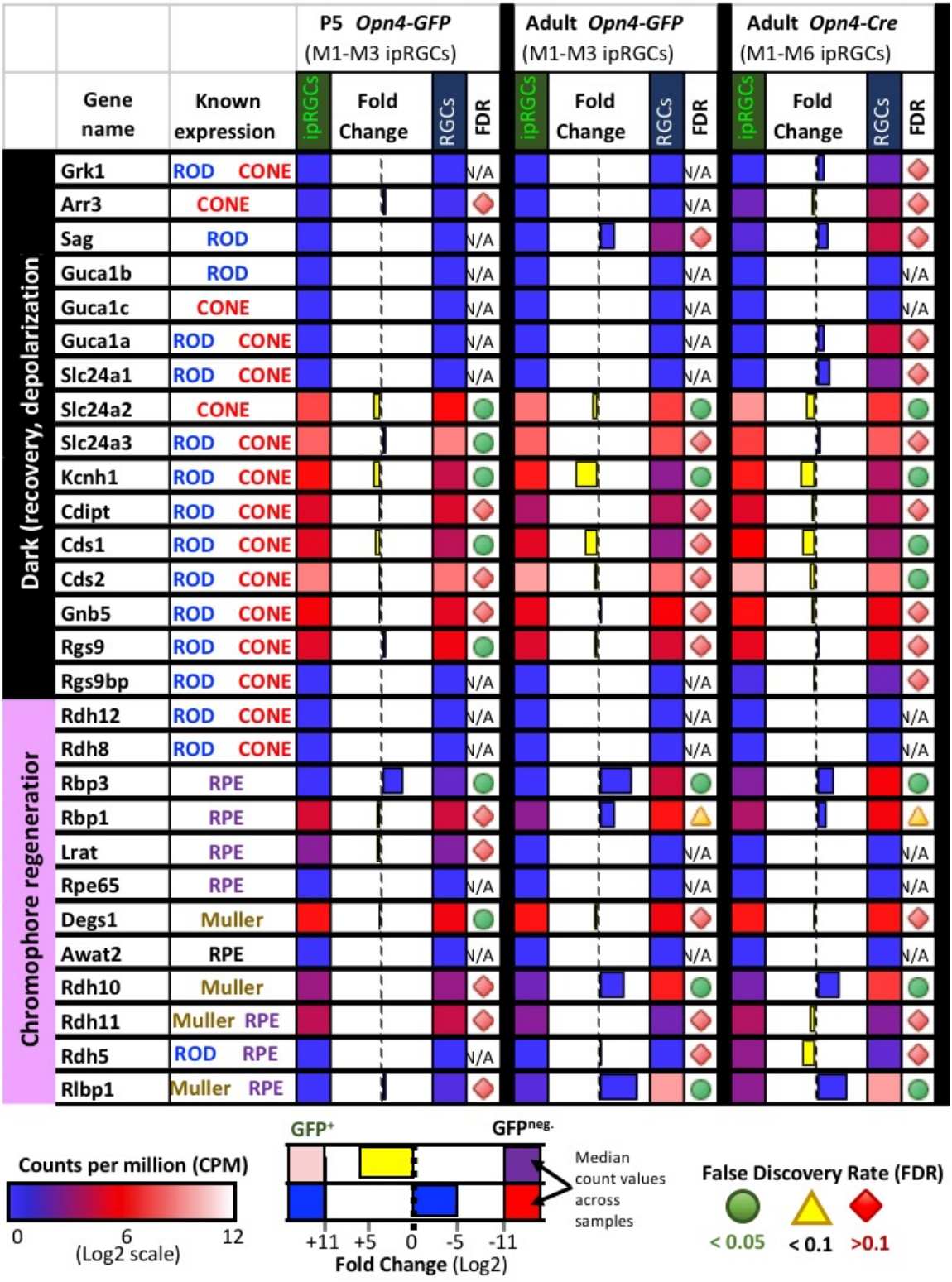

Figure 14. Heat map of genes encoding transcription factors that have a particular temporal pattern of differentially expression in ipRGCs (i.e., high P5 expression relative to adult expression). Relative expression levels, fold change, and FDR are color-coded as indicated in the figure.

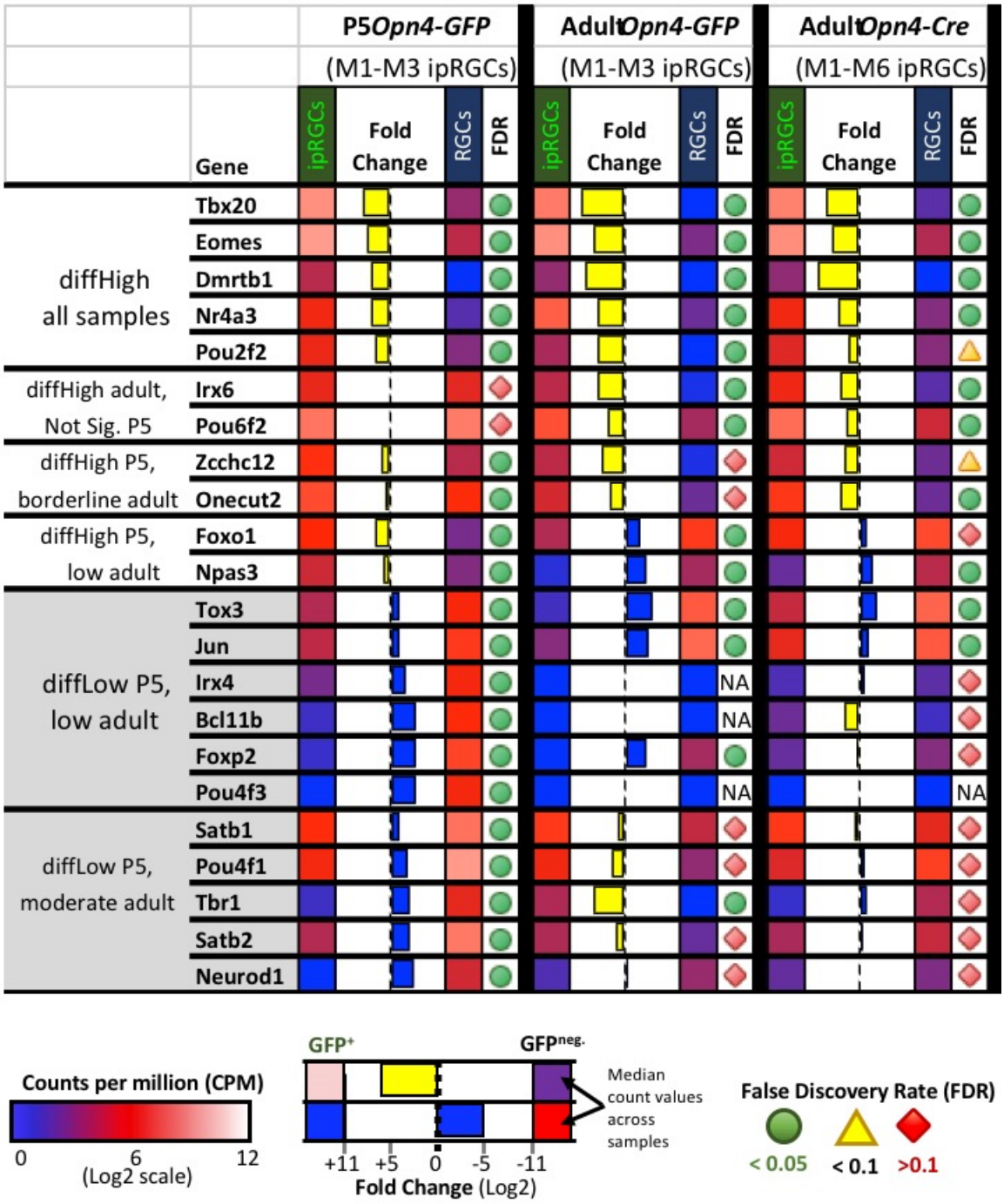

Figure 15A. Heat map of genes encoding for nicotinic acetylcholine, dopamine, and serotonin receptors. Relative expression levels, fold change, and FDR are color-coded as indicated in the figure.

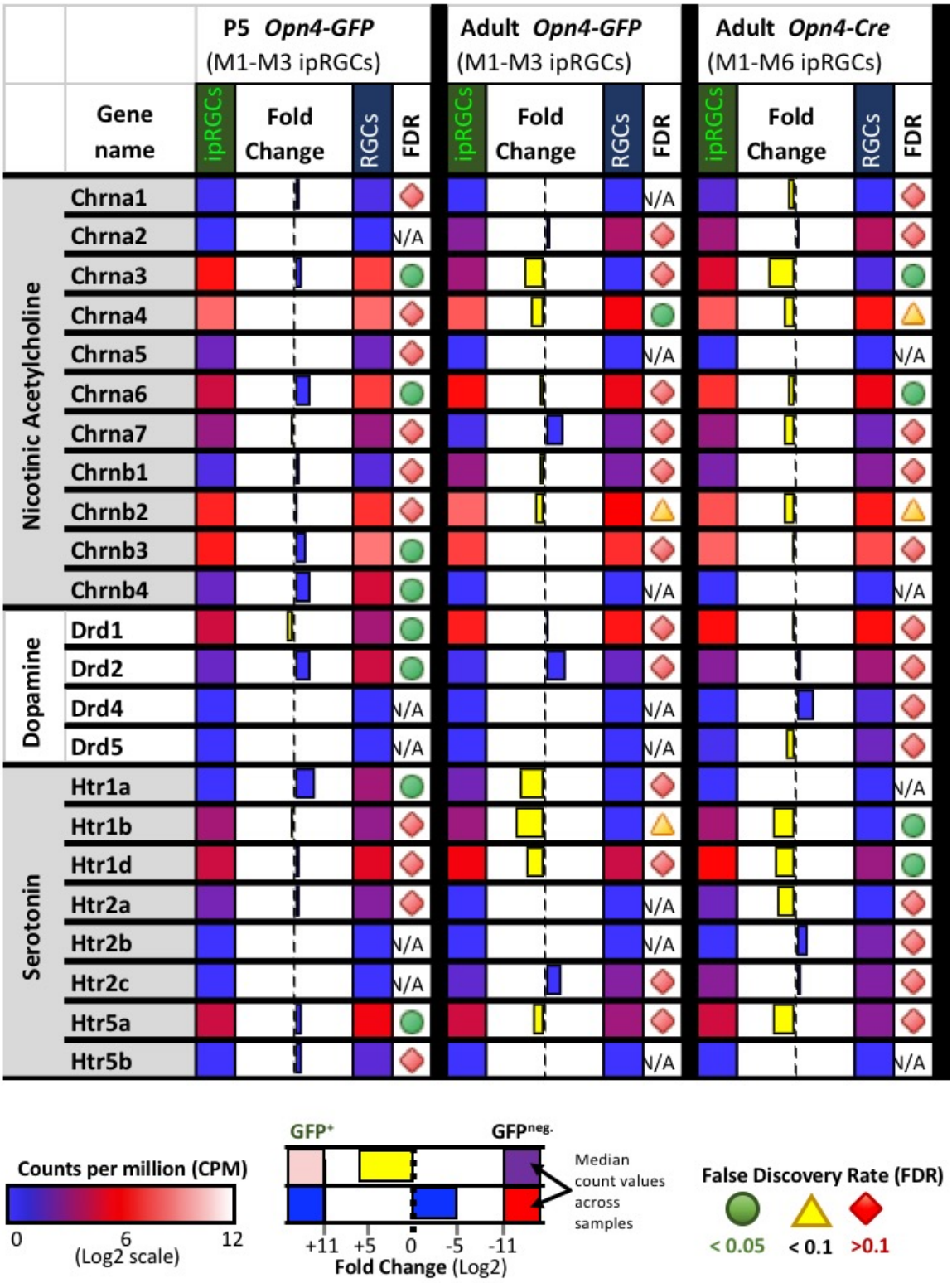

Figure 15B. Heat map of genes encoding for glycine, glutamate, and melatonin receptors. Relative expression levels, fold change, and FDR are color-coded as indicated in the figure.

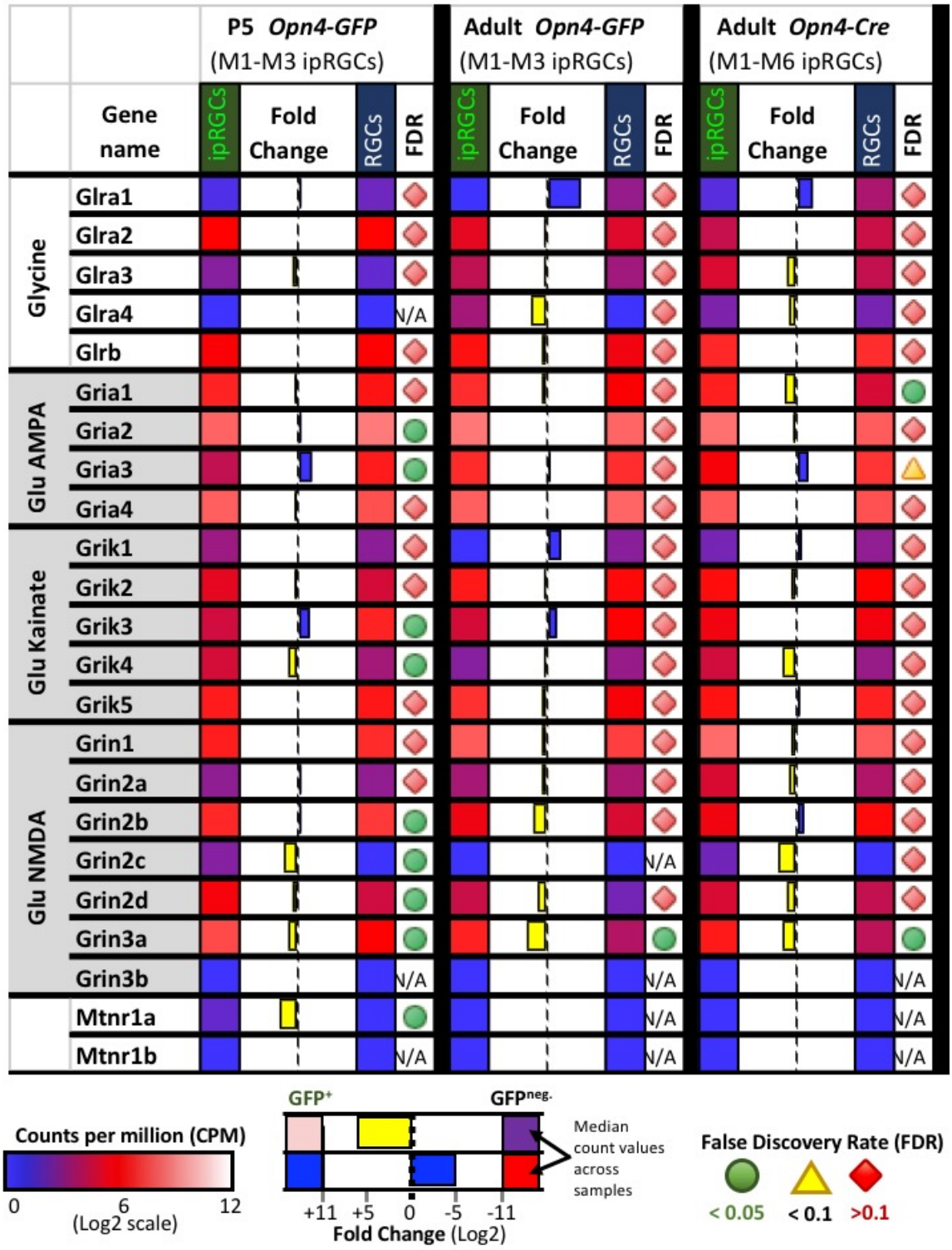

Figure 16. Heat map of genes differentially expressed in adult ipRGCs labeled by the *Opn4-Cre/ZEG* reporter (M1-M6 ipRGCs) compared to *Opn4-GFP* (M1-M3 ipRGCs). Relative expression levels, fold change, and FDR are color-coded as indicated in the figure.

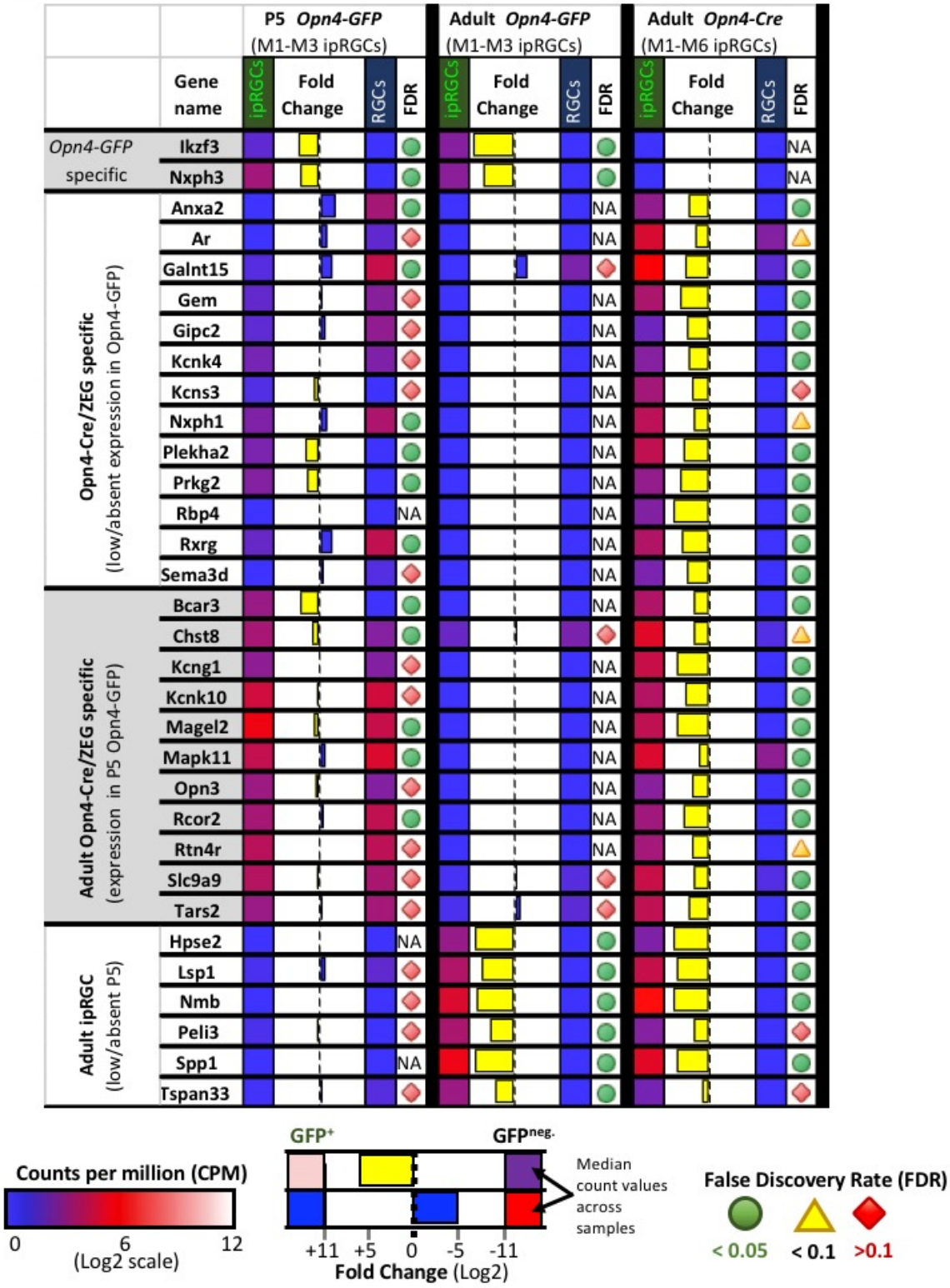

Figure 17. Heat map of genes relevant for development of ipRGCs. Relative expression levels, fold change, and FDR are color-coded as indicated in the figure.

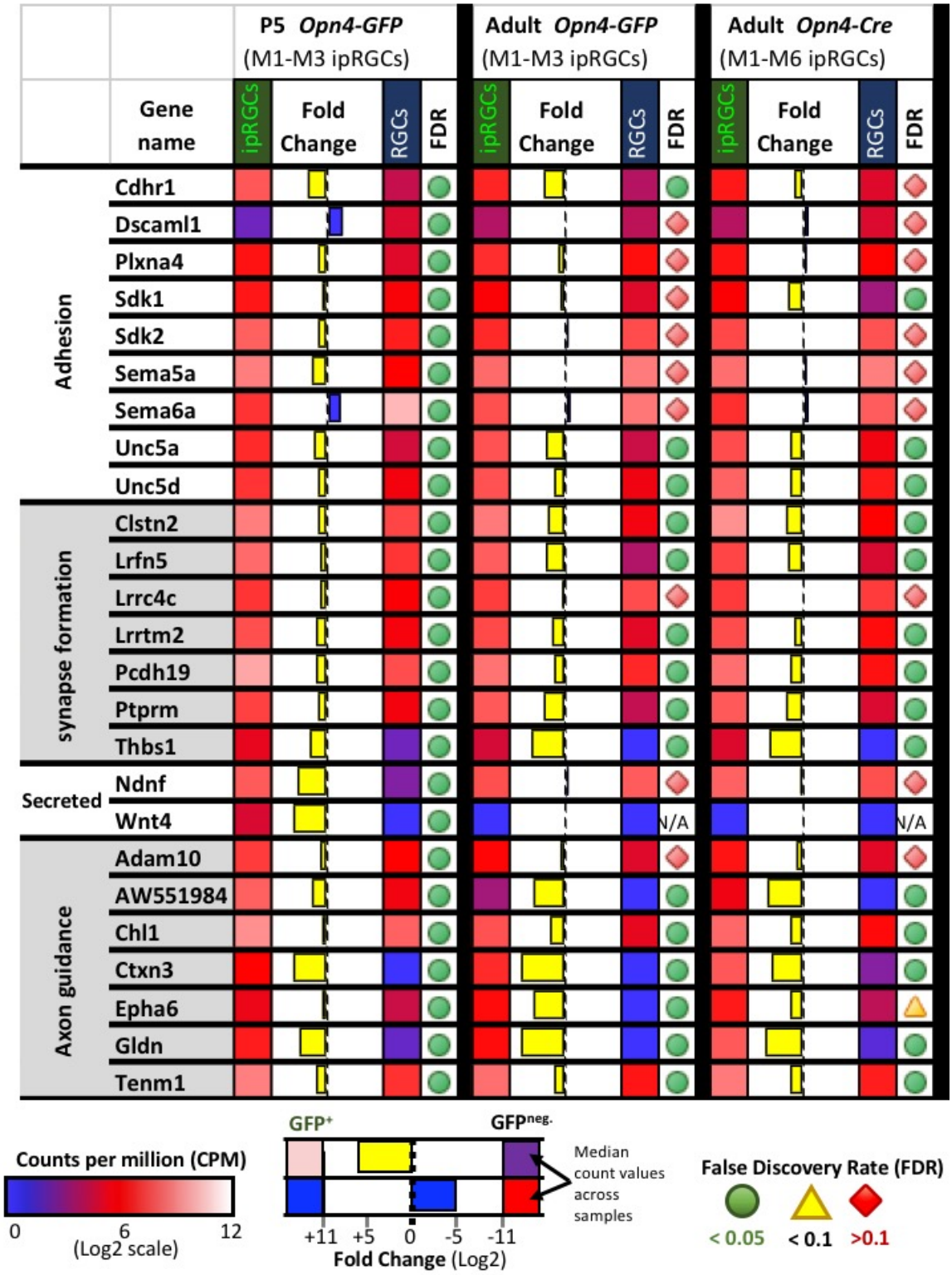

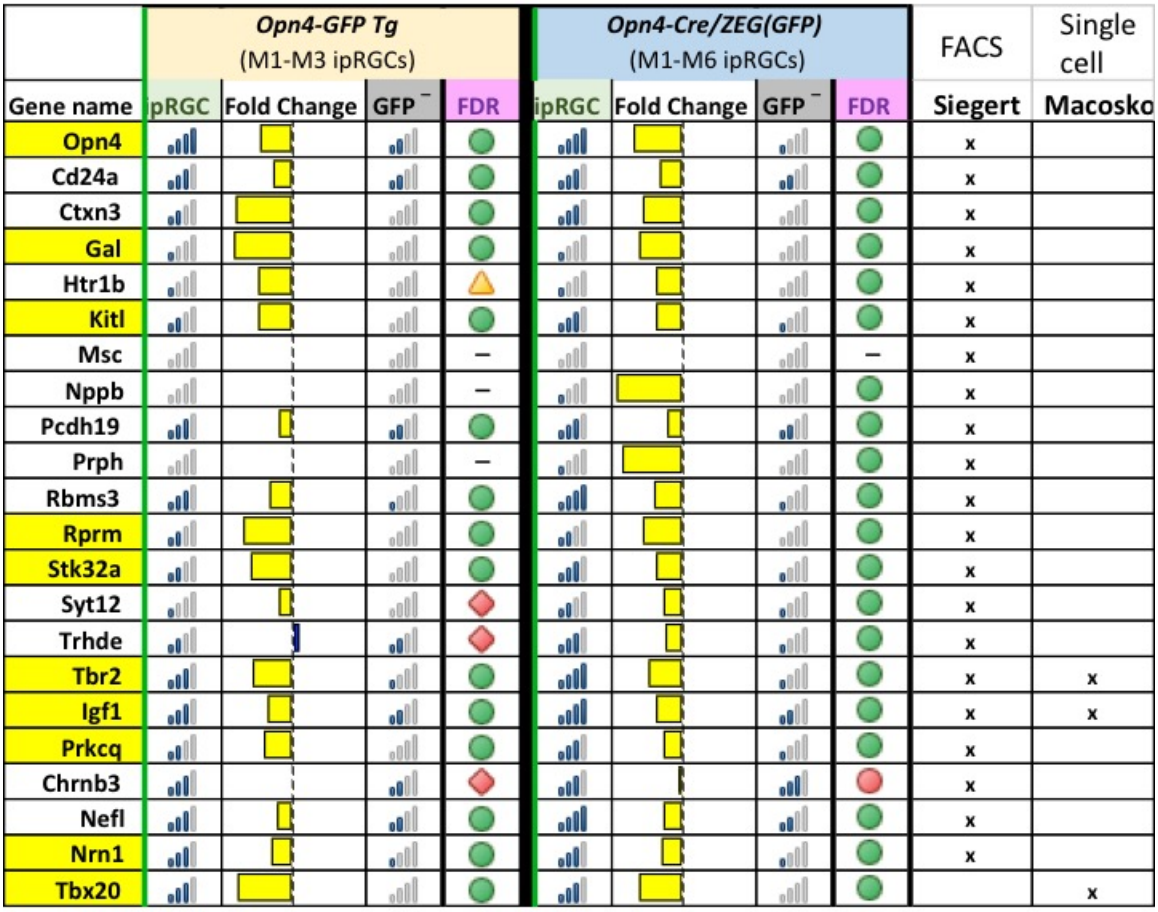

Figure 18. Comparison of other gene expression studies of ipRGCs to our dataset. Siegert et al., 2012 similarly used FACS of *Opn4-Cre* reporter system while Macosko et al., performed single cell analysis on whole retina.

CHAPTER 3:

Molecular Diversity of the Intrinsically Photosensitive Ganglion Cells Regulating Circadian Photoentrainment

Research was designed by DJ Berg and DM Berson.

Experiments were conducted, analyzed, and reported by DJ Berg except for the following:

- Brain injections of retrograde tracer into SCN was conducted by M. Leyrer. Immunofluorescence study of retrograde labeling in the retina was conducted and analyzed by DJ Berg.
- Rasgrp1 expression was quantified in relation to ipRGC subtypes by Katie Kartheiser.
- Tbx20 expression was quantified in relation to ipRGC subtypes by Alexandra Saali.

INTRODUCTION

Rasgrp1 provides specialized Ras signaling at the Golgi

Rasgrp1 is one of four members of the RasGRP family, which are membrane-bound guanine nucleotide-exchange factors (GEFs) capable of converting membrane-bound Ras-GDP to Ras-GTP (Johnson et al., 2007). Rasgrp1 expression is known to have limited expression across multiple tissues, with selective expression in lymphocytes and subpopulations of neurons in multiple brain regions that include the hippocampus, olfactory system, and the striatum (Ebinu et al., 1998; 2000; Pierret et al., 2000b; Toki et al., 2001).

The structure of Rasgrp1 contains EF hands that bind calcium, a diacylglycerol-binding C1 domain, and a catalytic region that has a REM (Ras exchange motif) and a CDC25 (cell division cycle 25) domain (Ebinu et al., 1998; Tognon et al., 1998; Lorenzo et al., 2000). This structure suggested that the Ras GEF activity of Rasgrp1 is mediated by the second messengers, calcium and diacylglycerol (DAG). Indeed, the generation of DAG by phospholipase C (PLC), following receptor stimulation, was demonstrated to be important for recruiting Rasgrp1 to the membrane for subsequent activation of Ras (Ebinu et al., 1998; Tognon et al., 1998). This Rasgrp1 signaling pathway might be engaged during Opn4-mediated phototransduction in ipRGCs. Light stimulation of Opn4 leads to the activation of PLCβ and generation of DAG, as well as inositol triphosphate (IP_3) from the hydrolysis of phosphatidylinositol 4,5-bisphosphate (PIP_2) (Hubbard and Hepler, 2006; Mizuno and Itoh, 2009). IP_3 is a second messenger that is known to trigger the intracellular release of calcium that is stored within the endoplasmic reticulum. It is possible that the effect of the increase of DAG and Ca^{2+} is to activate several TRPC cation channels present on the plasma membrane and important for the generation of action potentials (Panda et al. 2005; Qiu et al. 2005; Graham et al. 2008; Xue et al. 2011). However, applying analogues of DAG or IP3 were not found

to alter the photoresponses of ipRGCs (Graham et al., 2008). Therefore, the role of DAG and phosphoinositol signaling in Opn4-mediated phototransduction remains a mystery (Hankins et al., 2008; Do and Yau, 2010; Hughes et al., 2012; Díaz et al., 2016). We hypothesize that Rasgrp1 links Opn4-mediated phototransduction to specialized Ras signaling in at least a subset of ipRGCs.

The discovery that Rasgrp1 activates Ras signaling on the Golgi apparatus by Bivona and colleagues (2003) made the cell signaling field feel like they found, "Life on Mars" (Di Fiore, 2003). Their findings broke the established paradigm that Ras proteins signal solely at the plasma membrane and primarily function to regulate transcription (Willingham et al., 1980; Willumsen et al., 1984; Vieira et al., 1996; Di Fiore and Gill, 1999; Rajalingam et al., 2007). Translocation of Rasgrp1 to the Golgi requires DAG and PLC activity (Bivona et al., 2003a; Zhang et al., 2010). The Golgi complex is now considered to be a relay station for cellular signaling (Cancino and Luini, 2013). Signaling cascades initiated at the plasma membrane, such as classical ligand-receptor systems, may become modulated by passing through the Golgi and lead to different signaling outcomes (Inder et al., 2008). Studies of T-cells in the immune system has determined that activation of Rasgrp1 stimulates the mitogen-activated protein (MAP) kinase pathway (Ras–Raf–MEK–ERK) (Ebinu et al. 2000; Dower et al. 2000; Stone 2011; Shen et al. 2011; Golec et al. 2013; Kortum et al. 2013). The physiological difference between Golgi and plasma membrane activation of Ras is still unclear (Farhan and Rabouille, 2011; Wilson et al., 2011). Several groups have found that the kinetics of Ras activation of the Raf–MEK–ERK pathway is more sustained, graded, and delayed when compared to activation at the plasma membrane, which is generally more rapid and transient (Chiu et al., 2002; Rocks et al., 2005; Yasuda and Kurosaki, 2008). In neurons, Ras signaling has been linked to specific types of memory formation and synaptic plasticity (Adams and Sweatt 2002; Ye and Carew 2010; Sharma et al. 2003; Kelleher 3rd et al.,

2004; Yasuda 2012; Knafo and Esteban 2012). However, little is known about the role of specialized Ras signaling in RGCs or, more specifically, in ipRGCs.

Tbx20 has a dual role as both a transcriptional activator and repressor

The family of T-box genes encodes transcription factors play critical roles in development, cellular specification and differentiation in the nervous system and other diverse tissues (Naiche et al., 2005). T-box transcription factors recognize a highly conserved DNA binding region, the T-half site, which can vary in number as well as orientation in promoters of target genes (Sinha et al., 2000; Conlon et al., 2001; Stennard et al., 2003; Sakabe et al., 2012). To date, at least 18 T-box genes are identified in vertebrates with Tbx20 and Tbr2 being members of the Tbx1 and Tbr1 subfamilies, respectively (Sebé-Pedrós and Ruiz-Trillo, 2017). T-box family members are evolutionarily ancient, with Tbx20 having highly conserved roles in motor neuron axon targeting and cardiogenesis (Naiche et al., 2005). Many T-box proteins have either an activator or a repressor domain in their C-terminal regions, while some such as Tbx2 and Tbx20 are capable of both influences depending on promoter context (Paxton et al., 2002; Sakabe et al., 2012). Indeed, T-box factors often control target genes in combination with other transcription factors to contribute to promoter specificity (Garg et al., 2003; Stennard et al., 2003; Ghosh et al., 2009; Sakabe et al., 2012). This cooperativity may account for the tendency for T-box factors to be exquisitely sensitive to gene dosage (Naiche et al., 2005).

Tbx20 is an example of a transcription factor that possesses well-established roles in embryonic development, but are continuously required in mature cells to maintain their identities or carry out additional functional requirements during adulthood. The T-box genes Tbx20 and Tbx5 are important regulators of the molecular program driving myocardial proliferation and

patterning in heart development in vertebrates, as well as in *Drosophila* (Brown et al., 1998; Plageman and Yutzey, 2004; Chakraborty and Yutzey, 2012). In addition to its key developmental roles, Tbx20 has recently been demonstrated to be vital for maintaining the structure and function of cardiac muscle cells in the adult mouse heart (Stennard et al., 2003; Shen et al., 2011). Interestingly, Tbx20 has a dual role as a transcriptional activator in parallel to repressor activity, with each of these functions regulating distinct biological processes (Sakabe et al., 2012). In adult cardiomyocytes, Tbx20 is responsible for directly activating genes critical to normal adult cardiac function such as those required for ion transport and heart contraction (Shen et al., 2011; Sakabe et al., 2012). In contrast, genes directly repressed by Tbx20 have known roles in non-heart developmental programs, cell cycle, proliferation, and immune response (Sakabe et al., 2012). This signifies a dramatic reversal in transcriptional output since the main developmental function of Tbx20 is as a mediator of cardiac progenitor cell proliferation, whereas Tbx20 regulates an active anti-proliferative program in the adult heart (Cai et al., 2005; Takeuchi et al., 2005). Tbx20 cooperates with distinct cohorts of transcription factors to either promote or repress distinct molecular programs in a context-dependent manner (Sakabe et al., 2012). The co-binding of Tbx20 with factors known to have a role during heart embryogenesis (such as GATA4, GATA5, TBX5, or NKX2-5) plays a continuing role in the activation gene expression in the adult heart (Stennard et al., 2003; Sakabe et al., 2012). Additional factors seem to cooperate with Tbx20 to fine-tune active expression in response to intracellular or external factors. The cofactors responsible for promoting Tbx20 repressive transcriptional programs are less clear, but may include the transcription factor REST/NRSF which is known to repress pro-neural programs within non-neuronal tissues (Sakabe et al., 2012). The realization that Tbx20 has multiple motifs with different binding affinities adds an additional layer of gene target specificity that may in part explain the

dosage sensitivity of Tbox protein function. Therefore, Tbx20 may prove to have a similar reversal in its transcriptional activity when transitioning from embryonic to adulthood. Tbx20 has a known role as a repressor in early embryonic development of the eye (Carson et al., 2000; Pocock et al., 2008). Tbx20 is required for the expansion of the small pool of precursor cells in the optic vesicle(Carson et al., 2004). However, little is known about the function of Tbx20 in the adult retina.

When thinking about Tbx20 function, it would be useful to consider what is known about Tbr2, another Tbox family member that is known to have a critical role in the development of retinal ganglion cells (Mao et al., 2008), which later becomes essential to a restricted set of ipRGCs that participate in NIF visual circuits (Mao et al., 2014; Sweeney et al., 2014). Throughout the brain, as in the retina, binary cell fate specification is driven by complex genetic programs that require the simultaneous activation and repression of genes by transcription factors. For example, Tbr2 is integral to the neurogenesis and differentiation of multiple types of glutamatergic excitatory neurons not only in the retina, but also in the olfactory bulb, hippocampus, cerebellum, and neocortex (Englund et al., 2005; Fink et al., 2006; Hevner et al., 2006; Hodge et al., 2012; Kovach et al., 2013). In the neocortex, cortical progenitor cells progress through a series of stable identity transitions from symmetrically proliferating radial glial cells to become intermediate neuronal progenitor cells (INPs) capable of producing neurons (Noctor et al., 2004; Farkas and Huttner, 2008; Kowalczyk et al., 2009). Cortical progenitor cell transitions depend on the coordinated expression of a network of transcription factors. Radial glial cells initially express Pax6, a homeodomain transcription factor, which is required to maintain their radial glial identity as well as instigate the transition to INPs (Quinn et al., 2007). The proneural bHLH transcription factor Neurog2 promotes the radial glial cell to INP transition by activating Tbr2 transcription

(Arnold et al., 2008; Sessa et al., 2008; 2010). Tbr2 in turn directly represses Pax6 transcription, therefore blocking alternative cell fates (Kovach et al., 2012). Additionally, activation of Tbr2 by Ngn2 also specifies a dorsal glutamatergic projection neuron identity by direct repression of Ebf1, which specifies ventral GABAergic neuronal identity (Kovach et al., 2013). Therefore, Tbr2 is vital for neuronal identity in the developing neocortex primarily by eliminating alternative cell fates.

Tbr2 is also crucial for regulating synapse formation and maintaining precise neural connectivity, as exemplified by development of the olfactory bulb. The mitral and tufted cells of the bulb receive inputs from interrelated olfactory sensory neurons, project their dendrites into single glomeruli, and also convey odor information to higher olfactory centers (Ressler et al., 1994; Vassar et al., 1994). The local neuronal circuits constructed from the dendrodendritic synapses between the excitatory mitral/tufted cells and inhibitory GABAergic interneurons are important for refinement of odor-tuning specificity and discrimination (Gao and Strowbridge, 2009; Abraham et al., 2010; Dhawale et al., 2010). Tbr2 is required for the formation and maintenance of dendrodendritic synapses, with loss of Tbr2 leading to deficient lateral inhibition to mitral/tufted cells from local interneurons and a concurrent susceptibility to be activated by odorant stimuli (Mizughuchi et al., 2012). Additionally, the combinatorial expression of Tbr2 and the two Tbr1 subfamily members, Tbr1 and Tbx21, specify distinct subtypes of mitral/tufted cells by regulating the distinct expression of two vesicular glutamate transporters (Mizuguchi et al., 2012). Therefore, Tbr2 is required both for the differentiation of mitral/tufted cell subtypes and for the establishment and maintenance of the excitatory-inhibitory balance necessary for refined detection of odorants.

RESULTS

In Chapter 2, we identified more than 75 genes that were differentially expressed in adult ipRGCs. To begin this study, we sought to test our transcript-level differential expression analysis at the protein level and to determine whether their expression is selective for particular adult ipRGC subtypes. Ragrp1 and Tbx20 were two differentially expressed genes that we chose for particular focus, and we will consider results for each in turn.

Rasgrp1 is selectively expressed in ipRGCs

Transcriptional profiling suggested that Rasgrp1 is expressed differentially, possibly even selectively, in ipRGCs. However, differential mRNA expression does not guarantee a correspondence with protein product (Koussounadis et al., 2015). Therefore, we used the mouse monoclonal antibody m199, which was raised to recombinant Rasgrp1 (Puente et al., 2000), for immunofluorescence labeling and confocal imaging of Rasgrp1 protein in whole mount retinas from adult wild type mice. Rasgrp1-immunopositive cell bodies were present in the ganglion cell layer (GCL) as well as in the inner nuclear layer, which were likely amacrine cells and displaced ganglion cells considering their close proximity to the inner plexiform layer (IPL) (Figure 1). Robust Rasgrp1 immunostaining was observed in the cytoplasm and along the plasma membrane. Occasionally, particularly strongly Rasgrp1-labeled cells had additional labeling across the courser primary dendrites as well patchy labeling along the dendrites.

To test whether Rasgrp1 is expressed in RGCs, mouse retinas were immunostained for both Rasgrp1 and the RNA-binding protein Rbpms, which selectively labels all and only RGCs (Rodriguez et al., 2014). The majority of Rasgrp1-immunopositive cells in the GCL were found to be RGCs, as determined by co-labeling with Rbpms (56%, n=708 across three retinas, Figure 1).

Rasgrp1-expressing cells in the INL were rarely found to be displaced RGCs (Figures 1; data not shown). Together, these findings suggested that a subpopulation of RGCs express Rasgrp1. Rasgrp1 immunostaining was also observed in a subpopulation of photoreceptors in the outer retina (data not shown). Together, these results suggested that the antibody m199 labels a rare subpopulation of RGCs, along with many cells in the INL, plus vasculature and a subset of photoreceptors.

We used triple immunofluorescence for Rasgrp1, Opn4, and Rbpms to test the hypothesis that at least some of the Rasgrp1-expressing RGCs were ipRGCs (Figure 1). We quantified expression from confocal images of 49 regions that were topographically dispersed across three whole-mount adult mouse retinas. Nearly all Rasgrp1-expressing RGCs ($Rasgrp1^{+}$;$Rbpms^{+}$) were also Opn4-immunopositive (96%, n=412, Figure 1). In contrast, only a fraction of Opn4-immunopositive ipRGCs were Rasgrp1 immunopositive (34%, n=1169, Figure 1). Together, these findings support the idea that Rasgrp1 expression is confined to a subpopulation of ipRGCs.

We next tested whether the m199 antibody labeling of ganglion cells represented endogenous Rasgrp1 protein expression. The m199 antibody has been previously shown to specifically label Rasgrp1 protein expression in hippocampal neurons (Pierret et al., 2000b). As a further test for the specificity of the m199 antibody, we compared immunofluorescence labelling of whole mount retinas from normal and Rasgrp1-knockout mice generated by inserting *LacZ* and a *Neo* cassette into the Rasgrp1 gene to disrupt its expression (Dower et al., 2000). Our control experiments showed that the GCL and INL cellular labeling by the m199 antibody is absent in the Rasgrp1 knockout (Figure 1c). However, vasculature and photoreceptor cell labeling persisted in Rasgrp1-deficient mouse retinas, suggesting crossreactivity of m199 with other proteins. Vasculature labeling may be attributable to the anti-mouse-IgG secondary recognizing not only

the exogenous m199 monoclonal, but also other endogenous mouse IgGs in plasma that were fixed in the blood vessels.

Rasgrp1 expression is restricted to a diverse subpopulation of multiple ipRGC types

We next determined which of the established morphological subtypes of ipRGCs express Rasgrp1 into adulthood (Figure 2a). For this purpose, we used the established characteristics such as relative Opn4 expression, soma size, and detailed analysis of dendritic morphology to distinguish between the M1-M4 ipRGCs types(see Methods). We found that the majority of M1 cells expressed Rasgrp1 (72%, n=300 across three retinas), whereas only a fraction of M2 cells co-expressed Rasgrp1 (23%, n=389, Figure 2a). We determined that Rasgrp1-expressing M1 and M2 ipRGCs were uniformly distributed across the retina (Figure 2b). Additionally, Rasgrp1 was also observed to be co-expressed in a population of M5/6 ipRGCs in the GCL (31%, n=138, Figure 2a). In the INL, displaced M1 ipRGCs were found to express Rasgrp1 at a similar percentage as M1 cells in the GCL (72%, n=68). We found no examples of Rasgrp1 immunoreactivity in M4 cells (0%, n=172, Figure 2a). Of the Rasgrp1-expressing ipRGCs, two-thirds were M1 cells (67%), nearly a quarter were M2 (22%) and a small percent (11%) were M5/6 ipRGCs (n=396 $Rasgrp1^{+}/Opn4^{+}$ cells). Therefore, Rasgrp1 is selectively expressed in a diverse set of morphological ipRGC subtypes.

Spatial Distribution of ipRGCs and Rasgrp1-expressing ipRGCs

To observe how Rasgrp1 expressing ipRGCs fit into the known spatial distribution of ipRGCs, we placed a deep cut at the dorsal pole of the retina which allowed us to track the location of Rasgrp1

expressing ipRGCs and detect the presence of any distribution pattern trends. Our data did not suggest either a ventral-dorsal gradient or a naso-temporal gradient of M1-M3 ipRGC distribution across the retina (Figure 4—figure supplement 1C). We additionally observed the spatial distribution of M1 cells, both displaced and non-displaced, across the retina. We distinguished a minor difference between the number of M1s found in the nasal and temporal areas of the retina (Figure 4—figure supplement 1D). Next, we observed the spatial distribution of Rasgrp1-expressing RGCs, which we can infer are mostly ipRGCs (96%) from our previous results. We found that there was a minor ventral-dorsal gradient for Rasgrp1-expressing RGCs with a higher concentration in the ventral region of the retina as compared to the dorsal region (65% and 35%, respectively) (Figure 4—figure supplement 1E). Additionally, we identified a major center-peripheral gradient of Rasgrp1-expressing non-ganglion cells ($Rbpms^{neg.}$, presumptive displaced amacrine cells). We found that there was a much higher concentration of Rasgrp1-positive amacrine cells in the center of the retina (78%) as compared to the periphery (22%) (Figure 4—figure supplement 1F). While this analysis provides preliminary data about the spatial distribution of specific Rasgrp1-expressing cell types across the retina, more rigorous statistical analysis is needed to determine if the differences in cell populations are significant.

Tbx20 is expressed in a diverse subset of ipRGCs

The Tbx20 transcription factor was suggested from our gene expression analysis to be differentially expressed in ipRGCs. Tbx20 is functionally well-positioned to regulate the molecular program(s) important for maintaining adult ipRGC neuronal identity. To determine whether Tbx20 is expressed in adult ipRGCs, we studied Tbx20 expression using an antibody

specific to Tbx20 protein (see Methods for antibody information and validation, Figure 3). Immunofluorescence analysis of Tbx20 expression in 57 regions across four whole-mount retinas confirmed its enriched expression in a subset of Opn4-immunopositive ipRGCs (Figure 3). In-depth quantification of Tbx20 expression in ipRGC subtypes revealed that Tbx20 is expressed in most M1 cells (81%, n=514), but only a minority of M2 (25%, n=1305) and m5/6 ipRGCs (13%, n=603) (Figure 3). Half of displaced M1 (dM1) ipRGCs express Tbx20 (52%, n=153). Strikingly, Tbx20 was not expressed in M4 cells (0%, n=283, Figure 3). Therefore, Tbx20 is expressed in a diverse subset of ipRGCs.

Tbx20 is expressed in M5/6 ipRGCs

Many Tbx20 cells were not detectably immunopositive for Opn4. Only 41% of Tbx20 immunopositive were also Opn4-immunoreactive (23% were M1 ipRGCs; 15% were M2; and only 4% were M5/6 ipRGCs; n=2184; four retinas). The remaining Tbx20-immunopositive cells were RGCs, as confirmed by Rbpms-immunoreactivity (data not shown). Additionally, we observed that Tbx20-immunopositive RGCs that were Opn4-immunonegative were topographically enriched in the ventral region of the retina, with most Tbx20-positive cells in the dorsal retina being accounted for by Opn4-immunoreactivity (data not shown).

To investigate whether some or all of the Tbx20-immunopositive RGCs that were Opn4-immunonegative might be ipRGCs of the subtypes that exhibit little immunostaining, we used triple labeling: Tbx20-immunofluorescence; Opn4-immunofluorescence, to identify the "mystery" Tbx20 cells (Opn4-immunonegative); and all cells labeled in the *Opn4-Cre;Z/EG* mouse reporter that marks M5 and M6 cells, which have little if any melanopsin immunoreactivity. We observed examples of Tbx20-immunopositive cells that were GFP-positive (M1-M6 ipRGCs), but not

Opn4-immunopositive (M1-M4), which provided preliminary evidence that Tbx20 is expressed in at least a subset of M5/6 ipRGCs (data not shown).

The *Cdh3-GFP* mice permitted further analysis of the Tbx20-expression in M5/6 ipRGCs. Previous morphological studies of the *Cdh3-GFP* reporter have suggested that the GFP^+ cells can be divided into one abundant group consisting of bistratified M6 ipRGCs and two sparse groups of M5 and M2 ipRGCs (Quattrochi et al., in preparation; (Osterhout et al., 2011; 2014). The *Cdh3-GFP* reporter also labels a sparse population of brightly labeled amacrine cells that primarily reside in the INL. For the study of M5/6 cells in the *Cdh3-GFP*, we focused on GFP cells in the ganglion cell layer that are Opn4-immunonegative (to distinguish from M2 types). We proceeded to test Tbx20 immunoreactivity in the context of Opn4 immunofluorescence and *Cdh3-GFP* labeling (Figure 5B,C). At three weeks after birth, most *Cdh3-GFP* M5/6 cells express Tbx20 protein (78%, n=439 Figure 5C). Many, but not all, of the Opn4-immunonegative Tbx20-positive cells were GFP^+ in these experiments (27%, n=1277 $Tbx20^+$;$Opn4^-$ cells; four retinas). The dorsal-ventral pattern of Tbx20-positive cells that were Opn4-immunonegative was broadly similar to the retinal labeling of the *Cdh3-GFP* reporter. A large portion of Tbx20-immunopositive cells remained unclassified (43%; n=2184; Figure 5—figure supplement 1D). Finally, we determined whether Tbx20 expression correlates with the related T-box transcription factor Tbr2, a gene previously described to be enriched in adult ipRGCs (Mao et al., 2014; Sweeney et al., 2014). All Tbx20-expressing cells were strongly Tbr2-immunopositive, including M5/6 ipRGCs (n=328; four regions distributed across a single adult *Opn4-Cre/ZEG* retina; Figure 5—figure supplement 1C). Therefore, whereas Tbr2 is expressed in a broad range of types that includes the entire family of ipRGCs, Tbx20 expression is confined to a diverse subset of ipRGC types. In summary, we

determined Tbx20 to be expressed in a diverse subset of M1-M3 ipRGCs types, a subpopulation of the recently described M5/6 types, and an additional unidentified group of RGCs.

Molecular diversity of Rasgrp1 and Tbx20 expression in ipRGCs

Our expression studies revealed that Rasgrp1 and Tbx20 had a strikingly similar pattern of expression among ipRGC subtypes. Both genes were expressed in the majority of M1 cells, a minority of M2 cells, and a population of M5/6, but not in M4 ipRGCs. To directly test for co-expression, we compared and contrasted the expression patterns of Tbx20- and Rasgrp1-immunoreactivity in the context of M1-M4 subtypes revealed by Opn4-immunoreactivity (Figure 4). Confocal images for quantification of co-labeled cells were collected from 23 regions across three whole mount wild type mouse retina. Rasgrp1 co-expression with Tbx20 was only observed in a major fraction of M1 cells (29%; n=341 M1 cells; Figure 4). Further, M1 cells expressing either Rasgrp1 or Tbx20 alone account for similar fractions of M1 cells (25% and 39%, respectively; n=341 M1 cells). Only a small fraction of M1 cells were immunonegative for both Rasgrp1 and Tbx20 (7%; n=341 M1 cells). In contrast, half of M2 cells lacked Rasgrp1 and Tbx20 immunoreactivity (58%; n=388 M2 cells). Approximately a third of the M2 ipRGCs expressed Tbx20 (30%), while only 11% expressed Rasgrp1 (n=388 M2 cells). We did not observe an example of a M2 cell expressing both Rasgrp1 and Tbx20. Additionally, we did not observe any occurances of Rasgrp1 and Tbx20 co-expression outside of the M1-M3 ipRGC types, suggesting that their expression may diverge in the grouping we designated as M5/6 ipRGCs (see Methods). Together, these results provide further evidence for previously unrecognized molecular diversity in adult ipRGCs.

Molecular diversity of SCN-projecting ipRGCs

We further examined the Rasgrp1- and Tbx20-expressing ipRGC subtypes to seek intersectional expression patterns that would divide ipRGCs by their downstream visual pathways. Earlier studies showed that M1 cells could be subdivided based on their level of expression of Brn3b (Chen et al., 2011). We used quadruple immunolabeling to simultaneously test Brn3b expression with Rasgrp1- and Tbx20-immunoreactivity in the context of Opn4-immunolabeled ipRGCs (Figure 4). Co-expression was quantified from 23 regions across three wild type retinas. The minority of M1 ipRGCs that express Brn3b were also immunopositive for Tbx20 (8%; n=241 M1 cells (including displaced M1 and M3 ipRGCs); Figure 4a,b,e). However, the majority of Tbx20-immunopositive M1 ipRGCs were Brn3b-immunonegative (86%; n=183 $Tbx20^+$ M1 cells; Figure 4). We only found a single example of Brn3b and Rasgrp1 co-expressing in M1 cells(<1%; n=218 $Rasgrp1^+$ M1 cells), but a minority of M2 cells expressed Brn3b and Rasgrp1 (7%; 388 M2 cells; Figure 5e). Notably, every combination of single- and double-labeling of Brn3b, Tbx20, and Rasgrp1 was identified to varying degrees (Figure 5e). However, we found no examples of $Brn3b^+$;$Tbx20^+$;$Rasgrp1^+$ co-expression among all three genes (n=729 M1-M3 cells).

Our quadruple labeling study suggested that most SCN-projecting M1 cells (Brn3b-negative) might be molecularly diverse populations of cells (Figure 5). We correlated gene expression of Rasgrp1 and Tbx20 in the retina with retrograde labeling from the SCN (Figure 5a). We injected rhodamine-conjugated retrobeads in the SCN, followed by immunofluorescence labeling for Opn4, Rasgrp1, and Tbx20 (Figure 5b). All injection sites clearly involved the SCN, as revealed by DAPI labeling, but did not spread to the optic chiasm or tract (Figure 5a). Quantitative coexpression analysis was done using 18 confocal images collected across the contralateral and ipsilateral retinas. Nearly all retrolabeled cells were Opn4-immunopositive

(Rhodamine$^+$/Opn4$^+$ cells; 95%; n=250 retrolabeled cells), and these exhibited variable patterns of staining for the other proteins. Most expressed both Rasgrp1 and Tbx20 (Rasgrp1$^+$/Tbx20$^+$; 76%), but equal minorities expressed only Rasgrp1 (Rasgrp1$^+$/Tbx20$^-$; 12%) or only Tbx20 (Rasgrp1$^-$/Tbx20$^+$; 12%; n=235 Opn4$^+$;Retrobead$^+$). The pattern of expression seemed to be consistent between ipsilateral and contralateral retina (Figure 5d), as has been suggested previously by studies of bilateral input to the SCN (Hattar et al., 2006; Fernandez et al., 2016). Therefore, SCN-projecting ipRGCs are confirmed to have a complex pattern of Rasgrp1 and Tbx20 gene expression. Together, these results provide further evidence for previously unrecognized molecular diversity in adult ipRGCs.

To examine further the axonal projections of the Rasgrp1-positive RGCs, we obtained the BAC transgenic mouse, *Rasgrp1-Cre* (MMRRC P01). Though we recognize the potential for misleading expression in BAC systems, we considered that this may be a faithful reporter based on public databases brain labeling patterns for *Rasgrp1-Cre* (P01) mice crossed with Cre-dependent GFP reporter that matched the endogenous Rasgrp1 expression in the hippocampus and striatum (Pierret et al., 2000b; Gong et al., 2007; Gerfen et al., 2013). Additionally, significant labeling of RGC axons was visible in the optic nerve. Therefore, I injected a Cre-dependent virus with membrane-bound fluorescent protein into the *Rasgrp1-Cre* reporter to visualize brain targets of labeled RGCs (Figure 6a). As expected from the Rasgrp1 immunostaining, sparse RGCs were labeled in this line, and their axons could be traced into the optic nerve (data not shown). The brain targets of *Rasgrp1-Cre* expressing RGCs consisted of the complete set of the major known targets of ipRGCS including the SCN, OPN, lower quadrant of the dLGN (known M4 ipRGC brain target), IGL, and vLGN (Figure 6b). This was surprising since Rasgrp1 protein expression seemed to be limited to a partial subset of ipRGC types, with no observed expression in M4. Even more

surprising was the additional strong labeling of brain regions associated with the accessory optic system: the medial terminal nucleus (MTN), dorsal terminal nucleus (DTN), and nucleus of the optic tract (NOT). The accessory optic system (AOS) is responsible for mediating the optokinetic reflexes, which involve compensatory eye movements that stabilize images on the retina during perceived motion of the surrounding visual field. Crossing the *Rasgrp1-Cre* with a Cre-dependent reporter expressing membrane-bound GFP revealed extensive labeling in the major areas with known Rasgrp1-expression including the striatum and hippocampus (data not shown). However, the brain fibers across the brain limited our ability to accurately assess which axon terminals were of retina origin.

Functional testing of Rasgrp1

The signaling protein Rasgrp1, a Ras GEF, was selected for further study due to its potential role as a specialized Ras signaling regulator downstream of the Opn4-induced phototransduction cascade. To determine if some of the Rasgrp1 immunolabeling we had observed might be localized to the Golgi apparatus, we used an antibody towards Giantin, a specific marker for the perinuclear region of the neuronal Golgi complex(Linstedt and Hauri, 1993; Hughes and Stephens, 2008). There was a qualitatively good colocalization between the Giantin staining and intracellular localization of Rasgrp1 protein (Figure 7a). There was additional labeling of Rasgrp1 at the plasma membrane, which has been described in other studies using different cell systems such as lymphocytes (i.e., Bivona et al., 2003).

Rasgrp1 localization is dynamically regulated: upon activation by DAG at the membrane, Rasgrp1 will translocate to the Golgi apparatus and can be present in either location (Bivona et al., 2003a; Prior and Hancock, 2012). Rasgrp1 activity requires binding of DAG, a factor known to be

generated by Opn4-mediated phototransduction in ipRGCs (see Hughes et al., 2012, for review). Therefore, I tested the subcellular localization of Rasgrp1 in an $Opn4^{-/-}$ knockout mouse with that in littermate heterozygous littermate controls. Our preliminary data suggested that there was not a noticeable change in the subcellular localization in the absence of Opn4 (Figure 7b).

To assess other possible roles for Rasgrp1 in ipRGCs, we examined Opn4 immunostaining patterns and retinofugal projections in Rasgrp1 knockout (KO) mice, but we could find no consistent differences. In the retina, we did not observe any obvious phenotypes related to morphology or survival of Opn4-immunolabeled ipRGCs in the Rasgrp1 knockout (Figure 8a). We also used axonal tracing from the eye to examine retinofugal projections in the Rasgrp1-KO mouse. We saw no obvious difference in the visual brain targeting of RGCs as demonstrated by proper RGC axon terminations in the SCN, LGN, OPN, and the MTN (one of three brain regions of the accessory optic system) (Figure 8b).

DISCUSSION

There is limited knowledge of specific gene expression in ipRGCs and its subtypes, especially non-M1 ipRGCs. Our data demonstrate heterogeneity among ostensibly uniform ipRGC subtypes based on the expression of two interesting proteins: Tbx20, a transcription factor implicated in visual development; and Rasgrp1, a G-protein exchange factor that may interact with the melanopsin phototransduction cascade. Additionally, we determined that the combined expression pattern of Rasgrp1 and Tbx20 across ipRGCs is even more complex. Finally, through retrograde labeling, we demonstrate that M1 cells projecting to the SCN are more molecularly diverse than previously realized. Altogether, our identification of two novel molecular markers has already revealed further diversity than previous classifications of ipRGCs, and demonstrate the

importance of integrating molecular information with morphological and functional characteristics. Our contribution of additional endogenous markers of ipRGCs could provide a greater foundation for future gene expression studies and designing sophisticated, multi-locus mouse transgenic reporters.

What type(s) of adult ipRGCs express Rasgrp1?

Rasgrp1 expression has previously been described in hippocampal, olfactory, and striatal regions of the brain (Ebinu et al., 1998; Toki et al., 2001). To our knowledge, our study is the first to explore Rasgrp1 expression in the eye. Our immunofluorescence studies revealed the expression of Rasgrp1 a diverse subpopulation of ipRGC types, including the classic M1-M3 ipRGC types. A defining aspect of Opn4-immunolabeling of M1-M3 is the ability to identify dendritic morphology from the high expression of membrane-bound Opn4 along the dendrites. In our hands, we were able to optimize the immunofluorescence labeling procedure to reveal low levels of Opn4-immunoreactivity in large-soma ipRGCs, a reliable means of identifying the M4-type. We did not find any evidence for Rasgrp1 expression in M4-type cells. Additionally, we observed an unknown ipRGC type expressing Rasgrp1 that we characterized as having low Opn4-immunoreactivity in small somas and lack of decipherable dendritic labeling, distinct from M1-M3 ipRGCs. The lack of dendritic labeling made further classification a challenge, but the recently described M5 and M6 type exhibiting a weak intrinsic light response are currently the best candidates (Estevez et al., in preparation; Quattrochi et al., in preparation; Ecker et al., 2010). The M5 and M6 ipRGCs are more diverse than previously realized (Estevez et al., in preparation; Quattrochi et al., in preparation; Ecker et al., 2010). Although M5 ipRGCs currently do not have a specific molecular reporter, the M6 is suggested to be enriched in the *Cdh3-GFP* reporter line (Quattrochi et al., in preparation).

Our studies suggest that Tbx20 may prove to be a good additional marker for M6-type of ipRGCs (~80% coexpression *Cdh3-GFP*). We tested Rasgrp1 coexpression with Tbx20 and determined that there is a complex coexpression pattern among M1-M3 ipRGCs, but they are otherwise anti-correlated in M5/6 ipRGCs. Therefore, further testing could reveal Rasgrp1 as a novel marker for the M5 type, or the identification of another novel type of ipRGC. The level of Rasgrp1-immunoreactivity was variable across ipRGCs. Qualitatively, the level of Rasgrp1 protein expression did not coincide with Opn4-expression, but further quantification is required in relation to the expression levels of Opn4 and other ipRGC markers.

What is the function of Rasgrp1 in adult ipRGCs?

The function of Rasgrp1 in ipRGCs remains unknown, but our preliminary results should help inform and narrow the focus of future studies. At the cellular level, we suggest that the main ipRGC phototransduction cascade is independent of Rasgrp1 signaling. Although Rasgrp1-expressing RGCs were determined to be Opn4-immunopositive and therefore selective for ipRGCs, Rasgrp1 was not found to be expressed in some of the highest expressing ipRGC types (Rasgrp1-immunonegative in 28% of M1s and 77% of M2). Further, Rasgrp1 activation may be independent of Opn4 phototransduction. The known mechanism of Rasgrp1 activation and subsequent translocation to the Golgi is through binding to DAG and calcium, both of which are generated by light-activated Opn4 phototransduction cascade. Our preliminary subcellular localization studies suggest that Rasgrp1 may indeed be enriched on the Golgi and in position to activate specialized Ras signaling cascades in ipRGCs. However, our initial studies suggest that Rasgrp1 translocation to the Golgi may be independent of Opn4-mediated phototransduction cascade. Rasgrp1 subcellular localization anecdotally seemed to be unchanged on the Golgi despite

elimination of Opn4 by an Opn4-knockout. Further quantification of this localization correlation would be necessary to rule out more subtle changes that were missed such as altered concentration comparing plasma membrane signal to the Golgi compartment localization. However, the expression of Rasgrp1 in low expressing ipRGC type(s) further supports that Rasgrp1 biological function does not tie directly to Opn4-expression. Finally, testing Opn4-expression in Rasgrp1-knockout mice did not reveal an obvious cellular phenotype in ipRGCs, but this does not rule out subtle defects or a phenotype of physiological origin. We did not adequately explore many of the potential cell physiological effects such as circadian photoperiod, neuronal excitability, ligand activation of non-Opn4 GPCR signaling, or stress-induced signaling in disease models of vision loss.

An important survival mechanism in M1 ipRGCs is the maintainence of mTOR expression that is dependent on Opn4-phototransduction (Duan et al., 2015; Li et al., 2016). The DAG-mediated Rasgrp1-Ras-Mek1/2-Erk1/2 pathway has been demonstrated to be important for mTOR activation in thymocytes (Gorentla et al., 2011). Further, the percentage of M1 cells determined to express Rasgrp1 (72%) in our studies is strikingly similar to the survival rate of M1 cells after damaging the optic nerve (~70%, Li et al., 2016). Testing whether Rasgrp1 is required for the maintained mTOR levels in surviving M1 ipRGCs would be interesting to pursue in the future. Recent studies have also clarified different mechanisms being responsible for M1 survival and the regeneration potential of alpha-RGCs such as M4 ipRGCs (Duan et al., 2015; Li et al., 2016). Despite surviving well, M1 ipRGCs were not capable of regenerate their axons(Li et al., 2016). In contrast, alpha-RGCs had a unique capability to regenerate their axons that was promoted by their high levels of mTOR expression as well as osteopontin/Spp1 expression coupled with the growth factor IGF-1(Duan et al., 2015). Whereas M1 ipRGCs were found to maintain mTOR expression

after axon injury, M4 ipRGCs and other alpha RGC types were demonstrated to have diminished mTOR expression levels (Li et al., 2016). Our studies suggest that the M4 ipRGCs do not seem to express Rasgrp1, which may explain the lack of maintained mTOR expression after injury. Therefore, a previously recognized link between Rasgrp1 and mTOR in lymphocytes may potentially promote the survival of a subset of M1 ipRGCs, but testing this association was beyond the scope of our current research program.

Of course, Rasgrp1 has the potential to affect any number of neuronal signaling pathways. Ras signaling pathways are enormously complex and the cross talk between pathways makes it even harder to identify specific effects. One basic mechanism for specificity in Ras signaling is the distinct subcellular targeting of downstream components of the signaling pathway. As mentioned, localized Ras signaling of Rasgrp1 occurs preferentially on the Golgi apparatus, which is a rare form of compartmentalized Ras signaling. The Golgi apparatus in neurons provides the posttranslational protein modifications required for organizing protein and organelle trafficking throughout the cell. Rasgrp1 could play a crucial role in orchestrating a specific set of post-translational modifications at the Golgi. Whatever the role of Rasgpr1 may be in ipRGCs, it is possible that research in ipRGCs may inform the function that Rasgrp1 plays in other parts of the nervous system. Rasgrp1 is also known to be expressed in the hippocampus, striatum and olfactory structures but its function remains unknown in these areas as well (Ebinu et al., 1998; Toki et al., 2001).

Central brain targets of Rasgrp1-expressing ipRGCs

At the circuit level, Rasgrp1 is not anticipated to be an essential regulator of circadian photoentrainment. The majority of M1 ipRGCs are known to provide the primary retinal input to

the SCN, while a subset of M1 ipRGCs send input to the OPN to regulate the pupillary reflex. Our results that Rasgrp1 was expressed in the majority of M1 ipRGCs suggested to us that it might correlate directly and completely with the SCN-projecting M1s. However, retrograde tracing experiments from the SCN revealed that some SCN-projecting M1 cells were Rasgrp1-immunonegative. Accumulating research suggests that the SCN is more compartmentalized than previously recognized (Bedont and Blackshaw, 2015). The question of whether Rasgrp1 is expressed in a subset of M1 ipRGCs that targets a specific compartment of the SCN remains to be determined.

Rasgrp1 is almost certainly expressed not only in SCN-projecting ipRGCs, but also in additional ipRGC types with different visual targets. In addition to M1 ipRGCs, Rasgrp1 were determined to be expressed in a subset of M2-ipRGCs as well as an as yet unidentified low-expressing ipRGC type. These types remain less well annotated and correlated to brain targets than the M1-type. We conducted additional experiments to test which visual brain areas receive input from Rasgrp1-RGCs. Unfortunately, testing with a randomly integrated BAC transgenic reporter mouse, Rasgrp1-Cre, remains inconclusive due to suspected off-target RGC labeling by the reporter. Notably, the seemingly complete labeling of all brain targets from both the ipRGC and accessory optic system suggests that this mouse line could be useful for other purposes, perhaps in combination with a non-Cre based reporter system.

What type of amacrine cells express Rasgrp1?

Rasgrp1 is expressed in an extensive subpopulation of amacrine cells but remains uncharacterized. There are at least 42 distinct types of amacrine cells, making them the most diverse cell class in the retina but most of the class remains poorly understood (Masland, 2012).

They can be classified with a similar type of criteria as retinal ganglion cells: circuitry with their pre- and postsynaptic partners; morphology in the way of dendrititic field size and stratification; physiological and molecular markers such as the type of neurotransmitter expression. The soma labeling of the Rasgrp1 unfortunately does not provide much in the way of morphological assessment, but coexpression studies with known markers (i.e. GABA or Glycine) may help to begin narrowing the candidate list of amacrine types expressing Rasgrp1. Interestingly, amacrine cells make specific contacts with post-synaptic RGC partners and generally seem to be responsible for the correlated firing between RGCs that share a given amacrine cell type's input (Vaney, 1994; Masland, 2012). One recent example of this is the gap-junction coupling of ipRGCs with AII amacrine cells (Müller et al., 2010; Reifler et al., 2015). In addition, identifying the amacrine cell types expressing Rasgrp1 may also help inform the functional role performed by Rasgrp1.

Future directions of Rasgrp1 studies

The generation of a faithful, sensitive reporter for Rasgrp1 expression in the retina and brain targets of Rasgrp1-ipRGCs would serve many purposes. Our attempts at using a Rasgrp1-Cre reporter was unsuccessful most likely due to integration of the reporter cassette in a genomic region that altered reporter expression. What the *Rasgrp1-Cre* RGCs brain targets have in common is their involvement in subconscious, reflexive visual functions. Unfortunately, it is common that BAC transgenics, which rely on random integration of reporter cassette into the genome, adopt unintended expression patterns that are not in correspondence to endogenous gene expression of intended genetic locus. Therefore, we could not confidently decipher the Rasgrp1-expressing ipRGC brain targets using the *Rasgrp1-Cre* reporter system. A targeted knock-in of Cre-recombinase directly into the start codon of Rasgrp1 gene locus would likely provide a more

specific labeling pattern. The Cre-based system is useful because it enables identification of eye-specific brain terminations by intraocular viral reporter eye injections that would be potentially masked by a more general reporter labeling of all Rasgrp1-expressing cells. Using a Cre-dependent membrane bound fluorescent protein reporter packaged in the virus would also allow morphological reconstruction of the Rasgrp1-RGCs and –amacrine cells. Genetically crossing a transgenic ChR2-mCherry reporter would allow for labeling of the entire Rasgrp1-expressing population.

The translocation of Rasgrp1 to the Golgi and subsequent Ras activation is another area for future study. Further quantification of cellular localization would need to be done to decipher the relative abundance of Rasgrp1 protein across these two compartments in ipRGCs. Of course, there are other means that the translocation of Rasgrp1 to the Golgi could be effected since Opn4 phototransduction is undoubtedly not the only mode that the ubiquitous DAG and calcium signaling molecules are generated inside the Rasgrp1-expressing cells. Anecdotally, the amacrine cells may also have spatially organized Rasgrp1 localization in the Golgi despite not expressing Opn4, further suggesting that Opn4 is not required for dynamic localization of Rasgrp1. Exquisite fluorescent probes have been developed in cell culture systems for the *in vivo* visualization of Ras activation on the Golgi (Bivona et al., 2003b; Philips, 2005). Although possible in mammalian systems, this would prove to be a challenging undertaking due to the complexity of the multi-part genetic system that would be required. An easier method is to use antibodies specifically generated to detect activated Ras and test for enrichment on the Golgi. The ubiquitous nature of Ras may make this approach challenging. If the dynamic localization of Rasgrp1 in ipRGCs can be tested, then this should prove a useful tool to decipher subtler Rasgrp1 cell localization phenotypes.

In summary, our interest in Rasgrp1 was originally inspired by our differential gene expression studies of ipRGCs. Our follow-up studies demonstrate that Rasgrp1 protein is expressed in a subpopulation of multiple established subtypes of ipRGCs, suggesting a complex expression pattern and further molecular diversity across ipRGC subtypes than was previously appreciated. Studies of Rasgrp1 subcellular localization suggests that it may be preferentially translocating to the Golgi, where it is known to activate Ras through a pathway distinct from canonical mode that leads to activation of Ras on the plasma membrane. The biological function and specific visual pathway of Rasgrp1-expressing ipRGCs remains unclear.

Tbx20 is expressed in a diverse set of ipRGC subtypes

Tbx20 was another gene, like Rasgrp1, that was differentially expressed according to our gene expression studies of adult ipRGCs. Testing of Tbx20 protein expression revealed that many of the labeled cells were also Opn4-immunoreactive. Similar to Rasgrp1, Tbx20 was determined to be expressed in most M1 ipRGCs (75%) and a minority of M2 cells (40%) and an additional population of RGCs whose identity was not immediately obvious. We decided to then compare Tbx20 against other known molecular patterns in ipRGCs. Whereas most RGCs follow a Brn3b-dependent developmental program, the M1 ipRGCs that project to the SCN do not express Brn3b while OPN-projecting M1 ipRGCs express Brn3b. We found that Brn3b-expressing M1 cells are also Tbx20-immunopositive. The Brn3b-negative M1 cells are split between cells that express Tbx20 and those that do not. This finding already suggested to us that ipRGCs are more molecularly diverse than anticipated: Tbx20 is expressed in ipRGCs with differing brain targets, Tbx20 is expressed across multiple morphologically defined subtypes, and Tbx20 is not expressed in all of any one type. The exploration of Tbx20 coexpression with Rasgrp1 introduced further

diversification in the ipRGC family. Therefore, Tbx20 was found to be expressed across ipRGCs that belong to multiple morphological types, have diverse molecular expression, differing physiology, and is involved with multiple visual brain circuits.

Further studies are required to fully clarify Tbx20 expression in M6 ipRGCs. The *Cdh3-GFP* reporter is currently the best means to identify M6 ipRGCs, but it is randomly integrated BAC transgenic that has not been confirmed to endogenously express Cdh3 gene product. The lack of fluorescent reporting in adult M6 ipRGCs by Cdh3-GFP limits the research capabilities to study M6 ipRGCs into adulthood. Importantly, continued expression of Tbx20 in adult M6 cells suggests that Tbx20 reporter systems could prove to be a more complete, biologically relevant genetic reporter than *Cdh3-GFP* for further study in the future. However, there were additional Tbx20-expressing RGCs not accounted for by either the *Cdh3-GFP* or Opn4 labeling, which may be due to the incomplete labeling by the *Cdh3-GFP* reporter or other RGC types that express Tbx20.

What is the function of Tbx20 in adult ipRGCs?

Tbx20 may play fundamental roles in instructing ipRGC type identity by regulating cell-specific transcriptional programs and repressing alternate fates. Although outside the scope of this research program, characterizing the function of Tbx20 in late development and adulthood could be important for understanding the specification and maintenance of adult ipRGC subtype identity. Due to the vital role of Tbx20 during early development, constitutive knockout results in lethality during embryogenesis (Cai et al., 2005). Additionally, Tbx20 plays well-established global roles in the retina during embryogenesis (Carson et al., 2004). Therefore, a conditional allele of Tbx20 is required to study its function in the mature retina. A 'floxed' allele of Tbx20 ($Tbx20^{fl/fl}$) has been

generated by flanking exon 2 with loxp sites and has been demonstrated to be an effective conditional null of Tbx20 (Cai et al., 2005; Shen et al., 2011). In principle, the *Opn4-Cre* mice would be an ideal means to conditionally knockout gene expression in ipRGCs. However, the embryonic expression of Opn4 would not allow temporal control of Tbx20 gene disruption. Additionally, our laboratory has realized that the *Opn4-Cre* suffers from incomplete recombination, especially in the low Opn4 expressing M4-M6 ipRGC subtypes (our studies, personal communication with R. Maloney and L. Quattrochi). Another option for temporal and controlled knockdown in ganglion cells would be the "SLICK" mouse transgenics (Single-neuron Labeling with Inducible Cre-mediated Knockout), which uses the Thy1 promoter to drive CreER, a tamoxifeninducible form of the Cre recombinase, along with yellow fluorescent protein (Deisseroth et al., 2006; Young et al., 2008; Heimer-McGinn and Young, 2011). Importantly, different available founder lines of SLICK were determined to have variable expression patterns throughout the nervous system, but founder line H (SLICK-H, Jax 012708) has particularly strong labeling in retinal ganglion cells (Young et al., 2008). Conditional knockout of Tbx20 in adult RGCs would be possible by injecting young adult $Tbx20^{fl/fl}$/SLICK mice with tamoxifen (Shen et al., 2011). If Tbx20 is continuously required for the maintenance of ipRGC identity into adulthood, then the knocking out in differentiated ipRGCs may result in dramatic loss of viability or acquisition of alternative fates. Whereas Tbx20 promotes proliferation early during formation of the eye cup, those same genes may become repressed with altered cofactor binding that are presently unknown. Loss of Tbx20 function as repressor of alternate fates and proliferation capacity may lead to dedifferentiation and reentry into the cell cycle. These striking phenotypes would clearly demonstrate that Tbx20 is crucial not only for promoting retinal development but also for maintaining the identity of terminally differentiated ipRGCs. If this is the case, then this

loss of cell identity can be tested further for a behavioral phenotype. For example, if $Tbx20^{fl/fl}$/SLICK mice lost their retinal axon projections to the OPN, then a pupilary light reflex behavioral defect could be tested.

Classification of ipRGC subtypes

The retina has become an excellent model system for conceptualizing what constitutes a neuronal subtype. The current strategy to identify neuronal subtypes is by using a combination of four criteria: morphology, gene expression, mosaicism, and physiology(Sanes and Masland, 2015). In the beginning, there was one type of intrinsically photosensitive retinal ganglion cell that fit the criteria of cell type classification very well. The M1 morphology was stereotyped and distinct in the uppermost OFF layer; they uniquely responded to light independent of rods and cones; they were dispersed across the retina; they expressed a special protein related to their physiology; and they send irradiance information to regions in the brain such as the SCN that makes sense for behavior. Over the last 15 years, the sole M1 has grown to a family of six members (Figure 9). The central tenet that holds the family together is intrinsic photosensitivity. The trend of highest expressing M1 ipRGCs being discovered first and scaling down to the M6 type having a very weak response to light is not an accident. The special capability to autonomously respond to light is directly relatable to the level of Opn4 expressed. Further, the way that most of the new types of ipRGCs were discovered was due to increasing the sensitivity to visualize expression (i.e., transgenic reporters and immunofluorescence) and link it to a given type with follow-up experiments (such as dye-filling and physiology). The physiological response to light under normal circumstances is surprisingly similar from M1 to M6 type ipRGCs, having an ON-sustained light response whether they have an OFF arbor or not (Figure 9). Currently Opn4 continues to be the

defining molecule of the family. However, the introduction of molecularly distinct M1 types deciphered by absent Brn3b expression has provided hints that there might be more than meets the eye. We pursued our studies to try to relate molecular programs with the many known distinguishing characteristics of ipRGCs (i.e., Opn4 related to phototransduction). Additionally, we hoped to further refine the classification of ipRGC types. Our integration of the differentially-expressed genes Rasgrp1 and Tbx20 focused primarily on the initially described M1-M3 ipRGC subtypes because there is the most knowledge and tools available (Figure 9). Our studies suggest that there is even further molecular specialization in the SCN-projecting ipRGC types than previously considered (Figure 9).

In addition to Tbx20 expression in a subset of SCN-projecting M1s, Tbx20 may also regulate the molecular program of ipRGCs projecting to the OPN and control the pupillary light reflex (Figure 9). The Brn3b-expressing M1 ipRGCs, a subset of M2 ipRGCs and *Cdh3-GFP* labeled M6 ipRGCs are all known to project to the OPN, and all express Tbx20. However, this is not a direct association and further retrograde or Tbx20 conditional knockout studies are required, especially to determine the function of Tbx20-expressing M2s.

Our studies will allow future mosaic analysis of ipRGCs expressing Rasgrp1 and Tbx20, including counts of total cells, analysis of dendritic overlap, and the regularity of the array of somas and dendritic fields (i.e., Berson et al., 2010). Previous studies determined that the dendritic fields of both M1 and M2 cells appear to have exuberant overlap with those of other cells of the same type; the dendrites of three to four cells typically overlap any retinal point (Berson et al., 2010). This may be a characteristic feature of these RGC subtypes, but it may also signal that there are subtypes of M1 or M2 cells, each with its own orderly spatial arrangement yielding complete retinal coverage.

Identification of genes differentially expressed in adult ipRGCs

We are encouraged that our gene expression profiling data of ipRGCs lead us to the identification of Tbx20 and Rasgrp1 as novel, selectively expressed genes in ipRGCs. These results serve as a good proof of principal for the validity of our gene expression profiling results. In addition, the stable, specific expression in adult ipRGCs suggests that the differential gene expression of Rasgrp1 and Tbx20 were not simply due to transient, stress-induced molecular program resulting from the harsh processing steps prior to sequencing. The more than 75 genes suggested to be differentially expressed in ipRGCs will be useful for the identification of marker genes for ipRGC types, comparison of gene expression across types, understanding the intracellular gene networks underlying ipRGC phenotypes, and the testing for conservation of ipRGC molecular programs across mammalian species.

METHODS

Animals:

All experiments were conducted in accordance with NIH guidelines under protocols approved by the Brown University (Providence, RI) Animal Care and Use Committee. Both male and female adult mice (P30 to P90) were used unless otherwise stated. *Opn4*$^{cre/cre}$ mice (Ecker et al. 2010) crossed with floxed-stop reporter mice: "*Z/EG*" (*Jax#003920*); the offspring express GFP in *cre*-expressing cells (M1-M6), as described by Ecker et al., 2010. *Opn4-GFP(ND100Gsat)* is a BAC transgenic originated from the GENSAT project at Rockefeller University. Rasgrp1-KO (Rasgrp1^{tm1Jstn}, Dower et al., 2000) was initially provided generously by Robert Barrington, U. of Alabama for initial testing. A colony was created inhouse from stock at Jackson labs (Jax 022353). *Rasgrp1-Cre*(PO1 founder line) was rederived from Jackson Labs (#34811-UCD). *Cdh3-GFP* reporter is a BAC transgenic originally generated by the Gensat project (MMRRC, BK102Gsat/MMNC) and has been used previously (Osterhout et al., 2011, 2014; Sümbül et al., 2014). This mouse line has been backcrossed in wild type background for at least 10 generations. *Cdh3-GFP* mice were three weeks old or younger unless otherwise stated.

Antibodies for i*mmunohistochemistry:*

For these studies, the following primary antibodies were used: rabbit anti-melanopsin (Advanced Targeting Systems; 1:10,000), guinea pig anti-RBPMS (PhosphoSolutions 1832-RBPMS), rabbit anti-green fluorescent protein (GFP; Invitrogen); Goat anti-Brn3b antibody (Santa Cruz #sc-6026); mouse anti-Rasgrp1 (Santa Cruz sc-8430); guinea pig anti-Tbx20[1:8500] (Song et al., 2006)Rabbit anti-Giantin (Abcam ab24586). Secondary antibodies consisted of Alexa Fluor 350,

488, 594 or 647 donkey anti-goat, Alexa Fluor 594 donkey anti-rabbit and Alexa Fluor 594 goat anti-guinea pig.

Retina Tissue Preparations and Solutions

Mice were euthanized by inhalation of CO2. Prior to removing the eye, the dorsal margin of the cornea was marked with a cautery and this was used to guide the placement of a large relieving cut in the dorsal retina as a subsequent guide to retinal orientation. Eyes were removed immediately after death and placed in Hibernate-A solution preheated to 37 °C. To keep track of retinal orientation, the right and left eye were identified and processed separately.

Immunohistochemistry

After the retina was removed from the eye, it was placed on Millipore nitrocellulose paper. The retinas were fixed for 30 minutes at room temperature using 4% paraformaldehyde freshly prepared in 0.1M phosphate buffered saline (PBS; pH 7.4). The tissue was then washed for 15 minutes in PBS three times. The tissue was then incubated in a blocking solution of 0.5% Triton-X and 5% Goat Serum in PBS for two hours at room temperature. The tissue was incubated for two nights at 4 °C while on a shaker in the primary antibodies diluted in this same blocking solution. The following day, the samples were washed six times for 20 minutes in 0.1% Tween-20 in PBS. The tissue was then incubated for two hours in the appropriate Invitrogen or Jackson labs secondary antibodies diluted 1:1000 in the blocking solution at room temperature. The tissue was then washed six times for 10 minutes in 0.1% Tween-20 in PBS. The retinas were then mounted in Aquamount, coverslipped, and sealed with fingernail polish.

For Rasgrp1 immunofluorescence studies, an additional antigen retrieval step was included. antigen retrieval the tissue was then placed in Tris-EDTA (pH 8.0) for 30 minutes at 80 °C. The samples were then allowed to return to room temperatures (about 15-30 minutes) before they were removed from the Tris-EDTA solution and washed three times for 15 minutes in PBS.

Image Acquisition

Immunofluorescent images were captured on a Zeiss Confocal (LSM 510) and Nikon Eclipse microscope (Micro Video Instruments, Inc. E614, Avon, MA) with a built in Spot Camera (Diagnostic Instruments, Inc. HRD 100-NIK Sterling Heights, MI). Confocal images were taken with a 20x objective (Plan Apochromat, WD 0.55 mm) at a resolution of 2048 pixels. To enhance clarity, image files were pseudocolored and the brightness and contrast was adjusted using ImageJ 1.47 (National Insistute of Heath, Bethesda, MD). All final images were constructed using ImageJ and Powerpoint (Microsoft Corporation, Redmond, WA).

Analysis of Rasgrp1 expression in ipRGC subtypes.

Because M1 and M2 cells have the highest levels of melanopsin expression of the ipRGC population, their dendrites were clearly visible and decipherable with immunostaining. M1 cells were identified by their dendritic projections to the OFF layer of the inner plexiform layer (IPL). M2 cells were identified by their dendrites which monostratify the ON sublamina of the IPL (Berson et al. 2010; Schmidt and Kofuji 2009). M3 cells bistratify the ON and OFF sublamina of the IPL (Schmidt and Kofuji 2011) and because these cells have similar levels of melanopsin expression and soma size as M2 cells, it is likely that M3 cells were included in the M2 population quantified in this study.

M4-M6 cells have the lowest levels of melanopsin-expression of the ipRGC population and their dendrites were not visible or decipherable with immunostaining. However, at least some members of the M4/M5/M6 population had lightly immunoreactive somas. M4 cells were identified by their large soma size, low melanopsin immunodetectability and the lack of dendritic labeling. The M5 and M6 cells we observed were identified by their low levels of melanopsin labeling and M2-sized somas (Schmidt et al. 2011).

Analysis of Tbx20 expression in Cdh3-GFP mice.

ipRGC subtypes were identified using a combination of morphological clues and process of elimination. In the case of M1 and M2 cells, which express the highest levels of melanopsin, confocal images of their immunofluorescence reveal dendritic information. As a result, unique dendritic features distinguish M1 and M2 cells. Cells with dendrites stratifying in the OFF layer of the IPL were identified as M1 cells, whereas cells stratifying in the ON layer were identified as M2 cells (Berson et al. 2010; Schmidt and Kofuji 2009). Using this method, M3 cells, which stratify in the ON and OFF sublamina of the IPL, were included in the M1 cell population unless otherwise noted (Schmidt and Kofuji 2011). As a result of their low levels of melanopsin, M4 and M5/6 cells are weakly labeled using anti-melanopsin immunohistochemistry with only some of their somata, but no dendrites, visible. Therefore, the method employed for deciphering M1 and M2 cells cannot be used to identify M4 and M5/6 cells. Instead, M4 cells were categorized by their lack of dendritic labeling, and their large soma size. M5/6 cells were characterized by their lack of dendritic labeling, M2-sized somata, and process of elimination (Schmidt et al. 2011). In

other words, cells that were not stained by the melanopsin antibody (which would detect M1-M3), but were labeled by GFP (labeling M1-M6), and had small somata, fell into the M5/6 category.

Viral vectors

To express ChR2 in optic axons for brain studies, AAV1-ChR2-mCherry (Penn vector core) was injected into the right eyes of young adult mice. Two weeks later, the brain was sectioned and labeling was enhanced by anti-mcherry immunofluorescence.

Ocular injections

Mice were anesthetized with isoflurane (3% in O2), and eyes were protruded and stabilized using forceps. A glass pipette tip was then inserted at the corneal-scleral margin, and 1-2µl of tracer or virus was injected using gentle pressure over 1 minutes. After a 1-minute waiting period, the pipette was removed. Eyes were then coated with ophthalmic ointment and animals were recovered on a heating pad.

Brain injection of retrobeads into suprachiasmatic nucleus

Adult wild type mice (P30-P60) were anaesthetized with isofluorance and fluorescently labelled rhodamine latex microspheres (RetroBeads, Lumafluor) were injected into the ipsilateral suprachiasmatic nucleus to retrogradely label RGCs with axon terminals at the injections site. Three to five days later, the brain was removed and immediately fixed overnight. The following day, the brain was rinsed in 0.1M PBS and sectioned at 50um in the coronal plane. The slices were incubated with DAPI staining for 10 minutes was done in order to provide a reference for SCN location as indicated by concentrated cellular staining at the SCN. The slices were imaged for

DAPI in UV channel and overlayed with rhodamine channel to identify the injection site in relation to SCN location. Special attention was paid to ensure that the injection did not extend into optic nerve and confound results by introducing off-target RGC labeling of fibers of passage.

Brain histology

Animals were sacrificed via transcardial perfusion, and brains were removed and incubated in 4% paraformaldehyde overnight. Brains were sectioned at 50μm in the coronal plane. To reveal individual processes in viral tracing experiments, virallyexpressed EYFP was enhanced using rabbit-anti-gfp (1:1000) and goat-anti-rabbit alexa 488 (1:500). To observe parvalbumin expression in OPN neurons, parvalbumin immunohistochemistry was performed using mouse-anti-parvalbumin (1:1000) followed by goat-anti-mouse alexa 488.

Stained and sliced brain slices were mounted on glass cover slides and imaged using a SPOT RT Slider digital microscope camera mounted to a Nikon (Diagnostic Instruments) as described previously (Berson et al., 2010; Estevez et al., 2012). Images were assembled in Adobe Photoshop CS3.

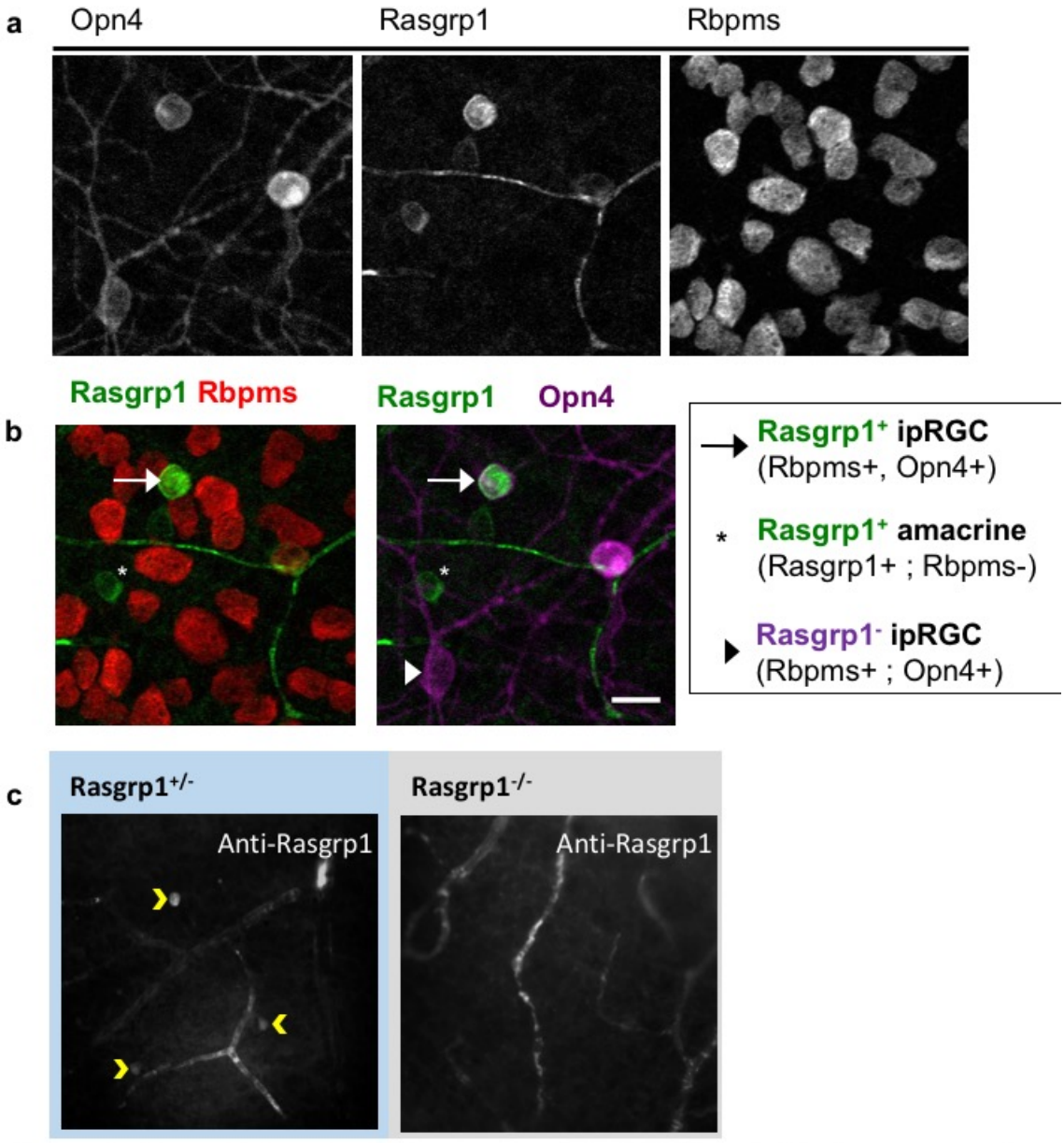

Figure 1. Rasgrp1 is selectively expressed in ipRGCs. a) Whole mount retina immunofluorescence study of the ganglion cell layer (GCL) immunostained for Opn4, Rasgrp1, and the pan-RGC marker RBPMS (Rodriguez et a., 2014). **b)** Rasgrp1 is expressed in a subpopulation of amacrine cells and RGCs (Rbpms-positive and –negative, respectively). The vast majority (97%) of Rasgrp1-RGCs are Opn4-immunopositive and therefore ipRGCs. Scale bar is 20um. **c)** Testing specificity of Rasgrp1 antibody (sc-8430) in Rasgrp1-/- knockout and heterozygous mice suggests a lack of off-target antiody staining.

a. **Quantification of Rasgrp1 expression in established ipRGC subtypes.**

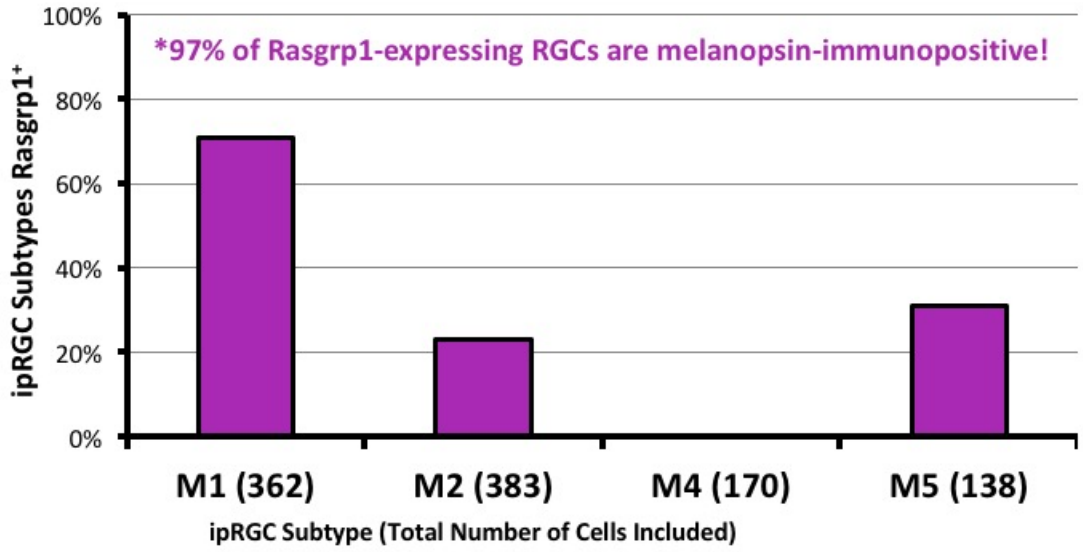

b. Spatial distribution of M1 and M2 ipRGCs

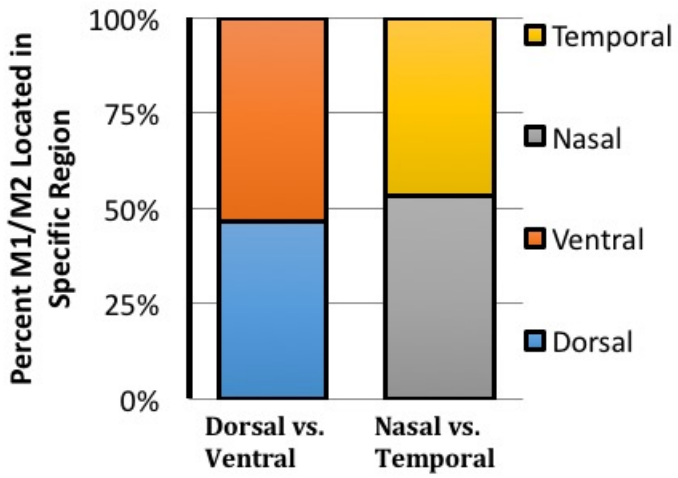

Figure 2. Rasgrp1 is selectively expressed in a subset morphologically diverse set of ipRGC subtypes. a) Rasgrp1 immunofluorescence is concentrated in ipRGCs, especially the M1 subtype, but also M2 cells and small soma, low Opn4 expression cells (presumptive M5). b) Analysis of the M1/M2 population in the right whole mount wild type shown in Figure 7 revealed no evident gradient of ipRGC spatial distribution across the retina. Seven frames were used to represent each area of the retina to maintain equal spatial contribution.

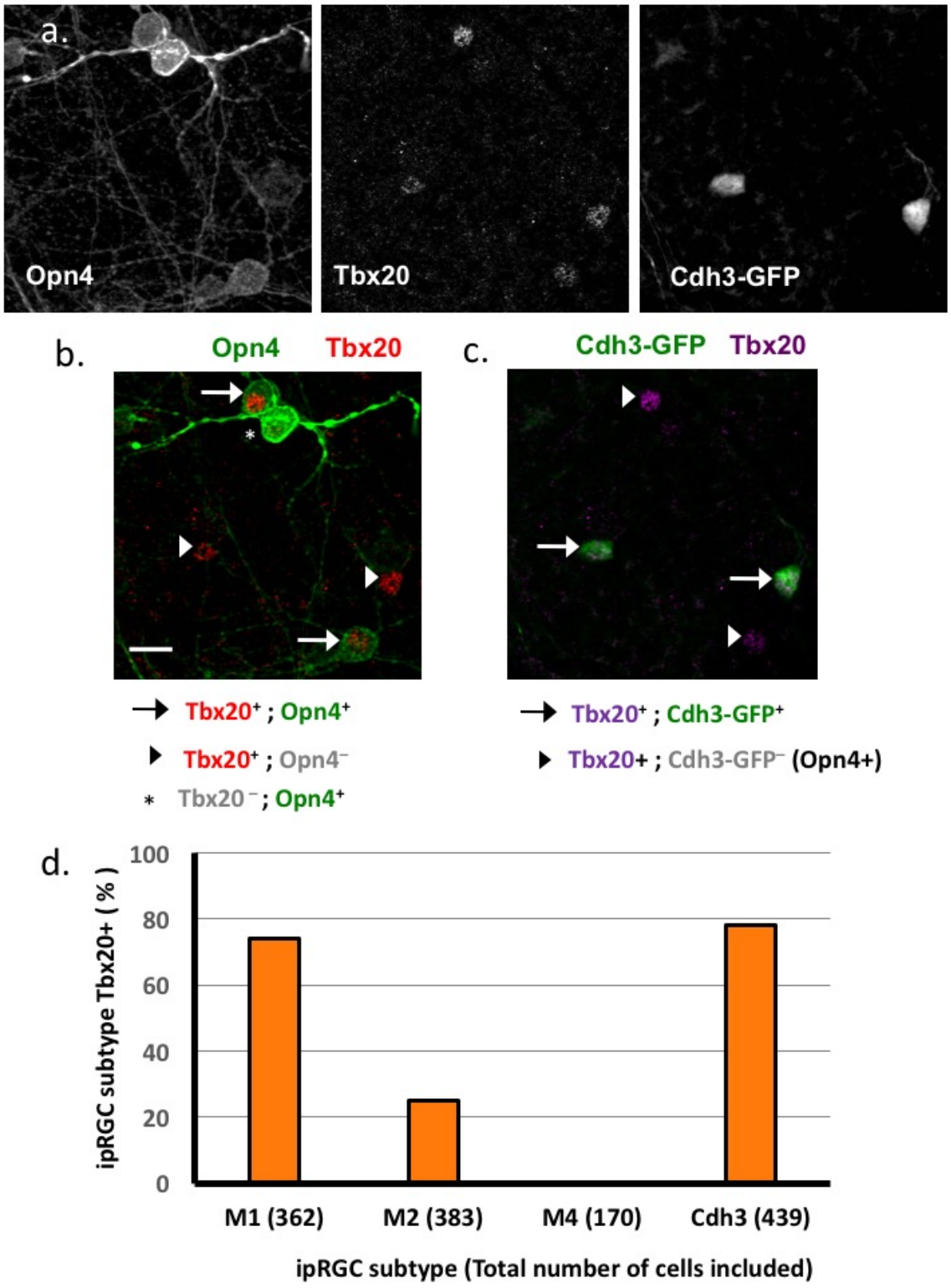

Figure 3. Colocalization study of Tbx20-expression in ipRGC subtypes. a. Triple immunofluorescence of Opn4, Tbx20, and Cdh3-GFP (M6-type enriched). b) Tbx20-expression in subset of M1-M3 ipRGCs (not M4). b,c)Tbx20 is concentrated in the nucleus of most Cdh3-GFP-cells.

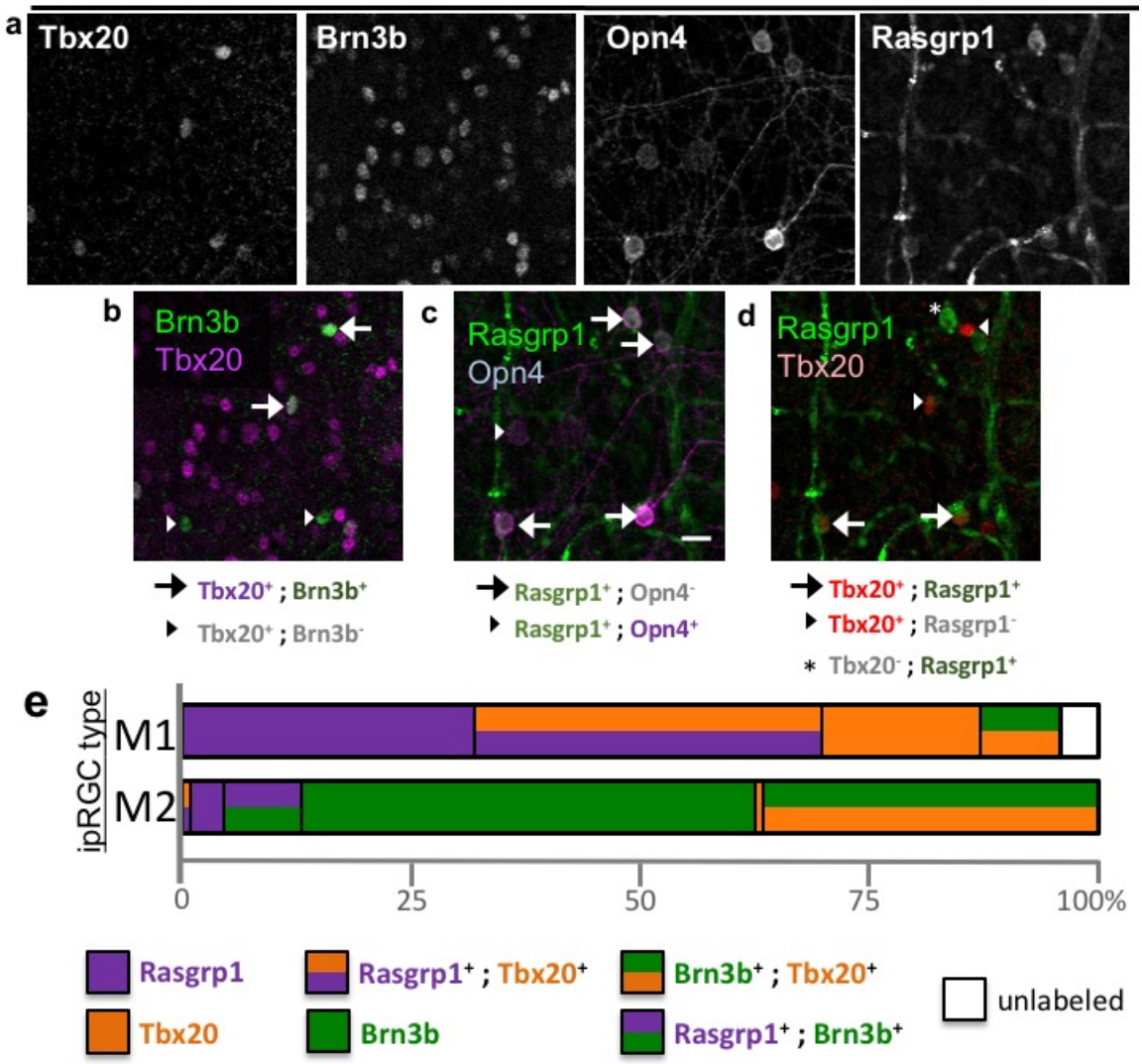

Figure 4: Complex pattern of Rasgrp1-Tbx20-Brn3b co-expression suggests further diversity in ipRGC family. a) Quadruple immunofluorescence study of Tbx20, Brn3b, Opn4, and Rasgrp1. b) Brn3b is expressed in a subpopulation of Tbx20-expressing cells. c) Rasgrp1 and Opn4 were quantified for ipRGC subtype expression prior to incorporating Tbx20 and Brn3b expression. d) Rasgrp1 and Tbx20 expression is partially overlapping. e) integrated expression patterns of Brn3b, Rasgrp1, and Tbx20 with M1 and M2 ipRGC subtypes. These correlation studies suggest unexpected additional diversity in the ipRGC family.

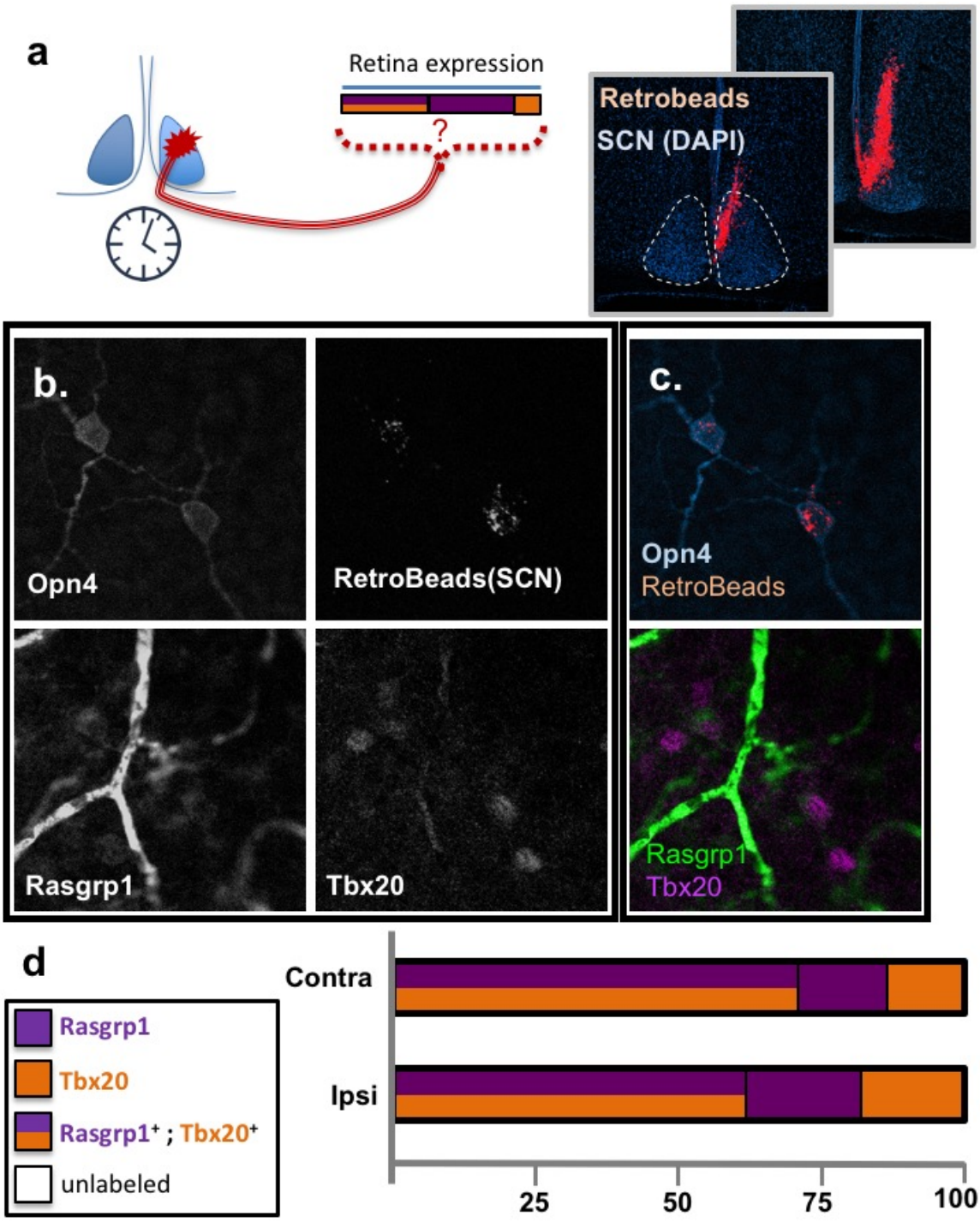

Figure 5. SCN-projecting ipRGCs are molecularly diverse patterns of Rasgrp1 and Tbx20 expression. a) Experimental design of fluorescent bead injection to SCN, followed by examination of Rasgrp1 and Tbx20 expression in retrograde labeled RGCs. Verification that retrograde injection is within the SCN, but not the optic nerve. b) Triple immunofluorescence of Opn4, Rasgrp1, and Tbx20 as well as fluorescent Retrobeads c) Opn4-Retrobeads coexpression further validates clean injection. d) SCN-projecting ipRGCs are molecularly diverse for Tbx20 and Rasgrp1.

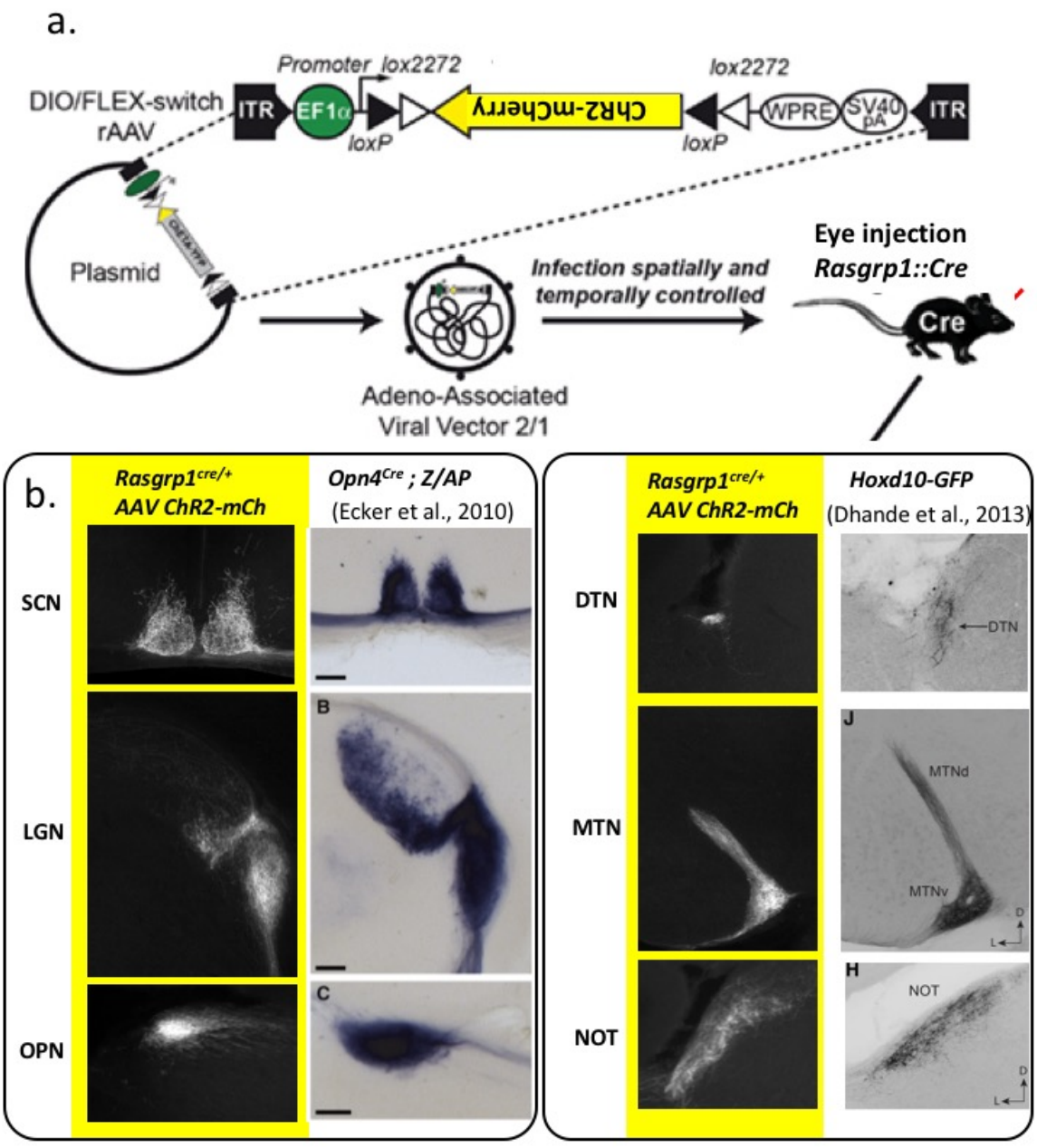

Figure 6. Rasgrp1-Cre expressing RGCs have axon terminals in a wide range of subconscous visual targets. a) Experimental design involved the injection of viruses packaged with Cre-dependent membrane-bound fluorescent reporter and injected into right eye of Rasgrp1-Cre mice. b) Rasgrp1-cre RGCs projections include a distinct, complete pattern of axon terminals reminiscent of Opn4-Cre labeling of M1-M6. Additional labeling was seed of the three major accessory optic regions.

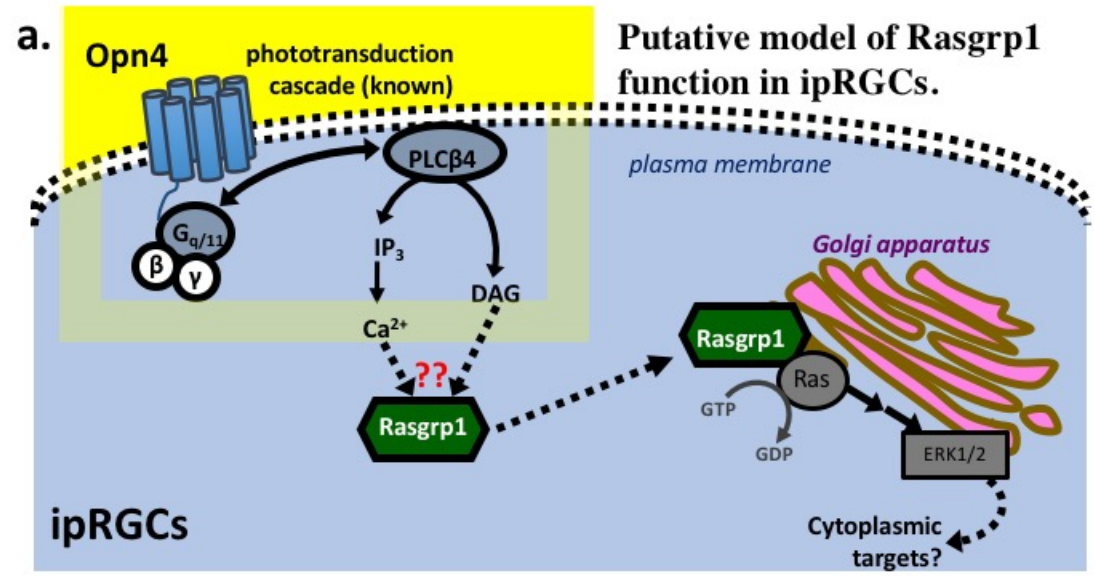

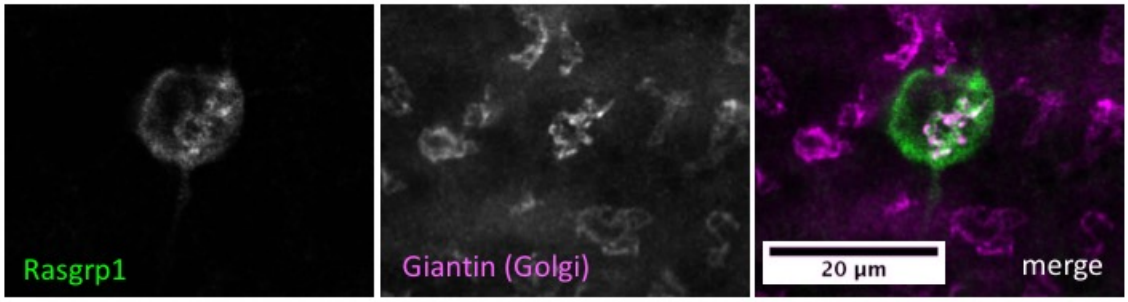

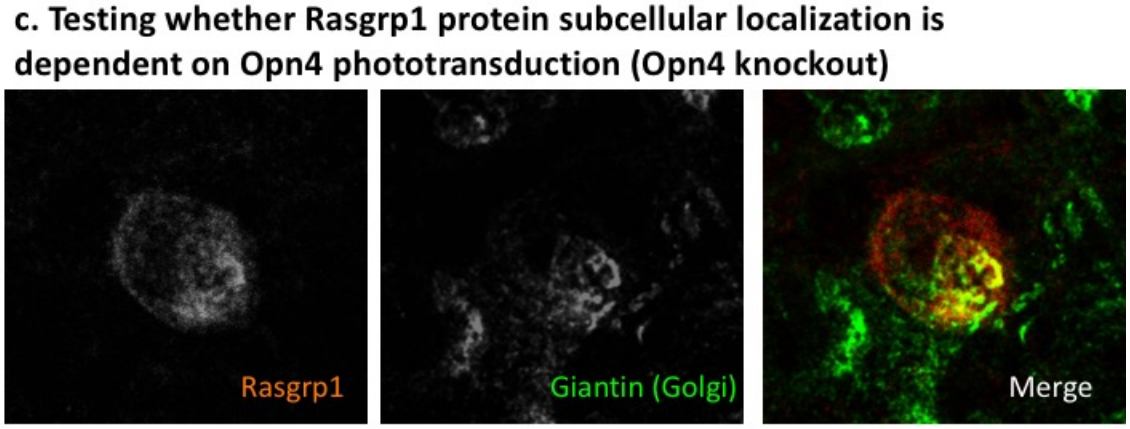

Figure 7. Rasgrp1 is localized to the Golgi in ipRGCs via an Opn4-independent process. a) ipRGC phototransduction elevates diacylglycerol and intracellular calcium, both known to activate Rasgrp1. Certain ipRGCs may utilize a specialized form of Ras signaling in the Golgi body. **b)** Preliminary evidence that Rasgrp1 (Green) may be colocalized with Giantin (magenta), a marker of the Golgi apparatus. Additional Rasgrp1 labeling is also present across the plasma membrane. c) Rasgrp1 translocation to Golgi is Opn4-independent.

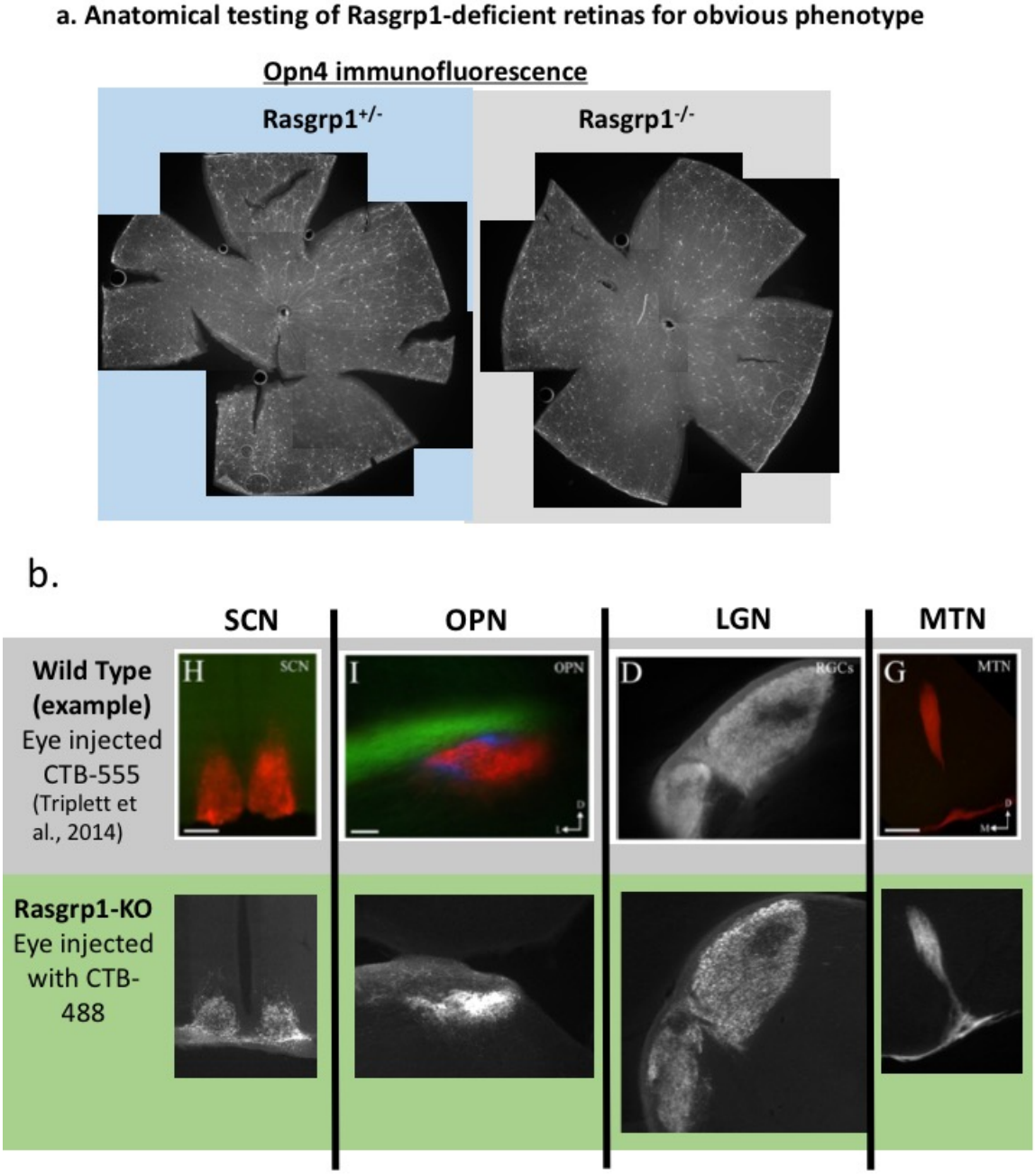

Figure 8. Phenotype analysis of anatomical defects suggest Rasgrp1 does not have an important circuit-based neuron function. a) Retinas of Rasgrp1-knockout mice appear normal, with no obvious phenotype. b) Rasgrp1-KO visual brain targets of RGCs also appear relatively normal.

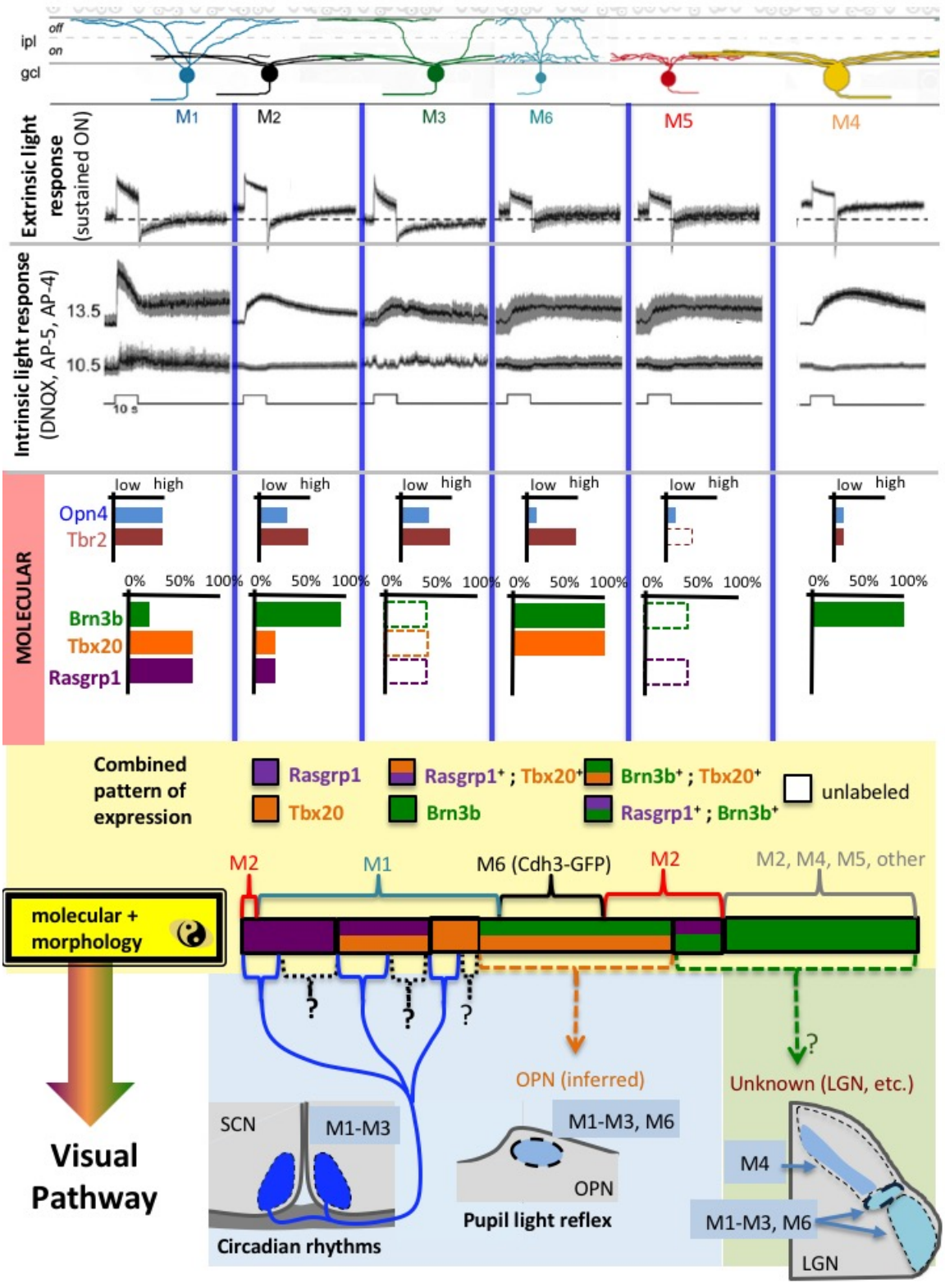

Figure 9. Current model of ipRGC family members integrating molecular, physiology, brain circuitry, and morphology.

REFERENCES

Abe T, Fujimori T (2013) Reporter Mouse Lines for Fluorescence Imaging. Dev Growth Differ 55:390–405.

Abraham NM, Egger V, Shimshek DR, Renden R, Fukunaga I, Sprengel R, Seeburg PH, Klugmann M, Margrie TW, Schaefer AT, Kuner T (2010) Synaptic inhibition in the olfactory bulb accelerates odor discrimination in mice. Neuron 65:399–411.

Adachi N, Oyasu M, Taniguchi T, Yamaguchi Y, Takenaka R, Shirai Y, Saito N (2005) Immunocytochemical localization of a neuron-specific diacylglycerol kinase beta and gamma in the developing rat brain. Brain Res Mol Brain Res 139:288–299.

Aikawa J, Grobe K, Tsujimoto M, Esko JD (2001) Multiple isozymes of heparan sulfate/heparin GlcNAc N-deacetylase/GlcN N-sulfotransferase. Structure and activity of the fourth member, NDST4. J Biol Chem 276:5876–5882.

Alban FBVS (1620) Novum Organum. In: The Oxford Francis Bacon, Vol. 11: The Instauratio magna Part II: Novum organum and Associated Texts (Rees G, Wakely M, eds), pp 48–586 Novum organum and Associated Texts. Oxford University Press.

Alvarez VA, Arttamangkul S, Dang V, Salem A, Whistler JL, Zastrow Von M, Grandy DK, Williams JT (2002) mu-Opioid receptors: Ligand-dependent activation of potassium conductance, desensitization, and internalization. J Neurosci 22:5769–5776.

Amundson R (2005) The Changing Role of the Embryo in Evolutionary Thought. Cambridge: Cambridge University Press.

Anders S, Huber W (2010) Differential expression analysis for sequence count data. Genome Biology 2010 11:10 11:R106.

Anders S, McCarthy DJ, Chen Y, Okoniewski M, Smyth GK, Huber W, Robinson MD (2013) Count-based differential expression analysis of RNA sequencing data using R and Bioconductor. Nature Protocols 8:1765–1786.

Andreazzoli M (2009) Molecular regulation of vertebrate retina cell fate Moody SA, ed. Birth Defects Research Part C: Embryo Today: Reviews 87:284–295.

Arendt D (2003) Evolution of eyes and photoreceptor cell types. Int J Dev Biol 47:563–571.

Arendt D (2008) The evolution of cell types in animals: emerging principles from molecular studies. Nature Reviews Genetics 9:868–882.

Arendt D, Hausen H, Purschke G (2009) The “division of labour” model of eye evolution. Philos Trans R Soc Lond, B, Biol Sci 364:2809–2817.

Arendt D, Musser JM, Baker CVH, Bergman A, Cepko C, Erwin DH, Pavlicev M, Schlosser G, Widder S, Laubichler MD, Wagner GP (2016) The origin and evolution of cell types. Nature

Reviews Genetics 17:744–757.

Arendt D, Tessmar-Raible K, Snyman H, Dorresteijn AW, Wittbrodt J (2004) Ciliary photoreceptors with a vertebrate-type opsin in an invertebrate brain. Science 306:869–871.

Arlotta P, Molyneaux BJ, Chen J, Inoue J, Kominami R, Macklis JD (2005) Neuronal Subtype-Specific Genes that Control Corticospinal Motor Neuron Development In Vivo. Neuron 45:207–221.

Arnold SJ, Huang G-J, Cheung AFP, Era T, Nishikawa S-I, Bikoff EK, Molnár Z, Robertson EJ, Groszer M (2008) The T-box transcription factor Eomes/Tbr2 regulates neurogenesis in the cortical subventricular zone. Genes Dev 22:2479–2484.

Atlasz T, Szabadfi K, Kiss P, Racz B, Gallyas F, Tamas A, Gaal V, Marton Z, Gabriel R, Reglodi D (2010) Pituitary adenylate cyclase activating polypeptide in the retina: focus on the retinoprotective effects. Ann N Y Acad Sci 1200:128–139.

Baden T, Berens P, Franke K, Román Rosón M, Bethge M, Euler T (2016) The functional diversity of retinal ganglion cells in the mouse. Nature 529:345–350.

BARLOW HB (1953) Summation and inhibition in the frog's retina. The Journal of Physiology 119:69–88.

BARLOW HB, HILL RM, LEVICK WR (1964) RETINAL GANGLION CELLS RESPONDING SELECTIVELY TO DIRECTION AND SPEED OF IMAGE MOTION IN THE RABBIT. The Journal of Physiology 173:377–407.

Barres BA, Hart IK, Coles HSR, Burne JF, Voyvodic JT, Richardson WD, Raff MC (1992) Cell death and control of cell survival in the oligodendrocyte lineage. Cell 70:31–46.

Barres BA, Silverstein BE, Corey DP, Chun LLY (1988) Immunological, morphological, and electrophysiological variation among retinal ganglion cells purified by panning. Neuron 1:791–803.

Bassett EA, Wallace VA (2012) Cell fate determination in the vertebrate retina. Trends in Neurosciences 35:565–573.

Bastien J, Rochette-Egly C (2004) Nuclear retinoid receptors and the transcription of retinoid-target genes. Gene 328:1–16.

Baver SB, Pickard GE, Sollars PJ, Pickard GE (2008) Two types of melanopsin retinal ganglion cell differentially innervate the hypothalamic suprachiasmatic nucleus and the olivary pretectal nucleus. European Journal of Neuroscience 27:1763–1770.

Bedont JL, Blackshaw S (2015) Constructing the suprachiasmatic nucleus: a watchmaker's perspective on the central clockworks. Front Syst Neurosci 9:74.

Beech DJ, Barnes S (1989) Characterization of a voltage-gated K+ channel that accelerates the

rod response to dim light. Neuron 3:573–581.

Beglopoulos V, Montag-Sallaz M, Rohlmann A, Piechotta K, Ahmad M, Montag D, Missler M (2005) Neurexophilin 3 is highly localized in cortical and cerebellar regions and is functionally important for sensorimotor gating and motor coordination. Mol Cell Biol 25:7278–7288.

Benjamini Y, Hochberg Y (1995) Controlling the false discovery rate: a practical and powerful approach to multiple testing. Journal of the royal statistical society Series B (….

Bergström AL, Hannibal J, Hindersson P, Fahrenkrug J (2003) Light-induced phase shift in the Syrian hamster (Mesocricetus auratus) is attenuated by the PACAP receptor antagonist PACAP6-38 or PACAP immunoneutralization. Eur J Neurosci 18:2552–2562.

Berson DM, Castrucci AM, Provencio I (2010) Morphology and mosaics of melanopsin-expressing retinal ganglion cell types in mice. Journal of Comparative Neurology 518:2405–2422.

Berson DM, Dunn FA, Takao M (2002) Phototransduction by Retinal Ganglion Cells That Set the Circadian Clock. Science 295:1070–1073.

Beyer K, Goldstein J, Ramakrishnan R, Shaft U (1999) When Is "Nearest Neighbor" Meaningful? In: Database Theory — ICDT'99, pp 217–235 Lecture Notes in Computer Science. Berlin, Heidelberg: Springer Berlin Heidelberg.

Béguin P, Nagashima K, Gonoi T, Shibasaki T, Takahashi K, Kashima Y, Ozaki N, Geering K, Iwanaga T, Seino S (2001) Regulation of Ca2+ channel expression at the cell surface by the small G-protein kir/Gem. Nature 411:701–706.

Bharadwaj A, Bydoun M, Holloway R, Waisman D (2013) Annexin A2 heterotetramer: structure and function. Int J Mol Sci 14:6259–6305.

Bivona TG, de Castro IP, Ahearn IM, Grana TM, Chiu VK, Lockyer PJ, Cullen PJ, Pellicer A, Cox AD, Philips MR (2003a) Phospholipase C|[gamma]| activates Ras on the Golgi apparatus by means of RasGRP1. Nature 424:694–698.

Bivona TG, Pérez De Castro I, Ahearn IM, Grana TM, Chiu VK, Lockyer PJ, Cullen PJ, Pellicer A, Cox AD, Philips MR (2003b) Phospholipase Cgamma activates Ras on the Golgi apparatus by means of RasGRP1. Nature 424:694–698.

Blackshaw S, Fraioli RE, Furukawa T, Cepko CL (2001) Comprehensive Analysis of Photoreceptor Gene Expression and the Identification of Candidate Retinal Disease Genes. Cell 107:579–589.

Blackshaw S, Harpavat S, Trimarchi J, Cai L, Huang H, Kuo WP, Weber G, Lee K, Fraioli RE, Cho S-H, Yung R, Asch E, Ohno-Machado L, Wong WH, Cepko CL (2004) Genomic Analysis of Mouse Retinal Development William Harris, ed. PLOS Biol 2:e247.

Bloom JS, Khan Z, Kruglyak L, Singh M, Caudy AA (2009) Measuring differential gene expression by short read sequencing: quantitative comparison to 2-channel gene expression microarrays. BMC Genomics 10:221.

Bocksteins E (2016) Kv5, Kv6, Kv8, and Kv9 subunits: No simple silent bystanders. J Gen Physiol 147:105–125.

Bocksteins E, Snyders DJ (2012) Electrically silent Kv subunits: their molecular and functional characteristics. Physiology (Bethesda) 27:73–84.

Borst A, Euler T (2011) Seeing things in motion: models, circuits, and mechanisms. Neuron 71:974–994.

Boycott BB, Wässle H (1974) The morphological types of ganglion cells of the domestic cat's retina. The Journal of Physiology 240:397–419.

Brennaman LH, Moss ML, Maness PF (2014) EphrinA/EphA-induced ectodomain shedding of neural cell adhesion molecule regulates growth cone repulsion through ADAM10 metalloprotease. J Neurochem 128:267–279.

Brewer GJ (1997) Isolation and culture of adult rat hippocampal neurons. Journal of Neuroscience Methods 71:143–155.

Brewer GJ, Torricelli JR (2007) Isolation and culture of adult neurons and neurospheres. Nature Protocols 2:1490–1498.

Brewer GJ, Torricelli JR, Evege EK, Price PJ (1993) Optimized survival of hippocampal neurons in B27-supplemented neurobasal™ , a new serum-free medium combination. Journal of Neuroscience Research 35:567–576.

Brown NL, Kanekar S, Vetter ML, Tucker PK, Gemza DL, Glaser T (1998) Math5 encodes a murine basic helix-loop-helix transcription factor expressed during early stages of retinal neurogenesis. Development 125:4821–4833.

Bungers SR (2010) The Role of the Ras Guanyl-Nucleotide Exchange Factor Rasgrp1 in Synaptic Transmission.

Cahoy JD, Emery B, Kaushal A, Foo LC, Zamanian JL, Christopherson KS, Xing Y, Lubischer JL, Krieg PA, Krupenko SA, Thompson WJ, Barres BA (2008) A transcriptome database for astrocytes, neurons, and oligodendrocytes: a new resource for understanding brain development and function. J Neurosci 28:264–278.

Cai C-L, Zhou W, Yang L, Bu L, Qyang Y, Zhang X, Li X, Rosenfeld MG, Chen J, Evans S (2005) T-box genes coordinate regional rates of proliferation and regional specification during cardiogenesis. Development 132:2475–2487.

Cajal SRY (1892) The structure of the retina. Charles C. Thomas Publisher.

Cameron EG, Robinson PR (2014) β-Arrestin-Dependent Deactivation of Mouse Melanopsin Craft CM, ed. PLoS ONE 9:e113138.

Cancino J, Luini A (2013) Signaling circuits on the Golgi complex. Traffic 14:121–134.

Carcieri SM, Jacobs AL, Nirenberg S (2003) Classification of retinal ganglion cells: a statistical approach. Journal of Neurophysiology 90:1704–1713.

Caretti E, Devarajan K, Coudry R, Ross E, Clapper ML, Cooper HS, Bellacosa A (2008) Comparison of RNA amplification methods and chip platforms for microarray analysis of samples processed by laser capture microdissection. Journal of Cellular Biochemistry 103:556–563.

Carrasco AE, McGinnis W, Gehring WJ, De Robertis EM (1984) Cloning of an X. laevis gene expressed during early embryogenesis coding for a peptide region homologous to Drosophila homeotic genes. Cell 37:409–414.

Carson CT, Kinzler ER, Parr BA (2000) Tbx12, a novel T-box gene, is expressed during early stages of heart and retinal development. Mechanisms of Development 96:137–140.

Carson CT, Pagratis M, Parr BA (2004) Tbx12 regulates eye development in Xenopus embryos. Biochemical and Biophysical Research Communications 318:485–489.

Casagrande VA (1994) A third parallel visual pathway to primate area V1. Trends in Neurosciences 17:305–310.

Catherine Faivre-Sarrailh JJD (2013) Neuro-glial interactions at the nodes of Ranvier: implication in health and diseases. Frontiers in Cellular Neuroscience 7:196.

Cayouette M, Poggi L, Harris WA (2006) Lineage in the vertebrate retina. Trends in Neurosciences 29:563–570.

Cepko CL (1999) The roles of intrinsic and extrinsic cues and bHLH genes in the determination of retinal cell fates. Current Opinion in Neurobiology 9:37–46.

Cepko CL, Austin CP, Yang X, Alexiades M, Ezzeddine D (1996) Cell fate determination in the vertebrate retina. PNAS 93:589–595.

Chakraborty S, Yutzey KE (2012) Tbx20 regulation of cardiac cell proliferation and lineage specialization during embryonic and fetal development in vivo. Developmental Biology 363:234–246.

Chen SK, Badea TC, Hattar S (2011) Photoentrainment and pupillary light reflex are mediated by distinct populations of ipRGCs. Nature 476:92–95.

Chen SK, Ecker JL, Hattar S (2010) Understanding the Complexity of ipRGCs Targeting and Functions. Invest Ophthalmol Vis Sci 51:664–664.

Cherry TJ, Trimarchi JM, Stadler MB, Cepko CL (2009) Development and diversification of retinal amacrine interneurons at single cell resolution. Proc Natl Acad Sci USA 106:9495–9500.

Chiu VK, Bivona T, Hach A, Sajous JB, Silletti J, Wiener H, Johnson RL, Cox AD, Philips MR (2002) Ras signalling on the endoplasmic reticulum and the Golgi. Nat Cell Biol 4:343–350.

Chow RL, Lang RA (2003) Early Eye Development in Vertebrates. http://dxdoiorg/101146/annurevcellbio171255 17:255–296.

Cleland BG, LEVICK WR (1974) Properties of rarely encountered types of ganglion cells in the cat's retina and an overall classification. The Journal of Physiology 240:457–492.

Clément-Ziza M, Gentien D, Lyonnet S, Thiery J-P, Besmond C, Decraene C (2009) Evaluation of methods for amplification of picogram amounts of total RNA for whole genome expression profiling. BMC Genomics 10:246.

Conlon FL, Fairclough L, Price BM, Casey ES, Smith JC (2001) Determinants of T box protein specificity. Development 128:3749–3758.

Cook JE, Noden AJ (1998) Somatic and dendritic mosaics formed by large ganglion cells in the retina of the common house gecko (Hemidactylus frenatus). Brain Behav Evol 51:263–283.

Cook T (2003) Cell diversity in the retina: more than meets the eye. BioEssays 25:921–925.

Craig AM, Kang Y (2007) Neurexin-neuroligin signaling in synapse development. Current Opinion in Neurobiology 17:43–52.

Cui Q, Ren C, Sollars PJ, Pickard GE, So KF (2015) The injury resistant ability of melanopsin-expressing intrinsically photosensitive retinal ganglion cells. Neuroscience 284:845–853.

Dacey DM, Liao H-W, Peterson BB, Robinson FR, Smith VC, Pokorny J, Yau K-W, Gamlin PD (2005) Melanopsin-expressing ganglion cells in primate retina signal colour and irradiance and project to the LGN. Nature 433:749–754.

Dang VC, Williams JT (2005) Morphine-Induced mu-opioid receptor desensitization. Mol Pharmacol 68:1127–1132.

Daniele LL, Adams RH, Durante DE, Pugh EN, Philp NJ (2007) Novel distribution of junctional adhesion molecule-C in the neural retina and retinal pigment epithelium. J Comp Neurol 505:166–176.

Darwin C (1859) On the origin of species by means of natural selection, or, The preservation of favoured races in the struggle for life /. London :: John Murray.

Dasen JS (2009) Chapter 4 Transcriptional Networks in the Early Development of Sensory–Motor Circuits. In: Development of Neural Circuitry, pp 119–148 Current Topics in Developmental Biology. Elsevier.

Dawkins R (1978) Replicator selection and the extended phenotype. Z Tierpsychol 47:61–76.

de Sevilla Müller LP, Sargoy A, Rodriguez AR, Brecha NC (2014) Melanopsin Ganglion Cells Are the Most Resistant Retinal Ganglion Cell Type to Axonal Injury in the Rat Retina Tosini G, ed. PLoS ONE 9:e93274.

de Sousa Abreu R, Penalva LO, Marcotte EM, Vogel C (2009) Global signatures of protein and mRNA expression levels. Mol Biosyst 5:1512–1526.

Deisseroth K, Feng G, Majewska AK, Miesenböck G, Ting A, Schnitzer MJ (2006) Next-generation optical technologies for illuminating genetically targeted brain circuits. J Neurosci 26:10380–10386.

Delgado R, Muñoz Y, Peña-Cortés H, Giavalisco P, Bacigalupo J (2014) Diacylglycerol activates the light-dependent channel TRP in the photosensitive microvilli of Drosophila melanogaster photoreceptors. J Neurosci 34:6679–6686.

Dell AL, Fried-Cassorla E, Xu H, Raper JA (2013) cAMP-induced expression of neuropilin1 promotes retinal axon crossing in the zebrafish optic chiasm. J Neurosci 33:11076–11088.

DeParis S, Caprara C, Grimm C (2012) Intrinsically photosensitive retinal ganglion cells are resistant to N-methyl-D-aspartic acid excitotoxicity. Mol Vis 18:2814–2827.

Devries SH, Baylor DA (1997) Mosaic arrangement of ganglion cell receptive fields in rabbit retina. Journal of Neurophysiology 78:2048–2060.

Dhande OS, Estevez ME, Quattrochi LE, El-Danaf RN, Nguyen PL, Berson DM, Huberman AD (2013) Genetic dissection of retinal inputs to brainstem nuclei controlling image stabilization. J Neurosci 33:17797–17813.

Dhande OS, Stafford BK, Lim J-HA, Huberman AD (2015) Contributions of Retinal Ganglion Cells to Subcortical Visual Processing and Behaviors. Annual Review of Vision Science 1:291–328.

Dhawale AK, Hagiwara A, Bhalla US, Murthy VN, Albeanu DF (2010) Non-redundant odor coding by sister mitral cells revealed by light addressable glomeruli in the mouse. Nature Neuroscience 13:1404–1412.

Di Fiore PP, Gill GN (1999) Endocytosis and mitogenic signaling. Curr Opin Cell Biol 11:483–488.

Diaz A, Ruiz F, Flórez J, Hurlé MA, Pazos A (1995) Mu-opioid receptor regulation during opioid tolerance and supersensitivity in rat central nervous system. J Pharmacol Exp Ther 274:1545–1551.

Díaz NM, Morera LP, Guido ME (2016) Melanopsin and the Non-visual Photochemistry in the Inner Retina of Vertebrates. Photochemistry and Photobiology 92:29–44.

Do MTH, Kang SH, Xue T, Zhong H, Liao H-W, Bergles DE, Yau K-W (2009) Photon capture and signalling by melanopsin retinal ganglion cells. Nature 457:281–287.

Do MTH, Yau K-W (2010) Intrinsically photosensitive retinal ganglion cells. Physiol Rev 90:1547–1581.

Doğrul A, Yeşilyurt O, Işimer A, Güzeldemir ME (2001) L-type and T-type calcium channel blockade potentiate the analgesic effects of morphine and selective mu opioid agonist, but not to selective delta and kappa agonist at the level of the spinal cord in mice. Pain 93:61–68.

Dougherty JD, Geschwind DH (2005) Progress in Realizing the Promise of Microarrays in Systems Neurobiology. Neuron 45:183–185.

Dower NA, Stang SL, Bottorff DA, Ebinu JO, Dickie P, Ostergaard HL, Stone JC (2000) RasGRP is essential for mouse thymocyte differentiation and TCR signaling. Nat Immunol 1:317–321.

Doyle JP, Dougherty JD, Heiman M, Schmidt EF, Stevens TR, Ma G, Bupp S, Shrestha P, Shah RD, Doughty ML, Gong S, Greengard P, Heintz N (2008) Application of a Translational Profiling Approach for the Comparative Analysis of CNS Cell Types. Cell 135:749–762.

Drager UC (1985) Birth Dates of Retinal Ganglion Cells Giving Rise to the Crossed and Uncrossed Optic Projections in the Mouse. Proceedings of the Royal Society of London B: Biological Sciences 224:57–77.

Duan X, Qiao M, Bei F, Kim I-J, He Z, Sanes JR (2015) Subtype-Specific Regeneration of Retinal Ganglion Cells following Axotomy: Effects of Osteopontin and mTOR Signaling. Neuron 85:1244–1256.

Dumitrescu ON, Pucci FG, Wong KY, Berson DM (2009) Ectopic retinal ON bipolar cell synapses in the OFF inner plexiform layer: Contacts with dopaminergic amacrine cells and melanopsin ganglion cells. Journal of Comparative Neurology 517:226–244.

Dyer MA, Livesey FJ, Cepko CL, Oliver G (2003) Prox1 function controls progenitor cell proliferation and horizontal cell genesis in the mammalian retina. Nature Genetics 34:53–58.

Eberhard DA, Brown MD, VandenBerg SR (1994) Alterations of annexin expression in pathological neuronal and glial reactions. Immunohistochemical localization of annexins I, II (p36 and p11 subunits), IV, and VI in the human hippocampus. Am J Pathol 145:640–649.

Ebihara S, Tsuji K (1980) Entrainment of the circadian activity rhythm to the light cycle: Effective light intensity for a Zeitgeber in the retinal degenerate C3H mouse and the normal C57BL mouse. Physiology & Behavior 24:523–527.

Ebinu JO, Bottorff DA, Chan EY, Stang SL, Dunn RJ, Stone JC (1998) RasGRP, a Ras guanyl nucleotide- releasing protein with calcium- and diacylglycerol-binding motifs. Science 280:1082–1086.

Ebinu JO, Stang SL, Teixeira C, Bottorff DA, Hooton J, Blumberg PM, Barry M, Bleakley RC, Ostergaard HL, Stone JC (2000) RasGRP links T-cell receptor signaling to Ras. Blood 95:3199–3203.

Ecker JL, Dumitrescu ON, Wong KY, Alam NM, Chen S-K, LeGates T, Renna JM, Prusky GT, Berson DM, Hattar S (2010) Melanopsin-Expressing Retinal Ganglion-Cell Photoreceptors: Cellular Diversity and Role in Pattern Vision. Neuron 67:49–60.

Eide EJ, Woolf MF, Kang H, Woolf P, Hurst W, Camacho F, Vielhaber EL, Giovanni A, Virshup DM (2005) Control of mammalian circadian rhythm by CKIepsilon-regulated proteasome-mediated PER2 degradation. Mol Cell Biol 25:2795–2807.

Emanuel AJ, Do MTH (2015) Melanopsin Tristability for Sustained and Broadband Phototransduction. Neuron 85:1043–1055.

Englund C, Fink A, Lau C, Pham D, Daza RAM, Bulfone A, Kowalczyk T, Hevner RF (2005) Pax6, Tbr2, and Tbr1 are expressed sequentially by radial glia, intermediate progenitor cells, and postmitotic neurons in developing neocortex. J Neurosci 25:247–251.

Enroth-Cugell C, Robson JG (1966) The contrast sensitivity of retinal ganglion cells of the cat. The Journal of Physiology 187:517–552.

Ereshefsky M (2000) The Poverty of the Linnaean Hierarchy. Cambridge University Press.

Erskine L, Herrera E (2014) Connecting the retina to the brain. ASN Neuro 6:175909141456210.

Estevez ME, Fogerson PM, Ilardi MC, Borghuis BG, Chan E, Weng S, Auferkorte ON, Demb JB, Berson DM (2012) Form and function of the M4 cell, an intrinsically photosensitive retinal ganglion cell type contributing to geniculocortical vision. J Neurosci 32:13608–13620.

Fahrenkrug J, Nielsen HS, Hannibal J (2004) Expression of melanopsin during development of the rat retina. NeuroReport 15:781–784.

Farah MH, Easter SS (2005) Cell birth and death in the mouse retinal ganglion cell layer. Journal of Comparative Neurology 489:120–134.

Farhan H, Rabouille C (2011) Signalling to and from the secretory pathway. J Cell Sci 124:171–180.

Farkas LM, Huttner WB (2008) The cell biology of neural stem and progenitor cells and its significance for their proliferation versus differentiation during mammalian brain development. Curr Opin Cell Biol 20:707–715.

Farrow K, Masland RH (2011) Physiological clustering of visual channels in the mouse retina. Journal of Neurophysiology 105:1516–1530.

Farrow K, Teixeira M, Szikra T, Viney TJ, Balint K, Yonehara K, Roska B (2013) Ambient

illumination toggles a neuronal circuit switch in the retina and visual perception at cone threshold. Neuron 78:325–338.

Fink AJ, Englund C, Daza RAM, Pham D, Lau C, Nivison M, Kowalczyk T, Hevner RF (2006) Development of the deep cerebellar nuclei: transcription factors and cell migration from the rhombic lip. J Neurosci 26:3066–3076.

Fink M, Lesage F, Duprat F, Heurteaux C, Reyes R, Fosset M, Lazdunski M (1998) A neuronal two P domain K+ channel stimulated by arachidonic acid and polyunsaturated fatty acids. EMBO J 17:3297–3308.

Fischer R, Wei Y, Anagli J, Berchtold MW (1996) Calmodulin binds to and inhibits GTP binding of the ras-like GTPase Kir/Gem. J Biol Chem 271:25067–25070.

Ford K (2011) Cellular Mechanisms Underlying Retinal Wave Generation.

Ford KJ, Feller MB (2012) Assembly and disassembly of a retinal cholinergic network. Visual Neuroscience 29:61–71.

Fornaro M, Raimondo S, Lee JM, Giuseppina Giacobini-Robecchi M (2007) Neuron-specific Hu proteins sub-cellular localization in primary sensory neurons. Annals of Anatomy - Anatomischer Anzeiger 189:223–228.

Foster RG, Provencio I, Hudson D, Fiske S, De Grip W, Menaker M (1991) Circadian photoreception in the retinally degenerate mouse (rd/rd). J Comp Physiol A 169:39–50.

Fox MA, Guido W (2011) Shedding light on class-specific wiring: development of intrinsically photosensitive retinal ganglion cell circuitry. Mol Neurobiol 44:321–329.

Freedman MS, Lucas RJ, Soni B, Schantz von M, Muñoz M, David-Gray Z, Foster R (1999) Regulation of Mammalian Circadian Behavior by Non-rod, Non-cone, Ocular Photoreceptors. Science 284:502–504.

Frings S, Brüll N, Dzeja C, Angele A, Hagen V, Kaupp UB, Baumann A (1998) Characterization of ether-à-go-go channels present in photoreceptors reveals similarity to IKx, a K+ current in rod inner segments. J Gen Physiol 111:583–599.

Gamsiz ED, Ouyang Q, Schmidt M, Nagpal S, Morrow EM (2012) Genome-wide transcriptome analysis in murine neural retina using high-throughput RNA sequencing. Genomics 99:44–51.

Gan L, Xiang M, Zhou L, Wagner DS, Klein WH, Nathans J (1996) POU domain factor Brn-3b is required for the development of a large set of retinal ganglion cells. PNAS 93:3920–3925.

Gao Y, Strowbridge BW (2009) Long-term plasticity of excitatory inputs to granule cells in the rat olfactory bulb. Nature Neuroscience 12:731–733.

Garg V, Kathiriya IS, Barnes R, Schluterman MK, King IN, Butler CA, Rothrock CR, Eapen RS,

Hirayama-Yamada K, Joo K, Matsuoka R, Cohen JC, Srivastava D (2003) GATA4 mutations cause human congenital heart defects and reveal an interaction with TBX5. Nature 424:443–447.

Gavériaux-Ruff C, Kieffer BL (2007) Conditional gene targeting in the mouse nervous system: Insights into brain function and diseases. Pharmacology & Therapeutics 113:619–634.

Gehring WJ (1998) Master Control Genes in Development and Evolution. Yale University Press.

Gehring WJ (2012) The animal body plan, the prototypic body segment, and eye evolution. Evol Dev 14:34–46.

Georgoussi Z, Leontiadis L, Mazarakou G, Merkouris M, Hyde K, Hamm H (2006) Selective interactions between G protein subunits and RGS4 with the C-terminal domains of the μ- and δ-opioid receptors regulate opioid receptor signaling. Cellular Signalling 18:771–782.

Gerfen CR, Paletzki R, Heintz N (2013) GENSAT BAC cre-recombinase driver lines to study the functional organization of cerebral cortical and basal ganglia circuits. Neuron 80:1368–1383.

Gerke V, Creutz CE, Moss SE (2005) Annexins: linking Ca2+ signalling to membrane dynamics. Nat Rev Mol Cell Biol 6:449–461.

Gerke V, Moss SE (2002) Annexins: from structure to function. Physiol Rev 82:331–371.

Ghiselin MT (1966) An Application of the Theory of Definitions to Systematic Principles. Systematic Zoology 15:127.

Ghiselin MT (1974) A Radical Solution to the Species Problem. Systematic Zoology 23:536.

Ghiselin MT (1997) Metaphysics and the Origin of Species. SUNY Press.

Ghiselin MT (2005) Homology as a relation of correspondence between parts of individuals. Theory Biosci 124:91–103.

Ghiselin MT, Breidbach O, The Hegeler Institute (2007) The Search for the Basis of Natural Classification Sugden SJB, ed. Monist 90:483–498.

Ghosh TK, Song FF, Packham EA, Buxton S, Robinson TE, Ronksley J, Self T, Bonser AJ, Brook JD (2009) Physical interaction between TBX5 and MEF2C is required for early heart development. Mol Cell Biol 29:2205–2218.

Goldberg JL, Vargas ME, Wang JT, Mandemakers W, Oster SF, Sretavan DW, Barres BA (2004) An oligodendrocyte lineage-specific semaphorin, Sema5A, inhibits axon growth by retinal ganglion cells. J Neurosci 24:4989–4999.

Goldblum D, Mittag T (2002) Prospects for relevant glaucoma models with retinal ganglion cell damage in the rodent eye. Vision Research 42:471–478.

Gong S, Doughty M, Harbaugh CR, Cummins A, Hatten ME, Heintz N, Gerfen CR (2007) Targeting Cre Recombinase to Specific Neuron Populations with Bacterial Artificial Chromosome Constructs. J Neurosci 27:9817–9823.

Goodman T, Crandall JE, Nanescu SE, Quadro L, Shearer K, Ross A, McCaffery P (2012) Patterning of retinoic acid signaling and cell proliferation in the hippocampus. Hippocampus 22:2171–2183.

Gorentla BK, Wan C-K, Zhong X-P (2011) Negative regulation of mTOR activation by diacylglycerol kinases. Blood 117:4022–4031.

Gould SJ (2002) The Structure of Evolutionary Theory. Harvard University Press.

Gould SJ, Lewontin RC (1979) The spandrels of San Marco and the Panglossian paradigm: a critique of the adaptationist programme. Proc R Soc Lond, B, Biol Sci 205:581–598.

Graham DM, Wong KY, Shapiro P, Frederick C, Pattabiraman K, Berson DM (2008) Melanopsin Ganglion Cells Use a Membrane-Associated Rhabdomeric Phototransduction Cascade. Journal of Neurophysiology 99:2522–2532.

GRÜNERT U, JUSUF PR, LEE SCS, NGUYEN DT (2011) Bipolar input to melanopsin containing ganglion cells in primate retina. Visual Neuroscience 28:39–50.

Güler AD, Ecker JL, Lall GS, Haq S, Altimus CM, Liao H-W, Barnard AR, Cahill H, Badea TC, Zhao H, Hankins MW, Berson DM, Lucas RJ, Yau K-W, Hattar S (2008) Melanopsin cells are the principal conduits for rod–cone input to non-image-forming vision. Nature 453:102–105.

Hacking I (2007) Natural Kinds: Rosy Dawn, Scholastic Twilight. Royal Institute of Philosophy Supplement 61:203–239.

Haeryfar SMM, Hoskin DW (2004) Thy-1: More than a Mouse Pan-T Cell Marker. The Journal of Immunology 173:3581–3588.

Hankins MW, Peirson SN, Foster RG (2008) Melanopsin: an exciting photopigment. Trends in Neurosciences 31:27–36.

Hannibal J, Hindersson P, Knudsen SM, Georg B (2002a) The photopigment melanopsin is exclusively present in pituitary adenylate cyclase-activating polypeptide-containing retinal ganglion cells of the …. J Neurosci.

Hannibal J, Hindersson P, Nevo E, Fahrenkrug J (2002b) The circadian photopigment melanopsin is expressed in the blind subterranean mole rat, Spalax. NeuroReport 13:1411.

Hartline HK (1938) The discharge of impulses in the optic nerve of Pecten in response to illumination of the eye. Journal of Cellular and Comparative Physiology 11:465–478.

Hartwick ATE, Bramley JR, Yu J, Stevens KT, Allen CN, Baldridge WH, Sollars PJ, Pickard

GE (2007) Light-evoked calcium responses of isolated melanopsin-expressing retinal ganglion cells. J Neurosci 27:13468–13480.

Hatori M, Le H, Vollmers C, Keding SR, Tanaka N, Schmedt C, Jegla T, Panda S (2008) Inducible Ablation of Melanopsin-Expressing Retinal Ganglion Cells Reveals Their Central Role in Non-Image Forming Visual Responses Hendricks M, ed. PLoS ONE 3:e2451.

Hattar S, Kumar M, Park A, Tong P, Tung J, Yau K-W, Berson DM (2006) Central projections of melanopsin-expressing retinal ganglion cells in the mouse. J Comp Neurol 497:326–349.

Hattar S, Liao HW, Takao M, Berson DM, Yau KW (2002) Melanopsin-Containing Retinal Ganglion Cells: Architecture, Projections, and Intrinsic Photosensitivity. Science 295:1065–1070.

Haverkamp S, Inta D, Monyer H, Wässle H (2009) Expression analysis of green fluorescent protein in retinal neurons of four transgenic mouse lines. Neuroscience 160:126–139.

He S, LEVICK WR, Vaney DI (1998) Distinguishing direction selectivity from orientation selectivity in the rabbit retina. Visual Neuroscience 15:439–447.

Heiman M, Schaefer A, Gong S, Peterson JD, Day M, Ramsey KE, Suárez-Fariñas M, Schwarz C, Stephan DA, Surmeier DJ, Greengard P, Heintz N (2008) A Translational Profiling Approach for the Molecular Characterization of CNS Cell Types. Cell 135:738–748.

Heimer-McGinn V, Young P (2011) Efficient inducible Pan-neuronal cre-mediated recombination in SLICK-H transgenic mice. Genesis 49:942–949.

Henson MA, Roberts AC, Pérez-Otaño I, Philpot BD (2010) Influence of the NR3A subunit on NMDA receptor functions. Progress in Neurobiology 91:23–37.

Hevner RF, Hodge RD, Daza RAM, Englund C (2006) Transcription factors in glutamatergic neurogenesis: conserved programs in neocortex, cerebellum, and adult hippocampus. Neurosci Res 55:223–233.

Hinman MN, Lou H (2008) Diverse molecular functions of Hu proteins. Cell Mol Life Sci 65:3168–3181.

Hobert O (2011) Regulation of Terminal Differentiation Programs in the Nervous System. http://dxdoiorg/101146/annurev-cellbio-092910-154226 27:681–696.

Hodge RD, Nelson BR, Kahoud RJ, Yang R, Mussar KE, Reiner SL, Hevner RF (2012) Tbr2 is essential for hippocampal lineage progression from neural stem cells to intermediate progenitors and neurons. J Neurosci 32:6275–6287.

Hu C, Hill DD, Wong KY (2013) Intrinsic physiological properties of the five types of mouse ganglion-cell photoreceptors. Journal of Neurophysiology 109:1876–1889.

Hubbard KB, Hepler JR (2006) Cell signalling diversity of the Gqalpha family of heterotrimeric

G proteins. Cellular Signalling 18:135–150.

Hubel DH, Wiesel TN (1962) Receptive fields, binocular interaction and functional architecture in the cat's visual cortex. The Journal of Physiology 160:106–154.

Huberman AD, Feller MB, Chapman B (2008a) Mechanisms Underlying Development of Visual Maps and Receptive Fields. Annual review of neuroscience 31:479–509.

Huberman AD, Manu M, Koch SM, Susman MW, Lutz AB, Ullian EM, Baccus SA, Barres BA (2008b) Architecture and activity-mediated refinement of axonal projections from a mosaic of genetically identified retinal ganglion cells. Neuron 59:425–438.

Huberman AD, Wei W, Elstrott J, Stafford BK, Feller MB, Barres BA (2009) Genetic identification of an On-Off direction-selective retinal ganglion cell subtype reveals a layer-specific subcortical map of posterior motion. Neuron 62:327–334.

Hughes A (1979) A rose by any other name... on "naming of neurones" by Rowe and Stone. Brain Behav Evol 16:52–64.

Hughes S, Hankins MW, Foster RG, Peirson SN (2012) Melanopsin phototransduction: slowly emerging from the dark. Prog Brain Res 199:19–40.

Hughes S, Jagannath A, Hickey D, Gatti S, Wood M, Peirson SN, Foster RG, Hankins MW (2015) Using siRNA to define functional interactions between melanopsin and multiple G Protein partners. Cell Mol Life Sci 72:165–179.

Inder K, Harding A, Plowman SJ, Philips MR, Parton RG, Hancock JF (2008) Activation of the MAPK module from different spatial locations generates distinct system outputs. Mol Biol Cell 19:4776–4784.

Isoldi MC, Rollag MD, Castrucci A, Provencio I (2005) Rhabdomeric phototransduction initiated by the vertebrate photopigment melanopsin. PNAS 102:1217–1221.

Ivanova E, Lee P, Pan Z-H (2013) Characterization of multiple bistratified retinal ganglion cells in a purkinje cell protein 2-Cre transgenic mouse line. Journal of Comparative Neurology 521:2165–2180.

Iwasaki H, Akashi K (2007) Hematopoietic developmental pathways: on cellular basis. Oncogene 26:6687–6696.

Jain V, Ravindran E, Dhingra NK (2012) Differential expression of Brn3 transcription factors in intrinsically photosensitive retinal ganglion cells in mouse. Journal of Comparative Neurology 520:742–755.

Jeon C-J, Strettoi E, Masland RH (1998) The Major Cell Populations of the Mouse Retina. J Neurosci 18:8936–8946.

Jessell TM (2000) Neuronal specification in the spinal cord: inductive signals and transcriptional

codes. Nature Reviews Genetics 1:20–29.

Ji M, Zhao W-J, Dong L-D, Miao Y, Yang X-L, Sun X-H, Wang Z (2011) RGS2 and RGS4 modulate melatonin-induced potentiation of glycine currents in rat retinal ganglion cells. Brain Research 1411:1–8.

Jin Z, Zhang J, Klar A, Chédotal A, Rao Y, Cepko CL, Bao Z-Z (2003) Irx4-mediated regulation of Slit1 expression contributes to the definition of early axonal paths inside the retina. Development 130:1037–1048.

Johnson J, Wu V, Donovan M, Majumdar S, Rentería RC, Porco T, Van Gelder RN, Copenhagen DR (2010) Melanopsin-dependent light avoidance in neonatal mice. Proc Natl Acad Sci USA 107:17374–17378.

Johnson JE, Goulding RE, Ding Z, Partovi A, Anthony KV, Beaulieu N, Tazmini G, Cornell RB, Kay RJ (2007) Differential membrane binding and diacylglycerol recognition by C1 domains of RasGRPs. Biochem J 406:223–236.

Kamme F, Salunga R, Yu J, Tran D-T, Zhu J, Luo L, Bittner A, Guo H-Q, Miller N, Wan J, Erlander M (2003) Single-cell microarray analysis in hippocampus CA1: demonstration and validation of cellular heterogeneity. J Neurosci 23:3607–3615.

Kay JN, la Huerta De I, Kim I-J, Zhang Y, Yamagata M, Chu MW, Meister M, Sanes JR (2011) Retinal ganglion cells with distinct directional preferences differ in molecular identity, structure, and central projections. J Neurosci 31:7753–7762.

Kaylor JJ, Yuan Q, Cook J, Sarfare S, Makshanoff J, Miu A, Kim A, Kim P, Habib S, Roybal CN, Xu T, Nusinowitz S, Travis GH (2013) Identification of DES1 as a vitamin A isomerase in Müller glial cells of the retina. Nature Chemical Biology 9:30–36.

Keeler CE (1927) Iris movements in blind mice. American Journal of Physiology--Legacy Content.

Kim AY, Tang Z, Liu Q, Patel KN, Maag D, Geng Y, Dong X (2008a) Pirt, a Phosphoinositide-Binding Protein, Functions as a Regulatory Subunit of TRPV1. Cell 133:475–485.

Kim I-J, Zhang Y, Meister M, Sanes JR (2010) Laminar restriction of retinal ganglion cell dendrites and axons: subtype-specific developmental patterns revealed with transgenic markers. J Neurosci 30:1452–1462.

Kim I-J, Zhang Y, Yamagata M, Meister M, Sanes JR (2008b) Molecular identification of a retinal cell type that responds to upward motion. Nature 452:478–482.

Kock JH, Mecke E, Orlov OY, Reuter T, Väisänen RA, Wallgren JE (1989) Ganglion cells in the frog retina: discriminant analysis of histological classes. Vision Research 29:1–18.

Kolb H, Nelson R, Ahnelt P, Cuenca N (2001) Cellular organization of the vertebrate retina. Prog Brain Res 131:3–26.

Komatsu Y, Watakabe A, Hashikawa T, Tochitani S, Yamamori T (2005) Retinol-binding protein gene is highly expressed in higher-order association areas of the primate neocortex. Cereb Cortex 15:96–108.

Kong J-H, Fish DR, Rockhill RL, Masland RH (2005) Diversity of ganglion cells in the mouse retina: unsupervised morphological classification and its limits. Journal of Comparative Neurology 489:293–310.

Koussounadis A, Langdon SP, Um IH, Harrison DJ, Smith VA (2015) Relationship between differentially expressed mRNA and mRNA-protein correlations in a xenograft model system. Sci Rep 5:10775.

Kovach C, Dixit R, Li S, Mattar P, Wilkinson G, Elsen GE, Kurrasch DM, Hevner RF, Schuurmans C (2013) Neurog2 simultaneously activates and represses alternative gene expression programs in the developing neocortex. Cereb Cortex 23:1884–1900.

Kowalczyk T, Pontious A, Englund C, Daza RAM, Bedogni F, Hodge R, Attardo A, Bell C, Huttner WB, Hevner RF (2009) Intermediate neuronal progenitors (basal progenitors) produce pyramidal-projection neurons for all layers of cerebral cortex. Cereb Cortex 19:2439–2450.

Koyanagi M, Kubokawa K, Tsukamoto H, Shichida Y, Terakita A (2005) Cephalochordate melanopsin: Evolutionary linkage between invertebrate visual cells and vertebrate photosensitive retinal ganglion cells. Curr Biol 15:1065–1069.

Krzyzosiak A, Szyszka-Niagolov M, Wietrzych M, Gobaille S, Muramatsu S-I, Krezel W (2010) Retinoid x receptor gamma control of affective behaviors involves dopaminergic signaling in mice. Neuron 66:908–920.

KUFFLER SW (1953) Discharge patterns and functional organization of mammalian retina. Journal of Neurophysiology 16:37–68.

Kühn R, Torres RM (2002) Cre/loxP recombination system and gene targeting. Methods Mol Biol 180:175–204.

Lacalli T (2004) Evolutionary biology: Light on ancient photoreceptors. Nature 432:454–455.

Laemle LK, Ottenweller JE (1998) Daily Patterns of Running Wheel Activity in Male Anophthalmic Mice. Physiology & Behavior 64:165–171.

LAKSO M, SAUER B, MOSINGER B, LEE EJ, MANNING RW, YU SH, MULDER KL, WESTPHAL H (1992) Targeted Oncogene Activation by Site-Specific Recombination in Transgenic Mice. PNAS 89:6232–6236.

Lamb TD (2013) Evolution of phototransduction, vertebrate photoreceptors and retina. Progress in Retinal and Eye Research 36:52–119.

Lamb TD, Collin SP, Pugh ENJ (2007) Evolution of the vertebrate eye: opsins, photoreceptors,

retina and eye cup. Nature Reviews Neuroscience 8:960–975.

Lane MA, Bailey SJ (2005) Role of retinoid signalling in the adult brain. Progress in Neurobiology 75:275–293.

Lawrence R, Yabe T, HajMohammadi S, Rhodes J, MCNEELY M, LIU J, LAMPERTI E, TOSELLI P, LECH M, SPEAR P (2007) The principal neuronal gD-type 3-O-sulfotransferases and their products in central and peripheral nervous system tissues☆. Matrix Biology 26:442–455.

Leamey CA, Glendining KA, Kreiman G, Kang N-D, Wang KH, Fässler R, Sawatari A, Tonegawa S, Sur M (2008) Differential gene expression between sensory neocortical areas: potential roles for Ten_m3 and Bcl6 in patterning visual and somatosensory pathways. Cereb Cortex 18:53–66.

Leamey CA, Merlin S, Lattouf P, Sawatari A, Zhou X, Demel N, Glendining KA, Oohashi T, Sur M, Fässler R (2007) Ten_m3 regulates eye-specific patterning in the mammalian visual pathway and is required for binocular vision. Harris WA, ed. PLOS Biol 5:e241.

Leamey CA, Sawatari A (2014) The teneurins: new players in the generation of visual topography. Seminars in Cell & Developmental Biology 35:173–179.

Lee K, Kim Y, Lee S-J, Qiang Y, Lee D, Lee HW, Kim H, Je HS, Südhof TC, Ko J (2013) MDGAs interact selectively with neuroligin-2 but not other neuroligins to regulate inhibitory synapse development. Proc Natl Acad Sci USA 110:336–341.

LEVICK WR (1967) Receptive fields and trigger features of ganglion cells in the visual streak of the rabbit's retina. The Journal of Physiology 188:285–307.

LEVICK WR, Thibos LN (1983) Chapter 11 Receptive fields of cat ganglion cells: Classification and construction. Progress in Retinal Research 2:267–319.

Levit GS, Meister K (2006) The history of essentialism vs. Ernst Mayr's ‘Essentialism Story’: a case study of German idealistic morphology. Springer-Verlag.

Levkovitch-Verbin H, Quigley HA, Martin KRG, Harizman N, Valenta DF, Pease ME, Melamed S (2005) The transcription factor c-jun is activated in retinal ganglion cells in experimental rat glaucoma. Experimental Eye Research 80:663–670.

Li S, Yang C, Zhang L, Gao X, Wang X, Liu W, Wang Y, Jiang S, Wong YH, Zhang Y, Liu K (2016) Promoting axon regeneration in the adult CNS by modulation of the melanopsin/GPCR signaling. Proc Natl Acad Sci USA 113:1937–1942.

Li S-Y, Yau S-Y, Chen B-Y, Tay DK, Lee VWH, Pu M-L, Chan HHL, So K-F (2008) Enhanced Survival of Melanopsin-expressing Retinal Ganglion Cells After Injury is Associated with the PI3 K/Akt Pathway. Cell Mol Neurobiol 28:1095–1107.

Li Y, Wongsiriroj N, Blaner WS (2014) The multifaceted nature of retinoid transport and

metabolism. Hepatobiliary Surg Nutr 3:126–139.

Linné CV (1751) Philosophia botanica : in qua explicantur fundamenta botanica cum definitionibus partium, exemplis terminorum, observationibus rariorum, adjectis figuris aeneis / Caroli Linnæe. Stockholmiæ,: apud Godofr. Kiesewetter.

Linné von C (2010) Fundamenta Botanic.

Liu W, Wang JH, Xiang M (2000) Specific expression of the LIM/Homeodomain protein Lim-1 in horizontal cells during retinogenesis. Developmental Dynamics 217:320–325.

Livesey FJ, Cepko CL (2001) Vertebrate neural cell-fate determination: Lessons from the retina. Nature Reviews Neuroscience 2:109–118.

Livesey FJ, Young TL, Cepko CL (2004) An analysis of the gene expression program of mammalian neural progenitor cells. Proc Natl Acad Sci USA 101:1374–1379.

Lobo MK, Karsten SL, Gray M, Geschwind DH, Yang XW (2006) FACS-array profiling of striatal projection neuron subtypes in juvenile and adult mouse brains. Nature Neuroscience 9:443–452.

Lorenzo PS, Beheshti M, Pettit GR, Stone JC, Blumberg PM (2000) The guanine nucleotide exchange factor RasGRP is a high -affinity target for diacylglycerol and phorbol esters. Mol Pharmacol 57:840–846.

Lucas RJ, Douglas RH, Foster RG (2001) Characterization of an ocular photopigment capable of driving pupillary constriction in mice. Nature Neuroscience 4:621–626.

Lucas RJ, Freedman MS, Muñoz M, Garcia-Fernández J-M, Foster RG (1999) Regulation of the Mammalian Pineal by Non-rod, Non-cone, Ocular Photoreceptors. Science 284:505–507.

Lyuksyutova AI, Lu C-C, Milanesio N, King LA, Guo N, Wang Y, Nathans J, Tessier-Lavigne M, Zou Y (2003) Anterior-posterior guidance of commissural axons by Wnt-frizzled signaling. Science 302:1984–1988.

Mackie GO (1970) Neuroid conduction and the evolution of conducting tissues. The Quarterly Review of Biology 45:319–332.

Macosko EZ, Basu A, Satija R, Nemesh J, Shekhar K, Goldman M, Tirosh I, Bialas AR, Kamitaki N, Martersteck EM, Trombetta JJ, Weitz DA, Sanes JR, Shalek AK, Regev A, McCarroll SA (2015) Highly Parallel Genome-wide Expression Profiling of Individual Cells Using Nanoliter Droplets. Cell 161:1202–1214.

Maden M (2007) Retinoic acid in the development, regeneration and maintenance of the nervous system. Nature Reviews Neuroscience 8:755–765.

Madureira P, Waisman D (2013) Annexin A2: The Importance of Being Redox Sensitive. Int J Mol Sci 14:3568–3594.

Maguire J, Santoro T, Jensen P, Siebenlist U, Yewdell J, Kelly K (1994) Gem: an induced, immediate early protein belonging to the Ras family. Science 265:241–244.

Maier T, Güell M, Serrano L (2009) Correlation of mRNA and protein in complex biological samples. FEBS Lett 583:3966–3973.

Maingret F, Fosset M, Lesage F, Lazdunski M, Honoré E (1999) TRAAK is a mammalian neuronal mechano-gated K+ channel. J Biol Chem 274:1381–1387.

Malone JH, Oliver B (2011) Microarrays, deep sequencing and the true measure of the transcriptome. BMC Biol 9:34.

Mao C-A, Kiyama T, Pan P, Furuta Y, Hadjantonakis A-K, Klein WH (2008) Eomesodermin, a target gene of Pou4f2, is required for retinal ganglion cell and optic nerve development in the mouse. Development 135:271–280.

Mao C-A, Li H, Zhang Z, Kiyama T, Panda S, Hattar S, Ribelayga CP, Mills SL, Wang SW (2014) T-box transcription regulator Tbr2 is essential for the formation and maintenance of Opn4/melanopsin-expressing intrinsically photosensitive retinal ganglion cells. J Neurosci 34:13083–13095.

Mao C-A, Tsai W-W, Cho J-H, Pan P, Barton MC, Klein WH (2011) Neuronal transcriptional repressor REST suppresses an Atoh7-independent program for initiating retinal ganglion cell development. Developmental Biology 349:90–99.

Mao H, Zhao Q, Daigle M, Ghahremani MH, Chidiac P, Albert PR (2004) RGS17/RGSZ2, a novel regulator of Gi/o, Gz, and Gq signaling. J Biol Chem 279:26314–26322.

Marioni JC, Mason CE, Mane SM, Stephens M, Gilad Y (2008) RNA-seq: an assessment of technical reproducibility and comparison with gene expression arrays. Genome Res 18:1509–1517.

Masland R (2001) Neuronal diversity in the retina. Current Opinion in Neurobiology 11:431–436.

Masland RH (2004) Neuronal cell types. Curr Biol 14:R497–R500.

Masland RH (2012) The tasks of amacrine cells. Visual Neuroscience 29:3–9.

Mathes A, Engel L, Holthues H, Wolloscheck T, Spessert R (2007) Daily Profile in Melanopsin Transcripts Depends on Seasonal Lighting Conditions in the Rat Retina. Journal of Neuroendocrinology 19:952–957.

Matsuoka RL, Nguyen-Ba-Charvet KT, Parray A, Badea TC, Chédotal A, Kolodkin AL (2011) Transmembrane semaphorin signalling controls laminar stratification in the mammalian retina. Nature 470:259–263.

Matsushima D, Heavner W, Pevny LH (2011) Combinatorial regulation of optic cup progenitor

cell fate by SOX2 and PAX6. Development 138:443–454.

MATURANA HR, LETTVIN JY, MCCULLOCH WS, PITTS WH (1960) Anatomy and physiology of vision in the frog (Rana pipiens). J Gen Physiol 43(6)Suppl:129–175.

Mayr E (1963) Animal Species and Evolution. Cambridge, MA and London, England: Harvard University Press.

Mayr E (1968) Theory of biological classification. Nature 220:545–548.

Mayr E (1982) The Growth of Biological Thought. Harvard University Press.

Mayr E, Bock WJ (2002) Classifications and other ordering systems. Journal of Zoological Systematics and Evolutionary Research 40:169–194.

McGinnis W, Levine MS, Hafen E, Kuroiwa A, Gehring WJ (1984) A conserved DNA sequence in homoeotic genes of the Drosophila Antennapedia and bithorax complexes. Nature 308:428–433.

McNeill DS, Sheely CJ, Ecker JL, Tudor C Badea, Morhardt D, Guido W, Hattar S (2011) Development of melanopsin-based irradiance detecting circuitry. Neural Development 2011 6:1 6:8.

MELLOR H, PARKER PJ (1998) The extended protein kinase C superfamily. Biochemical Journal 332:281–292.

Melyan Z, Tarttelin EE, Bellingham J, Lucas RJ, Hankins MW (2005) Addition of human melanopsin renders mammalian cells photoresponsive. Nature 433:741–745.

Missler M, Hammer RE, Südhof TC (1998) Neurexophilin binding to alpha-neurexins. A single LNS domain functions as an independently folding ligand-binding unit. J Biol Chem 273:34716–34723.

Mizuguchi R, Naritsuka H, Mori K, Mao C-A, Klein WH, Yoshihara Y (2012) Tbr2 deficiency in mitral and tufted cells disrupts excitatory-inhibitory balance of neural circuitry in the mouse olfactory bulb. J Neurosci 32:8831–8844.

Mizuno N, Itoh H (2009) Functions and regulatory mechanisms of Gq-signaling pathways. Neurosignals 17:42–54.

Moises HC, Rusin KI, Macdonald RL (1994) Mu- and kappa-opioid receptors selectively reduce the same transient components of high-threshold calcium current in rat dorsal root ganglion sensory neurons. J Neurosci 14:5903–5916.

MOORE JA (1986) Science as a Way of Knowing—Genetics. American Zoologist 26:583–747.

Moore R, Decker M, Cotner S (2010) Chronology of the evolution-creationism controversy. Choice Reviews Online 47:47–6024–47–6024.

Morin LP, Studholme KM (2014) Retinofugal projections in the mouse. Journal of Comparative Neurology 522:3733–3753.

Morrow EM, Belliveau MJ, Cepko CL (1998) Two Phases of Rod Photoreceptor Differentiation during Rat Retinal Development. J Neurosci 18:3738–3748.

Morse AM, Carballo V, Baldwin DA, Taylor CG, McIntyre LM (2010) Comparison between NuGEN's WT-Ovation Pico and one-direct amplification systems. J Biomol Tech 21:141–147.

Moss SE, Morgan RO (2004) The annexins. Genome Biology 2010 11:10 5:219.

Mu X, Beremand PD, Zhao S, Pershad R, Sun H, Scarpa A, Liang S, Thomas TL, Klein WH (2004) Discrete gene sets depend on POU domain transcription factor Brn3b/Brn-3.2/POU4f2 for their expression in the mouse embryonic retina. Development 131:1197–1210.

Mu X, Fu X, Sun H, Beremand PD, Thomas TL, Klein WH (2005) A gene network downstream of transcription factor Math5 regulates retinal progenitor cell competence and ganglion cell fate. Developmental Biology 280:467–481.

Mu X, Klein WH (2004) A gene regulatory hierarchy for retinal ganglion cell specification and differentiation. Seminars in Cell & Developmental Biology 15:115–123.

Mulligan KA, Cheyette BNR (2012) Wnt signaling in vertebrate neural development and function. J Neuroimmune Pharmacol 7:774–787.

Müller LP de S, Do MTH, Yau K-W, He S, Baldridge WH (2010) Tracer coupling of intrinsically photosensitive retinal ganglion cells to amacrine cells in the mouse retina. Journal of Comparative Neurology 518:4813–4824.

Münch TA, da Silveira RA, Siegert S, Viney TJ, Awatramani GB, Roska B (2009) Approach sensitivity in the retina processed by a multifunctional neural circuit. Nature Neuroscience 12:1308–1316.

Naiche LA, Harrelson Z, Kelly RG, Papaioannou VE (2005) T-box genes in vertebrate development. Annu Rev Genet 39:219–239.

Nelson RJ, Zucker I (1981) Absence of extraocular photoreception in diurnal and nocturnal rodents exposed to direct sunlight. Comparative Biochemistry and Physiology Part A: Physiology 69:145–148.

Nelson SB, Sugino K, Hempel CM (2006) The problem of neuronal cell types: a physiological genomics approach. Trends in Neurosciences 29:339–345.

Niwa M, Aoki H, Hirata A, Tomita H, Green PG, Hara A (2016) Retinal Cell Degeneration in Animal Models. Int J Mol Sci 17:110.

Noble WS (2009) How does multiple testing correction work? Nature Biotechnology 27:1135–1137.

Noctor SC, Martínez-Cerdeño V, Ivic L, Kriegstein AR (2004) Cortical neurons arise in symmetric and asymmetric division zones and migrate through specific phases. Nature Neuroscience 7:136–144.

Novak A, Guo C, Yang W, Nagy A, Lobe CG (2000) Z/EG, a double reporter mouse line that expresses enhanced green fluorescent protein upon Cre-mediated excision. Genesis.

Novershtern N et al. (2011) Densely Interconnected Transcriptional Circuits Control Cell States in Human Hematopoiesis. Cell 144:296–309.

O'Donnell CD, Tiwari V, Oh M-J, Shukla D (2006) A role for heparan sulfate 3-O-sulfotransferase isoform 2 in herpes simplex virus type 1 entry and spread. Virology 346:452–459.

Okabe M, Ikawa M, Kominami K, Nakanishi T, Nishimune Y (1997) "Green mice" as a source of ubiquitous green cells. FEBS Lett 407:313–319.

Orkin SH, Zon LI (2008) Hematopoiesis: an evolving paradigm for stem cell biology. Cell 132:631–644.

Osterhout JA, El-Danaf RN, Nguyen PL, Huberman AD (2014) Birthdate and outgrowth timing predict cellular mechanisms of axon target matching in the developing visual pathway. Cell Rep 8:1006–1017.

Osterhout JA, Josten N, Yamada J, Pan F, Wu S-W, Nguyen PL, Panagiotakos G, Inoue YU, Egusa SF, Volgyi B, Inoue T, Bloomfield SA, Barres BA, Berson DM, Feldheim DA, Huberman AD (2011) Cadherin-6 mediates axon-target matching in a non-image-forming visual circuit. Neuron 71:632–639.

Owen R (1843) Lectures on the comparative anatomy and physiology of the invertebrate animals : delivered at the Royal College of Surgeons / By Richard Owen. London :: Longman, Brown, Green & Longmans.

Owen R (1849) On the nature of limbs. London :: John Van Voorst.

Oyster CW, BARLOW HB (1967) Direction-selective units in rabbit retina: distribution of preferred directions. Science 155:841–842.

Pack W, Hill DD, Wong KY (2015) Melatonin modulates M4-type ganglion-cell photoreceptors. Neuroscience 303:178–188.

Palczewski K (2006) G Protein–Coupled Receptor Rhodopsin. Annual review of biochemistry 75:743–767.

Panda S, Nayak SK, Campo B, Walker JR, Hogenesch JB, Jegla T (2005) Illumination of the

Melanopsin Signaling Pathway. Science 307:600–604.

Panda S, Provencio I, Tu DC, Pires SS, Rollag MD, Castrucci AM, Pletcher MT, Sato TK, Wiltshire T, Andahazy M, Kay SA, Van Gelder RN, Hogenesch JB (2003) Melanopsin Is Required for Non-Image-Forming Photic Responses in Blind Mice. Science 301:525–527.

Panda S, Sato TK, Castrucci AM, Rollag MD, DeGrip WJ, Hogenesch JB, Provencio I, Kay SA (2002) Melanopsin (Opn4) Requirement for Normal Light-Induced Circadian Phase Shifting. Science 298:2213–2216.

Paxton C, Zhao H, Chin Y, Langner K, Reecy J (2002) Murine Tbx2 contains domains that activate and repress gene transcription. Gene 283:117–124.

Peirson S, Foster RG (2006) Melanopsin: Another Way of Signaling Light. Neuron 49:331–339.

Peirson SN, Oster H, Jones SL, Leitges M, Hankins MW, Foster RG (2007) Microarray Analysis and Functional Genomics Identify Novel Components of Melanopsin Signaling. Current Biology 17:1363–1372.

Perez Leighton CE, Schmidt TM, Abramowitz J, Birnbaumer L, Kofuji P (2011) Intrinsic phototransduction persists in melanopsin-expressing ganglion cells lacking diacylglycerol-sensitive TRPC subunits. European Journal of Neuroscience 33:856–867.

Perez-Leon JA, Warren EJ, Allen CN, Robinson DW, Brown RL (2006) Synaptic inputs to retinal ganglion cells that set the circadian clock. Eur J Neurosci 24:1117–1123.

Pettem KL, Yokomaku D, Takahashi H, Ge Y, Craig AM (2013) Interaction between autism-linked MDGAs and neuroligins suppresses inhibitory synapse development. J Cell Biol 200:321–336.

Philips MR (2005) Compartmentalized signalling of Ras. Biochemical Society Transactions 33:657–661.

Pickard GE, Baver SB, Ogilvie MD, Sollars PJ (2009) Light-Induced Fos Expression in Intrinsically Photosensitive Retinal Ganglion Cells in Melanopsin Knockout (Opn4 –/–) Mice Mansvelder HD, ed. PLoS ONE 4:e4984.

Pierret P, Dunn RJ, Djordjevic B, Stone JC, Richardson PM (2000a) Distribution of ras guanyl releasing protein (RasGRP) mRNA in the adult rat central nervous system. J Neurocytol 29:485–497.

Pierret P, Dunn RJ, Djordjevic B, Stone JC, Richardson PM (2000b) Distribution of ras guanyl releasing protein (RasGRP) mRNA in the adult rat central nervous system. J Neurocytol 29:485–497.

Plachetzki DC, Fong CR, Oakley TH (2010) The evolution of phototransduction from an ancestral cyclic nucleotide gated pathway. Proceedings of the Royal Society of London B: Biological Sciences 277:1963–1969.

Plageman TF, Yutzey KE (2004) Differential expression and function of Tbx5 and Tbx20 in cardiac development. J Biol Chem 279:19026–19034.

Pocock R, Mione M, Hussain S, Maxwell S, Pontecorvi M, Aslam S, Gerrelli D, Sowden JC, Woollard A (2008) Neuronal function of Tbx20 conserved from nematodes to vertebrates. Developmental Biology 317:671–685.

Polyak SL (1941) The Retina.

Poulain FE, Yost HJ (2015) Heparan sulfate proteoglycans: a sugar code for vertebrate development? Development 142:3456–3467.

Prichard JR, Stoffel RT, Quimby DL, Obermeyer WH, Benca RM, Behan M (2002) Fos immunoreactivity in rat subcortical visual shell in response to illuminance changes. Neuroscience 114:781–793.

Prigge CL, Yeh P-T, Liou N-F, Lee C-C, You S-F, Liu L-L, McNeill DS, Chew KS, Hattar S, Chen S-K, Zhang D-Q (2016) M1 ipRGCs Influence Visual Function through Retrograde Signaling in the Retina. J Neurosci 36:7184–7197.

Prior IA, Hancock JF (2012) Ras trafficking, localization and compartmentalized signalling. Seminars in Cell & Developmental Biology 23:145–153.

Provencio I, Rodriguez IR, Jiang G, Hayes WP, Moreira EF, Rollag MD (2000) A novel human opsin in the inner retina. J Neurosci 20:600–605.

Puente LG, Stone JC, Ostergaard HL (2000) Evidence for protein kinase C-dependent and -independent activation of mitogen-activated protein kinase in T cells: potential role of additional diacylglycerol binding proteins. The Journal of Immunology 165:6865–6871.

Qiu X, Kumbalasiri T, Carlson SM, Wong KY, Krishna V, Provencio I, Berson DM (2005) Induction of photosensitivity by heterologous expression of melanopsin. Nature 433:745–749.

Quail MA, Kozarewa I, Smith F, Scally A, Stephens PJ, Durbin R, Swerdlow H, Turner DJ (2008) A large genome center's improvements to the Illumina sequencing system. Nat Methods 5:1005–1010.

Quinn JC, Molinek M, Martynoga BS, Zaki PA, Faedo A, Bulfone A, Hevner RF, West JD, Price DJ (2007) Pax6 controls cerebral cortical cell number by regulating exit from the cell cycle and specifies cortical cell identity by a cell autonomous mechanism. Developmental Biology 302:50–65.

Rachel RA, Dölen G, Hayes NL, Lu A (2002) Spatiotemporal features of early neuronogenesis differ in wild-type and albino mouse retina. The Journal of ….

Raghu P, Usher K, Jonas S, Chyb S, Polyanovsky A, Hardie RC (2000) Constitutive activity of the light-sensitive channels TRP and TRPL in the Drosophila diacylglycerol kinase mutant,

rdgA. Neuron 26:169–179.

Rajalingam K, Schreck R, Rapp UR, Albert S (2007) Ras oncogenes and their downstream targets. Biochim Biophys Acta 1773:1177–1195.

Ray J (1691) The wisdom of God manifested in the works of the creation / John Ray. London :: Printed by William Innys and Richard Manby.

Reese BE (2011) Development of the retina and optic pathway. Vision Research 51:613–632.

Reifler AN, Chervenak AP, Dolikian ME, Benenati BA, Li BY, Wachter RD, Lynch AM, Demertzis ZD, Meyers BS, Abufarha FS, Jaeckel ER, Flannery MP, Wong KY (2015) All Spiking, Sustained ON Displaced Amacrine Cells Receive Gap-Junction Input from Melanopsin Ganglion Cells. Current Biology 25:2763–2773.

Renna JM, Weng S, Berson DM (2011) Light acts through melanopsin to alter retinal waves and segregation of retinogeniculate afferents. Nature Neuroscience 14:827–829.

Ressler KJ, Sullivan SL, Buck LB (1994) Information coding in the olfactory system: evidence for a stereotyped and highly organized epitope map in the olfactory bulb. Cell 79:1245–1255.

Reyes R, Lauritzen I, Lesage F, Ettaiche M, Fosset M, Lazdunski M (2000) Immunolocalization of the arachidonic acid and mechanosensitive baseline traak potassium channel in the nervous system. Neuroscience 95:893–901.

Rieppel O (2009) Species as a process. Acta Biotheor 57:33–49.

Rivlin-Etzion M, Zhou K, Wei W, Elstrott J, Nguyen PL, Barres BA, Huberman AD, Feller MB (2011) Transgenic mice reveal unexpected diversity of on-off direction-selective retinal ganglion cell subtypes and brain structures involved in motion processing. J Neurosci 31:8760–8769.

Roberts A, Pachter L (2011) RNA-Seq and find: entering the RNA deep field. Genome Medicine 2011 3:11 3:74.

Roberts MR, Hendrickson A, McGuire CR, Reh TA (2005) Retinoid X receptor (gamma) is necessary to establish the S-opsin gradient in cone photoreceptors of the developing mouse retina. Invest Ophthalmol Vis Sci 46:2897–2904.

Robinson MD, Oshlack A (2010) A scaling normalization method for differential expression analysis of RNA-seq data. Genome Biology 2010 11:10 11:R25.

Rockhill RL, Euler T, Masland RH (2000) Spatial order within but not between types of retinal neurons. PNAS 97:2303–2307.

Rocks O, Peyker A, Kahms M, Verveer PJ, Koerner C, Lumbierres M, Kuhlmann J, Waldmann H, Wittinghofer A, Bastiaens PIH (2005) An acylation cycle regulates localization and

activity of palmitoylated Ras isoforms. Science 307:1746–1752.

Rodieck RW, Brening RK (1983) Retinal ganglion cells: properties, types, genera, pathways and trans-species comparisons. Brain Behav Evol 23:121–164.

Rodriguez AR, Sevilla Müller LP, Brecha NC (2014) The RNA binding protein RBPMS is a selective marker of ganglion cells in the mammalian retina. Journal of Comparative Neurology 522:1411–1443.

Rodríguez-Muñoz M, la Torre-Madrid de E, Sánchez-Blázquez P, Wang JB, Garzón J (2008) NMDAR-nNOS generated zinc recruits PKCγ to the HINT1–RGS17 complex bound to the C terminus of Mu-opioid receptors. Cellular Signalling 20:1855–1864.

Rose MR, Oakley TH (2007) The new biology: beyond the Modern Synthesis. Biol Direct 2:30.

Rousso DL, Qiao M, Kagan RD, Yamagata M, Palmiter RD, Sanes JR (2016) Two Pairs of ON and OFF Retinal Ganglion Cells Are Defined by Intersectional Patterns of Transcription Factor Expression. Cell Rep 15:1930–1944.

Rowe MH (2012) Still with us after all these years: issues of neuronal classification revisited. Brain Behav Evol 80:1–3.

Rowe MH, Stone J (1977) Naming of neurones. Classification and naming of cat retinal ganglion cells. Brain Behav Evol 14:185–216.

Rowe MH, Stone J (1979) The Importance of Knowing Our Own Presuppositions. Brain Behav Evol 16:65–80.

Rowe MH, Stone J (1980) The interpretation of variation in the classification of nerve cells. Brain Behav Evol 17:123–151.

Ruby NF, Brennan TJ, Xie X, Cao V, Franken P, Heller HC, O'Hara BF (2002) Role of Melanopsin in Circadian Responses to Light. Science 298:2211–2213.

Ruiz A, Mark M, Jacobs H, Klopfenstein M, Hu J, Lloyd M, Habib S, Tosha C, Radu RA, Ghyselinck NB, Nusinowitz S, Bok D (2012) Retinoid Content, Visual Responses, and Ocular Morphology Are Compromised in the Retinas of Mice Lacking the Retinol-Binding Protein Receptor, STRA6. Invest Ophthalmol Vis Sci 53:3027.

Rupke N (1994) Richard Owen: Victorian naturalist. Choice Reviews Online 32:32–1507–32–1507.

Safe S, Jin U-H, Morpurgo B, Abudayyeh A, Singh M, Tjalkens RB (2016) Nuclear receptor 4A (NR4A) family - orphans no more. J Steroid Biochem Mol Biol 157:48–60.

Sakabe NJ, Aneas I, Shen T, Shokri L, Park S-Y, Bulyk ML, Evans SM, Nobrega MA (2012) Dual transcriptional activator and repressor roles of TBX20 regulate adult cardiac structure and function. Hum Mol Genet 21:2194–2204.

Sakai JA, Halloran MC (2006) Semaphorin 3d guides laterality of retinal ganglion cell projections in zebrafish. Development 133:1035–1044.

Sakamoto K, Liu C, Tosini G (2004) Classical photoreceptors regulate melanopsin mRNA levels in the rat retina. J Neurosci 24:9693–9697.

Salvini-Plawen von L, Mayr E (1977) On the Evolution of Photoreceptors and Eyes. In: Evolutionary Biology, pp 207–263. Boston, MA: Springer US.

Sanes JR, Masland RH (2015) The Types of Retinal Ganglion Cells: Current Status and Implications for Neuronal Classification. http://dxdoiorg/101146/annurev-neuro-071714-034120 38:221–246.

Scamps F, Sangari S, Bowerman M, Rousset M, Bellis M, Cens T, Charnet P (2015) Nerve injury induces a Gem-GTPase-dependent downregulation of P/Q-type Ca2+ channels contributing to neurite plasticity in dorsal root ganglion neurons. Pflugers Arch 467:351–366.

Schlatter MC, Buhusi M, Wright AG, Maness PF (2008) CHL1 promotes Sema3A-induced growth cone collapse and neurite elaboration through a motif required for recruitment of ERM proteins to the plasma membrane. J Neurochem 104:731–744.

Schmidt TM, Kofuji P (2009) Functional and morphological differences among intrinsically photosensitive retinal ganglion cells. The Journal of neuroscience.

Schmidt TM, Kofuji P (2010) Differential cone pathway influence on intrinsically photosensitive retinal ganglion cell subtypes. J Neurosci 30:16262–16271.

Schmidt TM, Taniguchi K, Kofuji P (2008) Intrinsic and Extrinsic Light Responses in Melanopsin-Expressing Ganglion Cells During Mouse Development. Journal of Neurophysiology 100:371–384.

Schultze M (1866) Zur Anatomie und Physiologie der Retina. Archiv für Mikroskopische Anatomie 2:175–286.

Scott MP, Weiner AJ (1984) Structural relationships among genes that control development: sequence homology between the Antennapedia, Ultrabithorax, and fushi tarazu loci of Drosophila. PNAS 81:4115–4119.

Sebé-Pedrós A, Ruiz-Trillo I (2017) Evolution and Classification of the T-Box Transcription Factor Family. Curr Top Dev Biol 122:1–26.

Seipel K, Yanze N, Schmid V (2004) Developmental and evolutionary aspects of the basic helix-loop-helix transcription factors Atonal-like 1 and Achaete-scute homolog 2 in the jellyfish. Developmental Biology 269:331–345.

Sekaran S, Lupi D, Jones SL, Sheely CJ, Hattar S, Yau KW, Lucas RJ, Foster RG, Hankins MW (2005) Melanopsin-Dependent Photoreception Provides Earliest Light Detection in the

Mammalian Retina. Current Biology 15:1099–1107.

Sengupta A, Baba K, Mazzoni F, Pozdeyev NV, Strettoi E, Iuvone PM, Tosini G (2011) Localization of melatonin receptor 1 in mouse retina and its role in the circadian regulation of the electroretinogram and dopamine levels. Yamazaki S, ed. PLoS ONE 6:e24483.

Sessa A, Mao C-A, Colasante G, Nini A, Klein WH, Broccoli V (2010) Tbr2-positive intermediate (basal) neuronal progenitors safeguard cerebral cortex expansion by controlling amplification of pallial glutamatergic neurons and attraction of subpallial GABAergic interneurons. Genes Dev 24:1816–1826.

Sessa A, Mao C-A, Hadjantonakis A-K, Klein WH, Broccoli V (2008) Tbr2 directs conversion of radial glia into basal precursors and guides neuronal amplification by indirect neurogenesis in the developing neocortex. Neuron 60:56–69.

Sexton T, Buhr E, Van Gelder RN (2012) Melanopsin and mechanisms of non-visual ocular photoreception. J Biol Chem 287:1649–1656.

Shapley R, Hugh Perry V (1986) Cat and monkey retinal ganglion cells and their visual functional roles. Trends in Neurosciences 9:229–235.

Sheely C (2011) A population of melanopsin-expressing retinal ganglion cells develops independent of Math5.

Shekhar K, Lapan SW, Whitney IE, Tran NM, Macosko EZ, Kowalczyk M, Adiconis X, Levin JZ, Nemesh J, Goldman M, McCarroll SA, Cepko CL, Regev A, Sanes JR (2016) Comprehensive Classification of Retinal Bipolar Neurons by Single-Cell Transcriptomics. Cell 166:1308–1323.e1330.

Shen T, Aneas I, Sakabe N, Dirschinger RJ, Wang G, Smemo S, Westlund JM, Cheng H, Dalton N, Gu Y, Boogerd CJ, Cai C-L, Peterson K, Chen J, Nobrega MA, Evans SM (2011) Tbx20 regulates a genetic program essential to adult mouse cardiomyocyte function. J Clin Invest 121:4640–4654.

Shen Y, Liu X-L, Yang X-L (2006) N-methyl-D-aspartate receptors in the retina. Mol Neurobiol 34:163–179.

Sheng W-L, Chen W-Y, Yang X-L, Zhong Y-M, Weng S-J (2015) Co-expression of two subtypes of melatonin receptor on rat M1-type intrinsically photosensitive retinal ganglion cells. Barnes S, ed. PLoS ONE 10:e0117967.

Shepard AR, Rae JL (1999) Electrically silent potassium channel subunits from human lens epithelium. Am J Physiol 277:C412–C424.

Shulga YV, Topham MK, Epand RM (2011) Regulation and Functions of Diacylglycerol Kinases. Chemical Reviews 111:6186–6208.

Siegert S, Cabuy E, Scherf BG, Kohler H, Panda S, Le Y-Z, Fehling HJ, Gaidatzis D, Stadler

MB, Roska B (2012) Transcriptional code and disease map for adult retinal cell types. Nature Neuroscience 15:487–495.

Siegert S, Scherf BG, Del Punta K, Didkovsky N, Heintz N, Roska B (2009) Genetic address book for retinal cell types. Nature Neuroscience 12:1197–1204.

Simpson GG (1961) Principles of Animal Taxonomy. Columbia University Press.

Singh P (2007) Role of Annexin-II in GI cancers: interaction with gastrins/progastrins. Cancer Lett 252:19–35.

Sinha S, Abraham S, Gronostajski RM, Campbell CE (2000) Differential DNA binding and transcription modulation by three T-box proteins, T, TBX1 and TBX2. Gene 258:15–29.

Smith L (2011) Good planning and serendipity: exploiting the Cre/Lox system in the testis. Reproduction 141:151–161.

Soto I, Oglesby E, Buckingham BP, Son JL, Roberson EDO, Steele MR, Inman DM, Vetter ML, Horner PJ, Marsh-Armstrong N (2008) Retinal Ganglion Cells Downregulate Gene Expression and Lose Their Axons within the Optic Nerve Head in a Mouse Glaucoma Model. J Neurosci 28:548–561.

Star EN, Zhu M, Shi Z, Liu H, Pashmforoush M, Sauve Y, Bruneau BG, Chow RL (2012) Regulation of retinal interneuron subtype identity by the Iroquois homeobox gene Irx6. Development 139:4644–4655.

Stennard FA, Costa MW, Elliott DA, Rankin S, Haast SJP, Lai D, McDonald LPA, Niederreither K, Dolle P, Bruneau BG, Zorn AM, Harvey RP (2003) Cardiac T-box factor Tbx20 directly interacts with Nkx2-5, GATA4, and GATA5 in regulation of gene expression in the developing heart. Developmental Biology 262:206–224.

Sterling P (1983) Microcircuitry of the cat retina. Annual review of neuroscience 6:149–185.

Sternberg N (1981) Bacteriophage P1 site-specific recombination. III. Strand exchange during recombination at lox sites. J Mol Biol 150:603–608.

Stone J, Fabian M (1966) Specialized receptive fields of the cat's retina. Science 152:1277–1279.

Stone J, Fukuda Y (1974) The naso-temporal division of the cat's retina re-examined in terms of Y-, X- and W-cells. J Comp Neurol 155:377–394.

Stone J, Hoffman K-P (1972) Very slow-conducting ganglion cells in the cat's retina: a major, new functional type? Brain Research 43:610–616.

Sucher NJ, Lipton SA, Dreyer EB (1997) Molecular basis of glutamate toxicity in retinal ganglion cells. Vision Research 37:3483–3493.

Sugino K, Hempel CM, Miller MN, Hattox AM, Shapiro P, Wu C, Huang ZJ, Nelson SB (2006)

Molecular taxonomy of major neuronal classes in the adult mouse forebrain. Nature Neuroscience 9:99–107.

Sümbül U, Song Sen, McCulloch K, Becker M, Bin Lin, Sanes JR, Masland RH, Seung HS (2014) A genetic and computational approach to structurally classify neuronal types. Nature Communications 5.

Sweeney NT, Tierney H, Feldheim DA (2014) Tbr2 is required to generate a neural circuit mediating the pupillary light reflex. J Neurosci 34:5447–5453.

Takeuchi JK, Mileikovskaia M, Koshiba-Takeuchi K, Heidt AB, Mori AD, Arruda EP, Gertsenstein M, Georges R, Davidson L, Mo R, Hui C-C, Henkelman RM, Nemer M, Black BL, Nagy A, Bruneau BG (2005) Tbx20 dose-dependently regulates transcription factor networks required for mouse heart and motoneuron development. Development 132:2463–2474.

Tariq MA, Kim HJ, Jejelowo O, Pourmand N (2011) Whole-transcriptome RNAseq analysis from minute amount of total RNA. Nucleic Acids Res 39:e120–e120.

Thomson KS (2009) The young Charles Darwin. Choice Reviews Online 46:46–6191–46–6191.

Thorvaldsdóttir H, Robinson JT (2013) Integrative Genomics Viewer (IGV): high-performance genomics data visualization and exploration. Briefings in ….

Tognon CE, Kirk HE, Passmore LA, Whitehead IP, Der CJ, Kay RJ (1998) Regulation of RasGRP via a phorbol ester-responsive C1 domain. Mol Cell Biol 18:6995–7008.

Toki S, Kawasaki H, Tashiro N, Housman DE, Graybiel AM (2001) Guanine nucleotide exchange factors CalDAG-GEFI and CalDAG-GEFII are colocalized in striatal projection neurons. J Comp Neurol 437:398–407.

Toonen JA, Ronchetti A, Sidjanin DJ (2016) A Disintegrin and Metalloproteinase10 (ADAM10) Regulates NOTCH Signaling during Early Retinal Development. Kihara AH, ed. PLoS ONE 11:e0156184.

Topark-Ngarm A, Golonzhka O, Peterson VJ, Barrett B, Martinez B, Crofoot K, Filtz TM, Leid M (2006) CTIP2 associates with the NuRD complex on the promoter of p57KIP2, a newly identified CTIP2 target gene. J Biol Chem 281:32272–32283.

Tran H, Sawatari A, Leamey CA (2015) The glycoprotein Ten-m3 mediates topography and patterning of thalamostriatal projections from the parafascicular nucleus in mice. European Journal of Neuroscience 41:55–68.

Trapnell C, Roberts A, Goff L, Pertea G, Kim D, Kelley DR, Pimentel H, Salzberg SL, Rinn JL, Pachter L (2012) Differential gene and transcript expression analysis of RNA-seq experiments with TopHat and Cufflinks. Nature Protocols 7:562–578.

Trenholm S, Johnson K, Li X, Smith RG, Awatramani GB (2011) Parallel mechanisms encode

direction in the retina. Neuron 71:683–694.

Trenholm S, McLaughlin AJ, Schwab DJ, Awatramani GB (2013) Dynamic tuning of electrical and chemical synaptic transmission in a network of motion coding retinal neurons. J Neurosci 33:14927–14938.

Trimarchi JM, Stadler MB, Cepko CL (2008) Individual Retinal Progenitor Cells Display Extensive Heterogeneity of Gene Expression Callaerts P, ed. PLoS ONE 3:e1588.

Tu DC, Zhang D, Demas J, Slutsky EB, Provencio I, Holy TE, Van Gelder RN (2005) Physiologic Diversity and Development of Intrinsically Photosensitive Retinal Ganglion Cells. Neuron 48:987–999.

Tyner CF (1975) The naming of neurons: applications of taxonomic theory to the study of cellular populations. Brain Behav Evol 12:75–96.

Vacaru AM, Vitale J, Nieves J, Baron MH (2014) Generation of transgenic mouse fluorescent reporter lines for studying hematopoietic development. Methods Mol Biol 1194:289–312.

Van Hook MJ, Wong KY, Berson DM (2012) Dopaminergic modulation of ganglion-cell photoreceptors in rat. European Journal of Neuroscience 35:507–518.

Vaney DI (1994) Patterns of neuronal coupling in the retina. Progress in Retinal and Eye Research 13:301–355.

Vaney DI, Sivyer B, Taylor WR (2012) Direction selectivity in the retina: symmetry and asymmetry in structure and function. Nature Reviews Neuroscience 13:194–208.

Vassar R, Chao SK, Sitcheran R, ez JMN, Vosshall LB, Axel R (1994) Topographic organization of sensory projections to the olfactory bulb. Cell 79:981–991.

Verleysen M, François D (2005) The Curse of Dimensionality in Data Mining and Time Series Prediction. In: Database Theory — ICDT'99, pp 758–770 Lecture Notes in Computer Science. Berlin, Heidelberg: Springer Berlin Heidelberg.

Vieira AV, Lamaze C, Schmid SL (1996) Control of EGF receptor signaling by clathrin-mediated endocytosis. Science 274:2086–2089.

Viney TJ, Balint K, Hillier D, Siegert S, Boldogkoi Z, Enquist LW, Meister M, Cepko CL, Roska B (2007) Local Retinal Circuits of Melanopsin-Containing Ganglion Cells Identified by Transsynaptic Viral Tracing. Current Biology 17:981–988.

Visser JJ, Cheng Y, Perry SC, Chastain AB, Parsa B, Masri SS, Ray TA, Kay JN, Wojtowicz WM (2015) An extracellular biochemical screen reveals that FLRTs and Unc5s mediate neuronal subtype recognition in the retina. Elife 4:e08149.

Vuong HE, Hardi CN, Barnes S, Brecha NC (2015) Parallel Inhibition of Dopamine Amacrine Cells and Intrinsically Photosensitive Retinal Ganglion Cells in a Non-Image-Forming

Visual Circuit of the Mouse Retina. J Neurosci 35:15955–15970.

WAGNER G (2000) Character Identification in Evolutionary Biology: The Role of the Organism. Theory in Biosciences 119:20–40.

Wagner GP (2014) Homology, Genes, and Evolutionary Innovation. Princeton: Princeton University Press.

Walker MT, Brown RL, Cronin TW, Robinson PR (2008) Photochemistry of retinal chromophore in mouse melanopsin. Proc Natl Acad Sci USA 105:8861–8865.

Wang GY, Liets LC, Chalupa LM (2001) Unique functional properties of on and off pathways in the developing mammalian retina. J Neurosci 21:4310–4317.

Wang Y, Cheng X, Zhou Z, Wu H, Long L, Gu X, Xu G (2013) Increased expression of Gem after rat sciatic nerve injury. J Mol Histol 44:27–36.

Ward Y, Yap S-F, Ravichandran V, Matsumura F, Ito M, Spinelli B, Kelly K (2002) The GTP binding proteins Gem and Rad are negative regulators of the Rho-Rho kinase pathway. J Cell Biol 157:291–302.

Wässle H (2004) Parallel processing in the mammalian retina. Nature Reviews Neuroscience 5:747–757.

Wässle H, Peichl L, Boycott BB (1981) Dendritic territories of cat retinal ganglion cells. Nature 292:344–345.

Weitz D, Ficek N, Kremmer E, Bauer PJ, Kaupp UB (2002) Subunit Stoichiometry of the CNG Channel of Rod Photoreceptors. Neuron 36:881–889.

Wen H, Cao J, Yu X, Sun B, Ding T, Li M, Li D, Wu H, Long L, Xu G, Zhang F (2013) Spatiotemporal patterns of Gem expression after rat spinal cord injury. Brain Research 1516:11–19.

Weng S, Estevez ME, Berson DM (2013) Mouse ganglion-cell photoreceptors are driven by the most sensitive rod pathway and by both types of cones. Barnes S, ed. PLoS ONE 8:e66480.

Whewell W (1840) THE PHILOSOPHY OF THE INDUCTIVE SCIENCES. Рипол Классик.

Whewell W (1847) History of the inductive sciences, from the earliest to the present time. London: J.W. Parker.

Whewell W (1858) **Novum Organon Renovatum**. J. W. Parker and son.

Whitehead AN (1920) The Principles of Natural Knowledge.

WHITTLE AC, GOLDING DW (1974) Fine-Structure of Prostomial Photoreceptors in Eulalia-Viridis (Polychaeta-Annelida). Cell Tissue Res 154:379–398.

Wilkins JS (2009) Defining Species. Peter Lang.

Wilkins JS (2010) What is a species? Essences and generation. Theory Biosci 129:141–148.

Wilkins JS (2013) Essentialism in Biology. In: The Philosophy of Biology, pp 395–419 History, Philosophy and Theory of the Life Sciences. Dordrecht: Springer Netherlands.

Williams GC (1992) Natural Selection. Oxford University Press.

Willingham MC, Pastan I, Shih TY, Scolnick EM (1980) Localization of the src gene product of the Harvey strain of MSV to plasma membrane of transformed cells by electron microscopic immunocytochemistry. Cell 19:1005–1014.

Willumsen BM, Christensen A, Hubbert NL, Papageorge AG, Lowy DR (1984) The p21 ras C-terminus is required for transformation and membrane association. Nature 310:583–586.

Wilson C, Venditti R, Rega LR, Colanzi A, D'Angelo G, De Matteis MA (2011) The Golgi apparatus: an organelle with multiple complex functions. Biochem J 433:1–9.

Winsor MP (2003) Non-essentialist methods in pre-Darwinian taxonomy. Biology and Philosophy 18:387–400.

Winsor MP (2006) The creation of the essentialism story: an exercise in metahistory. Hist Philos Life Sci 28:149–174.

Wong KY (2012) A retinal ganglion cell that can signal irradiance continuously for 10 hours. J Neurosci 32:11478–11485.

Wong KY, Dunn FA, Graham DM, Berson DM (2007a) Synaptic influences on rat ganglion-cell photoreceptors. The Journal of Physiology 582:279–296.

Wong KY, Graham DM, Berson DM (2007b) The Retina-Attached SCN Slice Preparation: An In Vitro Mammalian Circadian Visual System. J Biol Rhythms 22:400–410.

Wright AG, Demyanenko GP, Powell A, Schachner M, Enriquez-Barreto L, Tran TS, Polleux F, Maness PF (2007) Close homolog of L1 and neuropilin 1 mediate guidance of thalamocortical axons at the ventral telencephalon. J Neurosci 27:13667–13679.

Xu F, Huang H, Wu Y, Lu L, Jiang L, Chen L, Zeng S, Li L, Li M (2014) Upregulation of Gem relates to retinal ganglion cells apoptosis after optic nerve crush in adult rats. J Mol Histol 45:565–571.

Xue T, Do MTH, Riccio A, Jiang Z, Hsieh J, Wang HC, Merbs SL, Welsbie DS, Yoshioka T, Weissgerber P, Stolz S, Flockerzi V, Freichel M, Simon MI, Clapham DE, Yau KW (2011) Melanopsin signalling in mammalian iris and retina. Nature 479:67–73.

Yang X, Dong X, Jia C, Wang Y (2013) Profiling of genes associated with the murine model of oxygen-induced retinopathy. Mol Vis 19:775–788.

Yasuda T, Kurosaki T (2008) Regulation of lymphocyte fate by Ras/ERK signals. Cell Cycle 7:3634–3640.

Yonehara K, Shintani T, Suzuki R, Sakuta H, Takeuchi Y, Nakamura-Yonehara K, Noda M (2008) Expression of SPIG1 reveals development of a retinal ganglion cell subtype projecting to the medial terminal nucleus in the mouse. Soares D, ed. PLoS ONE 3:e1533.

Young P, Qiu L, Wang D, Zhao S, Gross J, Feng G (2008) Single-neuron labeling with inducible Cre-mediated knockout in transgenic mice. Nature Neuroscience 11:721–728.

Young RW (1985) Cell differentiation in the retina of the mouse. The Anatomical Record 212:199–205.

Zhang D-Q, Wong KY, Sollars PJ, Berson DM, Pickard GE, McMahon DG (2008) Intraretinal signaling by ganglion cell photoreceptors to dopaminergic amacrine neurons. Proc Natl Acad Sci USA 105:14181–14186.

Zhang M, Xia H, Li X, Wang X, Dong Y, Zhang T, Yu H (2010) C1 domain mediates CalDAGIII localization to the Golgi. Mol Biol Rep 37:3481–3485.

Zhang X, Wang F, Sheng J (2016) "Coding" and “Decoding”: hypothesis for the regulatory mechanism involved in heparan sulfate biosynthesis. Carbohydr Res 428:1–7.

Zhao X, Stafford BK, Godin AL, King WM, Wong KY (2014) Photoresponse diversity among the five types of intrinsically photosensitive retinal ganglion cells. The Journal of Physiology 592:1619–1636.

Zheng J, Trudeau MC, Zagotta WN (2002) Rod cyclic nucleotide-gated channels have a stoichiometry of three CNGA1 subunits and one CNGB1 subunit. Neuron 36:891–896.

Zhong H, Molday LL, Molday RS, Yau K-W (2002) The heteromeric cyclic nucleotide-gated channel adopts a 3A:1B stoichiometry. Nature 420:193–198.

Zhou H, Yoshioka T, Nathans J (1996) Retina-derived POU-domain factor-1: a complex POU-domain gene implicated in the development of retinal ganglion and amacrine cells. J Neurosci 16:2261–2274.

Zhou ZJ (1998) Direct participation of starburst amacrine cells in spontaneous rhythmic activities in the developing mammalian retina. J Neurosci 18:4155–4165.

CHAPTER 4

A Cre mouse line for probing irradiance- and direction-encoding retinal networks

Shai Sabbah[1], Daniel Berg[1], Carin Papendorp[1], Kevin L. Briggman[2] and David M. Berson[1]

[1] Department of Neuroscience, Brown University, Providence, RI, 02912, USA

[2] National Institute for Neurological Disorders and Stroke, National Institute of Health, Bethesda, MD, 20892, USA

Author Contributions
D.B., S.S., and D.M.B. designed the study and developed the theoretical framework. S.S. performed all electrophysiological recordings and intracellular dye-fills. D.B. performed intraocular injections. D.B., S.S., and C.P. performed immunostaining of retinas and brains, and confocal imaging. K.L.B. acquired the serial EM dataset. S.S., C.P., and D.M.B reconstructed neurons in the serial EM dataset. S.S., D.M.B., and C.P. analyzed the data. S.S. and D.M.B. wrote the paper.

History:

Received February 28, 2017. Accepted April 10, 2017. **Published online April 18, 2017.**

eNeuro 18 April 2017, ENEURO.0065-17.2017; DOI: 10.1523/ENEURO.0065-17.2017

http://eneuro.org/content/early/2017/04/18/ENEURO.0065-17.2017

Summary

Cell-type-specific Cre driver lines have revolutionized the analysis of retinal cell types and circuits. We show that the transgenic mouse Rbp4-Cre selectively labels several retinal neuronal types relevant to the encoding of absolute light intensity (irradiance) and visual motion. In the ganglion cell layer, most marked cells are wide-field spiking polyaxonal amacrine cells (ACs) with sustained irradiance-encoding ON responses that persist during chemical synaptic blockade. Their arbors spread about a millimeter across the retina and are restricted to the inner half of the ON sublamina of the inner plexiform layer. There, they costratify with dendrites of M2 intrinsically photosensitive retinal ganglion cells (ipRGCs), to which they are tracer-coupled. We propose that synaptically-driven and intrinsic photocurrents of M2 cells pass through gap junctions to drive AC light responses. Also marked in this mouse are two types of retinal ganglion cells (RGCs). 'R-cells' have a bistratified dendritic arbor, weak directional tuning, and irradiance-encoding ON responses. However, they also receive excitatory OFF input, revealed during ON-channel blockade. Serial blockface electron microscopic (SBEM) reconstruction confirms OFF bipolar input, and reveals that some OFF input derives from a novel type of OFF bipolar cell. R-cells innervate specific layers of the dorsal lateral geniculate nucleus and superior colliculus. The other marked RGC type ('RDS') is bistratified, transient, and ON-OFF direction-selective. It apparently innervates the nucleus of the optic tract. The Rbp4-Cre mouse will be valuable for targeting these cell types for further study and for selectively manipulating them for circuit analysis.

Significance Statement

Genetically modified Cre strains permit cell-type-specific labeling and functional manipulations. We illustrate the utility of Rbp4-Cre mice for studying selected retinal cell types that encode the

intensity of light and the direction of motion. Intensity encoding is thought to be uniquely mediated by intrinsically photosensitive retinal ganglion cells (ipRGCs). ipRGCs transmit intensity signals not only to the brain, but also intraretinally, partly through gap junctions to polyaxonal amacrine cells. We show that these amacrine cells are tagged in Rbp4-Cre mice, confirm their persistent light responses under chemical synaptic blockade, and show that they co-stratify with, and are tracer-coupled to M2 ipRGCs. The line also labels a variant of direction-selective RGCs, and a RGC that lacks intrinsic photosensitivity but encodes intensity.

Introduction

The discovery and description of retinal cell types and circuits have been dramatically enhanced by the emergence of large numbers of strains of genetically modified mice with cell-type specific patterns of labeling. Of these, the most versatile are Cre lines, which permit diverse type-specific manipulations, including optogenetic and chemogenetic control. Here, we document the utility of a bacterial artificial chromosome (BAC) transgenic mouse, Rbp4-Cre, for studies of several inner retinal cell types. Some of these encode the irradiance (intensity) of light entering the eye. Among retinal ganglion cells (RGCs), such irradiance coding has been thought to be unique to those that are intrinsically photosensitive (ipRGCs). These ipRGCs all express melanopsin and respond directly to light, but are otherwise diverse in form, physiology and central projections (Sand et al., 2012). Two sublaminae of the inner plexiform layer (IPL) are strongly linked to ipRGCs. The first lies at the outer margin of the IPL, abutting the inner nuclear layer (INL). There, intermingled, lie the narrowly stratified dendrites of M1 ipRGCs, certain other ipRGC types, and dopaminergic amacrine cells (ACs). The second ipRGC-associated sublamina, containing most ipRGC dendrites, lies in the inner half of the ON sublayer, proximal to the ON cholinergic band. We

show that all Cre-expressing ACs in the Rbp4-Cre line stratify within these same two laminae, and that at least one of them is coupled to ipRGCs there.

Early efforts to define the functional roles played by ipRGCs focused on their outputs to the brain, especially to the hypothalamic and brainstem circuits responsible for circadian synchronization and the pupillary light reflex. Spiking by ipRGCs encodes environmental light intensity and triggers reflexive circadian and pupillary responses. However, recent work has identified several 'centrifugal' outputs, through which ipRGC signals are injected back into retinal networks. ipRGCs make both chemical and gap junctional contacts with other retinal neurons (Zhang et al., 2004; Zhang et al., 2007; Zhang et al., 2008; Muller et al., 2010; Reifler et al., 2015; Arroyo et al., 2016; Prigge et al., 2016) and ocular structures (Semo et al., 2014). They influence spontaneous retinal waves (Renna et al., 2011; Kirkby and Feller, 2013) and perinatal vascular development of the eye (Rao et al., 2013). Electrical coupling permits ipRGCs to inject excitatory currents into all ON displaced wide-field ACs (Reifler et al., 2015). Here, we demonstrate that in Rbp4-Cre mice, these ACs are tagged with enough selectivity to permit morphological reconstruction, targeted patch recordings, and tracer-coupling studies. We confirm that a component of their light responses persists under chemical synaptic blockade, and show that they are selectively tracer-coupled to the M2 ipRGC type, with which they co-stratify almost perfectly.

As a bonus, the Rbp4-Cre line also labels two distinct types of RGCs. The bistratified 'R-cell' costratifies incompletely with the cholinergic plexuses, exhibits weak and inconsistent direction selectivity, and has some capacity for irradiance encoding. These cells project to the superior colliculus and a defined lamina of the dorsal lateral geniculate nucleus (vLGN and dLGN) distinct

from that innervated by direction-selective (DS) cells. The other RGC, the 'RDS cell', is a bistratified direction-selective RGC that responds transiently at both light ON and OFF. The RDS cell appears to innervate the nucleus of the optic tract (NOT).

Methods

Animals

All procedures were in accordance with National Institutes of Health guidelines and approved by the Institutional Animal Care and Use Committee at Brown University. We used adult mice (2 - 2.5 months old; either sex) of the strain Rbp4:Cre (031125-UCD, MMRRC). In some experiments we used mice from crosses of the Rbp4-Cre line with the Cre-dependent tdTomato Cre-reporter mouse Ai14 (B6.Cg-*Gt(ROSA)26Sor*$^{tm14(CAG-tdTomato)Hze/J}$)(The Jackson Laboratory).

Intravitreal injections for Cre-dependent fluorescent labeling

Mice were anesthetized with isoflurane (3% in oxygen; Matrx VIP 3000, Midmark). A viral vector designed for Cre-dependent cell labeling with the mCherry fluorophore (rAAV2/Ef1a-DIO-hchR2(H134R)-mCherry; Vector Core, UNC; 1.5 –2 µl of ~1.5 x 10^{12} units/ml) was injected into the vitreous humor of both eyes through a glass pipette using a microinjector (Picospritzer III, Science Products GmbH). Animals were killed and retinas and brains harvested 14-21d later.

Tissue harvest and retinal dissection

Eyes were removed and immersed in oxygenated Ames medium (95% O_2, 5% CO_2; Sigma-Aldrich; supplemented with 23 mM $NaHCO_3$ and 10 mM D-glucose). Under dim red light, the globe was cut along the ora serrata, and cornea, lens and vitreous removed. Four radial relieving

cuts were made in the eyecup, the largest centered on the insertions of the lateral and medial recti, useful later as a reference axis. The other two were deliberately asymmetric (roughly dorsotemporal and ventral) to disambiguate retinal orientation. Using gentle suction, the retina was flat-mounted on a custom-machined hydrophilic polytetrafluoroethylene membrane (cell culture inserts, Millicell; Ivanova et al., 2013b) and secured in a chamber on the microscope stage. Retinas were continuously superfused with oxygenated Ames' medium (32–34°C).

Patch recording and dye filling of ganglion and amacrine cells

Whole-cell patch-clamp current-clamp and voltage-clamp recordings of isolated flat-mount retinas were performed as described (Van Hook and Berson, 2010), using a Multiclamp 700B amplifier, Digidata 1550 digitizer, and pClamp 10.5 data acquisition software (Molecular Devices; 10 kHz sampling). Pipettes were pulled from thick-walled borosilicate tubing (P-97; Sutter Instruments); tip resistances were 5–6 MΩ when filled with internal solution, which, for current-clamp recordings, contained (in mM): 120 K-gluconate, 5 NaCl, 4 KCl, 2 EGTA, 10 HEPES, 4 ATP-Mg, 7 phosphocreatine-Tris, and 0.3 GTP-Tris, pH 7.3, 270–280 mOsm). For voltage-clamp recordings, the internal solution contained (in mM): 120 Cs-methanesulfonate, 5 NaCl, 4 CsCl, 2 EGTA, 10 HEPES, 4 ATP-mg, 7 Phosphocreatine-tris, and 0.3 GTP-tris, pH 7.3, 270–280 mOsm). Green fluorescent dye (Alexa Fluor 488; Invitrogen) was added to the pipette for visual guidance under two-photon imaging and dye-filling for later morphological characterization.

We pharmacologically blocked various receptors and pathways with one or more chemicals: 1) L-AP4 (100 μM; a group III metabotropic glutamate receptor agonist; acting on the metabotropic glutamate receptor mGluR6); 2) D-AP5 (30 μM; an NMDA glutamate receptor antagonist); 3)

DNQX (40 μM; an AMPA/ kainate glutamate-receptor antagonist); or 4) ACET (1 μM; a selective GluR5-containing kainate-receptor antagonist). All were purchased from Tocris.

Whole-cell recordings and intracellular injections (described below) were conducted on a multiphoton Olympus FV1200MPE BASIC (BX-61WI) microscope equipped with a 25x, 1.05 NA water-immersion objective (XLPL25XWMP, Olympus) and an ultrafast pulsed laser (Mai Tai DeepSee HP, Spectra-Physics) tuned to 910 nm. Epifluorescence emission was separated into "green" and "red" channels with a 570 nm dichroic mirror and a 525/50 bandpass filter (FF03-525/50-32, Semrock, green channel) and 575-630 nm bandpass filter (BA575-630, Olympus, red channel), respectively. The microscope system was controlled by FluoView software (FV10-ASW v.4.1).

Visual stimulation

Patterned visual stimuli, synthesized by custom software using Psychophysics Toolbox under Matlab (The MathWorks), were projected (AX325AA, HP) and focused onto photoreceptor outer segments through the microscope's condenser (Borghuis et al., 2013). The projected display covered 1.5 x 1.5 mm; each pixel was 5×5 μm. The video projector was modified to use a single UV LED lamp (NC4U134A, Nichia). The LED's peak wavelength (385 nm) shifted to 395 nm after transmission through a 440 nm short-pass dichroic filter (FF01-440/SP, Semrock), a dichroic mirror (T425lpxr, Chroma), and various reflective neutral density filters (Edmund Optics).

Quantum catches were derived from the stimulus spectrum (measured using an absolute-irradiance-calibrated spectrometer [USB4000-UV-VIS-ES, Ocean Optics]) and spectral

absorbances of mouse rod, cone, and melanopsin pigments (Govardovskii et al., 2000; Berson et al., 2002). At the highest light stimulus intensity, quantum catches were very similar among rods, cones, and melanopsin (~13.5 log photons cm^{-2} s^{-1}), independent of the cones' relative expression of S- and M-cone pigments (Szel et al., 1992; Chang et al., 2013).

To study the cells' ability to encode the absolute irradiance level, we used bright circular spots on a dark background (diameter=1200 μm, Michelson contrast=0.95, stimulus duration=15 or 30 sec, inter-stimulus duration=15 sec, 4 repetitions) at 4 or 5 irradiance levels at the plane of the photoreceptors (11-13.5 log photons cm^{-2} s^{-1}). To assess directional tuning, we used a sinusoidal grating spanning two spatial periods (spatial frequency=0.132 cycle/degree, Michelson contrast=0.95, stimulus duration=3.65 sec, inter-stimulus duration=5 sec at uniform mean grating luminance) drifting in 8 randomized directions (45° interval, drift speed=4.5 degree/sec, 4 repetitions). To study receptive-field center-surround configuration, we used a series of 7 circular spots of intermediate intensity (12 log photons cm^{-2} s^{-1}) centered on the cell's soma and covering a range of diameters (50-1200 μm). For RGCs, we used an additional set of 7 spot diameters (50-400 μm) to sample smaller-spot responses more fully. For all stimuli, frames of the stimulus movie were brief but frequent, appearing for 50 μs during the short 185 μs interval between successive sweeps of the imaging laser. Response persistence allowed us to observe the evoked light responses even though no stimulus was present during the interval of laser scanning and associated imaging (300 μs/sweep). The very rapid stimulus flicker (>2000 Hz) was well above critical fusion frequency in mice (Dai et al., 2015).

Electrophysiology data analysis

Irradiance-response (IR) curves were calculated using the steady-state response, measured as the mean level over the 5 last sec of the 15 sec stimulus. The ability of cells to report the absolute irradiance was assessed by fitting the sigmoidal Naka-Rushton function (Naka and Rushton, 1966) to the cell's steady state response to various stimulus irradiance levels (R):

$$R = R_{\max} \cdot 10^{(nE)} / (10^{(nE)} + 10^{(nK)}) \quad (1)$$

Where $R_{\max}$ stands for the cell's predicted maximum response, n stands for the slope of the function, E stands for the irradiance measured in units of log photons cm^{-2} s^{-1}, and K stands for the cell's sensitivity.

The direction selectivity index (DSI) ranges between 0 (no direction selectivity) and 1 (maximal direction selectivity). It was calculated as (Kim et al., 2008):

$$\mathrm{DSI} = \left| \sum_{\varphi} r(\varphi) \mathrm{e}^{i\varphi} \right| \Big/ \sum_{\varphi} r(\varphi) \quad (2)$$

where r is the response amplitude to stimuli moving at direction φ (0°, 45°,…,315°). The orientation selectivity index (OSI), which similarly ranges between 0 and 1 was calculated as:

$$\mathrm{OSI} = (r_{\mathrm{p}} - r_{\mathrm{o}}) / (r_{\mathrm{p}} + r_{\mathrm{o}}) \quad (3)$$

where r_{p} stands for the response amplitude at the preferred orientation and r_{o} stands for the mean response at the two directions orthogonal to the preferred one (Zhao et al., 2013).

Prior to analysis, current and voltage traces were down-sampled to 0.1 KHz, and current traces were smoothed with a Gaussian filter (s.d. = 5). The response amplitude represented the

peristimulus-time histogram (PSTH) (for current-clamp recording under control conditions; bin width = 0.155 sec), lower envelope of the voltage response (for current-clamp recording under any pharmacological manipulation that blocked voltage spikes), or current response (for voltage-clamp recording under any condition). All data were analyzed using custom Matlab scripts.

Intracellular injections of Neurobiotin

For tracer-coupling analysis, selected tdTomato-positive ACs were injected with Neurobiotin. Fine glass pipettes (~50 MΩ resistance) were filled at their tips with green fluorescent dye (Alexa Fluor 488; Invitrogen) and 4% Neurobiotin [N-(2-aminoethyl) biotinamide hydrochloride; Neurobiotin, Vector], and backfilled with K-gluconate-based internal solution (described above; Muller et al., 2010). A current pulse (-20 nA; 100 ms) triggered cell penetration. Fluorescent dye was iontophoretically injected (20 - 60 biphasic current pulses; -2000 pA for 500 ms and +500 pA for 400 ms) until dendrites were well filled. Then, an additional set of current pulses of reversed polarity were applied to iontophoretically inject the Neurobiotin. Retinas were fixed (4% paraformaldehyde, 30 min, 20°C) and incubated overnight with streptavidin-AlexaFluor 488 (S32354, ThermoFisher Scientific) in 0.1 M PBS containing 0.3% TritonX (X-100, Sigma-Aldrich). Anti-melanopsin and anti-ChAT immunostaining was conducted as described below. Filled cells were documented in Z-stacks acquired in confocal (single-photon) mode.

Immunohistochemistry of retina and brain

After recording, retinas were fixed (4% paraformaldehyde, 30 min, 20°C) and counterstained with one or more antibodies: 1) rabbit anti-CART (1:1000, Cocaine and Amphetamine Regulated Transcript; H00362, Phoenix Pharmaceuticals) - a specific marker for most ON-OFF DS cells;

Kay et al., 2011); 2) guinea pig anti-RBPMS (1:1000, RNA-binding protein with multiple splicing; 1832-RBPMS, PhosphoSolutions), a pan-ganglion-cell marker; Rodriguez et al., 2014); 3) goat anti-ChAT (1:100, anti-choline acetyltransferase; AB144P, Millipore); 4) rat anti-mCherry (1:1000, EST202, Kerafast); or 5) rabbit anti-melanopsin (1:1000, Advanced Targeting Systems).

Reconstruction of retinal neurons and circuits by serial blockface electron microscopy

Tissue preparation and EM acquisition were performed as previously described (Ding et al., 2016). In short, a retina from an adult wild-type mouse (C57BL/6; postnatal day 30) was stained for EM while preserving the intracellular structure and details. A retinal block face (k0725) of ~200 x 400 μm was imaged using a serial block-face scanning electron microscope system. The incident electron beam had an energy of 2.0 keV and a current of ~110 pA. Images were acquired with a pixel dwell time of 2.5 μs and size of 13.2 nm × 13.2 nm. The section thickness was set to 26 nm. 10,112 consecutive block faces were imaged, resulting in aligned data volumes of 4,992 × 16,000 × 10,112 voxels, corresponding to an approximate spatial volume of 50 × 210 × 260 μm^3. The volume spanned the IPL and included parts of the GCL and INL. To facilitate viewing in KNOSSOS (http://www.knossostool.org), the data set was split into cubes comprising 128 × 128 × 128 voxels.

The skeletons of cells were manually traced using the KNOSSOS annotation platform.

All skeletons were traced by at least two observers and any discrepancies resolved to ensure accuracy. We assigned bipolar cells to established categories (Wassle et al., 2009; Helmstaedter et al., 2013; Kim et al., 2014) based on stratification level and lateral dimensions of the axonal arbor.

Where we had dense sampling of neighboring bipolar cells, the tiling pattern of arbors further aided the type assignment.

For each BC, we calculated the density of neurites as a function of IPL depth, where IPL 0% represents the INL-IPL boundary, and 100% represents the IPL-GCL boundary. We defined the INL-IPL boundary as lying at the level of the fifth percentile of neurite density of Type 2 BC axon terminals, and IPL-GCL boundary at the 95th percentile of neurite density for rod bipolar axon terminals. We accounted for the slight tilt of the retinal laminae relative to the ultramicrotome cutting plane when calculating IPL depth. All analyses on skeleton data were performed using MATLAB.

Results

Small subsets of amacrine and ganglion cells are marked in the Rbp4-Cre mouse

We revealed Cre expression in retinas of Rbp4-Cre mice by injections of Cre-dependent mCherry virus (AAV) or crosses with a tdTomato Cre-reporter strain (Ai14). In both cases, red fluorescence marked a minority of retinal ganglion cells (RGCs) and amacrine cells (ACs). Bipolar cells (BCs) were also sparsely labeled, along with a subset of photoreceptors, but we have not studied these further.

In one fully mapped retina from an Rbp4-Cre;Ai14 mouse (Fig. 1A,B), there were 1893 tdTomato-positive cells in the ganglion cell layer (GCL), corresponding to a mean density of 115 cells/mm^2 (retinal area = 16.4 mm^2). The density of labeled cells showed modest topographic dependence, being lowest in the dorso-nasal retina (Fig. 1C). Labeled cells in the GCL comprised a mixture of RGCs and ACs. The RGCs were identifiable from their clearly labeled axons, traceable into the optic fiber layer, and from their immunoreactivity for the pan-ganglion-cell marker RBPMS (RNA-binding protein with multiple splicing [Rodriguez et al., 2014], Fig. 1D-F). However, most fluorescent cells of the GCL lacked both of these features and were thus displaced ACs. About 90% of the fluorescent cells of the GCL (~1700 cells in total) were displaced ACs while the remainder (~200 cells in total) were RGCs, as determined by RBPMS staining. The relative abundance of these cell classes varied topographically, with RGCs making up only 2.5% of the labeled cells in the ventro-temporal GCL, but 14.6% of them nasally (Figure 1D-G).

Labeled RGCs were readily divisible into two distinct types. The first, more common type (here termed the '*R-cell*') was bistratified with a relatively small soma and compact dendritic field (Fig.

2A,B). The second, rarer type (here termed the '*RDS cell*') was also bistratified, but resembled classic direction-selective cells. These had distinctly larger somas and, typically, asymmetric dendritic arbors (Fig. 2A,C). An additional amacrine cell type was labeled in this line. These had small somata in the conventional position for ACs (inner margin of inner nuclear layer; INL) and a bistratified dendritic arbor. Figure 2D compares the patterns of stratification for each of these four types, and a fuller description of each follows.

Rbp4-Cre labels a unique population of displaced polyaxonal amacrine cells of the inner ON sublayer

For convenience, we refer to Rpb4-Cre-positive displaced amacrine cells (i.e., the labeled amacrine cells in the GCL) as "*RACs*." Their morphology is summarized in Figs. 2A and D, Fig. 3, and Table 1. Cell bodies were relatively large for ACs (11.2±1.4 μm diameter; average ± s.d.; n = 46), comparable to those of neighboring starburst ACs and the smallest RGCs. They were multipolar and extended their processes horizontally within the inner ON sublayer of the IPL (Fig. 3A). There, they were quickly lost in a dense feltwork of labeled processes dominated by very fine varicose fibers following mostly straight trajectories (Fig. 3A, magenta; Fig. 3B, red). This plexus occupied the inner third of the ON sublamina (S4/S5), entirely proximal to (below) the ON cholinergic band. This plexus was matched almost exactly in depth with the inner plexus of melanopsin immunoreactive processes (Fig. 2D, left), consisting mainly of the dendrites of M2 ipRGCs (Fig. 3C-F; Berson et al., 2010). Intracellular dye injections of Cre-labeled RACs revealed their morphology in better detail (Fig. 2A; Fig. 3A, green; Fig. 3G). Their processes spanned roughly 1mm, encompassing about a fifth of the retina each (Fig. 3G; diameters 970±130 μm; n = 4). The most widely spreading processes appeared axonal in form, having a uniform very fine

caliber with periodic swellings, but most primary processes seemed dendritic, with a gradually tapering caliber as well as some spines and appendages. We therefore conclude that RACs are a form of wide-field polyaxonal AC (Fig. 2A).

Rbp4-Cre labels a sparse population of conventionally-placed bistratified amacrine cells

A second type of Cre-labeled amacrine cell in this mouse line had conventionally placed somata in the INL (Fig. 2D purple; Fig. 3H-J). They were regularly spaced, suggesting possible mosaic organization (Fig. 3H), and of uniformly small size (diameter of 9.65±0.55 μm, average ± s.d., n = 23). Cre-dependent viral labeling revealed that their processes form a dense plexus in the outermost IPL, just proximal to their somata (Fig. 3H-J). Well-labeled cells almost invariably possessed a major dendritic process that descended through the IPL and branched, and apparently arborized, within the plexus of Cre-labeled RAC processes in the inner ON sublamina (Fig.2D, left; Fig. 3D-F). We could not determine from such material the dimensions of the ON-sublayer dendritic fields of these bistratified amacrine cells, nor what fraction of this inner amacrine-cell plexus was derived from these cells as opposed to RACs.

RACs have sustained irradiance-encoding light responses

A recent study in rat retina found that all ON sustained wide-field displaced ACs are electrically coupled to ipRGCs (Reifler et al., 2015). The RACs we identify among the labeled Rbp4-Cre cells are similar morphologically to these rat ACs, so we suspected that RACs might have similar functional properties. Indeed, whole-cell current-clamp recordings confirmed this inference. Cre-labeled RACs were tonically depolarized, and increased their spiking in response to prolonged whole-field illumination (Fig. 4A). Responses included a transient peak that decayed within a few

seconds to the steady-state level. Firing rates during this plateau phase varied as a function of stimulus irradiance. This is evident from spiking visible in individual voltage traces (Fig. 4A), from the average peri-stimulus-time histogram (PSTH; average ± s.e.m.; Fig. 4B), and from the irradiance-response function of pooled cells (Fig. 4C), derived from spike frequency during the 5 last seconds of the stimulus. We also examined the excitatory currents by voltage-clamping at the chloride reversal potential. Sustained excitatory inward currents persisted throughout the stimulus, with amplitudes correlated with stimulus irradiance (Fig. 4D,E). Light offset evoked an outward current (Fig. 4D) and modest hyperpolarization (Fig. 4A). These cells exhibited little evidence of an antagonistic surround (data not shown).

To probe the origin of these light-evoked inward currents, we blocked the ON pathway by bath application of L-AP4 (an agonist of the group III metabotropic glutamate receptors essential for light responses in ON bipolar cells). ON-channel blockade dramatically reduced the light-evoked depolarization and firing (Fig. 4F, lower trace; compare Fig. 4A), but low amplitude responses persisted (Fig. 4F, inset). For bright stimuli (>10^{12} photons cm^{-2} s^{-1}), these consisted of a rapid hyperpolarization (~1mV), followed by a larger, slowly developing sustained depolarization (Fig. 4F,G,I) that lasted at least 30s, and decayed over many seconds after stimulus offset (Fig. 4I). Dimmer stimuli evoked only a very small sustained hyperpolarization (Fig. 4G). At light intensities above threshold for the sluggish depolarization, response amplitude increased with stimulus irradiance (Fig. 4G,H). This response is strikingly similar to melanopsin-driven responses of ipRGCs; it is depolarizing and irradiance encoding, with a high threshold (~10^{12} photons cm^{-2} s^{-1}), sluggish onset and slow post-stimulus decay (Berson et al., 2002). Because these amacrine cells are melanopsin-immunonegative (Figs. 3B, 5G), our findings parallel those of Reifler et al.

(2015) in suggesting that the sluggish depolarizing response seen under these recording conditions derives from electrical coupling to ipRGCs.

RACs also appear to get modest excitatory input from the OFF channel. Blockade of the ON channel revealed a modest brisk depolarization at light offset (Fig. 4F,G,I). This was blocked (Fig. 4K,M) by supplementing the ON blocker L-AP4 with a mix of drugs designed to block the OFF channel. This 'OFF cocktail' included D-AP5 (an NMDA glutamate receptor antagonist), DNQX (an AMPA/ kainate glutamate receptor antagonist), and ACET (a selective GluR5-containing kainate receptor antagonist). The sluggish, irradiance-encoding, melanopsin-like response persisted under this more extensive blockade of chemical synaptic signaling (Fig. 4J,K,M).

RACs are tracer coupled to selected ipRGCs and ACs

We used tracer coupling to test the hypothesis that the melanopsin-like response seen in RACs is attributable to gap junctional coupling to ipRGCs (Reifler et al., 2015). In Rbp4-Cre;Ai14 mice, two fluorescently tagged RACs were injected with Neurobiotin, which passes through gap junctions to label coupled cells. Both injected cells were confirmed to be wide-field ACs, and one of these is illustrated in Figure 5. Tracer-coupled cells labeled in these experiments included M2 ipRGCs, identified by their melanopsin immunoreactivity and characteristic dendritic arbors (Fig. 5B,E,K,Q). Also tracer-labeled were displaced ACs, identified by their small soma size, and their immunonegativity for either melanopsin or the RGC marker RBPMS (Fig. 5H,I,N,O). These ACs were not RACs, because they were not labeled by the tdTomato Cre reporter (Fig. 5F,G, L, and M). A few tracer-coupled cells were melanopsin-immunonegative and weakly RBPMS immunopositive. It is unclear whether these are ipRGCs with weak melanopsin expression (M4 or

M5 cells) or some other RGC types. We conclude that RACs form an extensive electrically-coupled network comprising, at least, M2 ipRGCs and a distinct type of displaced ACs.

Rbp4-Cre marks two types of bistratified RGCs

To assess the general morphology of Cre-expressing RGCs in the Rbp4-Cre line, we labeled large numbers of them through genetic crosses with the Ai14 tdTomato Cre-reporter mice or by Cre-dependent viral labeling. Melanopsin and ChAT immunolabeling provided laminar benchmarks. We could relatively easily trace the coarser dendrites of the RGCs through the thicket of amacrine-cell processes in the inner ON sublayer and thus reconstruct their arbors with reasonable confidence. Two clear types emerged: the smaller *R-cell* (Fig. 2B) and the larger *RDS cell* (Fig. 2C). Both were bistratified, but they differed in many other respects, as outlined below.

Morphology of the *R-cell*

These RGCs were invariably bistratified. Their somas were small (diameter 12.9±1.0 μm); not much larger than those of starburst ACs, and smaller than those of M1 ipRGCs (Fig. 6F). Their dendritic fields were of intermediate size among murine RGCs, and their ON arbor (178±35 μm diameter) was typically slightly larger and more complex than the OFF arbor (138±36μm; Fig. 2B; 6A,C; Table 1). Though the two arbors were usually largely in spatial register, they were substantially offset from one another in a minority of cells. Local clusters of labeled R-cells had the appearance of fragmentary mosaics with well-spaced somas and a uniform plexus of moderately overlapping dendritic arbors in both the ON and OFF sublayers of the IPL (Fig. 6F,G). One tier of dendrites lay within the ON IPL sublayer, stratifying near the proximal margin of the ON ChAT band. These processes lay just distal to those of M2 ipRGCs and the wide-field

displaced RACs described above (Fig. 6D). The ON tier loosely co-fasciculated with the ON starburst processes (Fig. 6E). The OFF arbor was rather broadly stratified, filling the space between the plexus of OFF starburst AC dendrites and the plexus of M1 ipRGC dendrites marking the INL-IPL border (Fig. 2D right; Fig. 6D).

R-cells have sustained ON irradiance-encoding light-evoked responses

R-cells exhibited sustained ON responses to whole-field illumination, and only a brief hyperpolarization at OFF (Fig. 7A). Higher light intensities resulted in reduced spike amplitude and regularity (Fig. 7A), presumably due to partial sodium-channel inactivation. The average firing rate (Fig. 7B) and the irradiance-response function derived from it (Fig. 7C) revealed only modest dependence of spiking on stimulus intensity. However, when clamping the membrane at the chloride reversal potential, the irradiance-dependence of the steady-state, light-evoked inward current became more apparent (Fig. 7D,E). Inward currents at light offset were also observed (Fig.7D). The magnitudes of these, too, were irradiance-dependent.

Blocking the ON channel with L-AP4 reversed the sign of the steady-state light response from depolarization and spiking (Fig. 7A) to hyperpolarization (Fig. 7F). Though the hyperpolarization was relatively modest, it was accompanied by a reduction in membrane noise, and a dramatic suppression of spiking (Fig. 7F). Both onset and offset of the light stimulus evoked a small, transient hyperpolarization. Membrane voltage varied only modestly as a function of stimulus irradiance (Fig. 7G,H).

We next supplemented the ON-channel blockade with agents designed to silence the OFF pathway (namely, a mix of NMDA and AMPA/kainate blockers, D-AP5 and DNQX). Though this strongly attenuated the transient hyperpolarizations at light ON and OFF, we were surprised to find that this incompletely blocked the sustained ON hyperpolarization, and that light offset induced post-stimulus bursting in several cells (Fig. 7I). Membrane voltage was minimally related to stimulus irradiance under these conditions (Fig. 7J,K). We suspected that the residual light responses were due to incomplete kainate receptor blockade, so we added ACET (a selective antagonist for GluR5-containing kainate receptors). This rendered the cells largely irresponsive to light (Fig. 7L-N). Taken together, the data suggest that ON bipolar input normally dominates in R-cells, but that they also receive OFF bipolar input that is unmasked when the ON channel is silenced.

To study center-surround organization, we presented bright spots of various sizes (Fig. 7O). On average, the optimal spot diameter was 280 μm, which is substantially larger than the dendritic arbor. Larger spots attenuated the response, indicating the presence of an inhibitory surround (Fig. 7O, inset). R-cells generally showed some tuning for the direction or orientation of drifting gratings, but such tuning was inconsistent and typically weak (Fig. 7P,Q; direction selectivity index, DSI=0.21±0.13; orientation selectivity index, OSI=0.36±0.22).

Serial electron microscopy reconstruction of an R-cell and its synaptic inputs

To characterize the types of BCs that synapse onto R-cells, we mined a serial block-face electron microscopy (EM) volume (k0725) generated from a wild-type adult mouse retina (Ding et al., 2016). The volume ($50 \times 210 \times 260$ μm^3) spanned the IPL and the immediately adjacent portions

of the GCL and INL. The retina had been processed so as to reveal intracellular structures such as synaptic ribbons and vesicles.

Among many RGCs traced in the EM volume, we identified diverse bistratified forms. One of these RGCs closely resembled the R-cells as just characterized at the light-microscopic (LM) level (compare Fig. 8A and Fig. 2B). Several key morphological measures obtained from the EM-reconstructed presumptive R-cell fell within one standard deviation of the mean value of those measures for R-cells traced in confocal z-stacks (Table 1; compare R-cell and R-cell EM). The dendritic tree of the EM-reconstructed cell were similar in form to those of R-cells in branching structure, apparent dendritic field size and stratification (Fig. 8A). The outer arbor of the reconstructed R-cell stratified between the dendrites of reconstructed M1 ipRGCs and the OFF ChAT band (inferred from dendritic stratification of reconstructed ON-OFF direction-selective cells). The inner arbor resided within and just below the ON ChAT band (Fig. 8B and Fig. 6D). Though the soma diameter of this presumptive R-cell was larger than those of R-cells as assessed by confocal microscopy (16.1 vs. 12.9±1.0 μm), this might have resulted from osmotic factors during tissue fixation (Thorne and Nicholson, 2006; Mikula and Denk, 2015).

To identify the BC types that synapse onto the presumptive R-cell, we scanned its dendrites for ribbon synaptic contacts (Fig. 8A, red dots); subsequently, starting from randomly-selected identified dyad synapses (128 out of 281), we reconstructed the complete axon and axon terminal of 76 BCs. To identify BC types, we assessed the stratification of their arbors in relation to one another and to the cholinergic bands (Fig. 8C,G,H). Fig. 8D shows all reconstructed bipolar cells synapsing onto the presumptive R-cell as projected onto the plane of the retina (D, top; *en face*

view) or onto an orthogonal, vertical plane to show depth information (bottom). ON synaptic input to the presumptive R-cell was dominated by Type 7 ON cone BCs, while its OFF synaptic input derived almost entirely from Type 1 and 2 OFF cone BCs (Fig. 8D,E). Figure 8F-H quantify two features of axon terminals that distinguish bipolar types from one another — the dimensions of the terminal arbor (Fig. 8F) and their depth within the IPL (Fig. 8G,H). In general, the presumptive R-cell seemed to receive input from axon terminals of all BC types within its dendritic field, provided they co-stratified with the R-cell's dendrites. ON inputs were more common than OFF inputs (78 vs. 50 dyads in the inner and outer arbors; 53 vs. 25 ON and OFF cone BCs), paralleling the dominant ON response observed physiologically (Fig. 7A-E).

A novel bipolar cell type – cone BC Type 0

Among the presynaptic neurons providing ribbon synaptic contact onto the presumptive R-cell, we identified four cells that appear to belong to a previously unknown BC type (Fig. 9). They superficially resembled Type 1 and Type 2 OFF cone bipolar cells but were clearly different from both. Most of the Type 0 cells (3 of the 4) had cell bodies at the inner margin of the INL (the remaining cell's soma lay outside the volume). This is a highly atypical position for bipolar cell bodies, but is characteristic of amacrine cells. However, there is no precedent for synaptic ribbons in ACs, so for now we assume that this is a novel OFF cone bipolar cell type, which we provisionally term 'Type 0.'

Multiple features differentiated Type 0 from Type 1 ($n = 25$) or Type 2 ($n = 16$) bipolar cells. First, the arbors of Type 0 BCs were sparsely branched and significantly broader than those of Types 1 and 2 (Figure 9D; 1614 μm^2, 450 μm^2, and 618 μm^2 axon terminal field areas for Types 0, 1, and

2; permutation one-way ANOVA, $p < 0.001$; by post-hoc pairwise comparisons, arbor areas of Type 0 were significantly larger than those of Type 1 or Type 2, $p < 0.001$). Second, their axonal arbors stratified slightly more proximally (lower) in the IPL (Figure 9E,F; IPL depth of 16%, 12%, and 9% for Types 0, 1, and 2; permutation one-way ANOVA, $p > 0.05$; post-hoc pairwise comparisons, Type 0 axons arborized significantly deeper in the IPL than Type 2 axons [$p = 0.048$], whereas the depth difference with Type 1 axons did not reach statistical significance [$p = 0.173$]). Finally, their arbors did not fit into the mosaics of BC Type 1 and 2 axon terminal fields, and instead dovetailed with each other in a way that suggests an independent tiled mosaic in the IPL (Fig. 9A-C). Like other bipolar cells, Type 0 BCs make mainly dyadic ribbon contacts in the IPL.

Morphology and physiology of RDS cells

The other RGC type labeled in the Rbp4 line — the direction-selective cell here termed 'RDS' — was rarer than R-cells, and easily distinguishable from them by virtue of its much larger soma (RDS: 17.5±2 μm, $n = 4$; R-cells: 12.9±1.0 μm, $n = 16$). RDS cells also had larger dendritic arbors. This was because the OFF arbor was larger in RDS cells (diameter 194±27 μm; $n = 4$) than in R-cells (138±36 μm; $n = 13$); in contrast, ON arbor dimensions were very similar between the two types (RDS diameter: 177±15 μm; R-cell diameter: 178±35 μm). In branching structure and stratification, RDS cells strongly resembled other ON-OFF direction selective (DS) types (Fig. 2C; 10A; Huberman et al., 2009; Rivlin-Etzion et al., 2011; Trenholm et al., 2011; Dhande et al., 2013). Like those types, the RDS cell restricted its dendritic arbors to the two sublaminae containing processes of starburst amacrine cells, revealed by ChAT immunolabeling (Fig. 10B). Moreover, like other ON-OFF DS cells, the RDS cell's dendrites cofasciculated with the ChAT-immunopositive processes (Fig. 10C) and avoided the melanopsin immunoreactive plexuses at the

margins of the IPL (Fig. 10B). We confirmed the direction selectivity of RDS cells by showing that they responded differentially to the direction of motion of sinusoidal gratings and bars. RDS cells were ON-OFF cells, responding to both the leading and trailing edge of the moving bar (Fig. 10E). Though our sample is small, all recorded RDS cells preferred ventral motion on the retina (Fig. 10E-F). They are thus reminiscent of cells labeled in the Hb9-GFP mouse line, which are also ON-OFF DS cells that prefer ventral retinal motion (Trenholm et al., 2011). Like Hb9-GFP cells, RDS cells exhibited dendritic asymmetry (Fig. 10A), with the center of the dendritic arbor displaced from the cell body in the cell's preferred direction (compare Fig.10F and G).

Like most ON-OFF DS types (Kay et al., 2011; Dhande et al., 2013), RDS cells were clearly immunoreactive for Cocaine and Amphetamine Regulated Transcript (CART) (Fig. 10H,I; white arrows). To our surprise, the R-cell, the other RGC type labeled in this line, was also virtually always CART-immunopositive despite its weak directional tuning (Fig. 10H,I; hollow white arrowheads). In the GCL, 97% of all RGCs (identified by their RBPMS labeling) that exhibited Cre-driven labeling in the Rbp4-Cre mouse also expressed CART (n = 64), whereas all but a handful of Cre-labeled displaced amacrine cells (RACs; Fig. 10H,I, hollow blue arrowheads) were CART-negative. Two identified displaced Rbp4-Cre-labeled RGCs also lacked CART staining.

Axonal projections of Rbp4-Cre RGCs

To study the central projections of RGCs in the Rbp4-Cre line, we made intraocular injections of Cre-dependent mCherry viruses. The advantage of this viral approach, as compared to crossing Rbp4-Cre mice with Cre reporter mice, is that it ensured that all fluorescent axons were of retinal origin. Labeled axon terminal fields were prominent in the dLGN. There, they were concentrated

within a specific lamina, at roughly the transition between the external shell and main core of the nucleus (Fig. 11A,C), defined by their differential input from direction-selective or melanopsin-expressing RGCs, respectively (Huberman et al., 2009; Ecker et al., 2010; Kay et al., 2011; Rivlin-Etzion et al., 2011). The superior colliculus (SC) was also prominently labeled, with highly branched fine axonal arbors that terminated only very superficially in the upper retinorecipient layers (Fig. 11D). Additional terminal fields were detected in a thin sheet at the lateral margin of the ventral LGN (Fig. 11A,C), and in the nucleus of the optic tract (NOT), a component of the accessory optic system (Fig. 11A-C). No labeling was detected in any other targets of retinofugal axons, including the MTN and the suprachiasmatic nucleus.

These axon terminal fields represent the combined projections of R-cells and RDS-cells, because the intraocular virus used transduced both RGC types, judging from their somadendritic architecture. However, in one case, viral transfection was sparse enough to label only three RGCs across the whole retina. All three were clearly R-cells. Their three axons were easily traced to the optic nerve head and into the brain. Three distinct arbors were evident in the dLGN, vLGN and SC (Fig. 11E), but no axon terminals were detected in the NOT. These data suggest that R-cells innervate the LGN complex and SC, but not other retinorecipient targets, including the accessory optic system, while the RDS cells innervate at least the NOT.

Discussion

Rbp4-Cre mice offer the opportunity to study and manipulate several interesting retinal cell types and circuits. These include a pair of wide-field AC types closely linked to melanopsin and ipRGCs; an ON bistratified RGC type (the R-cell) with weak direction and orientation selectivity and outputs linked to spatial vision; and a variant of the direction-selective RGC class (the RDS cell).

The *Rbp4* gene codes for a retinol carrier protein. Because RACs are coupled to ipRGCs, which require retinoids for their intrinsic photosensitivity, we wondered whether the cells marked in the Rbp4-Cre mouse might be linked in some way to melanopsin phototransduction. However, pilot studies revealed no Rbp4-like immunoreactivity in the inner retina. Many transgenes are expressed in patterns unrelated to those of the targeted gene, presumably due to positional effects, and this may apply to the Rbp4-Cre BAC transgene in this mouse.

RACs form a wide-field lateral inhibitory network coupled to ipRGCs

Two types of ACs are selectively marked in Rbp4-Cre mice. Both types contribute to the Rbp4-Cre plexus in the inner ON sublayer, where they costratify with the dendrites of most ipRGC subtypes (M2, M3, M4 and M5 cells). The other AC labeled in this mouse line, the conventionally placed bistratified type, has an outer dendritic arbor that intermingles with the dendrites of M1 and M3 ipRGCs.

RACs don't merely costratify with ipRGCs; tracer coupling revealed that the processes of RACs and M2 ipRGCs make gap junctional contacts. This echoes the report of Perez De Sevilla Muller et al. (2007), who observed dye-coupling between M2 cells and displaced wide-field,

monostratified polyaxonal ACs (PA-S5) that may match our RACs. RACs were also tracer-coupled to melanopsin-immunonegative RGCs; these could be M4 or M5 ipRGCs, which often lack detectable melanopsin immunoreactivity (Ecker et al., 2010; Estevez et al., 2012). Indeed, Volgyi et al. (2009) found polyaxonal ACs tracer-coupled to two RGC types; G_1, which appears equivalent to M4 ipRGCs, also known as ON alpha cells (Estevez et al., 2012); and G_6, which may correspond to M5 ipRGCs (Ecker et al., 2010). In addition to their coupling to RGCs, RACs were also coupled to Rbp4-Cre-negative displaced ACs. Therefore, RACs anchor a complex electrically coupled network in the inner ON IPL that encompasses multiple RGC types (including some ipRGCs) and at least one other AC type.

Our results provide several lines of evidence suggesting that RACs are influenced by ipRGC signals transmitted through gap junctions: (1) M2 ipRGCs are coupled through gap junctions to RACs (Fig. 5). (2) With chemical synaptic transmission intact, RAC spiking and excitatory currents are sustained and irradiance-encoding, mirroring those of ipRGCs (Fig. 4A-E). (3) Under blockade of chemical synaptic transmission, light triggers excitatory currents and increased RAC spiking, mirroring the responses of ipRGCs recorded under similar conditions. As in ipRGCs, these RAC responses are sluggish and sustained, and they persist long after the light stimulus is turned off (Fig. 4J-M). Presumably, under these conditions, intrinsic photoresponses of ipRGCs propagate into RACs through electrical coupling. (4) The response threshold of ipRGCs and RACs also match; under synaptic blockade, residual RAC light responses are evident mostly at the two highest light intensities tested, which are suprathreshold for driving the melanopsin-based phototransduction in ipRGCs (Fig. 4J-M). Therefore, RAC coupling to ipRGCs likely accounts for the persistence of RAC light responses under chemical synaptic blockade, and for the

melanopsin-like sluggishness, insensitivity, sustained and irradiance-encoding nature of those light responses.

Reifler et al. (2015) were the first to describe such responses in displaced wide-field ON ACs in rat, and they proposed electrical coupling to ipRGCs as their basis. RACs resemble these rat ACs morphologically and may be homologous. Other possible equivalents are mouse polyaxonal ACs coupled to G_1 and G_6 RGCs (see above; Volgyi et al., 2009), WA4-1 cells (Lin and Masland, 2006), PA-S5 cells (Perez De Sevilla Muller et al., 2007), and 'Cluster 2' cells (Badea and Nathans, 2004). Like RACs, these are polyaxonal ACs with large displaced somata (12 μm in diameter), a relatively large sparse dendritic arbor (~450 μm diameter) and wide-ranging axonal arbors (1-2 mm diameter), both of which are restricted to the inner ON sublayer.

Residual RAC light responses were weak under synaptic blockade, but this probably understates the impact of electrical coupling *in vivo*. All ipRGCs, including M2 cells, exhibit robust light-evoked excitatory currents derived from BCs (Schmidt and Kofuji, 2010; Wong, 2012). These synaptically driven photic signals presumably pass through gap junctions to modulate AC excitability, just as melanopsin-driven photocurrents do. Synaptic blockade would eliminate this excitatory influence, along with direct bipolar drive to the RAC itself. Therefore, in the intact retina, RACs are likely to receive a mix of robust synaptically-driven and intrinsic irradiance-encoding currents from M2 ipRGCs.

The wide-field architecture of RACs and their coupled partners provide a substrate for extensive lateral spread of locally generated irradiance signals. Spikes presumably transmit such signals

throughout their sprawling polyaxonal arbors. Because RACs are almost certainly GABAergic, they probably inhibit target neurons in proportion to background light intensity, suggesting a role in network light adaptation. The postsynaptic targets of such inhibition are unknown, but could include ON cone BC terminals (Types 6-9), dendrites of most ipRGC types (M2-M5), and many AC types (Helmstaedter et al., 2013).

Cre expression in RACs provides experimental opportunities. Cre-dependent calcium or glutamate indicators would facilitate functional imaging. Relatively selective optogenetic activation or silencing is also possible, though complicated by the diversity of Cre-expressing cells in this line. A favorable location for such studies would be the ventrotemporal retina, where RACs represent nearly all of the Cre-expressing cells in the GCL.

The bistratified morphology of the other AC type might predict ON-OFF light responses, but it could be purely ON. Its outer arbor narrowly costratifies with processes of M1 ipRGCs and dopaminergic ACs, both targets of ectopic *en passant* ON bipolar synapses in the OFF sublayer (Dumitrescu et al., 2009; Hoshi et al., 2009; Reifler et al., 2015).

R-cell – an ON bistratified ganglion cell type

The R-cell is possibly a novel bistratified mouse RGC type. It has some features reminiscent of ipRGCs (sustained, irradiance-encoding ON excitatory drive) and others that link it to the DS system (weak directional tuning, CART-immunoreactivity, and partial co-stratification with starburst amacrine cells).

R-cells join a variety of ON-dominant bistratified neurons of the GCL, including the M3 ipRGCs (Schmidt and Kofuji, 2011), ON-DS cells (Dhande et al., 2013), ON-orientation selective (OS) cells (Nath and Schwartz, 2016), and bistratified wide-field ACs (Reifler et al., 2015). We wondered whether R-cell outer arbors might be another target of the ectopic ON bipolar synapses in the outer OFF sublamina, but they were not. Serial-EM reconstruction revealed no ectopic ON bipolar contacts onto the R-cell outer dendrites, but abundant OFF bipolar input (Fig. 8), and this was reflected in their photoresponses (Fig. 7). Among RGCs, only ipRGCs have been thought capable of stably encoding light intensity, but we find R-cells do so to some degree, despite lacking melanopsin expression and intrinsic photosensitivity.

The responses of R-cells to a steady wide-field light stimulus differ from those of ipRGCs; yet they do share certain aspects. The responses of both R-cells and ipRGCs adapt over the first few seconds of the light stimulus, and then stay rather stable. In both cases, the response lasts at least 15 sec, the longest light stimulus we used (Fig. 7B,D). The steady-state response of R-cells, expressed as a fraction of the maximum response, is smaller than for ipRGCs, and the dynamic range of the steady-state light response is much smaller for R-cells than for ipRGCs (R-cells: 18.5 pA; ipRGCs: 200-400 pA; data not shown). Thus, while R-cells encode irradiance (Fig. 7E), they do so over a relatively narrow range. On the other hand, the firing rate of R-cells did not show obvious irradiance-encoding (Fig. C). Thus, R-cell intrinsic mechanisms may largely temporally filter out the irradiance signal at the level of the cell's spike train.

Bipolar inputs to R-cells were heterogeneous (ON: mainly from Types 5 and 7; OFF: mostly from Types 1 and 2). Our SBEM reconstruction also revealed contact from a novel OFF BC we call

'Type 0'. Like other OFF BCs, Type 0 BCs' axon terminals contain ribbons and stratify exclusively in the OFF sublayer of the IPL. However, they are distinguishable from Type 1 and Type 2 OFF cone BCs by axon terminal arbor dimensions and by mosaic analysis. Furthermore, they are distinguishable from Type 3 and 4 OFF cone BCs based on stratification. Type 0 BCs bear some resemblance to GluMI cells (Della Santina et al., 2016) and the presumably equivalent BC1B cells (Shekhar et al., 2016). Like Type 0 BCs, both have a soma placed low in the INL, near AC somas, and an arbor stratifying roughly at the same depth as Type 1 and 2 BCs. However, Type 0 BCs have larger axonal arbors than GluMI/BC1B cells. Our SBEM volume omitted the outer retina, so we cannot say if Type 0 BCs lack a process in the OPL, as GluMI and BC1B cells do.

R-cells resemble ON vertical OS RGCs (Nath and Schwartz, 2016). Both are bistratified in the same IPL sublaminae, have a larger ON than OFF arbors, lack marked dendritic-field asymmetry, have an ON-dominant response, and some sensitivity to stimulus orientation. However, R-cells have smaller dendritic arbors, a distinct temporal response profile to light steps, and substantially broader tuning for orientation than vertical OS cells.

Another possible R-cell equivalent is the medium-sized bistratified RGC (m-BGC), labeled in the PCP2-Cre mouse (Ivanova et al., 2013a). However, the two cell types slightly differ in soma diameter (R-cell vs. m-BGC: 12.9±1.0 vs. 14.6±1.6 μm), dendritic field diameters (ON: 178±35 vs. 219±25 μm; OFF: 138±36 vs. 148±24 μm), and ratio of ON to OFF dendritic field diameters (1.3±0.2 vs. 1.5±0.1). Moreover, the inner arbor of R-cells which partly costratifies with the ON ChAT band, appears a bit more distal than that of m-BGCs. Also, m-BGCs exhibit many dendrites

that ascend to the outer IPL before descending to the inner IPL; we rarely saw these in R-cells. Retinofugal projections in the PCP2-Cre and Rbp4-Cre mice are generally similar, though the heterogeneity of RGC labeling in both lines complicates any interpretation. Other possible morphological equivalents of the R-cell include the G_{12} cell (Volgyi et al., 2009), Type 8 RGCs (Helmstaedter et al., 2013), and the 'V' RGCs (Sumbul et al., 2014), all of unknown physiological type.

RDS – A direction selective cell in the Rbp4-Cre mouse

The other RGC marked in this line, the RDS cell, is a variant of the ON-OFF DS RGC types. Superficially, the RDS cell resembles GFP-positive DS cells in the Hb9-GFP mouse (Trenholm et al., 2011). Like them, RDS cells prefer motion toward the ventral retina; they costratify and cofasciculate with both ON and OFF starburst processes in the IPL; they exhibit asymmetric ON and OFF dendritic arbors displaced from the soma toward the ventral retina; and they are CART-immunopositive (Kay et al., 2011; Trenholm et al., 2011). Additionally, the number of primary dendrites (4.0±0.8 vs. 3.1±0.6), total dendritic length (4965±981 vs. 5371±881 μm), and number of branch points (95±11 vs. 107±31) do not differ significantly between RDS and Hb9 cells (Welch t test for unequal variances - primary dendrites: t= -2.09, df=3.35, p=0.12; dendritic length: t= 0.79, df=3.47, p=0.48; branch points: t= 1.26, df=5.06, p=0.26; n_{RDS}=4, n_{Hb9}=42). However, differences do stand out. Global dendritic field diameter (229±6 vs. 192.8±2.7 μm) and soma diameter (17.5±2.0 vs. 12.7±1.4 μm) of RDS cells are significantly larger than those of Hb9 cells (dendritic field diameter: t= -10.57, df=6.71, p<0.001; soma diameter: t= -5.23, df=3.34, p=0.01; n_{RDS}=4, n_{Hb9}=42; all morphological statistics for Hb9 cells from Trenholm et al., 2011). Moreover, whereas several canonical ON-OFF DS subtypes are known to innervate the shell of the dLGN,

RDS cells appear to project to the NOT, a part of the accessory optic system. It remains to be systematically tested whether the RDS cell represents a novel DS cell type, or instead, the same cell type marked in the *Hb9-GFP* mouse.

Table 1. Summary (average ± s.d.) of morphological properties of RGCs and ACs in the GCL of Rbp4-Cre mouse

	R-cell (n = 13)	R-cell EM (n = 1)	RDS (n = 4)	RAC (n = 4)
Soma diameter (µm)	12.9±1.0 (n = 16)	16.1	17.5±2.0 (n = 4)	11.2±1.4 (n = 46)
ON dendritic field diameter (µm)	178±35	192	177±15	970±130
OFF dendritic field diameter (µm)	138±36	189	194±27	
Global dendritic field diameter (µm)	186±33	218	229±6	
Total dendrite length (µm)	2912±1076	3883	4965±981	6765±1595
Branch points	53±15	47	95±11	16±5
Primary dendrites	5±2	3	4±1	5±1
ON/OFF ratio of dendritic field diameter	1.3±0.2	1	0.9±0.1	
% of total branch points in inner IPL	61±8	55	42±3	
% of total dendritic length in inner IPL	62±7	58	34±6	

Soma diameters were estimated from photomicrographs of whole-mounted Rbp4-Cre;Ai14 retinas with exposures optimized for crisp definition of somatic profiles, thus avoiding overestimates from 'bloom' of intense somatic fluorescence. Global dendritic field diameter represents the diameter of a circle that has the same area as a convex polygon minimally enclosing both inner and outer arbors.

Figures and legends

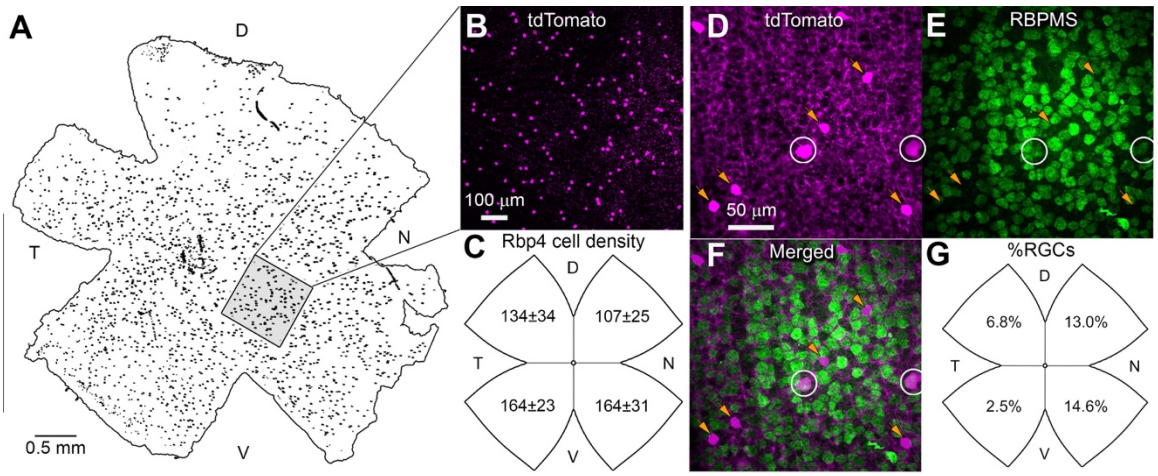

Figure 1. Density of Rbp4 ACs and RGCs varies across the retina

A. Photographic montages of a representative retinal wholemount from a Rbp4-Cre;Ai14 mouse showing tdTomato labeling in Cre-expressing cell bodies in the GCL (black dots). Fluorescence image has been inverted and binarized for clarity. D: dorsal, N: nasal, V: ventral; T: temporal. **B**. magnified view of retinal region marked by black square in (**A**). tdTomato fluorescence is pseudocolored magenta; focal plane is in the ganglion-cell layer. **C**. Density of tdTomato-positive cells in the GCL varies topographically, and is lowest in the dorsal-nasal retina. Values for each quadrant are mean densities (cells/mm^2) derived from counts in four fields, each 256 x 256 µm. **D-F**. tdTomato-labeled cells of the GCL (**D**) include RGCs (white circles) identifiable by their RBPMS-immunolabeling (**E**) and displaced amacrine cells (yellow arrows), which are RBPMS immunonegative. **G**. Topographic variation in the percentage of tdTomato-positive cells that are RGCs.

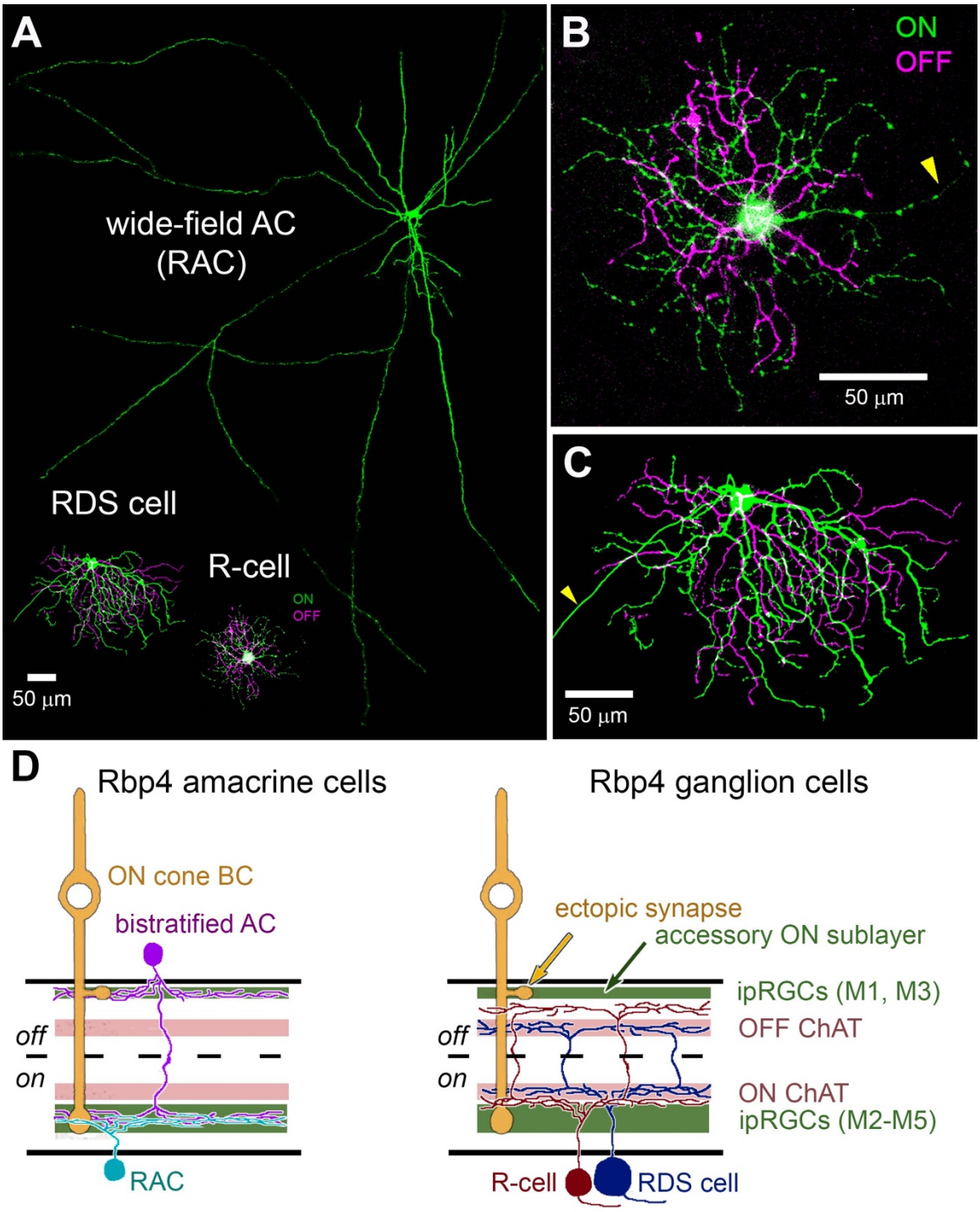

Figure 2. Morphology of Rbp4-Cre-positive cells of the inner retina.

A-C. Rbp4-Cre-positive cell types of the GCL. All images are maximum intensity projections showing the arbors as seen *en face*. To highlight the structure of the injected cell, images have been masked to hide extraneous fluorescence and pseudocolored to

distinguish between processes in the ON sublayer of the IPL (green) from those in the OFF sublayer (purple). All cells were filled by intracellular dye injection after targeted recording of a tdTomato-positive RGC or AC in the Rbp4-Cre-tdTomato mouse. **A.** wide-field Rbp4-Cre-labeled displaced AC ("RAC"), shown to scale with the two RGC types, the RDS-cell and R-cell. **B**. R-cell. **C**. RDS-cell. Arrowheads in (**B**) and (**C**) indicate axons. All scale bars, 50 μm. **D.** Schematic diagrams illustrating stratification of Rbp4-Cre-labeled ACs (left) and RGCs (right) relative to ipRGCs and starburst ACs (ON and OFF ChAT bands). Polyaxonal displaced ACs (RACs, cyan) restrict their processes to the inner ipRGC plexus (lower green band). Bistratified ACs (purple), which have conventionally placed somas in the INL, stratify within both the outer ipRGC plexus (upper green band; the 'accessory ON sublayer', locus of ectopic synapses from ON cone BCs) and in the inner ipRGC plexus. R-cells (red), the most abundant Rbp4-Cre-labeled RGC type, deploy an outer arbor between the OFF ChAT band and the outer ipRGC plexus; their inner arbor stratifies near the inner boundary of the ON ChAT band. RDS-cells (blue) deploy their dendrites strictly within the ON and OFF ChAT bands.

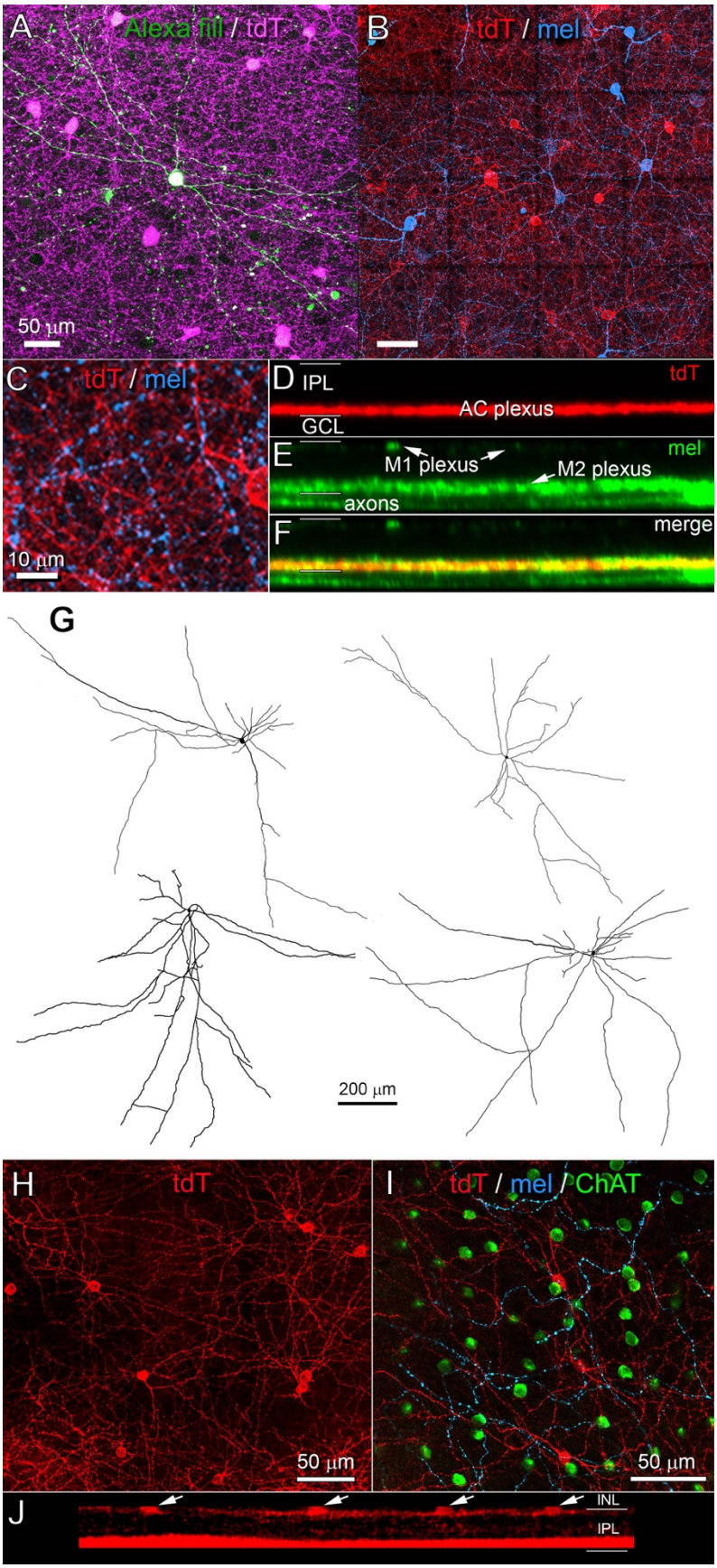
A
Alexa fill / tdT
50 µm
B
tdT / mel
C
tdT / mel
10 µm
D
IPL
tdT
AC plexus
GCL
E
mel
M1 plexus
M2 plexus
axons
F
merge
G
200 µm
H
tdT
50 µm
I
tdT / mel / ChAT
50 µm
J
INL
IPL

Figure 3. Morphology of ACs labeled in the Rbp4-Cre mouse line.

A-G. Morphology of RACs, the Rbp4-Cre-positive wide-field polyaxonal displaced amacrine cells. RAC processes form a dense plexus in the inner ON sublayer intermingled with dendrites of M2 ipRGCs. **A**. Single intracellularly dye-filled RAC (green) in relation to the dense plexus of fine, horizontally running tdTomato-positive processes in the Rbp4-Cre;Ai14 mouse (magenta). Maximum intensity projection of several optical sections through the GCL and inner ON sublayer of the IPL. **B**. Relationship of the same plexus of wide-field ACs processes (red: tdTomato reporter for Rbp4-Cre) in relation to the dendritic plexus of M2 ipRGCs (blue, anti-melanopsin). Tiled maximum intensity projection of ~10 optical sections spanning the plexus and adjacent GCL, but entirely proximal to ON ChAT. Scale bar, 50 μm. **C.** Magnified subregion from (**B**) showing numerous points of potential contact between the two cell types. Scale bar, 10 μm. **D-F**. Orthogonal projections of processes of Cre-positive ACs of the GCL (**D**), inner and outer ipRGC dendritic plexuses, marked by anti-melanopsin immunofluorescence (**E**), and a merged view (**F**) showing costratification of amacrine plexus with that of M2 melanopsin dendrites. **G**. Drawings of single dye-filled RACs. **H-J**. Cre-expressing wide-field bistratified ACs of the inner nuclear layer (INL). **H**. Somata and outer plexus of processes of these cells as shown in maximum intensity projection of a shallow z-stack of confocal optical sections spanning the INL-IPL border. **I**. Single optical section at the level of this plexus in the most distal IPL showing the processes of tdTomato-labeled AC processes (red) with the dendrites of M1 ipRGCs (cyan), labeled by anti-melanopsin immunofluorescence. Somata of OFF starburst ACs (green) are also visible at this level. **J**. Orthogonal maximal intensity projection of the z-stack from (**H**), showing the two plexuses of Rbp4-Cre-labeled

amacrine cells, an outer one (above) derived from the INL ACs (arrows) and the inner one (below) derived from both these INL amacrine cells and RACs. Scattered labeling between these plexuses comprise connecting dendrites of the INL amacrine cells. Somata in the GCL are not visible because the z-stack spanned only the IPL and proximal INL.

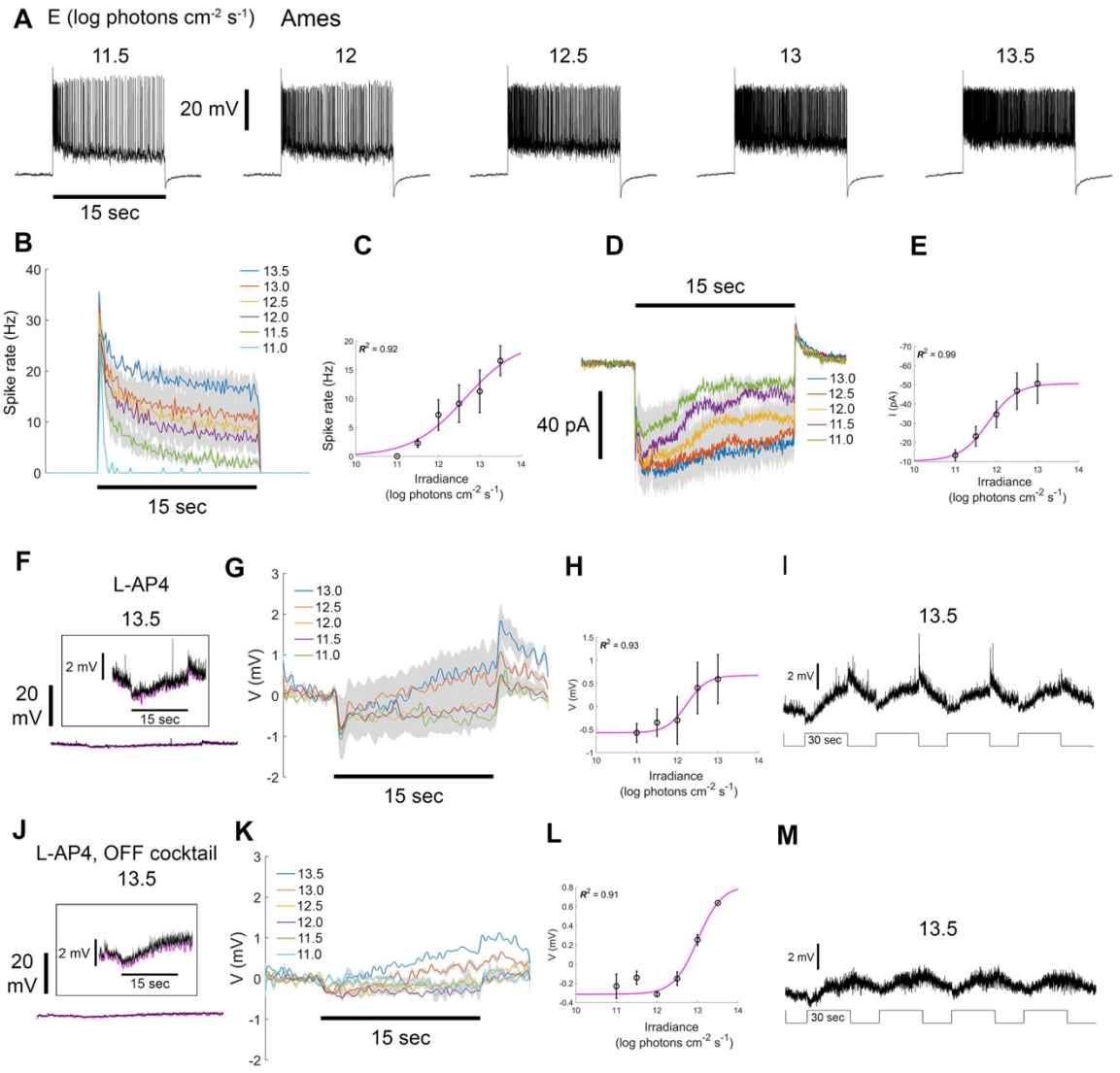

Figure 4. RACs have sustained irradiance-encoding light responses even under blockade of chemical synapses

A. Voltage responses, including spiking, of a single RAC stimulated with a series whole-field light steps of various irradiances under control conditions (Ames medium). Whole-cell current-clamp recordings. Irradiance levels in log photons cm^{-2} s^{-1} are indicated above traces. Horizontal black bar below the leftmost trace indicates the timing of the 15 sec stimulus (spot diameter 1200 μm). **B**. Average peri-stimulus time histograms (PSTHs) of spiking evoked by light steps of various irradiances (n = 3 cells; average ± s.e.m.). **C**.

Irradiance-response curve based on data presented in (**B**). Data points and error bars indicate the average ± s.e.m. of the steady state response, assessed during the last 5 seconds of the stimulus. Magenta line denotes the fitted sigmoidal Naka-Rushton function. The coefficient of determination (R^2) for the fit is indicated. **D**. Excitatory inward currents evoked by a series of stimulus irradiance steps under control conditions. Whole-cell recording with voltage clamped at the chloride reversal potential. **E**. Irradiance-response curve derived from data in (**D**). **F-I**. Effect of ON-channel blockade (bath applied L-AP4) on the voltage responses of RACs to light steps. Whole cell current-clamp recordings. **F-I.** Voltage responses of a representative RAC during ON-channel blockade. **F**. Response to the brightest light step tested (black trace; 13.5 log photons cm^{-2} s^{-1}). Lower trace is approximately to scale with those in (**A**). Inset: higher gain display showing transients at onset and offset of the stimulus, plus a slow depolarizing drift of the membrane potential during the stimulus. The lower envelope of the voltage trace is shown in magenta. **G**. Voltage responses at several irradiances (n = 3 cells; average ± s.e.m.). Lower voltage envelope is shown, rather than raw voltage, to minimize distortion by spikes. **H**. Irradiance-response relationship based on data in (**G**). **I**. Voltage responses to a series of four bright wide-field light steps each 30-sec long. Note the gradual depolarization during the stimulus and slow post-stimulus decay, which are characteristic of intrinsic melanopsin photoresponses in ipRGCs. **J-M**. Effects of combined OFF and ON channel blockade on RAC light responses obtained in whole-cell current-clamp configuration (bath applied L-AP4 plus an 'OFF cocktail' that included D-AP5, DNQX, and ACET; n = 3 cells), conventions the same as for matching plots in (**F-I)**. Light still drives a slow

depolarization, presumably due to persistence of melanopsin-dependent photoresponses in ipRGCs.

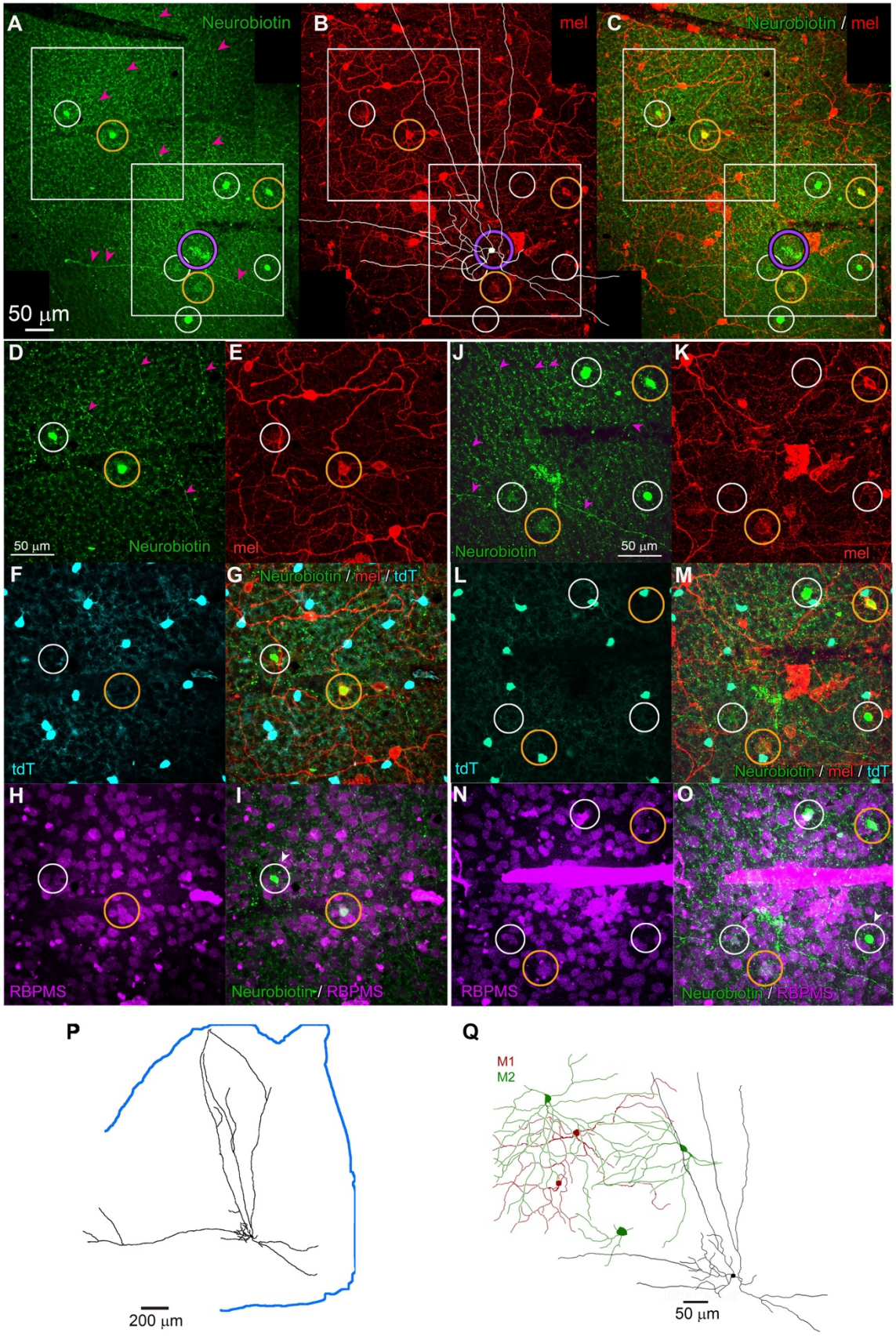
A
Neurobiotin
B
mel
C
Neurobiotin / mel
50 μm
D
E
J
K
50 μm
Neurobiotin
mel
Neurobiotin
50 μm
mel
F
G
Neurobiotin / mel / tdT
L
M
tdT
tdT
Neurobiotin / mel / tdT
H
I
N
O
RBPMS
Neurobiotin / RBPMS
RBPMS
Neurobiotin / RBPMS
P
200 μm
Q
M1
M2
50 μm

Figure 5. RACs are tracer-coupled to M2 ipRGCs and other neurons of the GCL.

A-C. Intracellular dye filling and tracer coupling of a Rbp4-Cre displaced amacrine cell (RAC) in relation to melanopsin immunoreactivity. Montage of collapsed z-stacks (maximum intensity projections) covering a portion of the RAC's arbor. **A.** Fluorescent streptavidin labeling of Neurobiotin-injected RAC (purple circle; partly obscured by artifacts) and in eight cells tracer-coupled to it (white and gold circles). Magenta arrowheads indicate the extremely slender processes of the dye-filled RAC. **B**. Anti-melanopsin immunolabeling. A tracing of the filled RAC is overlaid in white. Circles around tracer-coupled cells are color coded for the melanopsin immunoreactivity of the marked cell: gold for immunopositive cells and white for immunenegative ones. **C**. Merged view of (**A**) and (**B**). **D-I**. Identity of tracer coupled neurons in region marked by upper white square in (**A**-**C**). Conventions as in (**A**-**C**). **D**. Neurobiotin tracer. **E**. Anti-melanopsin immunofluorescence. **F**. Cre-dependent tdTomato labeling. **G**. Merge of (**D**-**F**). **H**. Immunofluorescence for the RGC marker RBPMS. **I**. Merge of Neurobiotin (**D**) and RBPMS labeling (**H**). White arrowhead indicates a tracer-coupled cell that is both RBPMS immunenegative, and thus an AC, and Cre-negative and thus not a RAC. **J-O**. Same cell as (**A-I**), but for the retinal region marked by the lower white square in (**A**-**C**). **P**. Tracing of the Neurobiotin-injected RAC, which nearly encompasses this retinal quadrant; retinal margin marked by blue line. **Q**. Drawings based on dendritic anti-melanopsin immunelabeling of three partially reconstructed M2 ipRGCs (green) that were tracer coupled to the Neurobiotin-filled RAC (black profile). Also traced are two M1 ipRGCs (red) in the same field that were not tracer-coupled to the injected RAC.

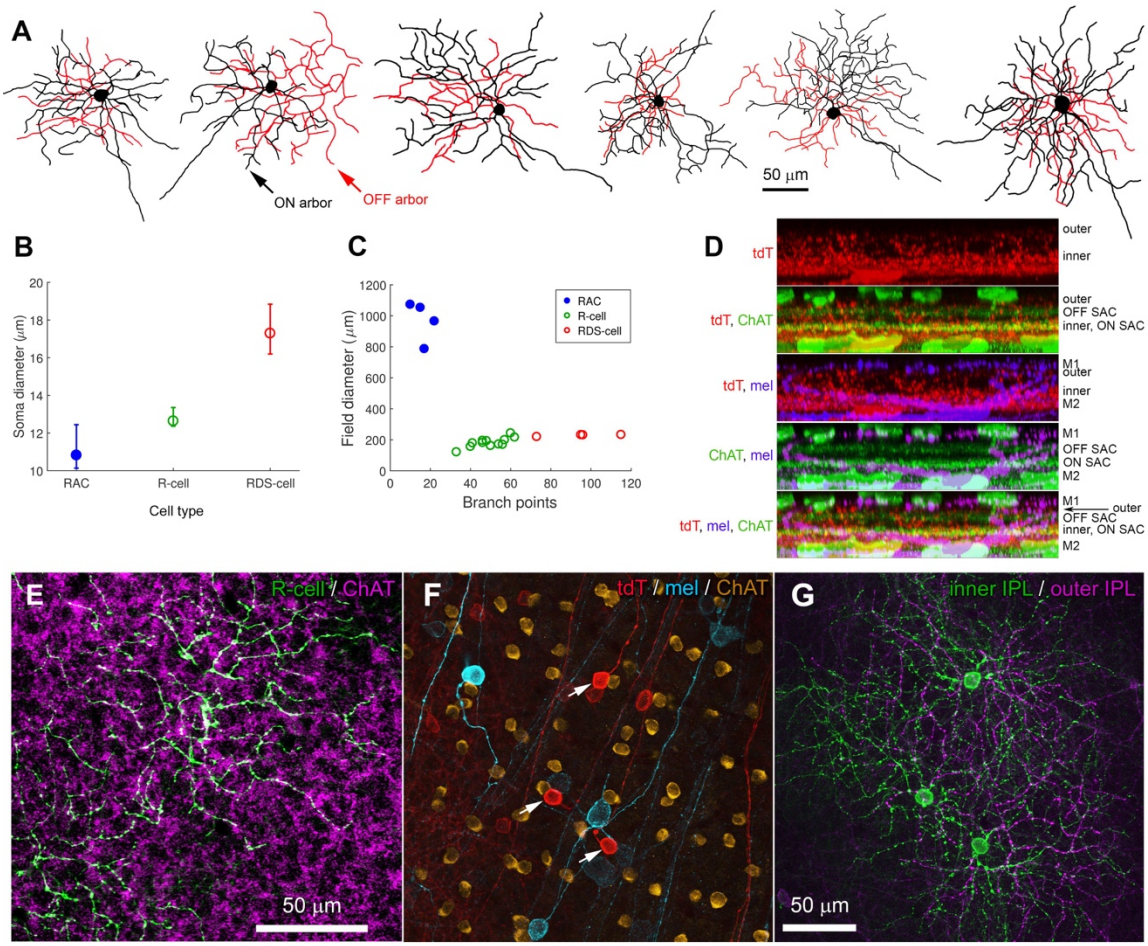

Figure 6. Morphology of the R-cell — a bistratified RGC labeled in the Rbp4-Cre line

A. Examples of the common tdTomato-positive RGCs — R-cell — in the Rbp4-Cre mouse. **B**. Variation in soma diameter across cell types in the GCL. Soma diameter differed significantly across the three cell types of the GCL (one-way ANOVA, $F_{2,65}$=90.9, $p < 0.001$; post-hoc pair-wise comparisons revealed that each cell type differed from the other two [$P < 0.001$]). **C**. Dendritic field diameter as a function of number of branch points for RACs, R-cells and RDS-cells. **D.** Stratification of R-cell processes. Side-view maximum intensity projections of processes in Rbp4-cre cells (red) in relation to processes of M1 and M2 ipRGCs (cyan; anti-melanopsin) and to starburst AC (SAC) processes (green; anti-ChAT). The fine Rbp4-cre-positive processes at the level of the inner melanopsin plexus

(M2 ipRGC dendrites) are derived from wide-field displaced RACs; the coarse processes are derived mainly from R-cells, and stratify near and within the ON ChAT band and between OFF ChAT and the outer melanopsin plexus (M1 ipRGC dendrites). **E**. Dendrites of the ON arbor of two virally labeled R-cells (green; flex AAV2-mCherry) tend to cofasciculate with the processes of ON starburst ACs (purple, anti-ChAT) which lie at or very near the same level as the R-cell ON processes. **F**. Three closely spaced R-cells (red; white arrows) with visible axons, labeled in the Rbp4-Cre-tdTomato mouse. The other red cells are Rbp4-Cre-labeled displaced ACs (RACs). Shown for comparison are the somas and axons of ipRGCs (cyan, anti-melanopsin) and the somas of ON starburst ACs (gold, anti-ChAT). **G**. The three closely spaced R-cells show a hint of mosaics formed by the dendritic arbors in both the ON (green) and OFF IPL sublayers (purple). Maximum intensity projection of several optical sections centered on the relevant arbor.

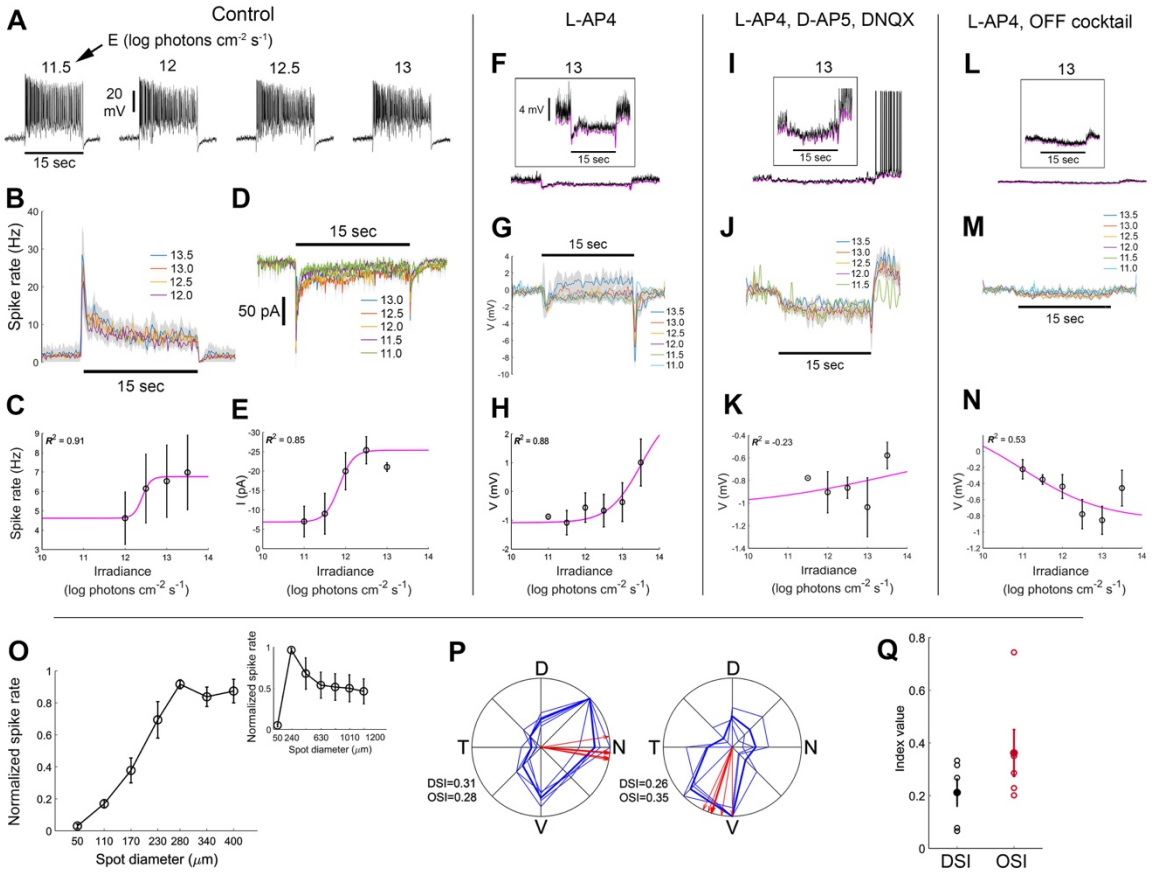

Figure 7. Rbp4 R-cells show sustained irradiance-encoding light-evoked responses

A. Light-evoked firing, obtained in whole-cell current-clamp configuration, to a series of stimulus intensities (irradiance) under control conditions (retina bathed in Ames medium only). Irradiances in log photons cm^{-2} s^{-1} are indicated above traces. Horizontal black bar below the leftmost trace indicates the duration of a 15 sec wide-field light step from darkness. **B**. Peri-stimulus time histograms (PSTHs) averaged across cells (n = 4 cells; average ± s.e.m.) for various irradiance levels. **C**. Irradiance-response (IR) curve based on data presented in (**B**). Data points and error bars indicate the steady state response (average ± s.e.m.). The coefficient of determination (R^2) of the fit is indicated. **D**. Light-evoked currents, obtained in whole-cell voltage-clamp configuration, to a series of stimulus irradiance levels under control conditions. The membrane voltage was clamped at the

chloride reversal potential. **E**. IR curve based on data presented in (**D**). **F-N**. Pharmacological analysis of circuitry underlying R-cell light responses. **F-H**. RGC responses, obtained in whole-cell current-clamp configuration, while blocking the ON pathway using L-AP4. **F**. Example of a cell's light-evoked voltage response (black trace) to the brightest stimulus tested (13 log photons cm^{-2} s^{-1}). The lower envelope of the voltage trace is shown in magenta. Inset, same trace at higher gain showing a sustained hyperpolarization in the voltage response as well as the lower voltage envelope throughout the stimulus duration. **G**. voltage envelope (n = 3 cells; average ± s.e.m.) for various irradiance levels. **H**. IR curve based on data presented in (**G**). **I-K**. RGC responses (n = 5 cells), obtained in whole-cell current-clamp configuration, while blocking both the ON and OFF pathways using L-AP4, D-AP5, and DNQX. Conventions in individual plots are the same as in (**F-H**). **L-N**. R-cell responses (n = 4 cells), obtained in whole-cell current-clamp configuration, after more complete synaptic blockade by further addition of the OFF channel blocker ACET to the L-AP4, D-AP5, and DNQX already in the bath. Conventions in individual plots are the same as in (**F-H**). **O**. Firing rate in response to a series of bright spots on a dark background at varying sizes (main plot, 50-400 μm; inset, 50-1200 μm; n = 3 cells). **P**. Example of direction and orientation selectivity tuning of two R-cells. Thick blue lines show the average cells' response to sinusoidal gratings drifting in each of eight different directions, 45° apart. Thin blue lines show data from each of four single trials. N, nasal; D, dorsal; T, temporal; V, ventral. Red lines indicate the preferred direction based on four individual repetitions (thin lines), and their average (thick line). The direction selectivity index (DSI), orientation selectivity index (OSI), and preferred direction (PD) of the cell are indicated. **Q**. Average ± s.e.m DSI and OSI across tested cells (n = 5 cells).

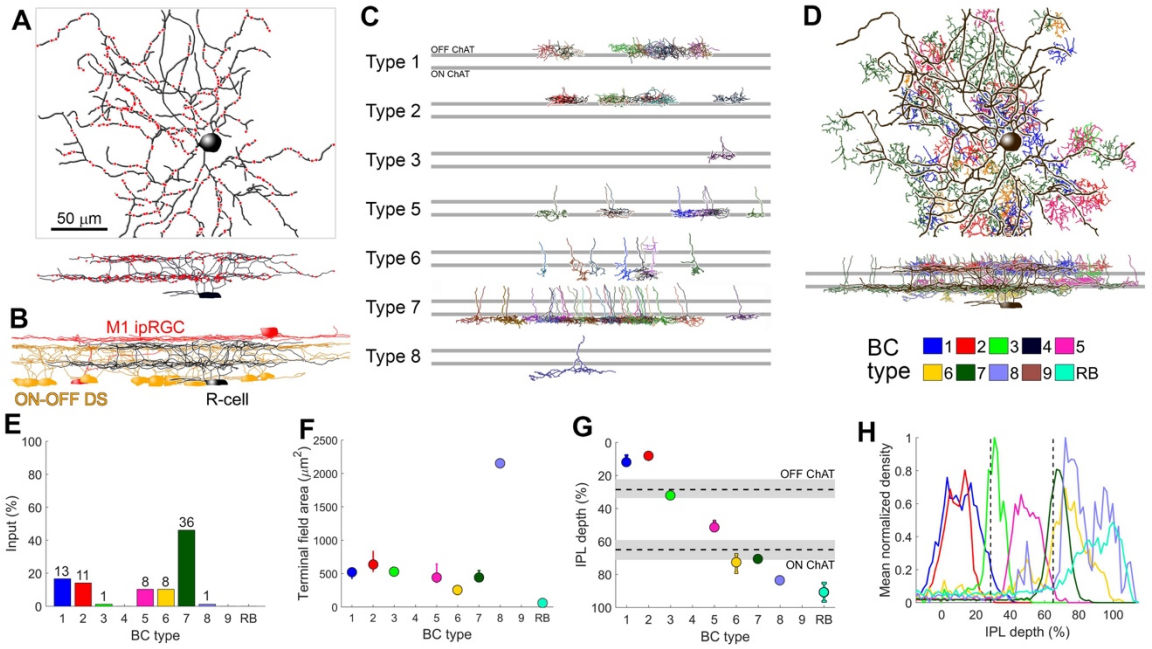

Figure 8. Serial electron microscopy reconstruction of an Rbp4 RGC and its synaptic inputs

A. EM reconstruction of a presumptive Rbp4 R-cell (black) along with dyad synapses made onto it (red dots), as viewed *en face* (top) and in an orthogonal plane (bottom). Scale bar, 50 µm applies to panels (**A**-**D**). **B.** Orthogonal view of the presumptive R-cell (black) along with traces of several ON-OFF DS RGCs (yellow) and two M1 ipRGCs (red). The outer dendritic arbor of the presumptive R-cell stratifies below the M1 ipRGC plexus and just above the OFF ChAT band; its inner arbor stratifies just below the ON ChAT band. **C.** Orthogonal view of BCs making identified ribbon synaptic contacts onto the presumptive R-cell. Top and bottom gray horizontal bars represent the OFF and ON ChAT bands, respectively. **D.** EM reconstruction of a presumptive R-cell (black) along with BCs that synapse onto it, as viewed *en face* (top) and in an orthogonal plane (bottom). Bipolar cell colors follow the scheme indicated in the key below. Note that the presumptive R-cell did

not receive input from rod BCs (RB) or cone BCs of Types 4 and 9. **E.** Percentage of all bipolar input to the presumptive R-cell as a function of BC type. OFF input derived mainly through Types 1 and 2, and ON input derived mainly through Type 7. **F.** Axon terminal field area (median and first and third quartiles) as a function of BC type. **G.** IPL depth (median and first and third quartiles) as a function of BC type. **H.** Mean normalized density of axonal processes as a function depth for each BC type. Though RB cells lacked synaptic contacts onto the presumptive R-cell, they were included in the analysis as a useful benchmark in the assessment of depth of axon-arbor stratification for BC types (see Methods).

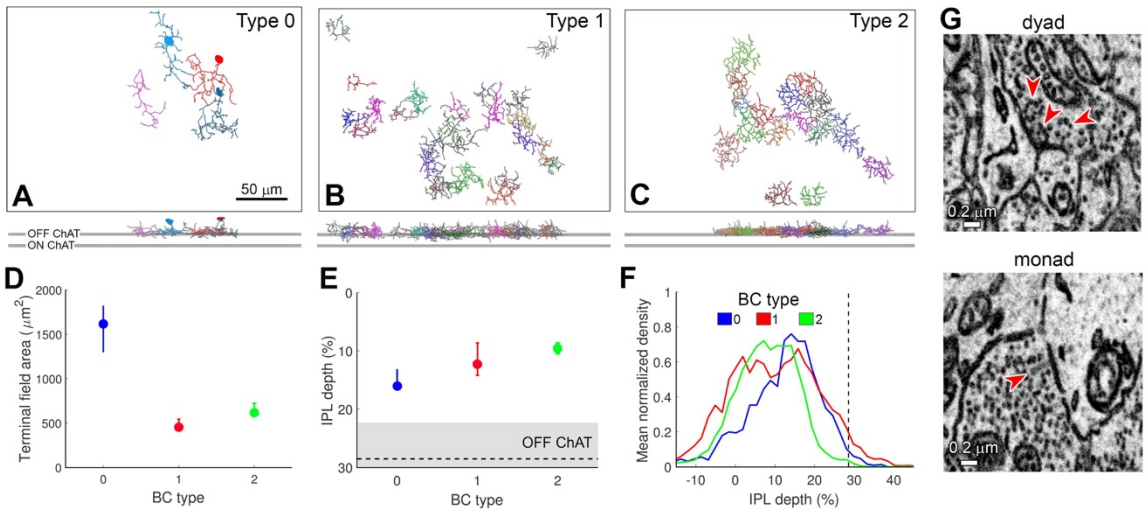

Figure 9. A novel OFF bipolar cell, Type 0

A-C. Partial mosaics of cone bipolar cell Types 0, 1 and 2, as viewed *en face* (top) and in an orthogonal plane (bottom). Top and bottom gray horizontal bars represent the OFF and ON ChAT bands, respectively. Scale bar, 50 µm. The soma of one type 0 was not included in the SBEM volume, perhaps due to slight variation in the orientation of the retina within the SBEM volume. **D.** Terminal field area (median and first and third quartiles) of Type 0 bipolar cells was larger than those of Types 1 and 2. **E.** IPL depth (median and first and third quartiles) of Type 0 cells was larger than those of Types 1 and 2. Gray horizontal bar represents the OFF ChAT band. **F.** Mean normalized density of axonal processes of Type 0 bipolar cells was slightly more peaked and narrow than Types 1 and 2. Vertical dashed line represents the OFF ChAT band. **G.** Type 0 BCs made both dyad and monad synapses; arrowheads mark ribbons. All contacts onto the presumptive R-cell were dyads; the postsynaptic partners of monads are unknown.

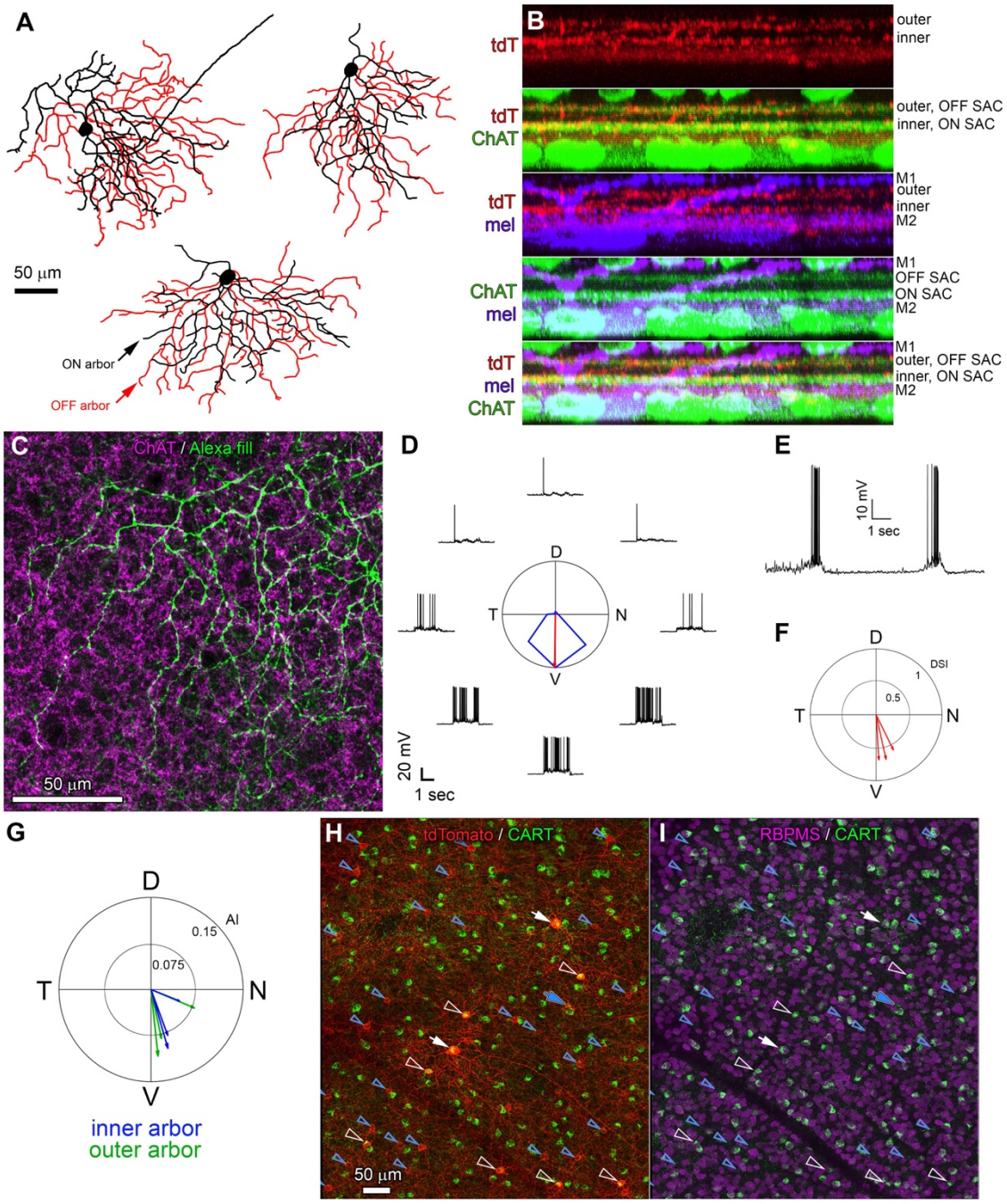

Figure 10. Morphology of DS RGCs in the Rbp4-Cre mouse

A. Drawings of three direction-selective RGCs labeled in the Rbp4-Cre mouse ('RDS cells'). **B.** Dendritic stratification of an RDS cell. Five views of the same rotated orthographic maximum intensity projection derived from z-stacks taken in the vicinity of a single labeled RDS cell are shown. Views (top to bottom) show the individual tdTomato

in the Rbp4:Cre;Ai14 mouse (tdT), tdTomato and anti-ChAT labeling (tdT/ChAT), tdTomato and anti-melanopsin labeling (tdT/mel), anti-ChAT and anti-melanopsin labeling (mel/ChAT), and tdT/mel/ChAT labeling. RDS dendrites with Rbp4-Cre-dependent viral labeling (red) match the depth of the ON and OFF ChAT bands (ON and OFF starburst AC [SAC] arbors, blue). Both Rbp4 (red) and ChAT (green) labeling appear below the outer M1 ipRGC plexus and above the inner M2 ipRGC plexus (purple). **C**. Dendrites of the inner arbor of a virally labeled RDS cell (green) cofasciculate with the processes of ON starburst amacrine cells (anti-ChAT) which lie at or very near the same levels as the RDS-cell inner processes. Scale bar, 50 μm. **D**. Voltage responses of a representative RDS cell to sinusoidal contrast gratings drifting in eight directions at 45° intervals. Polar plot shows response amplitude as a function of stimulus direction (normalized to maximum response). Red vector shows preferred direction in retinal coordinates (N, nasal; D, dorsal; T, temporal; V, ventral). **E**. Voltage traces for the same representative RDS cell, illustrating the ON and OFF responses to the leading and trailing edges of a drifting bright bar. **F**. A polar plot summarizing the direction preference (vector angle) and direction selectivity index (DSI, vector length). RDS cells preferred ventral motion on the retina. **G**. A polar plot summarizing the direction of dendritic arbor asymmetry (vector angle) and asymmetry index (AI, vector length), for the inner (blue) and outer (green) arbors. **H,I**. Both types of Rbp4-cre RGCs (R-cells and RDS cells) are CART immunoreactive. Triple labeling in the GCL for Rbp4-Cre-tdTomato (red), CART (green; an immunomarker for ON-OFF DS RGCs), and RBPMS (magenta; an immunomarker for RGCs). Cre-positive ganglion cells are indicated by white markers. Most are R-cells (hollow white arrowheads), but two are RDS cells (filled white arrows).

All of these are also immunopositive for RBPMS and CART (**I**). Cre-positive displaced amacrine cells (RACs), indicated by blue markers, are identifiable from their RBPMS immunonegativity (**I**). Virtually all of these lack CART immunolabeling (hollow blue arrowheads), but one RAC appeared to be CART-immunopositive (solid blue arrow). Scale bar, 50 μm.

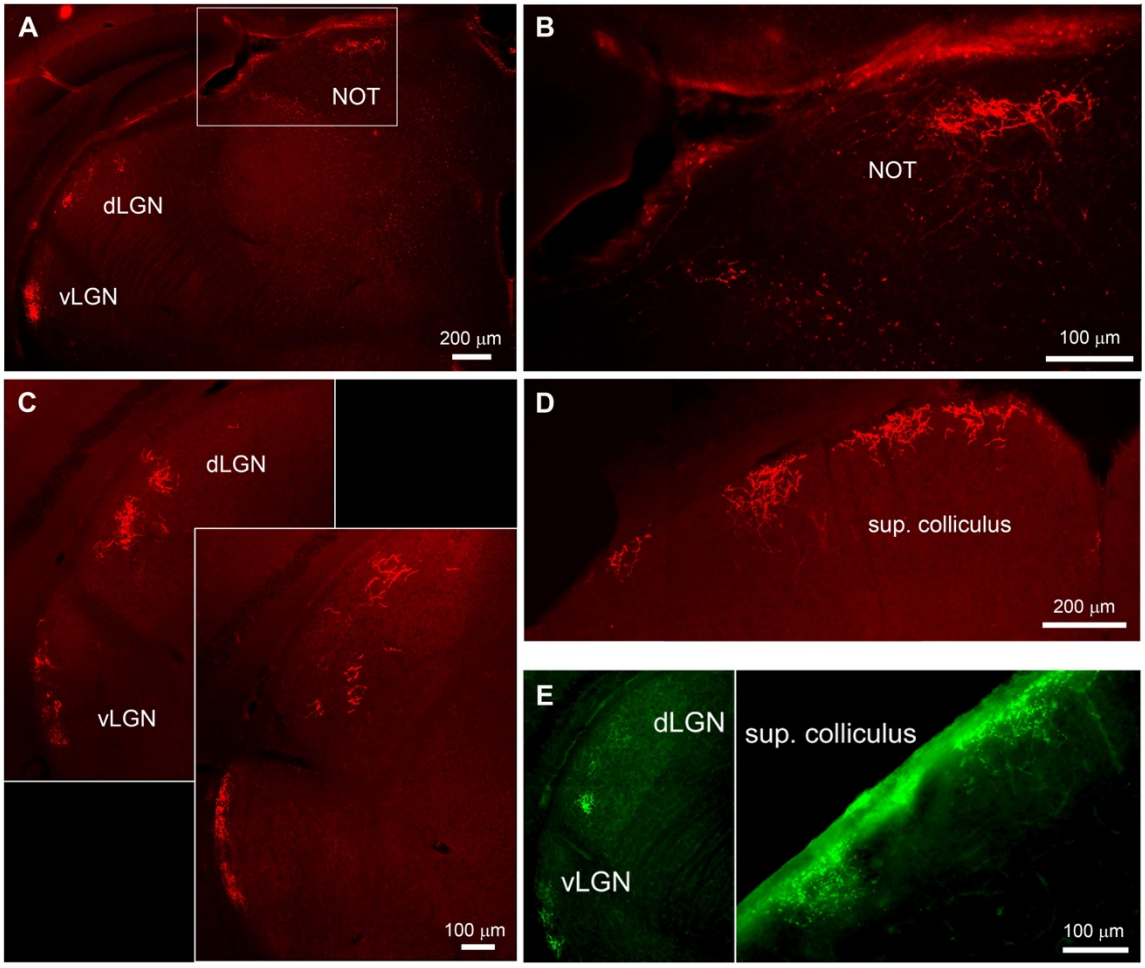

Figure 11. Brain projections of Rbp4 RGCs, and R-cells alone

A-**D**. Axon terminal labeling following injection of a Cre-dependent viral reporter. **A**. Labeling was evident in the lateral geniculate nucleus (LGN) (**A**,**C**) and nucleus of the optic tract (NOT) (**A**,**B**). **C**. Two coronal sections, consecutive along the rostral-caudal axis. Labeling was evident in the dorsal and ventral divisions of the LGN (dLGN, vLGN), but not in the intergeniculate leaflet (IGL). Labeling was restricted to a narrow band along the lateral margin of the vLGN. **D**. Intense labeling was evident also in the superficial layers of the superior colliculus (SC). **E**. Axon terminal labeling following sparse labeling of Cre-expressing neurons. Only three RGCs were detectably labeled in this retina, and all were bistratified R-cells. Axon terminal labeling was detected only in the dLGN (at the

boundary between core and shell regions), in the vLGN (left), and in the most superficial layers of the SC (right).

References

Arroyo DA, Kirkby LA, Feller MB (2016) Retinal waves modulate an intraretinal circuit of intrinsically photosensitive retinal ganglion cells. J Neurosci 36:6892-6905.

Badea TC, Nathans J (2004) Quantitative analysis of neuronal morphologies in the mouse retina visualized by using a genetically directed reporter. J Comp Neurol 480:331-351.

Berson DM, Dunn FA, Takao M (2002) Phototransduction by retinal ganglion cells that set the circadian clock. Science 295:1070-1073.

Berson DM, Castrucci AM, Provencio I (2010) Morphology and mosaics of melanopsin-expressing retinal ganglion cell types in mice. J Comp Neurol 518:2405-2422.

Borghuis BG, Marvin JS, Looger LL, Demb JB (2013) Two-photon imaging of nonlinear glutamate release dynamics at bipolar cell synapses in the mouse retina. J Neurosci 33:10972-10985.

Chang L, Breuninger T, Euler T (2013) Chromatic coding from cone-type unselective circuits in the mouse retina. Neuron 77:559-571.

Dai X, Zhang H, He Y, Qi Y, Chang B, Pang J-j (2015) The frequency-response electroretinogram distinguishes cone and abnormal rod function in rd12 mice. PLoS ONE 10:e0117570.

Della Santina L, Kuo SP, Yoshimatsu T, Okawa H, Suzuki SC, Hoon M, Tsuboyama K, Rieke F, Wong RO (2016) Glutamatergic monopolar interneurons provide a novel pathway of excitation in the mouse retina. Curr Biol 26:2070-2077.

Dhande OS, Estevez ME, Quattrochi LE, El-Danaf RN, Nguyen PL, Berson DM, Huberman AD (2013) Genetic dissection of retinal inputs to brainstem nuclei controlling image stabilization. J Neurosci 33:17797-17813.

Ding H, Smith RG, Poleg-Polsky A, Diamond JS, Briggman KL (2016) Species-specific wiring for direction selectivity in the mammalian retina. Nature 535:105-110.

Dumitrescu ON, Pucci FG, Wong KY, Berson DM (2009) Ectopic retinal ON bipolar cell synapses in the OFF inner plexiform layer: contacts with dopaminergic amacrine cells and melanopsin ganglion cells. J Comp Neurol 517:226-244.

Ecker JL, Dumitrescu ON, Wong KY, Alam NM, Chen S-K, LeGates T, Renna JM, Prusky GT, Berson DM, Hattar S (2010) Melanopsin-Expressing Retinal Ganglion-Cell Photoreceptors: Cellular Diversity and Role in Pattern Vision. Neuron 67:49-60.

Estevez ME, Fogerson PM, Ilardi MC, Borghuis BG, Chan E, Weng S, Auferkorte ON, Demb JB, Berson DM (2012) Form and function of the M4 cell, an intrinsically photosensitive retinal ganglion cell type contributing to geniculocortical vision. The Journal of neuroscience 32:13608-13620.

Govardovskii VI, Fyhrquist N, Reuter T, Kuzmin DG, Donner K (2000) In search of the visual pigment template. Vis Neurosci 17:509-528.

Helmstaedter M, Briggman KL, Turaga SC, Jain V, Seung HS, Denk W (2013) Connectomic reconstruction of the inner plexiform layer in the mouse retina. Nature 500:168-174.

Hoshi H, Liu WL, Massey SC, Mills SL (2009) ON inputs to the OFF layer: bipolar cells that break the stratification rules of the retina. J Neurosci 29:8875-8883.

Huberman AD, Wei W, Elstrott J, Stafford BK, Feller MB, Barres BA (2009) Genetic identification of an On-Off direction-selective retinal ganglion cell subtype reveals a layer-specific subcortical map of posterior motion. Neuron 62:327-334.

Ivanova E, Lee P, Pan ZH (2013a) Characterization of multiple bistratified retinal ganglion cells in a purkinje cell protein 2-Cre transgenic mouse line. J Comp Neurol 521:2165-2180.

Ivanova E, Toychiev AH, Yee CW, Sagdullaev BT (2013b) Optimized protocol for retinal wholemount preparation for imaging and immunohistochemistry. J Vis Exp:e51018.

Kay JN, De la Huerta I, Kim I-J, Zhang Y, Yamagata M, Chu MW, Meister M, Sanes JR (2011) Retinal ganglion cells with distinct directional preferences differ in molecular identity, structure, and central projections. J Neurosci 31:7753-7762.

Kim IJ, Zhang YF, Yamagata M, Meister M, Sanes JR (2008) Molecular identification of a retinal cell type that responds to upward motion. Nature 452:478-482.

Kim JS, Greene MJ, Zlateski A, Lee K, Richardson M, Turaga SC, Purcaro M, Balkam M, Robinson A, Behabadi BF, Campos M, Denk W, Seung HS, EyeWirers (2014) Space-time wiring specificity supports direction selectivity in the retina. Nature 509:331-336.

Kirkby LA, Feller MB (2013) Intrinsically photosensitive ganglion cells contribute to plasticity in retinal wave circuits. Proc Natl Acad Sci U S A 110:12090-12095.

Lin B, Masland RH (2006) Populations of wide-field amacrine cells in the mouse retina. J Comp Neurol 499:797-809.

Mikula S, Denk W (2015) High-resolution whole-brain staining for electron microscopic circuit reconstruction. Nat Methods 12:541-546.

Muller LPD, Do MTH, Yau KW, He SG, Baldridge WH (2010) Tracer coupling of intrinsically photosensitive retinal ganglion cells to amacrine cells in the mouse retina. J Comp Neurol 518:4813-4824.

Naka KI, Rushton WA (1966) S-potentials from luminosity units in the retina of fish (Cyprinidae). J Physiol 185:587-599.

Nath A, Schwartz GW (2016) Cardinal orientation selectivity is represented by two distinct ganglion cell types in mouse retina. J Neurosci 36:3208-3221.

Perez De Sevilla Muller L, Shelley J, Weiler R (2007) Displaced amacrine cells of the mouse retina. J Comp Neurol 505:177-189.

Prigge CL, Yeh PT, Liou NF, Lee CC, You SF, Liu LL, McNeill DS, Chew KS, Hattar S, Chen SK, Zhang DQ (2016) M1 ipRGCs influence visual function through retrograde signaling in the retina. J Neurosci 36:7184-7197.

Rao S, Chun C, Fan J, Kofron JM, Yang MB, Hegde RS, Ferrara N, Copenhagen DR, Lang RA (2013) A direct and melanopsin-dependent fetal light response regulates mouse eye development. Nature 494:243-246.

Reifler AN, Chervenak AP, Dolikian ME, Benenati BA, Li BY, Wachter RD, Lynch AM, Demertzis ZD, Meyers BS, Abufarha FS, Jaeckel ER, Flannery MP, Wong KY (2015) All spiking, sustained ON displaced amacrine cells receive gap-junction input from melanopsin ganglion cells. Current Biology 25:2878-2878.

Renna JM, Weng SJ, Berson DM (2011) Light acts through melanopsin to alter retinal waves and segregation of retinogeniculate afferents. Nature Neuroscience 14:827-829.

Rivlin-Etzion M, Zhou K, Wei W, Elstrott J, Nguyen PL, Barres BA, Huberman AD, Feller MB (2011) Transgenic mice reveal unexpected diversity of On-Off direction-selective retinal ganglion cell subtypes and brain structures involved in motion processing. J Neurosci 31:8760-8769.

Rodriguez AR, Muller LPD, Brecha NC (2014) The RNA binding protein RBPMS is a selective marker of ganglion cells in the mammalian retina. J Comp Neurol 522:1411-1443.

Sand A, Schmidt TM, Kofuji P (2012) Diverse types of ganglion cell photoreceptors in the mammalian retina. Prog Retin Eye Res 31:287-302.

Schmidt TM, Kofuji P (2010) Differential cone pathway influence on intrinsically photosensitive retinal ganglion cell subtypes. J Neurosci 30:16262-16271.

Schmidt TM, Kofuji P (2011) Structure and function of bistratified intrinsically photosensitive retinal ganglion cells in the mouse. J Comp Neurol 519:1492-1504.

Semo M, Gias C, Ahmado A, Vugler A (2014) A role for the ciliary marginal zone in the melanopsin-dependent intrinsic pupillary light reflex. Exp Eye Res 119:8-18.

Shekhar K, Lapan SW, Whitney IE, Tran NM, Macosko EZ, Kowalczyk M, Adiconis X, Levin JZ, Nemesh J, Goldman M, McCarroll SA, Cepko CL, Regev A, Sanes JR (2016) Comprehensive classification of retinal bipolar neurons by single-cell transcriptomics. Cell 166:1308-1323 e1330.

Sumbul U, Song S, McCulloch K, Becker M, Lin B, Sanes JR, Masland RH, Seung HS (2014) A genetic and computational approach to structurally classify neuronal types. Nat Commun 5:3512.

Szel A, Rohlich P, Caffe AR, Juliusson B, Aguirre G, Vanveen T (1992) Unique topographic separation of 2 spectral classes of cones in the mouse retina. J Comp Neurol 325:327-342.

Thorne RG, Nicholson C (2006) In vivo diffusion analysis with quantum dots and dextrans predicts the width of brain extracellular space. Proc Natl Acad Sci U S A 103:5567-5572.

Trenholm S, Johnson K, Li X, Smith RG, Awatramani GB (2011) Parallel mechanisms encode direction in the retina. Neuron 71:683-694.

Van Hook MJ, Berson DM (2010) Hyperpolarization-activated current (I(h)) in ganglion-cell photoreceptors. PLoS ONE 5:e15344.

Volgyi B, Chheda S, Bloomfield SA (2009) Tracer coupling patterns of the ganglion cell subtypes in the mouse retina. J Comp Neurol 512:664-687.

Wassle H, Puller C, Muller F, Haverkamp S (2009) Cone contacts, mosaics, and territories of bipolar cells in the mouse retina. J Neurosci 29:106-117.

Wong KY (2012) A retinal ganglion cell that can signal irradiance continuously for 10 hours. J Neurosci 32:11478-11485.

Zhang DQ, Zhou TR, McMahon DG (2007) Functional heterogeneity of retinal dopaminergic neurons underlying their multiple roles in vision. J Neurosci 27:692-699.

Zhang DQ, Stone JF, Zhou T, Ohta H, McMahon DG (2004) Characterization of genetically labeled catecholamine neurons in the mouse retina. Neuroreport 15:1761-1765.

Zhang DQ, Wong KY, Sollars PJ, Berson DM, Pickard GE, McMahon DG (2008) Intraretinal signaling by ganglion cell photoreceptors to dopaminergic amacrine neurons. Proc Natl Acad Sci U S A 105:14181-14186.

Zhao X, Chen H, Liu X, Cang J (2013) Orientation-selective responses in the mouse lateral geniculate nucleus. J Neurosci 33:12751-12763.

CHAPTER 5

Closing thoughts

Organisms are organized and integrated into multiple levels of increasing complexity. Atoms are components of molecules, which are organized into macromolecules such as proteins and DNA, which in turn form cells. Cells are parts of tissues, which form organs, which are components of organisms. For example, the eye at the highest level can be considered an optical device transducing light into a pattern of neural activity that is sent along the optic nerve to the central brain. The lower-level components include the transparent cornea that refracts incoming light before it passing through the pupil; the lens then tunes the focus of the light; and the light will finally be absorbed and transduced into neural signals by a thin sheet of specialized neural tissue forming the retina in the back of the eye. The retina is made of cells such as the photoreceptors, which change their membrane voltage in response to light stimulus intensity and wavelength, and the retinal ganglion cells that transmit multiple channels of visual information from the retina to the brain. At the molecular level, the rod photoreceptors, for example, contains the photopigment Rhodopsin that captures photons of light and mediates the phototransduction signaling cascade that leads to hyperpolarization of the cell.

Studying complex biological systems are generally considered according to top-down or bottom-up relationships across the levels. Darwin adopted a top-down approach for his studies of different species and the underlying complexities of evolutionary change. Classification studies have generally used a top-down approach to decompose complex spatial, temporal, and causal relationships into lower-level component parts. In contrast,

Mendel used a bottom-up approach to discover heritable "genes" that specifies the phenotypic characteristics of organisms. The discovery of the double-helix DNA as the physical basis of genetic material paved the way for understanding the 'transcription' of DNA into messenger RNAs that are then 'translated' into proteins (WATSON and CRICK, 1953). A genetic mutation is able to propagate across all higher levels of organization. The function of genes has been investigated by disrupting the coding region of genes and analyzing for consequential phenotypes (Strange, 2005, for review). Although these molecular approaches provided many insights into fundamental biological problems, the genotype-phenotype relationship was confounded by redundancy or a lack of discernible phenotypes (Brenner, 1994). Further, a gene by itself is not capable of causing an observable phenotypic trait and requires the context of many other genes in the cellular environment. Biological systems have emergent behavior in which the whole is more than the sum of the parts. In other words, the properties at one level of complexity are due to the interactions and relationships among their component parts. The innovation of genome-scale sequencing has generated the relatively new systems biology approach (Ideker et al., 2001; Kitano, 2002; Pennisi, 2003). Systems biology studies networks of interacting biological components using computational and mathematical models instead of focusing on identifying and characterizing individual molecular components. However, relying solely on inferred models of function of complex biological systems from systems biology has been insufficient due, in part, to the hazards of the inverse problem (Brenner, 2010). The inverse problem has at least two challenges described by (Tarantola, 2006). First, it can be a challenge to find even a single model that fits across the complex datasets that can sometimes span hundreds of dimensions, likened to finding a needle in a haystack. In

addition, multiple models may fit the same set of observations equally well. The hypothesis-neutral systems biology approach has similar overarching goals to study complex biological systems as integrated wholes as the classic hypothesis-driven physiology approach (Strange, 2005; Joyner, 2011; Noble, 2011). Increased synergy between molecular biology reductionism with systems biology and physiology approaches will be necessary to fully comprehend organisms from top to bottom and bottom to top, perhaps eventually necessitating a merger into 'Physiology 2.0' (Kuster et al., 2011).

The mammalian nervous system is the most complex biological system on the planet and has proven especially challenging to reach a complete integration across all levels from molecules to cells to circuits to animal behavior (Geschwind and Konopka, 2009; Koch, 2012; Samborska et al., 2016). Our study of mammalian retina cell types benefited from modern genomics capabilities for hypothesis-generation that we then complemented with the more hypothesis-driven approaches of molecular, cellular, and systems-level neuroscience. Our study joins a growing body of research that has revealed molecularly diversity within cell types across the nervous system (Mihaljević et al., 2014; Sanes and Masland, 2015; Sternson et al., 2016; Hamilton et al., 2017). Reaching a complete parts list at the cellular level has remained out of reach for the mammalian nervous system (Zhang et al., 2011; Masland, 2012; Sanes and Masland, 2015). Further, the sparse knowledge scattered across the biological levels of the nervous system has provided an impassible barrier to full integration.

Perhaps we can look to invertebrate model systems to gauge what will be required to reach an integrative understanding of mammalian systems. This would be similar to how sequencing of the *Caenorhabditis elegans* genome provided a framework for the

experimental pipeline required for the efficient completion of the Human Genome Project (C. elegans Sequencing Consortium, 1998; Sulston and Ferry, 2002; Hillier et al., 2005). The *C. elegans* nervous system contains less than 400 neurons and was recognized early on for its potential as a model system for studying neurobiological questions (Brenner, 1974; Corsi et al., 2015). Studying the relatively simple nervous system of the *C. elegans* nervous systems has generated a relatively complete representation of the cells and connections that make up the nervous system in an intact, whole organism. Currently, the classification of neurons in *C. elegans* is nearing completion, with all component neurons being catalogued based on their precise position, morphology, and wiring diagram (Hobert, 2016; Hobert et al., 2016). The accumulation of nearly 1000 reporter genes has distinguished molecular markers and combination of transcription factors that are expressed for nearly all (more than 90%) of the anatomically distinguished neuron types (Hobert, 2016; Hobert et al., 2016). However, neuron types are rarely distinguished by the expression of a single terminal selector, even in the relatively simple *C. elegans* nervous system (Hobert, 2016; Hobert et al., 2016). Regardless of its simplicity, *C. elegans* are capable of a surprisingly diverse set of behaviors that include response to environmental stimuli, locomotion, male and female reproductive behaviors, and social feeding (Trent et al., 1983; Bargmann, 1993; Bargmann et al., 1993; Riddle et al., 1997; de Bono and Bargmann, 1998). The 'brain-body-environment models' of the intact *C. elegans* have begun to relate the detailed understanding of neuron components to the whole animal as well as to its external environment (Izquierdo and Beer, 2016). Physiological analysis of whole-brain dynamics in a freely behaving *C. elegans* has recently been made possible using calcium indicators (Prevedel et al., 2014; Kato et al., 2015; Nguyen et al., 2016;

Venkatachalam et al., 2016). Despite the great progress that has been made integrating cell type models to *C. elegans* behavior, the full modeling of complex behaviors from molecules to cells to complex behaviors without gaps has remained out of reach even for *C. elegans*. Once completed, translating the framework of a model of invertebrate nervous systems to mammalian nervous systems is still anticipated to be an immense challenge. The mammalian nervous system has undergone a dramatic evolutionary diversification and increase in the number of neuron types(Katz et al., 2013). Further, a more elaborate and interconnected network of transcription factors is responsible for maintaining adult neuron identity in mammalian nervous system and a complex combination of transcription factors is expected to be responsible for co-regulating different specific subsets of target genes (Holmberg and Perlmann, 2012; Wagner, 2014; Arendt et al., 2016).

The 'grand challenge' of complete understanding of the mammalian nervous system is also burdened by the disorganized data flood that has been incoming from studies of the anatomical, physiological, and molecular properties of neurons (Ascoli and Wheeler, 2016; Hamilton et al., 2017). We will require increased collaboration, communication, and synthesis across a wide range of scientific fields, including close collaboration with computer scientists and engineers (Cohen, 2004; Padilla and Tsukimura, 2014; Padilla et al., 2014). Further, the neurons of the nervous system will need to be fully integrated with that of the overlapping network of glial cells (Samborska et al., 2016). Eventually the nervous system will become related across all biological levels, including system-wide physiological systems involved with regulating such diverse functions as blood flow and hormone secretion. Identifying 'individuated' evolutionary units could prove to be a powerful approach to distinguish natural subdivisions of components within the same level

(i.e., cell types) that share an evolutionary relationship with other individuated components in higher levels of complexity (Wagner, 2014; Arendt et al. 2016). Therefore, continuing to increase our comprehensive understanding of the nervous systems in other species is anticipated to increase understanding in humans. In the near future, research groups will need to become adept at generating and coordinating 'data ladders' in which datasets are interlinked in a way that provides a complete characterization of a brain area of study that spans the different levels of biological organization, including 'rungs' that relate what is known about humans with other species (Markram, 2013). There will not be an easy single answer to the profound question of how nervous systems accomplish the astounding computations that concurrently manage sensory processing, physiological maintenance, and behavior output. In the same way that organismal systems can integrate and organize diversity to generate astounding emergent behavior, so too will the ecosystem of scientists need to continue learning how to foster individuality while embracing diversity and collaboration in a way that the whole is greater than the sum of its parts.

REFERENCES

Arendt D, Musser JM, Baker CVH, Bergman A, Cepko C, Erwin DH, Pavlicev M, Schlosser G, Widder S, Laubichler MD, Wagner GP (2016) The origin and evolution of cell types. Nature Reviews Genetics 17:744–757.

Ascoli GA, Wheeler DW (2016) In search of a periodic table of the neurons: Axonal-dendritic circuitry as the organizing principle: Patterns of axons and dendrites within distinct anatomical parcels provide the blueprint for circuit-based neuronal classification. BioEssays 38:969–976.

Bargmann CI (1993) Genetic and cellular analysis of behavior in C. elegans. Annual review of neuroscience 16:47–71.

Bargmann CI, Hartwieg E, Horvitz HR (1993) Odorant-selective genes and neurons mediate olfaction in C. elegans. Cell 74:515–527.

Brenner S (1974) The genetics of Caenorhabditis elegans. Genetics 77:71–94.

Brenner S (1994) Loose ends. Current Biology 4:1052.

Brenner S (2010) Sequences and consequences. Philos Trans R Soc Lond, B, Biol Sci 365:207–212.

C. elegans Sequencing Consortium (1998) Genome sequence of the nematode C. elegans: a platform for investigating biology. Science 282:2012–2018.

Cohen JE (2004) Mathematics is biology"s next microscope, only better; biology is mathematics" next physics, only better. PLOS Biol 2:e439.

Corsi AK, Wightman B, Chalfie M (2015) A Transparent window into biology: A primer on Caenorhabditis elegans. WormBook:1–31.

de Bono M, Bargmann CI (1998) Natural Variation in a Neuropeptide Y Receptor Homolog Modifies Social Behavior and Food Response in C. elegans. Cell 94:679–689.

Geschwind DH, Konopka G (2009) Neuroscience in the era of functional genomics and systems biology. Nature 461:908–915.

Hamilton DJ, Wheeler DW, White CM, Rees CL, Komendantov AO, Bergamino M, Ascoli GA (2017) Name-calling in the hippocampus (and beyond): coming to terms with neuron types and properties. Brain Inform 4:1–12.

Hillier LW, Coulson A, Murray JI, Bao Z, Sulston JE, Waterston RH (2005) Genomics in C. elegans: so many genes, such a little worm. Genome Res 15:1651–1660.

Hobert O (2016) A map of terminal regulators of neuronal identity in Caenorhabditis elegans. Wiley Interdiscip Rev Dev Biol 5:474–498.

Hobert O, Glenwinkel L, White J (2016) Revisiting Neuronal Cell Type Classification in Caenorhabditis elegans. Curr Biol 26:R1197–R1203.

Holmberg J, Perlmann T (2012) Maintaining differentiated cellular identity. Nature Reviews Genetics 13:429–439.

Ideker T, Galitski T, Hood L (2001) A new approach to decoding life: Systems biology. Annu Rev Genomics Hum Genet 2:343–372.

Izquierdo EJ, Beer RD (2016) The whole worm: brain–body–environment models of C. elegans. Current Opinion in Neurobiology 40:23–30.

Joyner MJ (2011) Giant sucking sound: can physiology fill the intellectual void left by the reductionists? J Appl Physiol 111:335–342.

Kato S, Kaplan HS, Schrödel T, Skora S, Lindsay TH, Yemini E, Lockery S, Zimmer M (2015) Global brain dynamics embed the motor command sequence of Caenorhabditis elegans. Cell 163:656–669.

Katz P, Grillner S, Wilson R, Borst A, Greenspan R, Buzsáki G, Martin K, Marder E, Kristan W, Friedrich R, Chklovskii DM (2013) Vertebrate versus invertebrate neural circuits. Curr Biol 23:R504–R506.

Kitano H (2002) Computational systems biology. Nature 420:206–210.

Koch C (2012) Systems biology. Modular biological complexity. Science 337:531–532.

Kuster DWD, Merkus D, van der Velden J, Verhoeven AJM, Duncker DJ (2011) "Integrative Physiology 2.0": integration of systems biology into physiology and its application to cardiovascular homeostasis. The Journal of Physiology 589:1037–1045.

Markram H (2013) Seven challenges for neuroscience. Funct Neurol 28:145–151.

Masland RH (2012) The tasks of amacrine cells. Visual Neuroscience 29:3–9.

Mihaljević B, Benavides-Piccione R, Bielza C, DeFelipe J, Larrañaga P (2014) Bayesian Network Classifiers for Categorizing Cortical GABAergic Interneurons. Neuroinformatics 13:193–208.

Nguyen JP, Shipley FB, Linder AN, Plummer GS, Liu M, Setru SU, Shaevitz JW, Leifer AM (2016) Whole-brain calcium imaging with cellular resolution in freely behaving Caenorhabditis elegans. Proc Natl Acad Sci USA 113:E1074–E1081.

Noble D (2011) Systems: What's In a Name? Physiology 26:126–128.

Padilla DK, Daniel TL, Dickinson PS, Gruenbaum D, Hayashi C, Manahan DT, Marden JH, Swalla BJ, Tsukimura B (2014) Addressing Grand Challenges In Organismal Biology: The Need For Synthesis. Bioscience 64:1178–1187.

Padilla DK, Tsukimura B (2014) A New Organismal Systems Biology: How Animals Walk the Tight Rope between Stability and Change. Integr Comp Biol 54:218–222.

Pennisi E (2003) Systems biology: Tracing life's circuitry. Science 302:1646–.

Prevedel R, Yoon Y-G, Hoffmann M, Pak N, Wetzstein G, Kato S, Schrödel T, Raskar R, Zimmer M, Boyden ES, Vaziri A (2014) Simultaneous whole-animal 3D imaging of neuronal activity using light-field microscopy. Nat Methods 11:727–730.

Riddle DL, Blumenthal T, Meyer BJ, Priess JR, Emmons SW, Sternberg PW (1997) Male Development and Mating Behavior.

Samborska V, Gordleeva S, Ullner E, Lebedeva A, Kazantsev V, Ivanchenko M, Zaikin

A (2016) Mammalian Brain As a Network of Networks. opera medica et physiologica 2:11–26 Available at: http://operamedphys.org/OMP_2016_01_0024.

Sanes JR, Masland RH (2015) The Types of Retinal Ganglion Cells: Current Status and Implications for Neuronal Classification. http://dxdoiorg/101146/annurev-neuro-071714-034120 38:221–246.

Sternson SM, Atasoy D, Betley JN, Henry FE, Xu S (2016) An Emerging Technology Framework for the Neurobiology of Appetite. Cell Metab 23:234–253.

Strange K (2005) The end of "naive reductionism": rise of systems biology or renaissance of physiology? Am J Physiol, Cell Physiol 288:C968–C974.

Sulston J, Ferry G (2002) The Common Thread. Joseph Henry Press.

Tarantola A (2006) Popper, Bayes and the inverse problem. Nature Physics 2:492–494.

Trent C, Tsuing N, Horvitz HR (1983) Egg-laying defective mutants of the nematode Caenorhabditis elegans. Genetics 104:619–647.

Venkatachalam V, Ji N, Wang X, Clark C, Mitchell JK, Klein M, Tabone CJ, Florman J, Ji H, Greenwood J, Chisholm AD, Srinivasan J, Alkema M, Zhen M, Samuel ADT (2016) Pan-neuronal imaging in roaming Caenorhabditis elegans. Proc Natl Acad Sci USA 113:E1082–E1088.

Wagner GP (2014) Homology, Genes, and Evolutionary Innovation. Princeton: Princeton University Press.

WATSON JD, CRICK F (1953) Molecular Structure of Nucleic Acids - a Structure for Deoxyribose Nucleic Acid. Nature 171:737–738.

Zhang X, Serb JM, Greenlee MHW (2011) Mouse retinal development: a dark horse model for systems biology research. Bioinform Biol Insights 5:99–113.